The Role of the Atypical Chemokine Receptor D6 in the Placenta

Pek Joo Teoh
MBBChBAO MRCOG MRCPI MSc

Submitted in fulfilment of the requirements for the degree of
Doctor of Medicine

Reproductive and Maternal Medicine
Division of Developmental Medicine
School of Medicine
College of Medical, Veterinary and Life Sciences
University of Glasgow

July 2013

Summary

D6 is an atypical chemokine receptor related to CCR1-5 that binds to many inflammatory CC chemokines. Experiments using transfected cell lines have shown that upon binding to a chemokine ligand D6 does not trigger cellular signalling pathways, but rather acts to scavenge the bound ligand. It achieves this by constitutively travelling to and from the cell surface via early and recycling endosomes, internalising chemokines bound when it is at the cell surface. Over time, D6 removes a large amount of ligands from the extracellular compartment. In vivo, this scavenging activity is thought to regulate the level of CC chemokines, and thus controls inflammation locally and systemically. Lack of D6 has been shown to result in elevated amounts of bioavailable chemokines, and is associated with over exuberant inflammatory responses.

In human, D6 mRNA and protein is highly expressed in trophoblast-derived gestational tissues. The expression of D6 mRNA in the placenta is by far the highest, compared to other solid tissues being studied. The importance of D6 in protecting the offspring has been demonstrated in animals. In pigs, a defect in D6 expression was discovered in placental attachment sites in endometrium from arresting fetuses. In mice, lack of D6 results in an increase in fetal loss after challenge with lipopolysaccharide (LPS) or antiphospolipid autoantibodies (aPL), and an increase in the number of abnormal pups when mouse embryos are transferred into fully allogeneic pseudo-pregnant female recipients.

In view of these results suggesting a critical role for D6 in placental mediated complications, the expression and molecular function of D6 in primary human trophoblast cells were studied, as to date in vitro human studies have utilised the choriocarcinoma cell line BeWo or immortalised cell lines engineered to over-express exogenous D6. Secondly the impact of D6 deficiency on placental structure, chemokine expression and leukocyte abundance in mice was examined.

Chapter 3 presents the results of experiments on primary human trophoblasts. Protocols for routine primary trophoblast isolation, purification and culture from fresh term placentas were optimised in our laboratory. D6 mRNA was detected in these primary cells. Using Western blotting, immunofluorescence and flow

cytometry, D6 was shown to be present predominantly in the intracellular vesicles of the cells. Competition chemokine uptake assays, analysed by flow cytometry, showed that CCL2 was internalised by trophoblasts using D6. Competitive chemokine scavenging assays, analysed by quantitative Western blot, confirmed that D6 was functioning as a chemokine scavenger on primary human trophoblasts and that it progressively removed substantial quantities of chemokine from medium bathing the cells. This is the first set of experiments that confirms D6 is present, and functioning as a chemokine scavenger in primary human cells.

Chapter 4 contains the results from the mouse experiments. Even in an unchallenged environment it was shown that, on the DBA-1 genetic background, D6 deficiency in the mother and pups leads to higher rates of stillbirth and neonatal deaths, resulting in a reduction in the number of pups weaned per litter than their WT counterparts. By gestational age E14, pup weight was significantly smaller in the D6 KO mice. Using stereological techniques, the placenta of the D6 KO mice at this gestation was found to have a smaller labyrinthine zone. The volume of the labyrinthine zone was positively correlated with pup/placenta ratio. These phenotypes could be due to a maternal or fetal effect of D6 deficiency. To ascertain the answer to this question, the experiment at E14 was extended by breeding DBA-1 females heterozygous for the deleted D6 allele (D6 HET) with D6 deficient (D6 KO) males. In this model the phenotypes of D6 KO pups and placentas could be compared with their D6 HET siblings that developed in a mother expressing some D6 (i.e. D6 HET). Although there were no differences in pup weight, placental weight and pup/placenta ratio between these two groups, stereology revealed a decrease in labyrinthine zone volume fraction in the D6 KO placentas in comparison to their D6 HET siblings. The observed fetal compromise and placental defect at E14 was not apparent at the later gestational age of E18. Luminex multiplex protein assay showed an elevated level of circulating chemokine CCL2 in the serum of D6 KO pregnant mice in comparison to their WT counterpart, so loss of chemokine regulation could be responsible for the defects observed in D6 deficient placentas. In summary, D6 deficiency results in an increase in perinatal death, a fundamental defect in placental formation (reduced labyrinthine zone) and dysregulation of circulating chemokine levels.

Chapter 5 discusses the mechanisms of D6 in regulating placental formation and reproductive outcome and the novel insights that this work provided into placental D6 function. It also describes the design of future experiments to reveal the precise role of D6 in chemokine regulation and cell signalling in reproductive immunology, and discusses how D6 might contribute to pregnancy outcome in humans.

Table of Contents

List of Tables and Figures

Chapter 1

Chapter 2

Chapter 3

Chapter 4

Presentations of Work Undertaken in This Thesis to Learned Societies

- January 2013

The 8th Biennial Conference of the UK Fertility Societies (Fertility2013), Liverpool
(Oral Presentation)

- December 2012

Annual Academic Meeting of the Blair Bell Research Society, RCOG London
(Oral Presentation)

- May 2012

UK Specialty Registrar in Obstetrics and Gynaecology Annual Conference (SpROGs), Bristol
(Best Oral Presentation)

- February 2012

RCOG Scottish Senior Staff Conference, Dunkeld
(Invited Speaker)

- December 2011

Annual Meeting of Obstetrics and Gynaecology for Scottish Trainees (AMONGST), Glasgow
(Best Oral Presentation)

- March 2011

Society of Gynecological Investigation (SGI) Annual Meeting, Miami
(Poster Presentation)

Acknowledgements

Firstly I must thank both my supervisors Scott Nelson and Rob Nibbs, without their support and advice the completion of this project would not have been possible. Thanks also to Scott for helping me in my career advancement in reproductive medicine. Similarly I would like to thank Professor Graham Burton in Cambridge for his guidance and expertise in the technique of stereology. I am sincerely grateful especially to Fiona Menzies for her help and supervision in the laboratory. She has put in a lot of effort from the beginning in overseeing my work, to ensure I am heading towards the right direction to successfully complete the MD project.

I am thankful that all my colleagues have been very helpful and patient in guiding me through various laboratorial techniques. In 'desperate times' they have also willingly lent me some of their precious reagents. Both laboratorial teams at the reproductive medicine group, and the Nibbs's chemokine research group have been exceptionally friendly. I would like to especially thank those who have put in extra time to teach me in the lab: Ross Kinstrie in Western and FACS; Chris Hansell in FACS and Luminex; Helen Baldwin in FACS and immunofluorescence; Leah Marks in primary trophoblast culture; Mairi Clarke in genotyping; Rae Oldham for her advice in Flowjo and laboratorial reporting; Fiona Jordan for her advice in Western, qPCR and laboratorial reporting; Dr Dilys Freeman for her advice in the project; and last but not least Professor Mary Ann Lumsden, as my advisor, for her guidance and support in this project.

A special word of thanks to the staff and patients in Southern General Hospital, who have been exceptionally helpful during my frequent visits to collect placentas.

I would also like to thank Tenovus Scotland for providing consumable funding for this project.

Finally, my thanks are also due to my family for their relentless support for my education and career. Thank you papa and mama, and also sis's for your support and belief in me. Thank you my beloved wife, for being the most wonderful wife on earth. Despite having to cope with your busy full time job, you have been so

patient and dedicated in looking after both Eva and me throughout these years. Without your love, care and support I would not have completed this thesis. This thesis is dedicated to you. Thank you Eva for being such a good girl, mama and me are incredibly proud of you. Your arrival in this world has brought us endless joy. Lots of love to all of you.

Author's Declaration

I declare that, except where explicit reference is made to the contribution of others, that this thesis is the result of my own work and has not been submitted for any other degree at the University of Glasgow or any other institution.

Signature:

Printed name:

Abbreviations

2D two-dimensional

3D three-dimensional

7-AAD 7-aminoactinomycin D

ACKR atypical chemokine receptor

APC antigen presenting cell

aPL antiphospholipid autoantibodies

ApoE apolipoprotein E

APS antiphospholipid syndrome

bioCCL2 biotinylated CCL2

C3 complement component 3

CCL CC-chemokine ligand

$CCL2^{AF647}$ AlexaFluor647 CCL2

CCR CC-chemokine receptor

CCX-CKR chemocentryx chemokine receptor

CD cluster of differentiation

cDNA complementary deoxyribonucleic acid

COPD chronic obstructive pulmonary disease

CP chorionic plate

Crry complement receptor-1 related gene/protein Y

CTL cytotoxic T lymphocyte

CTLA cytotoxic T-lymphocyte-associated protein

CX_3CL CX_3C-chemokine ligand

CX_3CR CX_3C-chemokine receptor

CXCL CXC-chemokine ligand

CXCR CXC-chemokine receptor

DAF decay-accelerating factor

DAPI 4'-6-diamidino-2-phenylindole

DARC Duffy antigen receptor for chemokines

DB decidua basalis

DC-SIGN dendritic cell-specific intercellular adhesion molecule-3 grabbing nonintegrin

DM diabetes mellitus

DMEM Dulbecco's Modified Eagle Medium

DNAse deoxyribonuclease

EAE experimental autoimmune encephalomyelitis

ECM extracellular matrix

EDTA ethylenediaminetetraacetic acid

EVT extravillous cytotrophoblast

Exx embryonic day xx

FACS fluorescence-activated cell sorting

FITC fluorescein isothiocyanate

Foxp3 forkhead box p3

GAPDH glyceraldehyde 3-phosphate dehydrogenase

GDP guanosine diphosphate

GPCR G-protein-coupled receptor

GTP guanosine-5'-triphosphate

HEK293 human embryonic kidney 293

HEK-D6 HEK293 transfected with D6 expression constructs

HET heterozygous

HIV human immunodeficiency virus

HLA human leukocyte antigen

HRP horseradish peroxidase

IBD inflammatory bowel disease

iEVT interstitial extravillous cytotrophoblast

IFN-γ interferon-γ

Ig immunoglobulin

IL interleukin

IUGR intrauterine growth restriction

JZ junctional zone

KC keratinocyte chemoattractant

KIR killer inhibitory receptor

KSHV Kaposi's sarcoma herpesvirus

KO knockout

LDS lithium dodecyl sulfate

LEC lymphatic endothelial cells

LIF leukocyte inhibitory factor

LIR leukocyte immunoglobulin-like receptor

LPS lipopolysaccharide

LZ labyrinthine zone

MCP membrane cofactor protein

MFI mean fluorescence index

MHC major histocompatibility complex

MIF migration inhibitory factor

MIP macrophage inflammatory protein

MOG myelin oligodendroglial glycoprotein

mRNA messenger ribonucleic acid

MS multiple sclerosis

NaCl sodium chloride

NH_4Cl ammonium chloride

NK natural killer

NKG2 natural-killer group 2 receptor

NSCLC human non-small cell lung cancer

OVA chicken egg ovalbumin

PBS Dulbecco's phosphate buffered saline

PBST PBS-0.05% Tween 20

PCR polymerase chain reaction

PD-1 programme death-1 receptor

PDL programme death ligand

PGS PBS, 0.2% gelatine, 0.05% saponin

PIPES 4-piperazinediethanesulfonic acid

PMN polymorphonuclear

pNK peripheral blood natural killer cells

qPCR quantitative polymerase chain reaction

RA rheumatoid arthritis

RANTES regulated on activation, normal T cell expressed and secreted

RCF relative centrifugal force

RPE R-Phycoerythrin

rRNA ribosomal ribonucleic acid

SDS sodium dodecyl sulfate

SDS-PAGE sodium dodecyl sulfate polyacrylamide gel electrophoresis

siRNA small interfering ribonucleic acid

SNPs single nucleotide polymorphisms

ST syncytiotrophoblast

TAE Tris-acetate-EDTA

TCA trichloroacetic acid

TCR T-cell receptor

TGF transforming growth factor

Th T helper

TNF tumor necrosis factor

TOP-1 topoisomerase 1

Treg regulatory T cells

Tris-HCL Tris(hydroxymethyl)aminomethane hydrochloride

uNK uterine natural killer

VEGF vascular endothelial growth factor

vEVT endovascular extravillous cytotrophoblast

VT villous cytotrophoblast

WT wild type

XCL XC-chemokine ligand

XCR XC-chemokine receptor

1 Introduction

1.1 Adequate placentation is crucial for a successful pregnancy

Major adverse perinatal outcomes are increasingly recognised as having their origins in early pregnancy and abnormal placentation. Stillbirth is a devastating outcome of pregnancy for women and their families, with one in 170 babies affected (Office for National Statistics); (Bukowski et al., 2011). Pre-eclampsia, part of the spectrum of the gestational hypertensive disorders is also a major contributor to perinatal morbidity and mortality and affects 3% of pregnancies (Jacobs et al., 2003, Lee et al., 2004, Roberts et al., 2005, Geelhoed et al., 2010). Intrauterine growth restriction (IUGR), affects 10% of pregnancies and is associated with prematurity, cerebral palsy and neonatal death (Stoknes et al., 2012). All of these conditions have been associated with abnormal placental histology at delivery. More striking are the observations that these adverse events in late pregnancy have their origins in early pregnancy as demonstrated by first trimester assessment of placental biomarkers and fetal growth (Khong et al., 1986, Smith et al., 2004, Bukowski et al., 2011). Despite recognition of the major contribution of placentation to adverse perinatal outcomes the underlying pathophysiology remains poorly understood.

1.2 The placenta

The placenta is the first organ to form during pregnancy (Rossant and Cross, 2001), and is vital to support the survival and growth of the fetus in utero. Without the placenta, the procreation of the mammalian species is not possible.

The placenta forms an interface between the mother and fetus, performing its main function of facilitating the exchange of gases, nutrients and metabolic wastes. The placenta is also a barrier, protecting the fetus from the harmful attack of pathogens and the maternal immune system (Rossant and Cross, 2001). It produces hormones and growth factors which are needed for the advancement and flourishing of the pregnancy; they uphold the balanced physiological condition in the uterus for the continuation of the pregnancy. The hormones and growth factors produced also affect the physiological changes of the maternal body, to adapt to and support the pregnancy.

Some authors simplify human and rodent placentas into 3 major anatomical structures; each structure has their specific roles in providing support for the placenta to function as a whole unit (Watson and Cross, 2005). The outer maternal layer, which consists of the maternal decidual cells and vasculature, provides the blood supply to the placenta. The middle junctional layer contains giant cells and spongiotrophoblasts that anchor the placenta to the uterus, these cells may also play a role in the process of decidual remodelling (Adamson et al., 2002, Georgiades et al., 2002). The inner layer is the region where the maternal-fetal vasculature intertwines and closely approximates each other for the exchange of gases and nutrients.

The most important cells in the placenta are the fetal-derived trophoblasts. They are the main cells that line the maternal-fetal interface, the main structure for the placenta to serve its function (Rossant and Cross, 2001). Trophoblasts also have a major role to play in orchestrating the process of successful placental morphogenesis.

1.2.1 The human placenta

The mature human placenta is a discoid organ; its size and weight vary between individuals (Fig 1.1a). The mean radius of round placentas was estimated to be 9.1cm at term, with the mean thickness at the centre of 2.5cm (Salafia et al., 2010, Benirschke et al., 2012). The majority of placentas are round or oval in shape, however, in 10% of cases, the placentas have different shapes (Benirschke et al., 2012). They can have a smaller accessory (succenturiate) lobe (placenta succenturiata), be bilobal in shape (placenta bilobata) or, when the separation of the lobe is more pronounced, it can appear almost entirely detached from the main part of the placenta (placenta duplex). With these abnormal non-oval shaped placentas there is a significant association with lower placental efficiency linking with either maternal utero-placental or feto-placental vascular pathology (Salafia et al., 2010).

a)

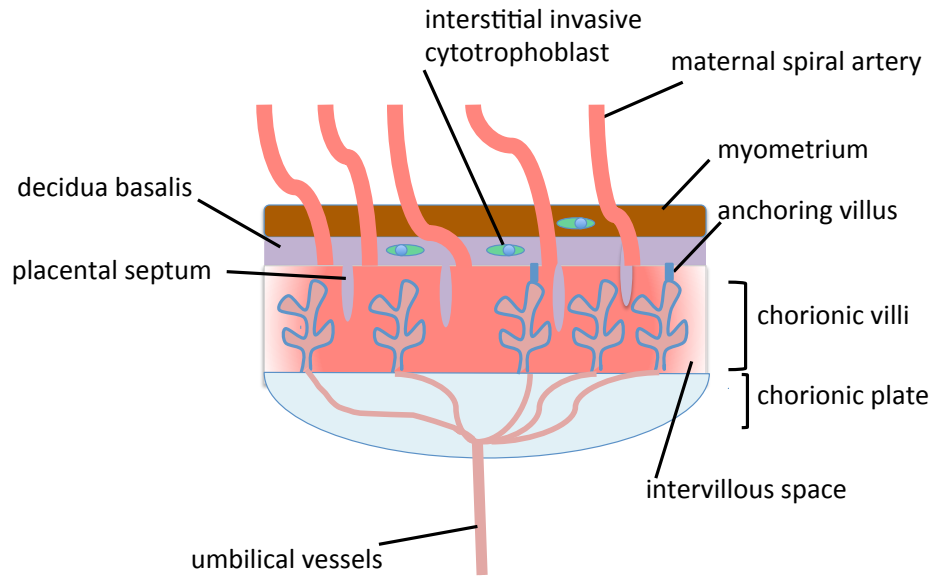

b)

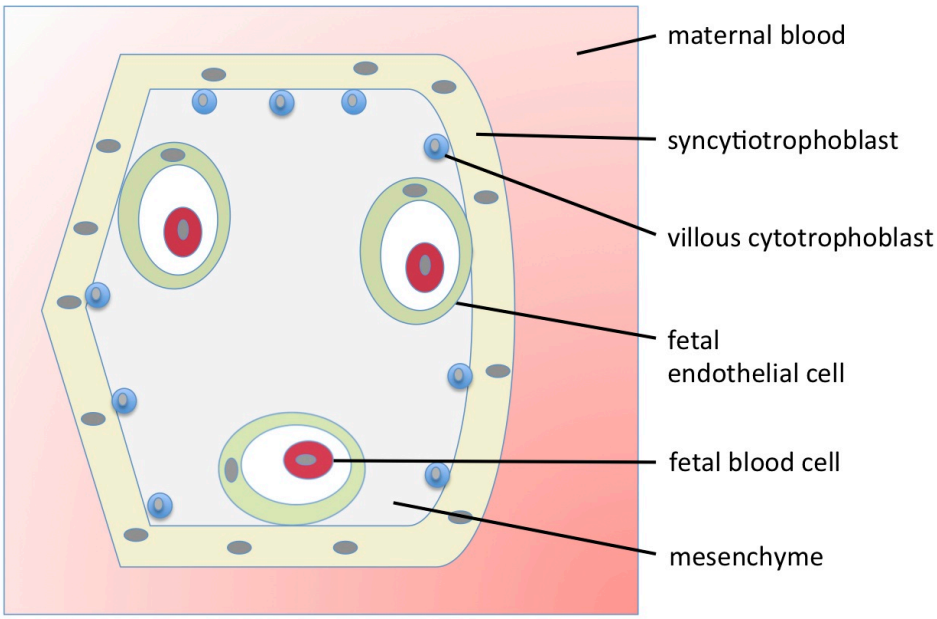

Figure 1.1 Schematic illustrations of the anatomy and chorionic villus of the full term human placenta. a) Fetal blood flows from the umbilical artery into the capillaries in the chorionic villi, which are bathed in the maternal blood in the intervillous space. b) The human placenta is monochorial, the syncytiotrophoblast is in direct contact with maternal blood. Gases and nutrients pass through one layer of syncytiotrophoblast, and the endothelium to reach the fetal circulation. Adapted from (Rossant and Cross, 2001).

a)

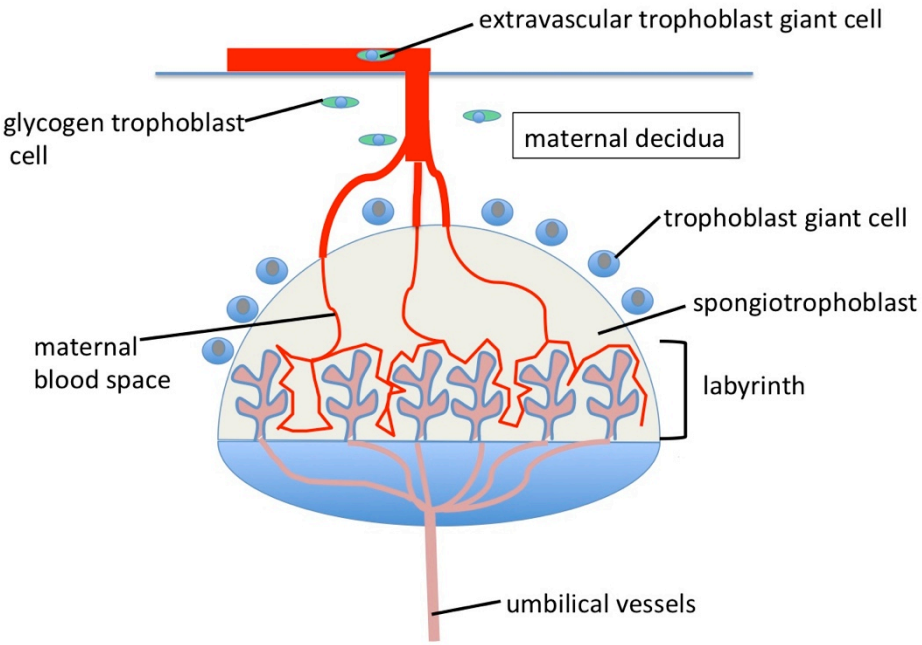

b)

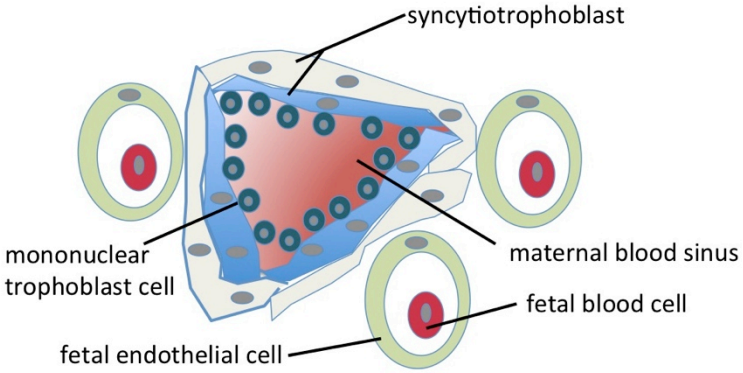

Figure 1.2 Schematic illustrations of the anatomy and labyrinth of mouse placenta. a) Maternal vessels and fetal umbilical vessels subdivide into capillaries in the labyrinth for fetal-maternal exchange. b) The mouse placenta is trichorial as there are 3 layers of trophoblasts (bilayer of syncytiotrophoblasts and a monolayer of mononuclear trophoblasts) in the fetal-maternal membrane, distinguishable in electron micrograph (Georgiades et al., 2002). Gases and nutrients have to pass through these three layers of trophoblasts, and another layer of endothelial cells before reaching the fetal circulation. Adapted from (Rossant and Cross, 2001).

The side of the placenta facing the amniotic cavity is the fetal surface, also called the chorionic or amniotic surface. This surface appears glossy, due to the avascular, intact epithelium of the amnion that covers the chorionic plate (Benirschke et al., 2012). From the fetal surface of the placenta, the umbilical cord connects to the fetus. It carries the communicative vessels between the fetus and the placenta, which comprises one umbilical vein and two arteries that spiral within the cord. Surrounding those vessels is the jelly like connective tissue called the Wharton's jelly. Wharton's jelly gives the cord its sponge like characteristic. The site of insertion of the cord to the placenta is usually off centre (Pathak et al., 2010). Eccentric umbilical cord insertion has been associated with a decrease in placental efficiency, but has not been found to be linking with adverse obstetric outcome (Yampolsky et al., 2009, Pathak et al., 2010). In slightly less than 1% of pregnancies, the cord inserts outwith the placenta into the membrane (velamentous cord insertion), with the blood vessels being exposed when they travel along the thin membrane (vasa praevia) before insertion into the chorionic plate (Sepulveda, 2006). This exposes the fetus to the danger of profuse blood loss if the vessels are punctured when the membrane ruptures either spontaneously or iatrogenically.

The basal (maternal) surface of the placenta is traversed by sets of grooves, which divide this part of the placenta into different lobes, or cotyledons. Each of these cotyledons contains one or several chorionic villous trees, the principal functioning units of the placenta (Benirschke et al., 2012). The sub-branches of the blood vessels from the umbilical cord form the chorionic villous trees. The most common classification of the subdivision of the chorionic villi is the one described by Kaufmann et al. in 1979 (Kaufmann et al., 1979). The stem villi are the main framework providing support for the villous tree, they are formed at the start of the ninth week of pregnancy. These stem villi branch out, forming extensions called immature intermediate villi by the 16^{th} week of pregnancy. Near the end of the second trimester, the stem villi also form mature intermediate villi, which are side branches more slender than the ones previously formed. By week 32, the mature intermediate villi begin to give rise to the terminal villi, which are grape-like capillaries forming the main fetal-maternal interface (Schoenwolf et al., 2009). The chorionic villi channel the fetal blood to the fetal-maternal interface; fetal blood flows from the umbilical

arteries to the villi, and then returns via the umbilical vein. The chorionic villi are bathed in the maternal blood, which flows directly into the intervillous space. The fetal-maternal interface of a mature human placenta is haemochorial, with the mono-layered barrier of the syncytiotrophoblast, and the fetal endothelium separating the fetal and maternal blood (Fig 1.1b). Between the syncytiotrophoblast, and the fetal endothelium, there is a non-continuous layer of mononuclear villous cytotrophoblast, also known as the Langhans cells. From the first trimester until around 20 weeks, the fetal-maternal membrane comprises four layers: syncytiotrophoblast, cytotrophoblast, villous connective tissue and endothelium of fetal capillaries (Moore et al., 2013). At this stage the cytotrophoblast forms a continuous layer. After the 20th week of gestation, the continuity of the cytotrophoblast layer in most of the villi is broken due to cellular changes. In some of the distal villi the fetal-maternal interface becomes thinner, forming a vasculosyncytial placental membrane where the syncytiotrophoblast directly contacts the endothelium of the fetal capillaries (Georgiades et al., 2002). This thin surface provides close proximity for the fetal and maternal blood, and thereby enhances the efficiency of fetal-maternal exchange.

At term, maternal blood flow to the placenta is estimated to be up to 700ml/minute (Wang and Zhao, 2010), with a surface area for fetal maternal exchange of more than 10m^2 (Ellery et al., 2009). This dynamism of placental function provides the support required for fetal survival until term pregnancy. It has been reported that maternal blood flow into the placenta is not established until at least after the first 12 weeks of pregnancy (Hustin and Schaaps, 1987), thereby protecting the early fetus from the oxidative stress and mechanical pressure from the maternal blood flow. During this period the delicate fetus is undergoing the important process of organogenesis (Georgiades et al., 2002).

1.2.2 The murine placenta

Murine placentas are widely used in research studies for greater understanding of the developmental, cellular and molecular structures and functions of the organ. Development of murine placentas is sensitive to genetic disruption (Rossant and Cross, 2001), and thus it is a good model for studies to gain new insights into the cellular and molecular biology of the placenta. Several

indispensible genes for mouse placental development, for example Mash2 and Gcm1, are also expressed in humans (Alders et al., 1997, Janatpour et al., 1999, Nait-Oumesmar et al., 2000), however the understanding of their functional role in human placental development is very limited (Rossant and Cross, 2001).

The detailed anatomies of the murine and human placentae are not exactly the same (Fig 1.1 and 1.2), but grossly there are certain similarities in the structure of the functional units, and also the cellular mechanisms underlying their development (Table 1.1) (Rossant and Cross, 2001).

Anatomical site	Structure/ cell		Function(s)
	Murine	Human	
Outer maternal layer	Trophoblast giant cell	Invasive extravillous cytotrophoblast	Invasion and modelling of decidua
Middle junctional layer	Giant cell (differentiated from spongiotrophoblast)	Cytotrophoblastic shell	Anchoring villus (human) and labyrinth (murine)
Inner layer	Labyrinth	Chorionic villus	Fetal-maternal interface
	Single cotyledon	Multiple cotyledon	Containing labyrinth (murine) and chorionic villus (human)

Maternal-fetal interface (Fig 1.1b and 1.2b)	Trichorial	haemochorial	Exchange of gases, nutrients and wastes. Physical barrier to hydrophilic substances. Invaginations on the surface facing maternal blood for both species, to increase absorption of substances.

Table 1.1 Structural and functional units of murine and human placentas. Summarised from (Georgiades et al., 2002, Rossant and Cross, 2001).

Mouse placenta, like human, is discoid. Both the maternal and fetal arteries subdivide into smaller branches, and eventually into smaller capillaries at the fetal-maternal interface. The capillaries are interconnected and form a maze-like architecture at the labyrinthine zone (LZ) in the inner layer of the placenta; the mouse placenta is described as a labyrinthine placenta (Georgiades et al., 2002). LZ is the most important zone in the placenta. This is the area where the placenta performs its vital role of supporting the fetus in utero; the fetal capillaries are situated in close proximity with maternal blood, forming the fetal-maternal interface for crucial exchanges described above. Unlike the haemochorial human placenta, fetal-maternal membrane in the trichorial mouse placenta comprises three layers of trophoblasts, and also the fetal endothelium (Fig 1.2b).

In mouse, it has been discovered that LZ continues to grow up to E18.5, even though the maximum volume of the placenta is reached at E16.5 (Coan et al., 2004). This leads to an increase in the representative proportion of LZ in the placenta, essential in supporting the bigger pup at this gestation. It has also been proven that smaller volume of LZ is related to fetal growth restriction, even after taking into account the size of the whole placenta in relation to the fetal weight (Coan et al., 2008, Coan et al., 2010). Within this functional zone, stereological analyses showed malformation of microstructures could also cause growth restriction in the fetuses. Stereology is a well established method for generating absolute three-dimensional (3D) quantities from two-dimensional (2D) paraffin and resin histological sections (Coan et al., 2004). This method of analysis showed that compromised fetuses had smaller surface area of fetal and maternal trophoblast membrane, shorter total capillary length, and also larger mean fetal-maternal membrane thickness; these lead to poorer theoretical diffusion capacity in the fetal-maternal interface (Coan et al., 2008).

Recent studies of placental development in rats show that the pattern of placental invasion of this species may be more representative of human placentation (Caluwaerts et al., 2005, Carter et al., 2006). Trophoblast invasion in rats involves a deeper part of the placental bed, leading to the development of an area called the mesometrial triangle. The mesometrial triangle is an extension of the decidua, consists of a mass of decidualised cells and uterine NK cells, and also numerous loops of spiral arteries (Caluwaerts et al., 2005, Carter

et al., 2006). In contrary, the invasion of trophoblasts in mice is merely restricted to the decidua. The mesometrial triangle in rat pregnancy is thought to be somewhat comparable to the invasion of the inner myometrium in human; structural arterial changes in this area has been studied to understand the process of uterine spiral arteries remodelling in rat pregnancy (Caluwaerts et al., 2005, Vercruysse et al., 2006, Geusens et al., 2010). It has been suggested that trophoblast invasion may play a more important role in rat pregnancy in comparison the mouse (Carter et al., 2006). It will be interesting to follow the development of further comparative studies. Perhaps in the future the rat will be more frequently used for placental research when more experimental genetic model systems are available for this species.

1.3 The critical role of successful placentation in pregnancy

For successful placentation, the decidua has to tolerate the invasion of the embryo, and also protect this semi-allogeneic tissue from maternal immunological rejection. The decidua is subjected to modification of the tissues and blood vessels for adequate formation of vasculature to the placenta for an increased and undisturbed blood supply (Georgiades et al., 2002).

As early as day six in human pregnancy, the blastocyst comes into the close proximity of the uterine epithelium, a process referred to as apposition (Hannan and Salamonsen, 2007). This is followed by the process of adhesion (Hannan and Salamonsen, 2007), and then invasion of the endometrium by syncytiotrophoblast at day seven to nine (implantation). Prior to implantation, the blastocyst consists of only 50-60 trophoblasts, thus vast proliferation of trophoblast happens after endometrial invasion (Cross, 2000). After implantation, cytotrophoblasts from the trophectoderm proliferate and emanate, breaking through the primitive syncytium to reach the basal plate (Knofler and Pollheimer, 2013). On the distal sites, proliferative cell columns of these cytotrophoblasts give rise to invasive extravillous trophoblasts. During placentation, the formation of vascular network involves branching morphogenesis of the epithelial surface along with underlying stroma. This is an embryonic developmental mechanism to construct large areas of maternal-fetal interface for exchanges of nutrients and gases (Cross et al., 2003).

In the subsequent weeks, the extravillous trophoblasts erode the maternal connective tissues and spiral arteries via two routes. The first route of invasion is directly into the decidual stroma, the extravillous trophoblasts that invade via this route are termed interstitial extravillous trophoblasts. The second group of extravillous trophoblasts, termed endovascular extravillous trophoblasts, migrate to the lumen of the spiral arteries following the erosion of the maternal endometrial tissues. These two groups of extravillous trophoblasts play a major role in the remodelling of the spiral arteries within the decidua and the inner third of the myometrium (Pijnenborg et al., 1980). They contribute to the destruction of the endothelium, vascular smooth muscle and elastic lamina, and the replacement of these structures by fibrinoid (Lyall et al., 2013). A recent study systematically quantified changes in spiral artery features in human; it revealed a major defect in myometrial spiral artery remodelling in pregnancies associated with pre-eclampsia and fetal growth restriction (Lyall et al., 2013). Immunostaining detected differences in the quantity and functional status of extravillous trohoblasts in the myometrial vessels between these pregnancies and the normal pregnancy. Less fibrinoid deposition was detected in abnormal pregnancies, associated with inadequate spiral artery remodelling. The study also demonstrated the capability of extravillous trophoblasts to migrate deeply into the myometrium during placentation. Endovascular extravillous trophoblasts are also believed to serve the purpose of controlling the timing and amount of maternal blood flow into the placenta (Hamilton and Boyd, 1966, Pijnenborg et al., 2006, Knofler and Pollheimer, 2013). This regulatory process of placentation eventually allow the flow of maternal plasma and blood into the intervillous space of the placenta in the late first trimester, forming the maternal-fetal interface for the placenta to carry out its primary function (Huppertz, 2007, Burton et al., 2010).

Human is not the only species with haemochorial placenta. The placenta from higher and lower simian primates are also haemochorial (Rosenberg and Trevathan, 2007, Cole, 2009). In comparison with trichorial placenta as described earlier, there are fewer layers separating the maternal-fetal blood in the haemochorial interface, allowing more efficient exchanges to happen. In human, the degree of trophoblast invasion is unusually deep in comparison to other mammalian species, and up to the first third of uterine myometrium and

spiral arteries are invaded by trophoblasts during the process of implantation (Hannan and Salamonsen, 2007). Even in higher simian primates like baboon and orang-utan, only one tenth of the myometrium is invaded (Cole, 2009). The depth of placental invasion in human gives rise to adequate remodelling of spiral arteries in both the decidua and myometrium, transforming them into distended, thin-walled flaccid vessels (Lyall et al., 2013). These remodelled vessels form a vast network for maternal blood flow into the placenta at low pressure, creating a large surface area for feto-maternal exchange without subjecting the placenta to the stress of high pressure flow. This mechanism provides sufficient blood supply to the feto-maternal membrane, bringing essential nutrients and oxygen needed for the development of the brain of the human fetus. Via evolution, human has a uniquely large brain to body mass ratio in comparison to other mammals, and even our closely related primates; relative to other mammals it is thought that the development of the human brain requires ultra high energy and nutritional provision from the maternal blood supply (Gibbons, 1998, Rosenberg and Trevathan, 2007, Cole, 2009, Carter and Pijnenborg, 2011). This high demand of placentation predisposes human to pathological processes, for example pre-eclampsia/eclampsia, which is believed by some to be unique to pregnancy of human species (Rosenberg and Trevathan, 2007, Cole, 2009). Humans also have a higher pregnancy failure rate (41% vs. ≤10%) in comparison to other mammalian species (Wilmut et al., 1986). Interestingly, pre-eclampia has been reported in gorillas and chimpanzees (Thornton and Onwude, 1992, Carter and Pijnenborg, 2011). Similar to human pregnancy, during placentation in these great apes deep invasion of the interstitial and spiral arteries extends into the inner myometrium (Carter and Pijnenborg, 2011).

A significant number of miscarriages and diseases in pregnancy are caused by failed implantation and inadequate placentation. While it is difficult to accurately determine the causes of miscarriages, it has been reported that failure of implantation accounts for up to 75% of miscarriages, which occurs in up to 50% of pregnancies before 20 weeks of gestation (Norwitz et al., 2001, Macklon et al., 2002, Christiansen et al., 2006). Failed implantation also potentially contributes to recurrent implantation failure in assisted conception.

Besides determining the continuation of pregnancy at the early stages, inadequate placentation has also been associated with complications in later

gestational ages. Shallow invasion and inadequate placental villous formation are linked with severe pre-eclampsia, intrauterine growth restriction (IUGR), late sporadic miscarriage and preterm labour (Kim et al., 2003, Ball et al., 2006, Brosens et al., 2011, Kovo et al., 2013, Lyall et al., 2013). At the other extreme, excessive invasion of the trophoblasts can result in abnormally adherent placenta to the myometrium (placenta accreta) or even the uterine serosa and adjacent organs (placenta percreta), collectively classified as placenta creta in pregnancy (Norwitz et al., 2001). This poses a risk of major haemorrhage during the time of delivery. Recent studies have shown the importance of the decidua in regulating extravillous trophoblast invasion and spiral artery modelling; the absence of decidua is associated with placenta creta (Tantbirojn et al., 2008, Hannon et al., 2012).

1.4 Communication between maternal and fetal cells during placentation

During implantation, the female reproductive tract is not immunologically inert. Specialised immune cells are recruited to precise locations to aid the appropriate invasion of the developing placenta into the endometrium, remodelling of the endometrial vessels, and also providing immunological sanctuary for the conceptus. During the female menstrual cycle, the number of immune cells (decidual leukocytes) increases substantially from proliferative towards mid-secretory phase to prepare for implantation of the embryo (Bulmer et al., 2010). In early pregnancy the majority of cells (up to 70%) in the decidua are leukocytes (Red-Horse et al., 2004). These immune cells consist of neutrophils, uterine natural killer (uNK) cells, macrophages, T cells and dendritic cells.

Optimal crosstalk between the maternal and fetal cells determines the success of implantation, and the outcome of pregnancy. The endometrium is only receptive to implantation during a very short period in the menstrual cycle during the mid-secretory phase, known as the ‘window of receptivity’ (Dimitriadis et al., 2010). Following the priming with oestrogen, and under the influence of progesterone, the endometrium undergoes decidualisation. Besides the infiltration of large number of leukocytes, the process is also characterised by the differentiation of stromal cells in the endometrium, the modification of

the extracellular matrix (ECM), and the increase in vascular permeability (Garlanda et al., 2008). In the mid-secretory phase, regulatory molecules such as LIF, CX_3CL1 and CCL14 are released into the uterine lumen (Dimitriadis et al., 2010), affecting the behaviour of the cells in the blastocyst coming into contact with the decidua. Fetal cells in the blastocyst are first presented to the uterine epithelial cells during apposition. At this very first stage of implantation, dialogues are established between these two groups of cells, utilising soluble mediators being released and regulated precisely locally. This crosstalk not only influences the receptivity of the endometrium to the implantation of the blastocyst, but also triggers the expression of a unique repertoire of surface adhesive molecules on both fetal and maternal cells, for example L-selectin on the trophoblasts, and integrins on the endometrium (Genbacev et al., 2003, Hannan and Salamonsen, 2007, Mangale and Reddy, 2007). Within the placenta throughout pregnancy, there are also other stages where fetal cells are in close contact and directly communicating with maternal cells: the migration of the invasive interstitial extravillous trophoblast into, but not through, the inner third of the myometrium; the remodelling of the wall of the uterine spiral arteries by the endovascular trophoblast; and the role served by villous syncytiotrophoblast as an endothelial-like lining soaking in maternal blood in the placental intervillous space (Huppertz, 2007). These cellular and molecular interactions ensure placentation is successful to serve its function in supporting and protecting the fetus throughout pregnancy, and at the same time not over adherent so that it can be separated after delivery to avoid haemorrhage.

1.5 Receptivity of decidua to the invasion of semi-allogeneic embryo

In prehistoric life, placental pioneers (the group of mammals whose young develop inside their bodies) appeared 135-65 million years ago in the Late Cretaceous period (Lambert et al., 2001). Prior to this era, even mammals are thought to have produced eggs where the shells separated the offspring from their mother's body. One reason for this is that placentation requires complex immunological regulation, and it took millions of years for this adaptation to emerge. Interestingly there are exceptions to this biological evolution. Monotremes such as duck-billed platypus and spiny anteaters are modern egg-laying mammals. Marsupials are pouched mammals which delivers their offspring

at a very early fetal stage, where the young lived in the pouch, completing the maturation by attaching to the teats which lactate milk with specific components, controlling the development of the babies (Trott et al., 2003). Although the pregnancy of marsupials occurs over a relatively short period of time, in some species of marsupials there is evidence showing the presence of maternal recognition of pregnancy, leading to changes necessary in the uterine environment to accommodate the growing fetus (Renfree, 1972, Renfree, 2000).

Understanding the immunological regulation of embryonic implantation into the decidua remains a huge challenge. The embryo carries histocompatibility antigens from the father (Bulmer et al., 2010), and yet the mother's decidua can tolerate the invasion of this foreign body and coexist with it until the delivery of the fetus. One experiment in the 1970s revealed female mice could carry the fetuses fathered by allogeneic or semi-allogeneic males, but readily rejected organs transplanted from the same males (Borland, 1975). This phenomenon shows the uniqueness of the immunomodulation of the female reproductive tract during the time of implantation and pregnancy. Different experiments have been performed to study the tolerogenic properties of the maternal immune system towards the placenta, leading to various models being constructed. The following sections provide a summary of some of the models described. The role of chemokines in pregnancy will be discussed later in section 1.7.

1.5.1 Regulation of antigen presentation in the placenta

During pregnancy in both humans and mice, there seems to be mechanisms in place to regulate the presentation of fetal antigens to the maternal immune system to avoid the phenomenon of graft rejection.

It is well known that T cells only recognize an antigen when it is associated with a major histocompatibility complex (MHC) molecule, in humans it is also called human leukocyte antigen (HLA). The MHC is a region of multiple loci that function as antigen-presenting structures; they play major roles in determining whether transplanted tissue will be accepted as self (histocompatible) or rejected as foreign (histoincompatible). T cells interact with the MHC either through the direct or indirect pathway. Most cells express MHC class I. In the direct pathway CD8+ T cells directly engage MHC I complexes on the surface of

the transplanted cells. Host CD8+ T cells that recognise peptides in the context of MHC I kill the transplanted cells by this direct pathway. In the indirect pathway, peptides have to be presented, or cross-presented, by host antigen presenting cells (APCs) in a host MHC-restricted fashion. MHC II are only expressed by APCs; CD4+ T cells are activated by engaging with these MHC complexes. APCs also prime CD8+ T cells by cross-presenting antigens on MHC I.

In mouse pregnancy, the fetal allograft is presented exclusively through the indirect pathway; T cell engagement requires the uptake and processing of fetal/placental antigen by maternal APCs (Erlebacher et al., 2007). Mouse pregnancy has the ability to avoid direct antigen presentation for T cell recognition. This relatively minor allorecognition pathway removes a major threat to fetal survival, since it avoids the large number of T cells that typically drive acute transplant rejection in mouse, through their ability to directly interact with foreign MHC I molecules. In these experiments it was also observed that T cells that indirectly recognise the fetus were poorly primed and underwent clonal deletion.

Collins et al described that the mouse fetus and placenta are encased by the decidua, a stromal cell-derived structure (Collins et al., 2009). The authors discovered that dendritic cells stationed at the fetal-maternal interface were unable to travel to the lymphatic vessels of the uterus and thus reach the draining lymph nodes. Dendritic cells function as critical antigen-presenting cells for naive T-cell activation. After capturing antigen in the tissues, dendritic cells usually migrate to various lymphoid organs where they present the antigen to lymphocytes. Entrapment of dendritic cells at the fetal maternal interface is therefore an important mechanism by which the alloantigen (fetus and placenta) can escape the T cell response.

In human, HLA class II molecules are immunogenic cell surface markers associated with allogeneic transplant graft rejection (Ober, 1998); thus prevention of direct antigen presentation may not effectively avoid fetal rejection. Fetal derived trophoblast cells have unique patterns of HLA expression in comparison to other nucleated cells. These trophoblasts, which are in contact with the maternal immune system, do not express HLA-A and HLA-B (HLA class I gene), or HLA-DR, HLA-DQ and HLA-DP (HLA class II genes) (Hunt et al., 1987,

Mattsson, 1998, Ober, 1998, Rizzo et al., 2011). Instead these cells express HLA-G, a non-classical class I molecule, and also low levels of HLA-C, HLA-E and HLA-F (Ishitani et al., 2003).

Although there is a lack of major histocompatibility complex (MHC) molecules expression in the trophoblasts, maternal antibodies against paternally derived HLA expressed by the fetus are detectable in pregnancies. The maternal immune system is probably sensitised by fetal nucleated cells that have escaped into the maternal circulation. Paradoxically, incompatibility of HLA expression between the parents is thought to be beneficial for pregnancies. In prospective and retrospective studies, HLA-A and HLA-B matched couples were observed to have higher miscarriage rates (Schacter et al., 1979, Ober, 1998). In pregnant subjects with rheumatoid arthritis (RA), women with pregnancy-induced amelioration of their RA had more maternal-fetal disparities in the alleles at HLA-DRB1, HLA-DQB1 and HLA-DQA1 loci, compared with pregnancies affected by active RA (Nelson et al., 1993). These observations suggest increased variability of HLA expressions in the offspring may have an important role in immunomodulation during pregnancy. The exact mechanism of this process is yet to be explored.

HLA-G is strongly expressed during pregnancy. It was initially detected only in fetal cells at the maternal-fetal interface, but expression was later found in thymus, cornea, erythroid and blood cells, and also in non-physiological environment in transplantation, cancer, infections and autoimmunity (Rizzo et al., 2011). HLA-G is a HLA gene that has an intron-exon structure identical to other class I genes, with a premature stop in exon 6 resulting in a much shorter cytoplasmic tail with six amino acids (RKKSSD) (Park et al., 2001). The truncated tail lost its potential endocytosis signals found in the cytoplasmic tail with a tyrosine or dileucine-based motif in all other MHC class I molecules. This results in a slower turnover and prolonged expression of HLA-G at the cell surface, and a diminished retrieval of this molecule upon assembly with high affinity peptides; HLA-G is not an efficient molecule to present exogenous peptides (Park et al., 2001). Due to this characteristic, it is thought this molecule's main function is in immunomodulation. HLA-G is presented in many different transmembrane and soluble isoforms due to alternative splicing; in the soluble

forms, transmembrane and cytoplasmic domains are absent in the molecules (Ober, 1998).

HLA-G has been found to suppress the proliferation and cytotoxic ability of T cells and natural killer (NK) cells. Through its ability (HLA-G5 isoform) to induce the differentiation of T cells into regulatory T cells (Treg), it may also be responsible for better graft acceptance (Le Rond et al., 2006). In another experiment, HLA-G1 transfected antigen-presenting cells (APCs) were capable of inhibiting the proliferation and induce anergy of $CD4^+$ T cells and providing non-antigen specific, inhibitory or proapoptotic signals (LeMaoult et al., 2004). Soluble HLA-G can induce apoptosis in $CD8^+$ T cells, possibly via the Fas ligand (FasL) pathway (Contini et al., 2003). In human placenta, HLA-E is found to be co-expressed in all cells that express HLA-G. It is thought that HLA-G and HLA-E act synergistically, binding to CD94/NKG2 receptor on NK cells, leading to their inhibition (Ishitani et al., 2003). In the context of in vitro fertilisation in assisted reproductive treatment, HLA-G expression was associated with better quality embryos with higher cleavage rates; pregnancy rates were better when their sibling embryos from the same treatment cycle were replaced (Jurisicova et al., 1996a, Jurisicova et al., 1996b).

1.5.2 The role of regulatory T cells (Treg) in pregnancy

Balance between the subtypes of CD4+ helper T cells is one of the classic models described in immunohomeostasis in pregnancy. CD4+ T cells can be classified into Th1 cells, which are involved in cellular immunity; Th2 cells, which are involved in humoral immunity; Th3 cells, which produce immunosuppressive cytokine transforming growth factor (TGF)-ß; Treg 1 cells, which produce immunosuppressive cytokine interleukin (IL)-10; and also $CD4^+CD25^+$ regulatory T cells ($CD4^+CD25^+$ Treg) (Saito et al., 2007). Other Th subsets have also been described more recently (e.g. Th17 cells). Traditionally the model of Th1/Th2 shift has been used in pregnancy, where successful pregnancy was believed to be a Th2 phenomenon; this model is now thought to be an oversimplification (Chaouat, 2007). The role of immunoactivation is played by Th1 and Th2 cells, while Th3 and Treg 1 cells are responsible for immunoregulation (Saito et al., 2007).

Recent studies discovered that $CD4^+CD25^+$ Treg is essential in maintaining tolerance of semi-allogeneic fetus in mouse. These cells are increased significantly during pregnancy. This phenomenon occurs in the conception of both syngeneic and semi-allogeneic fetuses, thus is independent of the exposure of paternal alloantigen (Aluvihare et al., 2004). Mice depleted of $CD4^+CD25^+$ Treg carrying semi-allogeneic fetuses are shown to have no successful pregnancy, while 50% of those carrying syngeneic fetuses had normal pregnancies (Aluvihare et al., 2004). In vitro, $CD4^+CD25^+$ Treg transfer has been shown to inhibit the proliferation and secretion of interferon-γ by lymphocytes from the spleen and decidua; in vivo it prevents fetal rejection in mice prone to abortion, produced by mating CBA/J females with DBA/2J males resulting in the initial abortion rate of 18% (Zenclussen et al., 2005). These results confirmed that $CD4^+CD25^+$ Treg have an important role in protecting fetuses in mice.

In human, systemic $CD4^+CD25^+$ Treg level is increased in pregnancy. It starts to elevate from the early gestational period, peaks during the second trimester, and declines after delivery (Somerset et al., 2004). A few theories of the regulation of $CD4^+CD25^+$ Treg in pregnancy have been presented. $CD4^+CD25^+$ Treg expresses chemokine receptor CCR4 (Curiel et al., 2004). CCR4 has two ligands, CCL17 and CCL22, which are known to be secreted by the maternal and fetal tissues in pregnancy. These chemokines may be responsible to attract Treg cells to the decidua, similar to the mechanism of Treg being attracted to tumours secreting CCL22 (Curiel et al., 2004). In a different study, the authors discovered oestrogen treatment increased the expression of Foxp3 in vivo and in vitro (Polanczyk et al., 2004). Foxp3 is a transcription factor that controls the phenotype and function of Treg, it is also a reliable marker for $CD4^+CD25^+$ Treg cells (Fontenot et al., 2003).

Collectively the above findings suggest pregnancy upregulates and attracts $CD4^+CD25^+$ Treg cells locally to modulate the maternal immune system. Recent observations suggest in human $CD4^+CD25^+$ Treg can be subgrouped into $CD4^+CD25^{high}$ and $CD4^+CD25^{low}$; $CD4^+CD25^{high}$ Treg has a strong immunoregulatory role, and should be studied specifically to ascertain the role of $CD4^+CD25^+$ Treg in pregnancy (Saito et al., 2005, Saito et al., 2007).

1.5.3 Uterine natural killer (uNK) cells

As part of the innate immune response, natural killer (NK) cells are bone marrow-derived lymphocytes that are able to secrete cytokines and kill target cells without prior sensitisation. This characteristic gives NK cells important roles in tumour immunity, host defence against intracellular pathogens, rejection of bone marrow transplants, and the development of acquired immunity through the production of specific cytokines (Riley and Yokoyama, 2008). During the first trimester of human pregnancy, more than 75% of the immune cells in the decidua are uterine natural killer (uNK) cells, a subset of NK cells with the cell surface phenotype of $CD56^{bright}/CD16^{-}$ (Bulmer et al., 1991, Moffett-King, 2002). In the periphery this subset only makes up 10% of the total number of peripheral blood NK (pNK) cells (Cooper et al., 2001). $CD56^{bright}/CD16^{-}$ NK cells produce abundant cytokines following activation by monocytes/macrophages, but have low cytotoxicity. When macrophages encounter pathogens as part of the innate immune response, they produce monocyte-derived cytokines (monokines) such as IL-12 and IL-15. When activated by these monokines, $CD56^{bright}/CD16^{-}$ NK cells produce much more interferon γ (IFN-γ) compared with $CD56^{dim}$ NK cell subset. The IFN-γ released by $CD56^{bright}/CD16^{-}$ NK cells is requisite for the elimination of the pathogens, it also elicits a positive feedback response resulting in further release of monokines from the monocytes (Cooper et al., 2001).

Comparison of uNK and $CD56^{bright}/CD16^{-}$ pNK cells showed differences in the expression of 278 genes, the majority of which encode surface proteins (Koopman et al., 2003). uNK cells in first trimester gravid uterus have also been found to be distinctive from the uNK cells in non-pregnant cycling endometrium (Kopcow et al., 2010). uNK cells in pregnancy (decidual NK) preferentially express cholesterol 25-hydroxylase, which may affect the synthesis of cholesterol and steroid hormones in the decidua (Kopcow et al., 2010). Other decidual NK cells specific molecules may have immunomodulatory functions during pregnancy, for example CCL4, interleukin 16 and CD9 (Koopman et al., 2003, Kopcow et al., 2010). These findings suggest uNK are specialised cells, playing an important role during pregnancy.

The receptors on uNK cells can be classed as activating (for example NKp46, NKp44, NKp30, NKG2d, and 2B4) or inhibitory (for example LIR-1, KIR2DL4, and CD94/NKG2A) (Bulmer et al., 2010). During pregnancy, the expression of KIR2D on uNK cells is upregulated (Verma et al., 1997, Sharkey et al., 2008, Male et al., 2011). The KIR2D receptor recognises maternal and fetal HLA-C, which is expressed on extravillous trophoblasts and uterine stromal cells when the endometrium transforms into decidua in pregnancy (King et al., 2000, Chazara et al., 2011, Male et al., 2011). This pregnancy related transformation biases uNK cells towards HLA-C interaction, which appears to regulate trophoblast invasion and vascular remodelling (Hanna et al., 2006, Lash et al., 2006, Male et al., 2011). The pattern of expression of KIR and HLA-C are highly polymorphic. While KIR2DL4, KIR3DL2 and KIR3DL3 are present in all individuals, the expression of other KIRs is variable (Nowak et al., 2011). Two different haplotypes are commonly described: “A” haplotypes consist of seven mostly inhibitory KIR genes, while “B” haplotypes have additional activating KIR genes in addition to the inhibitory ones; HLA-C is classified to C1 and C2 allotypes based on a dimorphism at position 80, each of these allotypes binds to different sets of KIRs with different affinities (Male et al., 2011). It is thought that the combination of different maternal and fetal KIR and HLA-C variants can affect the depth of placentation and the outcome of pregnancy (Hiby et al., 2004, Hiby et al., 2008, Hiby et al., 2010, Male et al., 2011). Women with KIR AA genotype have an increased risk of adverse pregnancy outcome, particularly if this is combined with certain maternal and fetal HLA-C genotypes (Hiby et al., 2010, Nowak et al., 2011).

As mentioned above, it is believed CD94/NKG2A reacts with HLA-G and HLA-E leading to the inhibition of uNK cells. Binding of HLA-G to KIR2DL4 on uNK cells led to the production of cytokine IFN-γ, which may have roles of controlling the invasion of trophoblasts, or modulating inflammation at the fetal-maternal interface (Rajagopalan et al., 2001, Hunt et al., 2005, Hu et al., 2006).

uNK cells also secrete many other different cytokines, some of which were found to stimulate (CXCL8 and CXCL10) or inhibit (TNF-α, TGF-ß1 and IFN-γ) trophoblast invasion (Bulmer et al., 2010). It was demonstrated that differences in gestational age affect the pattern of cytokines release from uNK cells (Lash et al., 2006, Bulmer et al., 2010). In theory, perhaps the cytokines produced by

uNK cells also differ depending on their location. This in turn can control the process of trophoblasts invasion up to the precise depth required. In human, research of uNK cells in pathological pregnancy has produced inconsistent results (Zenclussen et al., 2001, Bulmer et al., 2010). However, there is some evidence that an increased abundance of uNK cells in mid-secretory phase endometrium is linked to recurrent miscarriage, and is predictive of future miscarriage in subsequent pregnancy; severe IUGR and pre-eclampsia have also been associated with an alteration in the number of uNK cells in the decidua (Quenby et al., 1999, Eide et al., 2006, Bulmer et al., 2010).

1.5.4 Decidual macrophages

Macrophages are the second most abundant leukocytes in the decidua next to uNK cells. They represent 20% of white blood cells in the maternal-fetal interface during pregnancy (Lessin et al., 1988). In general, functionally polarised macrophages can be broadly grouped as classically activated, M1, or alternatively activated, M2 (Mantovani et al., 2004, Rozner et al., 2011). M1 has cytotoxic property, and usually responds to inflammatory stimuli; M2 is more involved in immunoregulatory processes, and also tissue remodelling and regeneration. Studies suggested macrophages in the decidua are distinctive subsets of cells, not fitting in the conventional pro-inflammatory (M1) or anti-inflammatory (M2) macrophages (Houser et al., 2011). Phenotypically, most of the decidual macrophages express CD14, with about 70% expresses C-type lectin CD209 (DC-SIGN) (Kammerer et al., 2003). CD14 is frequently used as a marker for the identification of decidual macrophages (Bulmer et al., 2010). The role of macrophages during placentation is not fully understood. Decidual macrophages constitutively produce abundant IL-10 and CCL18, suggesting their characteristic is closer to M2 (Lidstrom et al., 2003, Gustafsson et al., 2008, Erlebacher, 2013). Contradictorily, in vitro they have been shown to induce pro-inflammatory cytokines such as IL-6 and TNF-α with LPS stimulation (Li et al., 2009, Erlebacher, 2013). One study comparing the cells of Rhesus Monkey showed that decidual macrophages release higher level of CCL3 and CCL4, and same level of CCL2 and CXCL8 comparing to peripheral blood monocyte-derived macrophages (Rozner et al., 2011). Helige et al. revealed decidual macrophages have the ability to restrained uNK cells from killing extravillous cytotrophoblasts, controlled by a TGF-β dependent mechanism (Helige et al., 2013). There has

been some interest in studying the functional roles of the two separate groups of decidual macrophages: $CD209^{+}CD11C^{LO}$ macrophages and $CD209^{-}CD11C^{HI}$ macrophages (Houser et al., 2011, Erlebacher, 2013). As mentioned above, majority (~70%) of the macrophages consists of the earlier group. $CD209^{-}CD11C^{HI}$ macrophages are able to process protein antigen, and are believed to be the major antigen-presenting cells (APCs) in the decidua (Houser et al., 2011, Houser, 2012). They are not known to migrate to the draining lymph nodes of the decidua, thus provide the advantage of avoiding immune recognition by T cells. The lack of DCs in the decidua suggests that $CD209^{-}CD11C^{HI}$ decidual macrophages may be the most important APCs during placentation.

1.5.5 B7 family T-cell co-stimulatory molecules

There has been some research interest into the role B7 family of co-stimulatory molecules in regulating immune responses in pregnancy. Based on the two-signal model of T-cell activation, APCs interact with T cells by presenting the antigen associated with MHC, for ligation to the T-cell receptor (TCR) (first signal). A second co-stimulatory signalling between these two cells is provided by the co-stimulatory B7 receptors. This set of receptors regulates the immune response by their stimulatory or inhibitory effects upon binding to their ligands. B7-1 (CD80) and B7-2 (CD86) were expressed by cultured human decidual stromal cells, and the cells were able to stimulate allogenic T cells in vitro (Olivares et al., 1997). In vivo studies revealed that blockade of these receptors at the time of implantation inhibits maternal rejection of the allogenic fetuses in abortion prone mouse matings (Jin et al., 2005). At the fetal-maternal interface, inhibitory co-stimulatory receptors were also detected. Cytotoxic T-lymphocyte-associated protein 4 (CTLA-4), a negative regulator of T cell activation was detected on human placental fibroblasts throughout gestation (Kaufman et al., 1999). Paradoxically women with spontaneous miscarriage had a higher expression of this molecule. Recurrent miscarriage was associated with a higher ratio of expression of CTLA-4 to CD28, another co-stimulatory receptor, suggesting a more complex mechanism of action (Wang et al., 2006b). The programme death-1 (PD-1) receptor, as its name suggest, has the character of initiating inhibitory pathway (Khoury and Sayegh, 2004). Its ligands, PDL1 and PDL2, were detected in human trophoblasts and mouse placenta (Petroff et al.,

2003, Guleria et al., 2005). Blockade of PDL1 signalling was shown to result in rejection of allogeneic, but not syngeneic, concepti (Guleria et al., 2005).

1.5.6 Other modulating pathways

Complement regulatory proteins such as decay-accelerating factor (DAF, CD55), membrane cofactor protein (MCP, CD46) and CD59 were detected in human placenta from 6 weeks gestation until term (Holmes et al., 1992). The importance of these proteins was shown in the phenotype of mouse pregnancies in a study (Xu et al., 2000). Mouse *Crry* is a complement regulatory protein that controls C3 activation, like human DAF and MCP (Xu et al., 2000). Survival of *Crry*$^{-/-}$ mouse embryos was compromised, caused by C3 complement deposition resulting in placenta inflammation. The lethality of *Crry*$^{-/-}$ embryos was rescued by breeding to C3$^{-/-}$ phenotype, confirming the pathway of this protein in the regulation of fetal-maternal tolerance.

Other immunomodulatory models being studied in pregnancies include macrophage migration inhibitory factor (MIF), a cytokine being expressed at the fetal-maternal interface (Arcuri et al., 2001). MIF regulates innate and adaptive immunity by affecting the trafficking and behaviour of macrophages and lymphocytes (Vigano et al., 2007). During pregnancy, MIF is thought to play a role in modulating trophoblastic invasion of the decidua by regulating cytolytic activity of NK cells; and secondly by controlling macrophages trafficking in the placental bed (Vigano et al., 2007). Elevated level of MIF has been observed in patients with pre-eclampsia, supporting the role of aberrant inflammatory process involved in this pathological process (Todros et al., 2005). Recurrent miscarriage was associated with suppressed level of MIF (Yamada et al., 2003).

Collectively, these various studies have shown that during implantation, the interaction of the decidua with the semi-allogeneic embryo involves complex immunological pathways. A healthy immuno-regulatory environment is crucial to ensure a successful pregnancy. The evidence strongly suggests the presence of specialised leukocytes in the decidua is necessary during implantation. The trafficking of leukocytes to the organs in the body is highly dependent on chemoattractants. The family of chemokines is one of the most important groups

of chemoattractants; this group of proteins, and their receptors are explored in more details in the next section.

1.6 Chemokines and their receptors

1.6.1 Introduction to chemokines

Chemokines, a large family of chemotactic cytokines, are small secreted proteins (Calderon et al., 2005). They are essential for the chemoattraction and activation of leukocytes and other type of cells, with a role to selectively moving subsets of these cells into, and between, microanatomical domains within tissues (Mackay, 2001). A cysteine motif in the N-terminal region of the mature chemokine molecule is highly conserved and adopts distinct arrangements that are used to classify chemokines into four subgroups: C chemokines, CC chemokines, CXC chemokines, and CX_3C chemokines (Bacon et al., 2002, Calderon et al., 2005). In C chemokines there is only one cysteine residue in the N-terminal region; in CC chemokines two cysteine residues are directly juxtaposed; in CXC chemokines the two cysteine residues are separated by a non-conserved amino acid; and in CX_3C chemokines three amino acids separate the cysteine residues (Fig 1.3) (Zlotnik and Yoshie, 2000, Bacon et al., 2002). The cysteine residues are involved in forming disulphide bonds in the mature protein that maintain the structure of the protein. Chemokines act by binding to their G protein-coupled receptors on the surface of the target cells. The N-terminal tail of the chemokine is important in receptor activation, whilst the body of the chemokine mediates initial tethering of the chemokine to the receptor. Other determinants, particularly at the C-terminus, are involved in mediating interactions with extracellular matrix components, including glycosaminoglycans, and this is important for the function of chemokines in vivo. A two-step model has been described for the activation of chemokine receptors: after the initial binding of the body of the chemokine to the receptor (first step), the chemokine undergoes conformational change due to the flexible N-terminal tail (second step) (Fernandez and Lolis, 2002). The receptor is activated by the N-terminus of the chemokine following the conformational change, leading to the exchange of bound GDP to GTP in the α subunit of the G proteins. Subsequently, the G proteins dissociate from the receptor and trigger a cascade of signalling events within the cytoplasm of the cell (Fig 1.4). In relation

to leukocyte trafficking, each chemokine attracts a distinctive set of white blood cells (Le et al., 2004). Generally CC chemokines attract mononuclear cells, eosinophils and basophils; C chemokines attract T cells; CX_3CL1 is chemotactic to T cells, natural killer cells and monocytes. The CXC group of chemokines are further subclassified into ELR^+ and ELR^-, depending on the presence of a triplet amino aced motif (Glu-Leu-Arg) that precedes the first cysteine residue in the primary amino acid sequence of the chemokines. ELR^+ CXC chemokines have angiogenic property and attract neutrophil, while the ELR^- group is angiostatic and attracts lymphocytes (Le et al., 2004). CXCL12 is an exception, it is an angiogenic ELR^- CXC chemokine (Salcedo et al., 1999, Le et al., 2004).

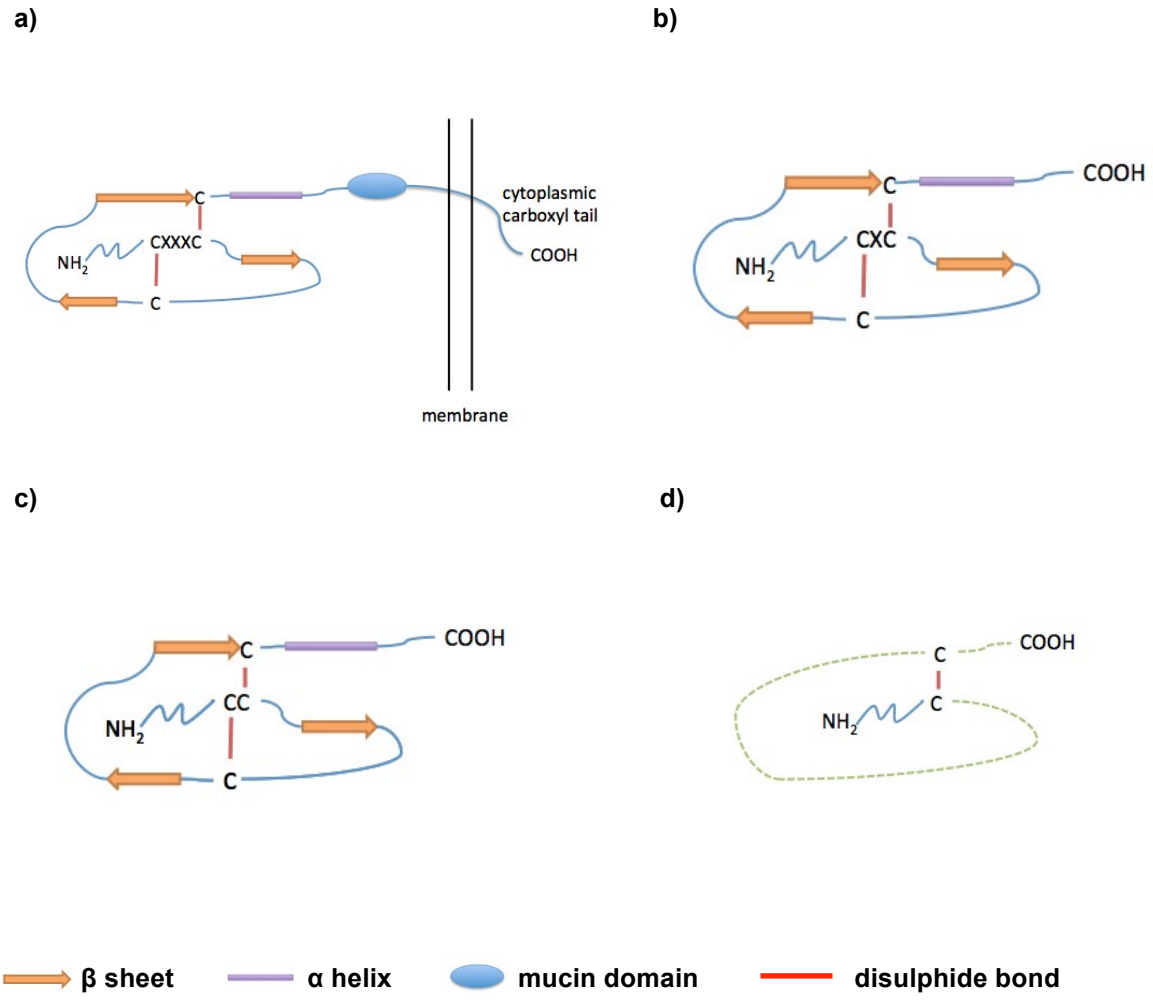

Figure 1.3 **Schematic illustrations of the major secondary structural motifs of the four chemokine subfamilies.** a) CX_3C chemokine, CX_3CL1 can occur as a transmembrane protein as shown, or after cleavage forming a soluble form; b) CXC chemokine; CXCL16, similar to CX_3CL1 as described above, is also produced as a transmembrane form that can be cleaved to be released as a soluble form; c) CC chemokine; d) C chemokine, depicted with dotted line as structure not fully known. Adapted from (Frederick and Clayman, 2001).

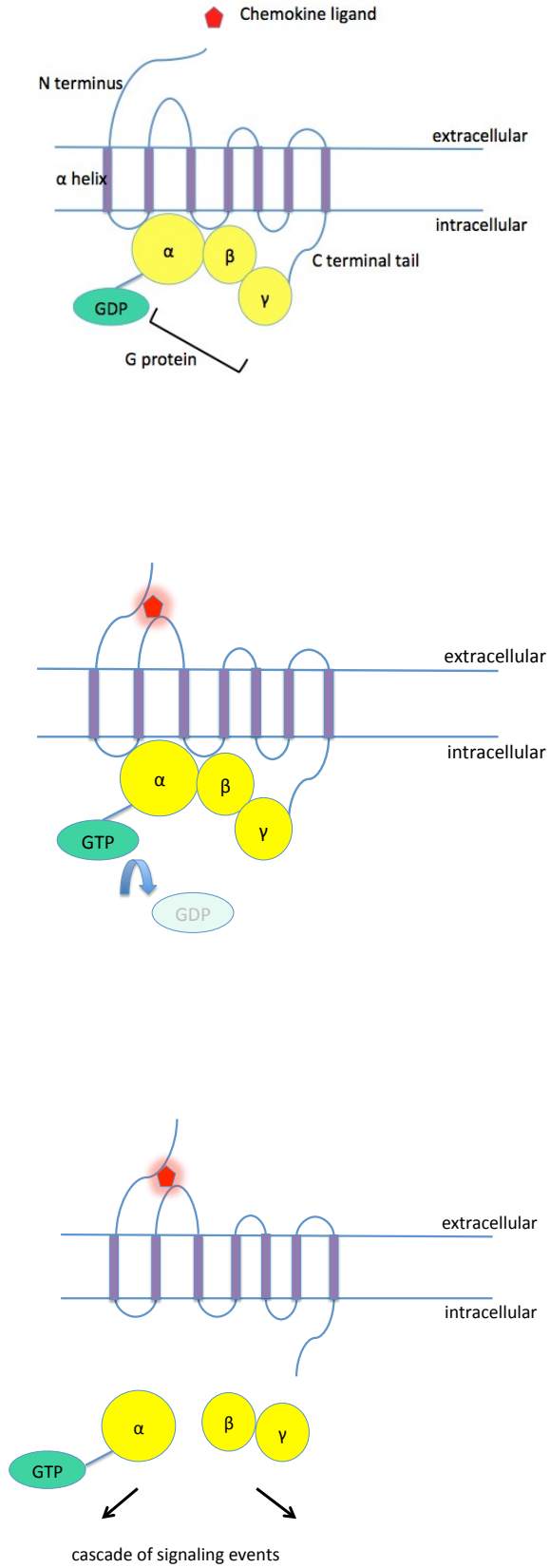

Figure 1.4 Structure and function of G protein coupled chemokine receptor. Interaction of chemokine ligand results in the exchange of GTP for GDP in the α subunit of the G protein. This dissociates the heterotrimeric G protein complex from the receptor into an α monomer and a β/γ dimer, triggering a cascade of signalling events. Information from (Fernandez and Lolis, 2002).

The production, localisation and destruction of chemokines are finely regulated by spatial and temporal controls (Comerford et al., 2007, Rodriguez-Sanabria et al., 2010). Chemokines are characterised as being either inflammatory or homeostatic. Inflammatory chemokines e.g. CCL3 are released in response to inflammatory stimulus, and they usually have rapid local effects and are short lived (Hannan and Salamonsen, 2007). Pathological conditions such as rheumatoid arthritis and airway inflammation have been associated with dysfunctional expression of inflammatory chemokines (Fox and Pease, 2005). Homeostatic chemokines are expressed constitutively for physiological maintenance of cells and tissues. For example CCL19 and CCL21 coordinate thymocyte trafficking within the thymus, and also control entry of T cells into, and movement within lymph nodes (Charo and Ransohoff, 2006, Teng et al., 2011). The distinction of chemokines for their inflammatory or homeostatic roles is not absolute, as some chemokines can have both characters (Fox and Pease, 2005), depending on the space and time of their release. The effects of chemokines locally and systematically are targeted and precise, but the mechanisms of their action can be very complex. In the process of cell signalling, chemokines have promiscuous interactions with the target cells; a responsive cell will usually have multiple receptors for different chemokines, and no chemokine is solely active on one leukocyte population (Borroni et al., 2008). When required chemokines exert their influence multi-dimensionally, by binding to different receptors they selectively recruit specific populations of cell types. As a consequence, chemokines are known to play major roles in the biological functions of lymphoid trafficking, lymphoid organ development, wound healing, Th1/Th2 development, angiogenesis/angiostasis, metastasis, cell recruitment, and inflammation (Table 1.2) (Rossi and Zlotnik, 2003).

Receptor	Chemokine ligands	Examples of physiological functions and pathological connections
CCR		
CCR1	CCL3 CCL5 CCL7 CCL14	RA; MS
CCR2	CCL2 CCL7 CCL8 CCL13 CCL16	atherosclerosis; RA; MS; resistance to intracellular pathogens; type 2 DM
CCR3	CCL5 CCL7 CCL8 CCL11 CCL13 CCL26 CCL28	allergic asthma & rhinitis
CCR4	CCL17 CCL22	parasitic infection; graft rejection; T-cell homing to skin
CCR5	CCL2 CCL3 CCL4 CCL5 CCL7 CCL8 CCL11 CCL13 CCL14 CCL16	transplant rejection
CCR6	CCL20	mucosal humoral immunity; allergic asthma; intestinal T-cell homing
CCR7	CCL19 CCL21	transport of T cells & dendritic cells to lymph node; antigen presentation; cellular immunity; T cells development in thymus
CCR8	CCL1	dendritic-cell migration to lymph node; type 2 cellular immunity; granuloma formation
CCR9	CCL25	homing of T cells & IgA+ plasma cells to the intestine; IBD; T cells development in thymus
CCR10	CCL27 CCL28	T-cell homing to intestine & skin
CXCR		
CXCR1	CXCL6 CXCL8	inflammatory lung disease; COPD
CXCR2	CXCL1 CXCL2 CXCL3 CXCL5 CXCL6 CXCL8	inflammatory lung disease; COPD; angiogenic for tumour growth; improvement of neutrophil homing
CXCR3-A	CXCL9 CXCL10 CXCL11	inflammatory skin disease; MS; transplant rejection; T cell homing to

		virally infected tissue
CXCR3-B	CXCL4 CXCL9 CXCL10 CXCL11	angiostatic for tumour growth
CXCR4	CXCL12	HIV-1 coreceptor (T-cell-tropic); tumour metastases; haematopoiesis; blood vessels, brain and heart development
CXCR5	CXCL13	formation of B-cell follicles; formation of lymph nodes and Peyer's patches
CXCR6	CXCL16	inflammatory liver disease; atherosclerosis
CX_3CR		
CX_3CR1	CX_3CL1	atherosclerosis
XCR		
XCR1	XCL1	RA; IgA nephropathy; tumour response

Table 1.2 Human chemokine receptors, their ligands, and involvement in physiological and pathological processes. RA: rheumatoid arthritis; MS: multiple sclerosis; DM: diabetes mellitus; IBD: inflammatory bowel disease; COPD: chronic obstructive pulmonary disease. Adapted from (Charo and Ransohoff, 2006), with updated information from (Bachelerie et al., 2014).

1.6.2 Chemokine receptors

Chemokine receptors are members of the G-protein-coupled receptors (GPCRs) superfamily. Their length ranges from 340 to 370 amino acids in general (Calderon et al., 2005). They display seven sequences of 20-25 hydrophobic residues that form α-helices that span the plasma membrane; an extracellular N-terminus; three extracellular loops; three intracellular domains; and an intracellular C-terminal tail that contains numerous serines and threonines that become phosphorylated upon ligand binding to the receptor (Fig 1.4) (Calderon et al., 2005, Valles and Domínguez, 2006). As described earlier, binding of chemokines leads to dissociation of G proteins from the receptors. The target cells, utilising their surface receptors, gather information about the chemokines present and respond accordingly. The signalling cascades can result in

cytoskeletal reorganisation, integrin activation, and other processes that lead to increased cellular adhesion, migration and activation (Calderon et al., 2005). Mutational analyses of chemokine receptors have identified the specific regions that react with the ligands. It is believed that the chemokine binding and receptor activation sites are not the same; binding sites are spread throughout the polypeptide (Fernandez and Lolis, 2002). The activity of some chemokine receptors is also affected by post-translational modifications, for example sulfation of tyrosines in CCR5 is essential for the receptor to function effectively (Farzan et al., 1999, Fernandez and Lolis, 2002).

Chemokine receptors are subdivided into groups depending on the subclass of chemokine that they typically bind to. Thus there are 10 CC chemokine receptors (CCR), six CXC chemokine receptors (CXCR), and one receptor each for CX_3CL1 and XCL1, termed CX_3CR1 and XCR1, respectively. Chemokines interact with their subgroup of receptors with considerable promiscuity. Most receptors bind to multiple ligands and most ligands interact with more than one receptor (Zlotnik and Yoshie, 2000, Mackay, 2001, Murphy, 2002). This is particularly prominent amongst chemokines and their receptors that are involved in controlling leukocyte migration during inflammation. It is thought that this brings flexibility and robustness to inflammatory responses. Pathogens, including viruses, bacteria and parasites have evolved ways of trying to subvert inflammatory chemokine networks and so receptor/ligand promiscuity may help ensure that leukocytes can still be recruited to infected tissues even if some of the components of the chemokine network have been subverted. Chemokine receptors have been detected on cancer and human immunodeficiency virus (HIV), thus they have received considerable attention in the search of therapeutic targets for these diseases (Frederick and Clayman, 2001).

1.6.3 Role of chemokines in diseases

The expression of chemokines has been studied in various disease models. The following sections provide a few examples of the role of chemokines in diseases.

1.6.3.1 Inflammatory diseases

A number of chemokines promote infiltration and activation of specific leukocytes into injured or infected tissues in acute and chronic inflammatory conditions. This process is necessary for the removal of foreign microbial invaders, and also dead cells in would repair (Le et al., 2004). In sepsis, CC chemokines, for example CCL3 and CCL5, exert their pro-inflammatory effect by regulating organ specific leukocyte influx (Standiford et al., 1995, VanOtteren et al., 1995, Le et al., 2004). In mouse, overexpression of CXCL1 in the lung has been shown to provide resistance to Klebsiella pneumonia (Tsai et al., 1998). CCL2 and CCL22 protect mice from lethality in peritoneal sepsis (Matsukawa et al., 1999, Matsukawa et al., 2000). Not all chemokines are protective in infection. In the case of fulminant hepatic failure induced by Propionibacterium acnes in mice, CCL17 can markedly worsen liver damage by recruiting $CCR4^+$ $CD4^+$ T cells (Yoneyama et al., 1998, Le et al., 2004). Interestingly, dysregulation of chemokine expression has also been implicated in a range of inflammatory disorders.

In asthma, it is thought that the airway epithelial cells and macrophages release chemokines to attract mainly eosinophils, and also other asthma-related leukocytes such as basophils and Th2 lymphocytes (Lukacs, 2001). CCL5, CCL7 and CCL13 have been detected in the airways of asthmatics (Wang et al., 1996, Lamkhioued et al., 2000). These are ligands for CCR3, which is highly expressed on eosinophils (Stellato et al., 1997). High levels of CCL2, CCL3 and CCL5 were associated with status asthmaticus, a life-threatening form of severe asthma (Tillie-Leblond et al., 2000, Lukacs, 2001). In patients with chronic obstructive pulmonary disease (COPD), CXCL8 and CXCL10 levels are increased, correlating with the infiltration of T cells expressing CXCR3, which is the receptor for CXCL10 (Saetta et al., 2002). Neutralisation of CXCL10 seems to depress allergic airway inflammation (Medoff et al., 2002).

In rheumatoid arthritis, high concentration of CXCL1, CXCL5 and CXCL8 were detected in the sera, synovial fluids and synovial tissues, believed to be responsible for promoting angiogenesis and the recruitment of neutrophils to the joints (Szekanecz et al., 2009). Abundant CCL2, CCL3 and CCL5 have also been found in the tissues; these chemokines are chemoattractants to monocytes (Le

et al., 2004). CXCL12 is also present, and is believed to recruit CXCR4-expressing CD4 memory T cells (Nanki et al., 2000). The chemokine may also block T cells from activation-induced apoptosis, and also induce the migration of dendritic cells from the blood stream into the local area (Le et al., 2004).

The role of chemokines in other inflammatory diseases has been studied. In animal models of acute glomerular or tubule-interstitial disease, CCL2, CCL3, CCL4 and CCL5 are expressed only in the diseased compartment of the kidney (Anders et al., 2003). Inhibition of CCL2 and CX_3CR1 in rats, and also CCL5 in mice has been shown to reduce leukocyte infiltration, resulting in the improvement of renal function (Lloyd et al., 1997, Wenzel et al., 1997, Feng et al., 1999, Anders et al., 2003). In patients with active Crohn's disease, mucosal biopsies showed a correlation of the expression of CXCL8 mRNA with clinical disease activity (Stallmach et al., 2004). Experiments using biopsies from inflammatory skin diseases including lichen planus and psoriasis demonstrated recruitment and maintenance of CXCR3 expressing T cells into the local area, regulated by the expression of CXCL9, CXCL10 and CXCL11 (Flier et al., 2001).

1.6.3.2 Multiple sclerosis (MS)

Multiple sclerosis (MS) is a chronic inflammatory demyelinating disorder of the central nervous system. It is associated with immune cells infiltration which consist of 10% $CD4^+$ and $CD8^+$ T cells, and 90% macrophages derived from infiltrating monocytes and resident microglia (Traugott et al., 1983, Charo and Ransohoff, 2006). The T cells express CCR5 and CXCR3; CCR7 expression in these activated effector cells is down-regulated (Balashov et al., 1999, Kivisakk et al., 2004). Infiltrating monocytes express CCR1, CCR2 and CCR5 (Simpson et al., 2000, Trebst et al., 2001). These monocytes down-regulate CCR1 when they mature into phagocytic macrophages in the later stages of MS (Trebst et al., 2001). The ligands for these receptors (CCL2, CCL3, CCL4, CCL5, CCL8 and CXCL10) were detected in the lesions of multiple sclerosis (Charo and Ransohoff, 2006). In animals, the model related to MS is autoimmune encephalomyelitis (EAE). This condition has similar pattern of chemokine expression as MS; expression of CCL2, CCL3, CCL4, CCL5 and CXCL10 is positively correlates with the severity of the disease (Godiska et al., 1995). Neutralising antibodies to

some of these chemokines can either inhibit the onset, or attenuate the severity of EAE (Karpus and Kennedy, 1997, Liu et al., 2001).

1.6.3.3 Atherosclerosis

The pathogenesis of atherosclerosis involves chronic inflammation of arterial blood vessels, characterised by accumulation of leukocytes, smooth muscle cells and lipids within the vessel wall (Ross, 1993, Reape and Groot, 1999, Calderon et al., 2005). The formation of fatty streaks, which consists of lipid-laden macrophages (foam cells), is the hallmark of early atherosclerotic lesions (Charo and Ransohoff, 2006). The expression of CCL2, CXCL8, CXCL12 and CX_3CL1 has been associated with atherosclerosis. Expression of CCL2 is increased in human atherosclerotic plaques (Nelken et al., 1991). Production of CCL2 in endothelial and smooth-muscle cells is induced by the presence of minimally oxidised low-density lipoprotein (LDL) cholesterol (Nelken et al., 1991). It is believed that CCL2 recruits foam cells into the vessel wall (Boring et al., 1998, Charo and Ransohoff, 2006). This chemokine has also been shown to enhance vascular smooth muscle proliferation in the presence of serotonin, a vasoconstrictor released by aggregated platelets (Watanabe et al., 2001). High level of serotonin is expressed in the coronary sinus of patients with coronary arterial disease (Rubanyl et al., 1987). In addition, CCL2 enhances the production of tissue factor by smooth muscle cells; tissue factor initiates the process of coagulation, and may play a role in the formation of thrombus and contribute to plaque instability (Schecter et al., 1997). In mice, deletion of CCL2 reduces the risk of diet-induced atherosclerosis (Gosling et al., 1999). In mice with apolipoprotein E deficiency ($ApoE^{-/-}$) which were fed with a high-fat diet, the deletion of CCR2 prevented macrophage accumulation and the formation of atherosclerosis (Boring et al., 1998). In contrast, the lack of CCR5, which is the receptor for CCL3, CCL4 and CCL5, in mice does not change their vulnerability to atherosclerosis (Kuziel et al., 2003). In human, the transcription of CCL2 gene is enhanced by a polymorphism in the promoter of CCL2, with the substitution of G for A at position -2518 (Rovin et al., 1999). Individuals who are homozygous for this polymorphism have an increased risk for conorary arterial disease (Szalai et al., 2001). CXCL8 is another chemokine with an increased expression in human atherosclerotic plaques (Wang et al., 1996). Similar to CCL2, CXCL8 and its receptor CXCR2 have been linked to macrophage recruitment to atherosclerotic

lesions (Boisvert et al., 1998). In addition, CXCL8 also induces vascular smooth muscle cells proliferation and migration (Yue et al., 1994). CXCL12, on the other hand, induces platelet aggregation and activation, and is believed to promote thrombus formation during plaque rupture and vessel occlusion (Abi-Younes et al., 2000, Calderon et al., 2005). CXCL12 is highly expressed by smooth muscle cells, endothelial cells and macrophages in human atherosclerotic plaques (Abi-Younes et al., 2000). The CX_3CL1 chemokine is found in human atherosclerotic lesions that contain high numbers of macrophages (Greaves et al., 2001). Genetic variation of its receptor CX_3CR1 results in a decreased number of CX_3CL1 binding sites on monocytes, fewer calcific atherosclerotic lesions formation and confers protection against coronary artery disease (McDermott et al., 2003, Calderon et al., 2005). In an animal model, the development of atherosclerosis was lower in the double knockout mice ($CX_3CL1^{-/-}$ and $ApoE^{-/-}$) in comparison to the $ApoE^{-/-}$ group (Combadiere et al., 2003).

1.6.3.4 Chemokines in tumour development

Chemokines regulate tumour growth broadly via the mechanisms of modulating angiogenesis and stimulating autocrine growth (Frederick and Clayman, 2001). Studies of G protein-coupled receptor (GPCR) encoded by Kaposi's sarcoma herpesvirus (KSHV) support the idea that chemokine is also responsible for cellular malignant transformation. KSHV-GPCR is somewhat similar to CXCR2; it is constitutively in an activated state, though its reactivity is further enhanced by binding to CXCL1 and CXCL8. In mice, overexpression of KSHV-GPCR is associated with the development of lesions with features resembling Kaposi's sarcoma (Yang et al., 2000). Constitutive activation can be induced in CXCR2 by introducing a point mutation. Cells transfected with this CXCR2 mutant undergo malignant changes (Burger et al., 1999).

CXC chemokines has been shown to play a central role in the dysregulation of angiogenesis required for tumour development. Increased expression of ELR positive CXC chemokines is discovered in several tumours (Frederick and Clayman, 2001, Rosenkilde and Schwartz, 2004). For instance, expression of CXCL8 has been shown to enhance the growth of human non-small cell lung cancer, metastatic melanoma, ovarian carcinoma and colon carcinoma (Smith et al., 1994, Brew et al., 1996, Kunz et al., 1999, Ivarsson et al., 2000); in

bronchogenic carcinomas this chemokine enhances tumourigenesis by accounting for 40-80% of angiogenesis of the tumour (Rosenkilde and Schwartz, 2004). The rate of tumour growth can be attenuated by neutralising antibodies against CXCL8 (Smith et al., 1994). Other ELR positive CXC chemokines that promote angiogenesis in tumours include CXCL1, CXCL3, CXCL5 and CXCL6 (Luan et al., 1997, Arenberg et al., 1998, Rosenkilde and Schwartz, 2004). For example, overexpression of CXCL1 and CXCL3 following transfection of non-tumourigenic mouse melanocytes results in the formation of highly vascular tumours in nude mice. Conditioned medium from these mice is shown to be angiogenic, and this character can be blocked by neutralising antibodies (Luan et al., 1997). Non-ELR CXC chemokines, via their angiostatic effect, has been shown to reduce tumour growth. CXCL9 and CXCL10 both have inhibitive effect on tumour growth (Arenberg et al., 1996, Addison et al., 2000). CXCL10 inhibits angiogenesis, tumour growth and spontaneous metastasis in a model of human non-small cell lung cancer (NSCLC) in severe combined immunodeficiency (SCID) mice; neutralisation antibodies against this chemokine resulted in enhanced tumour-derived angiogenic activity (Arenberg et al., 1996).

Some chemokines act as autocrine growth factors, in which they stimulate proliferation by binding to the receptors on the same tumour cells that produce them. An example for this includes CXCL1, which by binding to CXCR2 has growth stimulating activity on malignant melanoma (Richmond et al., 1988, Luan et al., 1997). CXCL8 is also an autocrine growth factor for certain melanomas and also tumour cells lines from cancers of the colon, stomach, liver, pancreas and skin (Miyamoto et al., 1998, Metzner et al., 1999, Brew et al., 2000, Fujisawa et al., 2000, Frederick and Clayman, 2001). Besides their autocrine effect, some chemokines are thought to play a role in the regulation of tumour metastasis. Chemokine receptors CXCR4 and CCR7 are highly expressed in human breast cancer cell lines and malignant breast tumours; their ligands CXCL12 and CCL21 have been detected in the metastatic organs of these tumour cells (Muller et al., 2001). The chemotactic effect of the CXCL12-CXCR4 reaction has been shown in a migratory assay of NSCLC cells (Phillips et al., 2003).

1.7 Chemokines and placentation

The distribution of expression of different chemokines in the endometrium and decidua has been found to be distinctive, suggesting their specific roles in the process of placentation. The kinetic of chemokine expression changes in different phases of the menstrual cycle; this dynamism is believed to play an important role in the process of endometrial modifications. In the early luteal phase of the menstrual cycle, the endometrium undergoes secretory changes, creating an optimal environment for embryo implantation. This transformation is induced by the progesterone released in the luteal phase. In human the patterns of chemokine expression in the endometrium have been studied. The expression of CXCL1 and CXCL14 in the endometrium is higher in the secretory phase in comparison to the proliferative phase (Nasu et al., 2001, Mokhtar et al., 2010). Endometrial stromal cells have been isolated to study the production of CXCL1; the expression of this protein is enhanced by in-vitro decidualisation of the cells by progestin treatment (Nasu et al., 2001). The exact role of these chemokines in the process of secretory changes of the endometrium is yet to be discovered; in vitro experiment showed CXCL14 is a chemoattractant for uterine natural killer (uNK) cells, which are the most abundant white blood cells during decidualisation (Mokhtar et al., 2010). Besides CXCL1 and CXCL14, elevated production of other chemokines such as CCL4, CCL8, CCL14 and CX_3CL1 has also been detected during the mid-secretory phase of menstrual cycle (Hannan et al., 2004, Jones et al., 2004, Hannan and Salamonsen, 2007).

During the late-secretory period, alteration of the chemokine profile has been discovered; this mechanism is believed to induce menstruation in the absence of embryo implantation. Progesterone withdrawal in mouse is associated with the expression of CXCL1, CXCL5 and CXCL14 (Cheng et al., 2007). In human, CCL7, CCL21, CCL22, CXCL8 and CX_3CL1 are detected close to the spiral arteries in the pre-menstrual phase (Jones et al., 2004, Evans and Salamonsen, 2012). Their presence at this phase of the menstrual cycle provides the mechanistic insight into the initiation of menstruation. It seems like menstruation is an inflammatory process induced by white blood cells bearing the receptors to the chemokines expressed. These leukocytes are chemoattracted to the endometrium in the late-secretory phase.

During pregnancy, the distribution of chemokine expression can be broadly categorised into 4 groups: diffuse expression originating from decidual stromal cells; focal expression from decidual leukocytes or fibroblasts; expression from invading cytotrophoblasts; and localised expression in cells lining the uterine vessels (Red-Horse et al., 2001, Red-Horse et al., 2004). The different chemokines expressed by the cells in the fetal-maternal interface are shown in Table 1.3. In placental development, it is believed chemokines act as regulators of leukocyte recruitment, trophoblast differentiation and localisation, and also angiogenesis. Table 1.4 summarises the chemokine receptor expression by human cytotrophoblasts and decidual leukocytes at the fetal-maternal interface. Interestingly, in a recent study miscarriage of human pregnancy has been associated with a reduction of CXCL8 expression (Pitman et al., 2013). In the in vitro experiment of the study, CXCL8 was shown to disrupt vascular smooth muscle morphology in a model of spiral artery remodelling. Perhaps lack of CXCL8 results in inadequate spiral artery remodelling and subsequently non-continuation of pregnancy.

Chemokine	Receptor/s	Ligand localisation		
		Endometrial epithelium mid-secretory	Decidual cells	Invasive cytotrophoblast
CCL				
CCL2	CCR2 & CCR5	+	+	NT
CCL3	CCR1 & CCR5	NT	+	+
CCL4	CCR5	+	+	NT
CCL5	CCR1, CCR3 & CCR5	NT	±	NT
CCL7	CCR1, CCR2, CCR3 & CCR5	+	+	NT
CCL8	CCR3 & CCR5	+	~	~
CCL11	CCR3 & CCR5	+	+	NT
CCL14	CCR1 & CCR5	+	+	+
CCL16	CCR1, CCR2 & CCR5	+	+	NT
CCL21	CCR7	+	+	NT
CCL22	CCR4	+	+	NT
CXCL				
CXCL1	CXCR2	+	+	-

CXCL6	CXCR1 & CXCR2	NT	+	+
CXCL8	CXCR1 & CXCR2	±	+	+
CXCL9	CXCR3	+	NT	NT
CXCL10	CXCR3	NT	+	NT
CXCL11	CXCR3	+	+	NT
CXCL12	CXCR4	NT	NT	+
CXCL14	Unknown	+	+	NT
CX_3CL				
CX_3CL1	CX_3CR1	+	+	NT

Table 1.3 Chemokine expression during human embryo implantation. + present; - not present; ± present/ not present (conflicting findings); ~ minimal expression; NT not tested. Adapted from (Hannan and Salamonsen, 2007), with updated information from (De Oliveira et al., 2010, Mokhtar et al., 2010, Pitman et al., 2013, Bachelerie et al., 2014).

Chemokine receptor	Expression in cytotrophoblasts	Expression in decidual leukocytes
CXCR		
CXCR1	+	+
CXCR2	+	+
CXCR3		+++
CXCR4	+++	+++
CXCR5		+
CXCR6	+++	+++
CCR		
CCR1		+++
CCR2	+	+++
CCR3	+	
CCR4		+
CCR5	+++	+++
CCR7	+++	+++
CCR8		+

CX_3CR		
CX_3CR1	+	+++

Table 1.4 Chemokine receptor expression at the fetal-maternal interface. +++ expression detected in the majority of samples tested; + expression detected in a minority of samples detected. Adapted from (Red-Horse et al., 2004), with updated information on the expression of CXCR1 in cytotrophoblasts (Pitman et al., 2013).

1.7.1 Leukocyte recruitment

As described earlier in section 1.4, the fetal-maternal interface is infiltrated with specific leukocytes to aid the process of implantation, and also modulate fetal tolerance. There is a striking concordance between the expression of chemokines in the human uterus and their corresponding receptors on decidual leukocytes, supporting the hypothesis of the recruitment of these white cells by the chemokines in the fetal-maternal interface (Red-Horse et al., 2001). In the uterine wall in human pregnancy, high RNA level of CX_3CR1, CXCR3, CCR1, CCR2, CCR5 and CCR7 were detected; these chemokine receptors are typically expressed by NK cells, T cells and monocytes. Complementary ligands, CX_3CL1, CXCL10, CCL2, CCL3, CCL14 and CCL21, were abundantly detected in the decidua in a reciprocal pattern (Red-Horse et al., 2001).

As described above, $CD56^{bright}/CD16^{-}$ natural killer (NK) cells are the most abundant leukocytes in the fetal-maternal interface. In the decidua these cells are termed uterine NK (uNK) cells, majority of NK cells in the decidua are displaying this phenotype; they also have a different gene expression in comparison to their counterpart in the peripheral blood (Koopman et al., 2003). The origin of uNK cells has long been debated. As mentioned earlier, microarray analysis of ~10,000 genes showed significant differences of 278 genes when uNK cells in the decidua were compared with peripheral NK cells (Koopman et al., 2003). This shows that uNK cells during pregnancy are distinctive cells, potentially a matured subset from the peripheral NK cells. Alternatively they may arise from a different haematopoietic precursor either originated from the

local tissue or homed from the peripheral blood or other organs. Reports from several experimental models supported the concept that uNK cells renew from local precursor cells in the endometrium. Xenotransplantation of normal human endometrial tissue into immunodeficient mice showed that local production of lymphocytes and uNK cells in the transplanted endometrial tissue was possible, in an environment where precursors for the white blood cells from the peripheral were lacking (Matsuura-Sawada et al., 2005). The presence of cells with haematopoietic stem cell phenotype in adult human endometrium has also been demonstrated (Lynch et al., 2007). On the other hand, it has been discovered that human $CD56^{bright}/CD16^{-}$ NK cells express receptors for all the chemokines produced by endothelial and stromal cells from the decidua, supporting the theory that peripheral NK cells are selectively chemoattracted to the endometrium, and further differentiate into uNK (Carlino et al., 2008). Potential haematopoietic precursors for uNK cells have also been discovered in the thymus, peripheral lymph nodes and blood in human and mouse (Freud et al., 2005, van den Heuvel et al., 2005, Vosshenrich et al., 2006). In a mouse model, the researchers confirmed the population of uNK cells in the decidua were recruited from other sites, rather than expanding locally through proliferation (Chantakru et al., 2002). In this experiment, uterine segments from NK cell-competent mice were grafted into NK/uNK cell-deficient or wild-type mice. uNK cells were only detected in wild-type recipients, concluding that uNK cells or their predecessors do not self-renew in the uterus. In another mouse model, L-selectin dependent adhesion of peripheral blood $CD56^{bright}$ cells became exaggerated during a peri-ovulatory window, potentially improving the migratory characteristic of these cells into the endometrium (van den Heuvel et al., 2005). The mechanism of NK cells recruitment to the pregnant uterus in mouse is probably CXCL14 dependent. In comparison to $CXCL14^{+/-}$ pregnant uteri, $CXCL14^{-/-}$ pregnant uteri had significantly decreased uNK cells (Cao et al., 2013). In view of the results from the experiments, some authors concluded that in human the origin of uNK cells is a mixture of progenitors from locally and also the periphery (Kitaya, 2008, Zhang et al., 2011).

The expression of chemokine receptors in uNK cells differs from the peripheral blood NK cells (Carlino et al., 2008). It has been discovered that human $CD56^{bright}/CD16^{-}$ uNK cells, in comparison to the $CD56^{bright}/CD16^{-}$ peripheral blood

NK cells, typically bear CXCR3, the receptor for CXCL9, CXCL10, and CXCL11, and also low levels of CXCR4, the receptor for CXCL12. In migratory assays, $CD56^{bright}/CD16^{-}$ peripheral blood NK cells were able to migrate through decidual endothelial and stromal cells following chemotaxis of CXCL10, CXCL12 and CX_3CL1. In contrast, $CD56^{bright}/CD16^{-}$ uNK cells migrated only to the first two, but not the last chemoattractant.

A recent study in mice showed that lack of chemokine expression in decidual cells is associated with impaired accumulation of T cells in the feto-maternal interface (Nancy et al., 2012). A mouse model was designed, in which wild-type females were crossed with males hemizygous for the Act-mOVA transgene to generate concepti expressing antigen chicken egg ovalbumin (OVA). OVA was expressed by the trophoblasts in direct contact with the fetal-maternal interface in as early as embryonic day 7.5 (E7.5). The exposure of maternal tissue to this surrogate antigen should in principle lead to priming of the T cells, thus resulting in the fetus being susceptible to the attack by antigen specific cytotoxic T lymphocytes (CTLs). However, in mice the antigen-specific fetal loss did not occur, even when systemic CTL activity was induced in late gestation (Erlebacher et al., 2007). In the samples, unexpectedly there was a lack of T cell infiltration in the decidual stromal cells. On the contrary, the accumulation of T cells in the adjacent myometrium, and endometrium from the interimplantation sites was clearly displayed. It was discovered that the expression of T helper (Th1) /T cytotoxic (Tc1) chemoattractants (CXCL9, CXCL10 and CCL5) in the decidua was low. Epigenetic silencing of these key T cell attracting inflammatory chemokine genes, CXCL9, CXCL10 and to an extent CCL5, was demonstrated in decidual stromal cells. In the experiment, the evidence of promoter accrual of repressive histone marks in these cells was displayed. This characteristic was not present in the adjacent myometrial stromal cells from the same experimental mouse samples. The findings led to the conclusion that during the process of decidualisation of endometrial stromal cells, epigenetic modification limits effector T cell trafficking to the feto-maternal interface, thus promoting feto-maternal immune tolerance.

At placentation sites in the first trimester, decidual macrophages, along with uNK cells, were found to be in close proximity to invasive trophoblasts, indicating these cells migrate towards the trophoblast invasion front (Helige et

al., 2013). In an in vitro experiment, Rhesus monkey decidual macrophages and primary Rhesus trophoblasts were co-cultured (Rozner et al., 2011). This co-culturing led to the decrease in the level of CCL3, CCL4 and CXCL8, when it was compared to the decidual macrophages being cultured alone. In the migratory assay, decidual macrophages migrated towards the trophoblasts. Reciprocally the trophoblasts also showed significantly enhanced migration towards the decidual macrophages; interestingly there was no migration of the trophoblasts towards peripheral-derived macrophages when they were co-cultured with these cells. In human, decidual macrophages have elevated expression of CCL2, supporting the theory that decidual macrophages recruit blood-borne monocytes, which subsequently differentiate into decidual macrophages (Gustafsson et al., 2008, Erlebacher, 2013). Some studies suggested that there is an exaggerated recruitment of macrophages in pathological pregnancies such as pre-eclampsia and miscarriage (Vassiliadou and Bulmer, 1996, Reister et al., 1999, Lockwood et al., 2006). In pre-eclampsia, it is thought that the expression of CCL2 is dysregulated by TNF-α and IL-1β, leading to the elevated number of macrophages (Bulmer et al., 2010). In one study, the expression of CCL2, CCL5, CXCL2, CXCL3 and CXCL8 was elevated up to 975-fold when cultured first trimester human decidual cells were exposed to IL-1β (Huang et al., 2006).

The recruitment of $CD4^+CD25^+$ Treg in mouse is regulated by CCR5. It was shown that more than 70% of $CD4^+CD25^+$ cells in the gravid uterus and placenta expressed CCR5, whereas CCR5 expression of Treg in the spleen, blood and other secondary lymphoid organs was less than 30% (Kallikourdis et al., 2007). In the in vitro experiment, the authors demonstrated that the majority of the $CD4^+$ cells that migrated towards CCL4 expressed CCR5. In one of the mouse models, semilymphopenic female recipients lacking $CD4^+$ T cells ($F5xRag1^{-/-}$) were adoptively transferred with wild-type CD25-depleted splenocytes reconstituted with $CD25^+$ cells prepared from either CCR5-deficient or wild-type mice. Then the females were allogeneically mated with BALB/c males. The average litter size (7) and the number of resorbing fetuses (2%) were similar between the control and the $F5xRag1^{-/-}$ mice that had received $CD25^+$ cells from wild-type mice. In contrary, the percentage of resorbing fetuses (17%) was significantly higher in the $F5xRag1^{-/-}$ mice that had received CCR-deficient $CD25^+$ cells. In order to follow Treg cells in vivo, the authors designed another experiment

where they transduced Treg cells from either wild-type mice or CCR gene deletion mutant mice with a retroviral vector carrying a constitutively expressed GFP gene, and then adoptively transferred the cells into wild-type females. The recipients were allogeneically mated. In the pregnant uteri they found only half as many tagged CCR-deficient Treg as their wild-type counterparts. From these experiments, the authors concluded that homing of $CD4^+CD25^+$ Treg into the gravid uterus in mouse is regulated by CCR5, the ligand responsible for this chemoattraction can be CCL4.

Collectively, the above findings show the complex regulation of leukocyte recruitment in the decidua during placentation. Human leukocytes, along with other cell types in the decidua, not only express chemokine receptors, but also release chemokines themselves (Red-Horse et al., 2001). The cellular pathway of implantation warrants further exploration in order to gain further understanding of this delicate process.

1.7.2 Trophoblast differentiation and localisation

Precise regulation of trophoblast outgrowth, invasion, differentiation and localisation is required for a successful pregnancy. During the process of apposition, the human blastocyst is immersed in the endometrial microenvironment dominated with chemokine molecules (Jones et al., 2004). Chemokine receptors, for example CCR1, CCR2, CCR3 and CX_3CR1 were detected in trophoblast cell lines, suggesting the importance of their ligands in influencing the character of these cells in vivo (Hannan et al., 2006). In vivo villous cytotrophoblasts (VT) undergo differentiation into syncytiotrophoblasts (ST), forming a thin multicellular layer in the fetal-maternal interface for efficient exchanges. Some other cytotrophoblasts differentiate into interstitial extravillous cytotrophoblasts (iEVT) and endovascular extravillous cytotrophoblasts (vEVT), for invasion and vascularisation during implantation (Fig 1.5) (Damsky et al., 1992, Shih et al., 2006, Ahmed et al., 2012). CX_3CR1 and CCR1 were detected in the human EVT, particularly the vEVT, indicating the specific function of the ligands of these receptors in regulating the migration of these specialised trophoblasts during placentation (Sato et al., 2003, Hannan et al., 2006). Migration assays have been used to demonstrate the migration of trophoblasts cell lines in response to CX_3CL1, CCL14 and CCL4, and also to

endometrial cell conditioned media, which contain these chemokines. Neutralising antibodies to CX_3CL1 and CCL4 attenuated the migration of these cells (Hannan et al., 2006). In a more recent study, invasion of EVT from human placental explants was shown to be stimulated by CXCL8. However, trophoblast invasion seems to be only partially regulated by this chemokine. Unstimulated CD8+ T cells did not alter EVT invasion, despite expressing CXCL8 at a level similar to uNK cells. Although the EVT invasion was stimulated by uNK cell supernatant, CXCL8 neutralising antibody only partially attenuated the degree of invasion (De Oliveira et al., 2010).

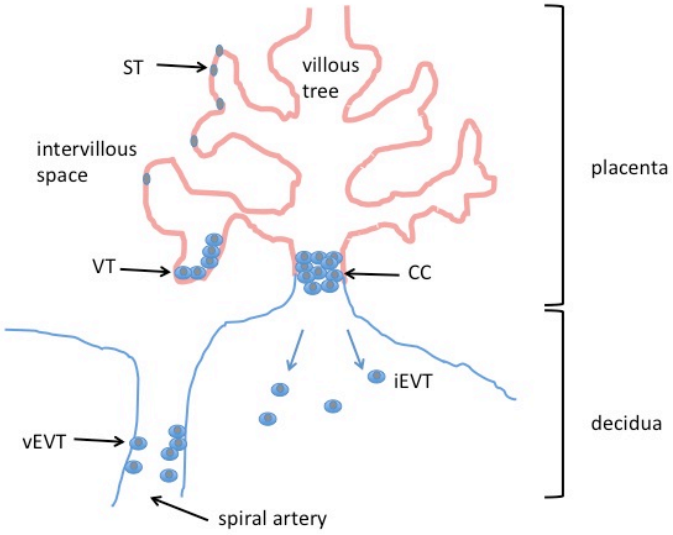

Figure 1.5 Villous trophoblasts undergo differentiation during placentation. Schematic representation of trophoblast populations surrounding the villous tree. ST= syncytiotrophoblasts; VT= villous cytotrophoblasts; CC= cell column; iEVT= interstitial extravillous trophoblasts; vEVT= endovascular extravillous trophoblasts. Adapted from (Hannan et al., 2006).

There are also findings showing trophoblasts control the level of chemokines, by expressing chemokines themselves, and also regulating the secretion of chemokines in the decidua. Human endometrial stromal cells treated with conditioned media from human trophoblasts had upregulated expression of CXCL1 and CCL8 (Hess et al., 2007). On the other hand, it has also been discovered that cytotrophoblasts express CCL3, and that cytotrophoblast conditioned medium has chemotactic effect on NK cells, monocytes and T cells (Drake et al., 2001). EVT expresses CXCL12, the ligand for CXCR4, which is

expressed on CD16- NK cells. CXCL12 is a chemoattractant for these cells (Hanna et al., 2003). This ligand-receptor interaction may be responsible for the precise localisation of trophoblasts and uNK cells during placentation, it may also induce differentiation of progenitors into uNK cells in the decidua.

Collectively, these findings confirm that chemokines play a central role in the regulation of trophoblast invasion and localisation. Alongside with careful localisation and activation of the decidual leukocytes, it is likely that successful placentation is indispensably dependent on the orchestration of chemokines in the decidua. Chemokines act as an essential communicative tool, aiding the crosstalk between trophoblasts, decidual cells and leukocytes.

1.7.3 Angiogenesis

Adequate vascularisation is important to ensure successful placentation, which is essential to support fetal growth, and prevent pathological conditions like pre-eclampsia. EVT has the role of shaping and remodelling maternal arteries in the decidua during implantation. As described above, these cells preferentially express specific chemokine receptors CX_3CR1 and CCR1, believed to be involved in targeting their migration into specific locations in and around the decidual blood vessels. They also secrete CXCL12, attracting CD16- NK cells, a phenotype of uNK cells, which in an in vitro study has been shown to work alongside EVT in the process of angiogenesis (Zhang et al., 2011).

The CXC group of chemokines has been discovered to have either angiogenic or angiostatic properties, depending on whether the particular molecule contains the ELR motif (Strieter et al., 1995). There is considerable interest in determining the expression of CXC chemokines in the fetal-maternal interface. CXCL11, and its receptor CXCR3 have been detected in human endometrial and placental cells (Hirota et al., 2006). In an experiment, the authors developed a complex three-dimensional spheroid model for in vitro studies of placental vasculogenesis with regard to cell-cell interactions (Baal et al., 2009). The expression of CXCL12 and its receptor CXCR4 was studied, as CXCL12/CXCR4 signalling plays a critical role in the process of embryonic vasculogenesis (Chen et al., 2007). In this model enhanced expression of CXCL12 and its receptor CXCR4 was detected in the physiological environment with low-oxygen

concentrations, in comparison to the pathological environment with high-oxygen concentrations. In another study, a trophoblast cell line was discovered to express CXCL2, CXCL3, CXCL6 and CXCL8 which are chemokines that bind to CXCR1 and CXCR2 receptors. These chemokines are known to stimulate angiogenesis. They were also shown to be chemoattractive to lymphocytes; the recruited lymphocytes may have an effect on spiral artery modelling via the release of angiogenic factors (Cavanagh et al., 2009). Another CXC chemokine, CXCL1 was also detected in human first-trimester trophoblasts; CXCL1 incited chemotaxis of NK cells and monocytes (Chen et al., 2010).

In mouse, CXCR3 deletion has been shown to reduce uNK cells recruitment to the decidua basalis, and mesometrial lymphoid aggregate of pregnancy; this was associated with abnormal formation of placental spiral arterioles with narrow lumen (Xie et al., 2005). $CXCR3^{-/-}$ mice also appeared to have hypocellular decidua basalis with increased intercellular space on the implantation sites. In another mouse study, treatment of gravid females with a CXCR4-specific inhibitor caused impaired homing of $CXCR4^{+}$DC during early gestation, resulting in a disorganised decidual vasculature (Barrientos et al., 2013). Later in gestation, this group of mice had impaired spiral artery modelling and a decrease in fetal survival. The authors showed that in a different model, DC depleted mice had similar phenotype of extremely low fetal survival. In this model, adoptive transfer of $CXCR4^{+}$DC into the mice rescued the pregnancy, by promoting vascular growth in the decidua, and enhancing the availability the VEGF. It is thought that VEGF is essential for adequate remodelling of the spiral arteries.

Collectively, these findings confirmed the important role of angiogenic CXCL in the process of placental angiogenesis. Angiogenic CXCL can exert a direct effect on angiogenesis; by recruiting the leukocytes they also further enhance the process to ensure adequate vascularisation of the placenta.

1.8 Atypical Chemokine Receptors

Atypical Chemokine Receptors (ACKRs), also known as chemokine decoy receptors, share structural similarity with other chemokine receptors. Not unlike other receptors, they have high affinity for specific subsets of chemokines.

However, upon binding to their ligands there is no activation of signalling pathways, as occurs with other G protein coupled receptors. At present four ACKRs have been described: DARC, D6, CCX-CKR and CXCR7 (Graham, 2009). The lack of signalling through these receptors, is thought to be due to subtle alterations in the canonical DRYLAIV motif found in the second intracellular loop of the signalling chemokine receptors; interestingly modification of the DKYLEIV motif of D6 to DKYLAIV results in weak ligand-induced signalling activity (Nibbs et al., 2009).

The ligands of the ACKRs are shown in Table 1.5. Based on in vitro study, it is thought that ACKRs can act as chemokine transporters to regulate chemokine abundance and localisation (Nibbs et al., 2003, Mantovani et al., 2006, Graham et al., 2012). D6, CXCR7 and CCX-CKR have also been found to have scavenging properties; in vitro these molecules have the ability to remove (scavenge) large quantities of extracellular ligands (Nibbs et al., 2009).

D6 is abundantly expressed in the placenta and forms a key focus of the studies described in this thesis. Thus, a more detailed of what is known about this molecule, and its potential reproductive function is described in different sections later in this chapter. The characteristics of DARC, CCX-CKR and CXCR7 are summarised below.

ACKRs		Ligands
DARC	Strong	CCL2 CCL5 CCL7 CCL11 CCL13 CCL14 CCL17 CXCL1 CXCL2 CXCL3 CXCL4 CXCL5 CXCL6 CXCL8 CXCL11
	Weak	CCL1 CCL8 CCL16 CCL18 CXCL9 CXCL10 CXCL13
D6		CCL2 CCL3 CCL3L1 CCL4 CCL5 CCL7 CCL8 CCL11 CCL13 CCL14 CCL17 CCL22
CCX-CKR		CCL19 CCL21 CCL25
CXCR7		CXCL11 CXCL12

Table 1.5 Ligands of atypical chemokine receptors (ACKRs) in human. Data from (Nibbs et al., 2009, Hansell et al., 2011a).

1.8.1 DARC (Duffy antigen receptor for chemokines)

DARC is traditionally known as the Duffy antigen. At first it was recognised as the entry point on erythrocyte for the malarial parasite Plasmodium Vivax (Rot, 2005). It is a seven transmembrane spanning receptor that binds inflammatory CC and CXC chemokines with high affinity (Gardner et al., 2004, Graham, 2009). Structurally DARC has 40% similarity with other chemokine receptors, however it lacks the DRY motif in the second intracellular loop (Chaudhuri et al., 1993, Graham, 2009). Besides erythrocytes, expression of DARC is detected on vascular endothelial cells; the expression of this receptor is upregulated in the presence of inflammatory stimuli (Lee et al., 2003a, Comerford et al., 2007). More than 95% Africans in malaria-endemic regions and 70% of African Americans lack expression of DARC in their erythrocytes, probably as a result of selection advantage provided by resistance against the infection of Plasmodium Vivax (Miller et al., 1976, Mantovani et al., 2006).

DARC binds promiscuously to 11 pro-inflammatory CC and CXC chemokines; it does not interact with homeostatic chemokines (Gardner et al., 2004). It has been shown that DARC is probably responsible for the process of transcytosis of

chemokines, where the proteins are internalised and transported across endothelial cells, and are presented on the tips of lumimal microvilli (Middleton et al., 1997, Hub and Rot, 1998, Nibbs et al., 2003). It has also been proposed that the presence of DARC on erythrocytes allow the cells to act as a 'sink' or reservoir for chemokines, regulating the amount of free pro-inflammatory chemokines available for binding with other receptors (Darbonne et al., 1991, Hadley and Peiper, 1997). DARC-deficient mice phenotypically have normal development and haematological parameters; in a model of endotoxaemia they show increased granulocytic infiltration in the lungs and liver (Dawson et al., 2000). In one experiment, mice where engineered to overexpress DARC on endothelial cells (Du et al., 2002). These mice showed reduced angiogenic responses to certain CXC chemokines, suggesting that DARC may be limiting the chemokines available for binding with CXCR2 on the endothelial cells. In a prostate cancer experiment using transgenic model, $DARC^{-/-}$ mice demonstrated greater tumour growth; they were unable to clear angiogenic chemokines produced by the cancer cells (Shen et al., 2006). This result is interesting, as African-American men, majority lacking DARC in the erythrocytes, has increased occurrence of mortality from prostate cancer (Lentsch, 2002). Wang et al. demonstrated that high DARC expression in breast cancer cell lines could limit tumour growth and metastasis (Wang et al., 2006a). Contradictorily, in a mouse model the level of injected CCL2 fell more rapidly in the plasma of $DARC^{-/-}$ mice (Fukuma et al., 2003). Similar pattern was noted in human, where erythrocyte DARC negative individuals have reduced CCL2 plasma levels (Jilma-Stohlawetz et al., 2001). Moreover, different experiments in DARC mouse model assessing the response of neutrophil infiltration following LPS administration produced conflicting results (Dawson et al., 2000, Lee et al., 2003b). Collectively these show the complexity of the regulation of pro-inflammatory chemokines by DARC.

1.8.2 CCX-CKR (Chemocentryx chemokine receptor)

CCX-CKR binds to CCL19, CCL21 and CCL25, homeostatic chemokines which involve in the regulation of leukocyte and thymocyte migration, and also formation of secondary lymphoid organs by interacting with CCR7 or CCR9 (Gosling et al., 2000). There is no signalling event when the ligands bind to CCX-CKR, thus CCX-CKR has been classified as an ACKR. This is due to the alteration of the DRY motif in the second intracellular loop of CCX-CKR to DRYVAVTKV in

human and DRYWACTKA in mouse (Comerford et al., 2007). CCX-CKR appears to be able to target their ligands for intracellular degradation. Unlike CCR7, there is no ligand-induced desensitisation in CCX-CKR. One study showed that CCX-CKR is able to continuously internalise and degrade large quantity of CCL19 over time (Comerford et al., 2006).

Initial assessment of the expression of CCX-CKR showed that this receptor is broadly expressed, for example in the haemopoietic cells, lymphoid tissues, and also the heart, kidneys and lungs (Gosling et al., 2000). In a separate study using CCX-CKR-EGFP heterozygous knock-in mice, CCX-CKR protein was not detected in the tissues previously shown, instead it was expressed in thymic epithelial cells, and also potentially in the lymph vessels of the gut, stromal cells in the lymph nodes and epidermis (Heinzel et al., 2007). In the same study, the authors demonstrated the role of CCX-CKR in modulating adaptive immunity, by affecting the transport of DC to skin-draining lymph nodes, and homing of embryonic thymic precursors to the thymic anlage. The effect of CCX-CKR on the thymus has been studied; in one study CCX-CKR deficient mice were found to have CCL25 dysregulation, and also marked differences in the localisation and abundance of thymocyte subsets (Bunting et al., 2013). However, this finding was not consistently demonstrated in another study (Heinzel et al., 2007). It has also been discovered that aged CCX-CKR knock out mice spontaneously developed autoimmune disease resembling Sjogren's Syndrome (Bunting et al., 2013).

1.8.3 CXCR7

CXCR7 is another ACKR that has the ability to degrade chemokines (Nibbs and Graham, 2013). Its ligands are CXCL11 and CXCL12 (Burns et al., 2006). Similar to other ACKRs this molecule lacks the typical canonical DRY motif (Nibbs and Graham, 2013). In mouse studies, this receptor was initially only detected in the fetus (Graham, 2009). During fetal development, high expression of CXCR7 was detected in cardiac microvessels, indicating its involvement in cardiac development. CXCR7 deficiency led to ventricular septal defect and malformation of the heart valves, resulting in an increased risk of mortality in perinatal period and adulthood (Sierro et al., 2007). The role of CXCR7 in primitive vertebrate development has been studied using zebrafish; it was shown

that this receptor has an important role in the coordination of primordial germ cell migration in the lateral line primordium (Valentin et al., 2007).

Expression of CXCR7 in adult mice has been detected recently by using $CXCR7^{GFP/+}$ reporter mice (Cruz-Orengo et al., 2011a, Cruz-Orengo et al., 2011b). CXCR7 expression was detected in the brain endothelial cells. CXCR7 antagonists inhibited CXCL12 internalisation by the receptor, leading to an increase in abluminal CXCL12 level. It was opined that this mechanism prevents $CXCR4^{+}$ leukocytes from preferentially migrating into the parenchyma. As a result, administration of the antagonists prophylactically and therapeutically decreased EAE disease activity induced by encephalogenic T cells. The benefit of CXCR7 antagonists is also shown in a collagen-induced arthritis model in mice (Watanabe et al., 2010). Administration of antagonists for CXCR7 improved the severity of arthritis; the group of mice that received antagonists had less blood vessel formation in the inflamed joints. Interestingly, in human $CXCR7^{+}$ vessels have been detected in patients with rheumatoid arthritis. These findings strongly suggest CXCR7 has an angiogenic effect in arthritis.

CXCR7 immunoreactivity has been detected on tumour cells and their vasculature in a number of human malignancies. In vitro studies showed that CXCR7 can regulate angiogenesis and also tumour cell proliferation and migration, thus may affect the survival and metastasis of cancers (Nibbs and Graham, 2013). CXCR7 exerts its regulatory mechanism by interacting with its ligand CXCL11 and CXCL12, and also by collaborating with CXCR4.

1.9 D6-mediated chemokine scavenging: evidence from in vitro and in vivo studies

D6 is related to chemokine receptors CCR1-5 structurally and binds to many inflammatory CC chemokines as shown above. However unlike the other CCRs, upon binding to the chemokine ligands it does not trigger a cellular signalling pathway e.g. calcium ion fluxes (Martinez de la Torre et al., 2007), instead D6 scavenges the ligands bound. It achieves this by constitutively travelling to and from the cell surface via early and recycling endosomes, internalising chemokines bound when it is at the cell surface (Weber et al., 2004). Unlike other chemokine receptors, there is no need for signalling induced by the ligands

for D6 to traffic into the cells. This mechanism has the advantage of avoiding receptor desensitisation and surface receptor depletion. The endosomes in the cells have very low pH; D6 is particularly sensitive to this change of acidity, and rapidly releases its bound ligands for retaining in the cells, which subsequently are degraded in the lysosomes. After releasing the ligands in the endosomes, D6 constitutively finds its path to the cell surface for performing its role in further chemokine scavenging. Over time, D6 removes a large amount of ligands from the extracellular compartment. This effect regulates the level of CC chemokines, and thus controls inflammation locally and systemically.

Different immune-regulatory in vitro and in vivo models have been used for the study of D6. In vivo studies have shown D6 KO mice have elevated amount of bioavailable chemokines, associated with over exuberant inflammatory responses (Jamieson et al., 2005). These findings were consistent with the results from in vitro experiments. Induction of skin inflammation led to a transient inflammatory reaction in wild type mice. On the contrary, mice lacking D6 have been shown to be associated with exacerbated inflammatory response, with close similarity to human psoriasis (Jamieson et al., 2005, Martinez de la Torre et al., 2005, Singh et al., 2012). This was associated with increased abundance of chemokines in the cutaneous sites and draining lymph nodes (Jamieson et al., 2005, Martinez de la Torre et al., 2005). In humans with psoriasis, skin biopsies showed expression of D6 was markedly elevated in uninvolved skin more than 8cm distant from the psoriatic plaques. In the psoriatic lesional and peri-lesional skin, there was a big drop in D6 expression (Singh et al., 2012). In an inflammation-driven skin tumourigenesis model, D6 KO mice were shown to have an increased susceptibility to invasive squamous cell carcinoma, associated with T cell and mast cell recruitment, which are known to contribute to skin tumours in the mouse model used (Nibbs et al., 2007). In humans, recently D6 has been discovered to have protective effect against disease progression of breast cancer. D6 expression in breast cancer is inversely correlated to lymph node metastasis and clinical stages, but positively correlated to disease-free survival rate (Wu et al., 2008).

In a colitis mouse model, D6 deficiency has been associated with an increased susceptibility to colitis-associated cancer in the distal colon (Vetrano et al., 2010). In a different study, D6 expression was discovered to be preventing

insulitis, and thus is protective against diabetes in mice (Lin et al., 2011). In this instance D6 inhibited the autoreactivity of lymphocytes, and prevented the migration of T and B lymphocytes into the pancreas. D6 also limited acute toxic liver injury in vivo, as lack of D6 was associated with increased protein levels of intrahepatic inflammatory chemokines CCL2, CCL3 and CCL5, leading to a higher amount of $CD45^+$ T and NK cells infiltration and inflammation (Berres et al., 2009). The role of D6 in altering the susceptibility of mouse to colitis is less well understood, with two different mouse studies producing contradictory results (Bordon et al., 2009, Vetrano et al., 2010).

Expression of D6 was detected in infarcted myocardium from human and mouse (Cochain et al., 2012). In mice with myocardial infarction, D6 deficiency increased the likelihood of cardiac rupture, and functional analysis showed features of adverse cardiac remodelling with left ventricle dilation and reduce ejection fraction. In the ischaemic hearts of these animals, there were increased levels of CCL2 and CCL3, with infarcts showing increased pathogenic neutrophils and monocytes infiltrations (Cochain et al., 2012). In a pulmonary model, low dose intranasal introduction of Mycobacterium tuberculosis into D6 KO mice, at a dosage similar to control WT mice, rapidly killed the former animal group. This was associated with abnormal elevation of chemokine ligands of D6 and cytokines, and also increased infiltrations of macrophages, dendritic cells, CD4 and CD8 T lymphocytes in the broncho-alveolar lavage locally and serum systematically. High levels of cytokines, tumour necrosis factor α, interleukin 1ß and interferon γ, were discovered in the mice with liver and kidney damage, resulting in failure of those organs (Di Liberto et al., 2008). In a different study, allergen ovalbumin was injected into the peritoneum of the mice. Experiments on the airway and lung parenchyma showed increased levels of CCL17 and CCL22, and high abundance of dendritic cells, T cells and eosinophils in D6 KO mice. Interestingly, these D6 KO mice showed attenuated airway reactivity to methacholine (Whitehead et al., 2007).

The role of D6 in lymphatic endothelium has been studied in in vitro and in vivo experiments. In human, D6 was detected in the lymphatic endothelial cells (LECs) (Nibbs et al., 2001). The receptor removes inflammatory CC-chemokines from lymphatic surfaces, minimises interaction of inflammatory leukocytes in this area, and therefore enhances chemokine-driven recirculation of leukocytes

through the lymphatics. In mice, D6 deficiency led to elevated CC chemokine ligands adherence to LECs, inducing inappropriate perilymphatic accumulation of inflammatory leukocytes, which caused lymphatic congestion at peripheral inflamed sites and draining lymph nodes. This subsequently resulted in impaired movement of antigen-presenting cells and fluid from inflamed sites to lymph nodes (Lee et al., 2011).

Besides the action of chemokine scavenging, there is evidence that D6 can regulate the immune system by other mechanisms. In the process of the resolution of acute inflammation in humans and rodents, the expression of D6 was detected in apoptotic inflammatory polymorphonuclear (PMN) cells (Pashover-Schallinger et al., 2012). In a mouse ex vivo model, the receptor improved the interactions of the PMN cells with macrophages, controlling their efferocytosis and cytokine secretion. These interactions were thought to enhance the immune silencing phenotype of the macrophages, leading to the resolution of inflammation. The immune silencing effect of macrophages was attenuated, when D6 deficient PMN cells were used to interact with these phagocytes (Pashover-Schallinger et al., 2012). In contrast to the above findings showing the immuno-regulatory character of D6, a couple of models showed D6 deficiency offered protection from disorders with pathologically elevated immune response in certain context. In one of the mouse model, D6 KO mice had increased number of $Ly6C^{high}$ monocytes in the circulation and secondary lymphoid tissues, regulated in a CCR2-dependent manner. This group of monocytes derived from D6 KO mice had enhanced immunosuppressive activity, inhibited the development of adaptive immune responses, and offered some protection against graft-versus-host-disease (Savino et al., 2012). In an experimental autoimmune encephalomyelitis (EAE) mouse model, D6 KO mice were unexpectedly resistant to the induction of EAE following the introduction of myelin oligodendroglial glycoprotein (MOG) peptide. There were reduced spinal cord inflammation and demyelination in the D6 KO mice. In the adoptive transfer experiment, MOG-primed $D6^{+/-}$ T cells equally triggered the disease in all the recipient groups regardless of their D6 expression status, whereas cells from D6 KO mice transferred the disease poorly even in $D6^{+/-}$ recipients (Liu et al., 2006).

In summary, the findings above confirmed the important role of D6 as a chemokine scavenger in the immune regulatory process. D6 also has an effect on other immune cells; in specific models these cells behave differently in the presence of D6.

1.10 D6 in reproductive immunology

In humans, in early studies D6 mRNA was found to be highly expressed in the placenta. In fact, the expression in the placenta was discovered to be by far the highest, compared to other solid tissues being studied (heart, brain, thymus, ovary, muscle, liver, kidney, spleen, lung) (Nibbs et al., 1997b). Apart from lymphatic endothelial cells and some leukocyte populations (Nibbs et al., 2001, McKimmie et al., 2008), D6 protein was highly abundant in first trimester and term placenta according to immunohistochemistry using a validated D6-specific antibody (Martinez de la Torre et al., 2007, Madigan et al., 2010). Immunostaining of other gestational tissues also showed exuberant expression of D6 in the decidua and membranes throughout pregnancy (Madigan et al., 2010).

D6 was found to be expressed exclusively by trophoblast-derived cells in the placenta, this was confirmed by staining of the adjacent sections with the trophoblast marker anti-cytokeratin 7 antibody (Madigan et al., 2010). In the chorionic villi from the first trimester placenta, D6 was detected in cytotrophoblasts and the syncytiotrophoblast layer. In the third trimester, the syncytium lining the chorionic villi was strongly stained. D6 protein was apical, clustering towards the surface of the villi where they were in contact with maternal blood. There was no consistent difference in the intensity of D6 immunoreactivity across samples from different gestational ages. In the gestational membranes of pregnancies between 32 and 41 weeks, the staining of D6 was abundant in the chorion laeve, separating the maternal decidua from the fetal amnion which themselves were D6 negative. On these trophoblast-derived cells, D6 protein was mostly localised inside the cells in a manner not unlike D6 transfected cell lines. From here, it is thought that D6 constitutively traffics to and from the cell surface to mediate chemokine scavenging. In the decidua, extravillous trophoblasts were expressing D6 when they were invading into the maternal decidua. This staining suggested that D6 plays a specific role in gestational tissues, delineating the fetal-maternal interface where the tissues

from mother and baby meet each other. By scavenging the surrounding chemokines, D6 probably was prepared to protect the fetal tissues from the attack of maternal chemokine-responsive leukocytes. It is also postulated that D6 may play an important role in controlling the action of trophoblasts, directing their movement during implantation, and affecting the formation of the placenta and wellbeing of the fetus. The expression of D6 was consistently strong in all the placental histological sections; in our laboratory placentas have been routinely used as a standard positive control for D6 expression studies. In pathological pregnancies (hydatidiform mole and choriocarcinoma), D6 expression is also retained by trophoblasts (Madigan et al., 2010). As before, this was determined by immunostaining of the adjacent sections with anti-cytokeratin 7 antibody. Similar to the normal placentas, D6 was strongly stained in organised trophoblast layers in a polarised manner in all the samples. In hydatidiform mole, D6 immunoreactivity was confined to the area of circumferential excess lined with trophoblasts; the staining of the swollen mucoid stromal core was negative. In choriocarcinomas, large patches of trophoblasts showed weak immunostaining, lacking the distinctive pattern seen in the villi and chorion in normal pregnancies.

At term, the chorionic villi in the placenta have an estimated surface area of about $10m^2$, and blood flow through the placenta is about 600-700ml/minute (Wang and Zhao, 2010). With the blood flowing over a large surface with abundant D6, it is not surprising if D6 can affect the systemic levels of its ligands in the maternal blood stream. In the placenta, high expression of chemokines (CCL2 and CCL3) has been shown by quantitative PCR. One would expect the protein level of these chemokines to be elevated during pregnancy. On the contrary, study of D6 ligands CCL2, CCL3 and CCL11 showed that the levels in the plasma of pregnant women are reduced in comparison to non-pregnant controls. The levels were reduced in first trimester, and continued to drop further in term pregnancies. There was no difference in the levels of non-D6 ligand CXCL10 between non-pregnant, first trimester and term samples. Interestingly in women with pre-eclampsia, which is associated with an exaggerated inflammatory response, the level of CXCL10 was significantly raised in pregnancy, whereas the levels of D6-binding chemokines were still subdued. Quantitative PCR of term placentas showed that the expression of D6 was

significantly higher in women with pre-eclampsia compared with controls. This shows the potential effectiveness of D6 as a scavenger, controlling the levels of D6-binding chemokines systematically, may prevent over exuberant inflammation in pregnancy (Madigan et al., 2010). In pathological condition like pre-eclampsia, D6 expression in the placenta may be increased to cope with a more pro-inflammatory environment.

The cellular in vitro studies nearest to reflecting the function of D6 in trophoblasts was performed using the choriocarcinoma cell line BeWo (Martinez de la Torre et al., 2007, Madigan et al., 2010). BeWo cells express D6 endogenously; prior to these studies, the detailed understanding of D6 structure and function has been primarily from experiments on transfected cell lines. Staining of D6 protein on BeWo cells showed D6 was predominantly found in intracellular vesicles, and was not detectable on the cell surface (Madigan et al., 2010). In these cells, D6 specifically internalised and degraded labelled CCL3, one of its ligands. The effect can be competed with other non-labelled D6 ligands, whereas non-D6 ligands had no competitive effect. Using siRNA, D6 was successfully knocked down, and the scavenging of labelled CCL3 was abolished. In the same study, the authors incubated term placental pieces with radiolabelled chemokines. They found the syncytiotrophoblast layer lining the chorionic villi positively interacted with radiolabelled CCL2, a D6 ligand, but not CXCL8, a non-D6 ligand. This provided further confirmation that trophoblasts in situ express D6 and specifically bind to its chemokine ligands.

In the mouse placenta, the expression of D6 mRNA is roughly the same as adult liver, and at a level much lower than the lungs (Madigan et al., 2010). In contrast to humans, where the placenta has the highest expression of D6, in the mouse placenta D6 is less abundantly expressed. However, the level of overall D6 expression in the mouse uterus still may be very high during mouse pregnancy, due to the multiparity nature of mouse pregnancy. Alternatively, one could postulate D6 expression in mouse placenta need not be as high, as the invasion of mouse trophoblasts into the decidua is not as drastic as the human placenta. The expression of D6 in the mouse placenta is fetal derived, as D6 deficient embryos, growing in heterozygous females (D6 HET) expressing D6, showed negative D6 detection in the placenta (Madigan et al., 2010). This

supports previous human findings of D6 being expressed exclusively by trophoblasts, which originate from the fetus.

In animal in vivo studies, D6 has been shown to play an important role in protecting the fetuses. D6 deficiency has been associated with adverse fetal outcomes. A defect in D6 expression was discovered in placental attachment sites in porcine endometrium from arresting fetuses. In healthy littermates no defect was detected (Wessels et al., 2007). In one key study, wild-type (WT) and D6-deficient mothers carrying D6-deficient pups where challenged with lipopolysaccharide (LPS) or antiphospholipid autoantibodies (aPL) purified from patients with antiphospholipid syndrome (APS) (Martinez de la Torre et al., 2007). LPS is an endotoxin that triggers inflammatory response associated with adverse pregnancy outcome, for example miscarriage, or preterm labour. Patients with APS have higher incidence of thrombosis, fetal loss, IUGR and pre-eclampsia. aPL-containing Ig fractions, when injected into pregnant mice, caused placental inflammation, necrosis and increased the rate of fetal loss; injection of IgG fractions from healthy women had no effect on pregnancy outcome (Martinez de la Torre et al., 2007).

Comparing WT and D6 deficient mice, LPS injection resulted in a significantly higher rate of fetal loss in the D6 deficient group. The increase in fetal loss could be completely reversed by the introduction of antibodies that blocked inflammatory CC chemokines. D6 binding chemokines were elevated in the placentas and sera of pregnant D6 deficient mice compared to WT counterparts. There were no differences in the levels of non-D6 binding chemokines between the two groups. Study of leukocyte infiltration revealed the number of macrophages and T lymphocytes were higher in the D6 deficient placenta, whereas the level of neutrophil was similar between the two groups. This finding led to a model in which D6 deficiency resulted in higher abundance of D6-binding CC chemokines, which selectively attracted macrophages and T lymphocytes. D6 deficiency also led to enhance aPL-induced fetal loss, confirming the role of D6 in protecting the fetus from inflammatory challenge (Martinez de la Torre et al., 2007).

In an unchallenged environment in normal mouse breeding, D6 is currently thought to be dispensable for successful pregnancy for both syngeneic and

semiallogeneic embryos. However, embryo transfer in mice was carried out to study the role of placental D6 in an unchallenged, but fully allogeneic environment (Madigan et al., 2010). In fully allogeneic pseudo-pregnant wild type female recipients, the proportion of abnormal fetuses was higher in the transferred D6 deficient littermates, in comparison to their D6 expressing siblings. This difference in phenotype was not observed when the embryos were transferred into syngeneic recipients. In the abnormal pups, the placentas were often structurally defective, and infiltrated with macrophages and T lymphocytes. Interestingly, recent work from the Nibbs/Nelson lab suggests that D6 deficiency in DBA-1 mice may lead to increased syngeneic pup loss. This observation forms the basis for one arm of my study.

1.11 Experimental design

Drawing on these published data, it was hypothesised that by scavenging chemokines, and regulating trophoblast responses to chemokines, D6 plays a role in placental function to limit fetal loss, stillbirth, and neonatal death.

Two specific areas of experimentation form the focus of the work. One arm of the study aims to investigate the molecular function of D6 in primary human trophoblasts; the second examines the basis for reproductive defects observed in D6 deficient DBA-1 mice. Collectively these studies aim to provide novel insights into the role of placental D6.

1.11.1 Molecular characterisation of D6 function in primary human trophoblasts

The function of D6 on primary cells has not been explored. The overall intention for this part of the research was to examine D6 expression, distribution and function in primary human trophoblast cultures from term placentas. Firstly, expression of D6 mRNA will be assessed by real time PCR. Following that the protein expression and localisation of D6 will be assessed by various protein detection techniques including flow cytometry, immunofluorescent staining and Western blotting. Transfected and untransfected HEK293 cell lines will be used as my controls.

To reveal the functional activities of D6, chemokine uptake assays will be carried out using fluorescent D6-binding chemokine CCL2. The uptake of this chemokine will be tracked by flow cytometry and immunofluorescence techniques. Known D6 ligands CCL2, CCL3L1, CCL4, CCL5, CCL7, CCL8, CCL11, CCL13, CCL17 and CCL22 will be used as competitive chemokines (Hansell et al., 2011a). CCL24 and CCL26 are not known to be D6 ligands, and will be used as negative controls. Once again HEK293 cells will be used as controls.

It is thought that the main task of the D6 molecule is to act as a scavenger. This characteristic will be studied by chemokine scavenging assays. This will be done by tracking the removal and destruction of biotinylated CCL2, over time, from media bathing cultured trophoblasts. The levels of biotinylated CCL2 at the various time points will be assessed by quantitative (relative) Western blot. Unlabelled CCL3L1 (D6 ligand) and CCL26 (non-D6 ligand) will be used as competitive chemokines.

Collectively these experiments will determine, for the first time, whether D6 is expressed in primary human trophoblasts in culture, and if so whether this D6 can mediate the uptake and scavenging of chemokines. This will provide novel, physiologically-significant insight into D6 function at the feto-maternal interface, and aid the interpretation of subsequent in vivo experiments.

1.11.2 Impact of D6 deficiency on placental structure, chemokine expression and leukocyte abundance

The trends of increased perinatal deaths, and decreased pup weaned/litter were observed in D6 deficient mice in comparison to their WT counterparts in DBA-1 background. A complete and expanding dataset will be collected from Central Research Facility, University of Glasgow to confirm this finding. To ascertain the wellbeing of the pups postnatally, perinatal deaths and weight changes during neonatal period will be followed up for a cohort of mice.

It was hypothesised that D6 deficient mice on this genetic background have fundamental defects in the structure of the placenta. To test this, a detailed temporal comparative analysis of placentas from WT and D6 deficient DBA-1 mice will be performed. First, in close collaboration with Professor Burton

(University of Cambridge), a detailed stereological analysis of the placenta across gestation at E10, E14 and E18 will be carried out. Wet weights of placentas and whole fetuses will also be recorded. These analyses will provide detailed comparative insight into the placentas from these animals, allowing the study of the differences in the three dimensional (3D) volumes of the functional zones in the placentas. The impact of the differences in these placental functional volumes to the fetal growth (weight) will be explored. If there are differences in the placentas between WT and D6 deficient group, heterozygous DBA-1 mice will be used to ascertain whether the observed phenotype is due to either fetal or maternal effect of D6 deficiency.

Alongside this structural analysis, the impact of D6 deficiency on local and systemic chemokine expression and abundance, and also infiltration of white blood cells will be examined. Real time PCR will be used to compare the expression of the genes of D6-binding chemokines CCL2, CCL3, CCL4, CCL5, CCL11, CCL12, CCL17 and CCL22 in the placentas of WT and D6 deficient mice. Depending on the results of the expressions of these chemokines, markers of relevant white blood cell infiltration will be assessed using real time PCR on the placentas. To study the systemic effect of D6 scavenging property, Luminex multiplex protein assay will be performed on the serum of the pregnant mice to assess the differences in the levels of D6 binding chemokines between WT and D6 deficient group.

These animal experiments will define indispensable roles for D6 in controlling placental structure, function and leukocyte content; identify the principal chemokines involved in leukocyte/trophoblast regulation in this tissue; and provide insight into how D6 regulates the local and systemic abundance of these chemokines. Along with the human trophoblast work above, this study will provide new insight into the role of D6 in the placenta.

2 Materials and Methods

2.1 In vitro study (primary human trophoblasts)

2.1.1 Trophoblast isolation and culture

The isolation and purification of trophoblasts from term placentas was performed using a modification of Kliman's technique (Kliman et al., 1986).

2.1.1.1 Preparation of reagents

Cytomedium and Percoll solutions were prepared before obtaining the placentas for these experiments. The cytomedium was made up of medium 199 (Invitrogen, Life Technologies, Paisley, UK) supplemented with 10% heat inactivated fetal bovine serum (Sigma-Aldrich, Dorset, UK) and 1% antibiotic/antimycotic solution (Gibco, Life Technologies, Paisley, UK). Different concentrations of Percoll solutions were made up in 50ml centrifuge tubes and stored in 4^{o}C (Table 2.1). The different concentrations of Percoll were layered in three Kimber round bottom glass centrifuge 30ml tubes (Fisher Scientific UK Ltd, Loughborough, UK) to form a gradient of different densities, for separating different cell types from a placenta and allowing the identification of trophoblast layers (Table 2.2). To prevent disruption of the layers, the three tubes of Percoll gradient were kept at 4^{o}C until the purification step when it was used in the procedure.

Concentration (%)	Percoll volume (ml)	Sterile water volume (ml)	10x HBSS volume (ml)	Total volume (ml)
70	35	10	5	50
60	30	15	5	50
55	27.5	17.5	5	50
50	25	20	5	50
45	22.5	22.5	5	50
40	20	25	5	50
35	17.5	27.5	5	50
30	15	30	5	50
20	10	35	5	50
10	5	40	5	50

Table 2.1 Solutions for different Percoll concentrations. The stock Percoll solution was from Sigma-Aldrich**,** Dorset, UK; the 10x HBSS was from Invitrogen, Life Technologies, Paisley, UK.

Percoll gradient
Top 2ml 10% 2ml 20% 4ml 30% ----------mark tube 2ml 35% 2ml 40% 2ml 45% 2ml 50% 2ml 55% ----------mark tube 2ml 60% 3ml 70%

Table 2.2 Layering of the Percoll gradient for separating trophoblasts from other cells in the placenta. Trophoblasts typically layered out in between the two marked lines in the glass tubes after centrifugation.

2.1.1.2 Collection and dissection of placenta

The study was approved by the West of Scotland Research Ethics Committee 5 (REC reference number: 10/S1001/14). Term placentas were collected from patients having elective Caesarean sections, with written consent obtained. In a primary cell culture sterile cabinet, the umbilical cord and the edge of the placenta were removed. Vertical dissections of the placenta were performed, cutting the placenta into two to three inches long cubes. The placenta was dissected in such a way that the cubes contained both the chorionic and basal surfaces for better orientation. The cubes were washed in sterile PBS twice. The basal plate from the cubes was removed for access to healthy tissues within the cubes. Following that, villous material was dissected into smaller pieces, about $5mm^3$ in size. Areas that were pink were preferable, as overall these tissues typically gave a higher purity of trophoblasts. Tissues with visible blood vessels, fibrous area, and clotted blood were avoided. A small amount of PBS was needed to moisten the tissue. These steps were continued until about 45g of tissue was obtained. Then it was rinsed through gauze with PBS. Following this the tissue was minced with fine scissors, removing remaining visible vessels.

2.1.1.3 Isolation of cells

The placental fragment underwent three steps of digestion with HBSS (Invitrogen, Life Technologies, Paisley, UK), 2.5% trypsin (Invitrogen, Life Technologies, Paisley, UK) and DNAse (Roche Diagnostics Corporation, Indianapolis, IN, USA). Multiple digestion steps are required for adequate yield of trophoblasts; this method has been performed in most experiments of trophoblast isolation in the past (Kliman et al., 1986, Le Bellego et al., 2009). The HBSS and trypsin were pre-warmed and maintained at 37^{o}C. Firstly, placenta was placed in a 1L conical flask, incubated with 150ml of HBSS, 15ml of trypsin and 76200Kunitz units of DNAse for 30 minutes, on a shaker at 100rpm at 37^{o}C. After the incubation period, 100ml of the supernatant was removed. 25ml of the supernatant was layered over 5ml of heat inactivated newborn bovine serum (Invitrogen, Life Technologies, Paisley, UK) in a centrifuge tube; the trypsin in the cell suspension would be neutralised when it was centrifuged through the newborn bovine serum. The process was repeated until four tubes were obtained using up all the 100ml supernatant collected. For the second digestion, 100ml of HBSS, 10ml of trypsin and 50800Kunitz units of DNAse were added into the conical flask containing the explants for similar incubation as the first step. 100ml of the supernatant was collected for the same treatment as before. In the last digestion, 75ml of HBSS, 7.5ml of trypsin, and 38100 Kunitz units of DNAse were used. After the incubation, as much supernatant was pipetted and layered onto newborn bovine serum as before. While removing the supernatant, care was taken not to include the solid materials in the flask. Typically 100-150ml of supernatant was collected in the third digestion. The layered supernatant with newborn bovine serum was centrifuged at relative centrifugal force of 500 gravities (RCF) for 10 minutes. After centrifugation, the supernatant, including the white fluffy layer at the bottom, was decanted. About 1ml of DMEM was added to each pellet. The pellets were disrupted, and pooled into a centrifuge tube. The combined cell solution was topped up with DMEM to about 50ml in total to fill up the centrifuge tube. It was centrifuged at 500RCF for 10 minutes. The supernatant was discarded after centrifugation.

2.1.1.4 Purifying and maintaining the trophoblasts

Following the above steps, 6ml of DMEM was added to the pellet. 3ml of cell solution was layered at the top of each of the first two tubes of Percoll gradient prepared. The remaining cell solution left was layered at the top of the third tube of Percoll gradient. The Percoll/cell layers were centrifuged for 30 minutes at 1000RCF, with the brake off.

After centrifugation, different cells and tissues were localised in different Percoll layers. Bands of trophoblasts, with densities between 1.028 and 1.062g/ml, could be visually identified between the two lines marked at 35% and 55% Percoll concentrations (Fig 2.1). The lower density layers above the marked lines consist of mostly debris, Hofbauer cells and fibroblasts. Below the marked lines, the higher density cells were mostly white cells (Blaschitz et al., 2000). Tissues and cells of the layers above the trophoblast layers were removed carefully, with the aim to remove as many non-trophoblastic cells as possible while not disrupting the trophoblast layers. Then the trophoblasts were collected, leaving the other layers at the bottom of the tubes. The trophoblasts collected were pooled together in a centrifuge tube and topped up with cytomedium to the rim, with the total volume of at least 45ml. The trophoblast solution was centrifuged at 500RCF for 10 minutes. The pellet was resuspended with 1ml of cytomedium. Cells were counted and plated out according to the needs of the subsequent experiments to be performed on the cells. The number of cells was counted manually under the light microscope using the Neubauer haemocytometer. The number of cells in the four corner and the middle 1/25mm squares was counted. The count from these five squares was divided by 0.02 to give the total number of cells in a cubic millimetre. The number of cells in a millilitre (cells/ml), the same as 1 cubic centimetre, was obtained by multiplying the last number of count by 1000. Generally, for maintaining the trophoblasts, they were plated on 90mm petri dishes. The maximum cell count plated out was 13×10^6 cells in each dish.13ml of cytomedium was needed to cover the culture surface of each dish. The cells were incubated in a humidified atmosphere of 5% CO_2/95% air with standard level of 20% O_2 at 37^oC. 3ml of cytomedium was added into each dish daily for supplementation of the cytomedium. For the reporting of the in vitro experiments using the

trophoblasts, the day of the placenta collection and trophoblast isolation will be described as day 0.

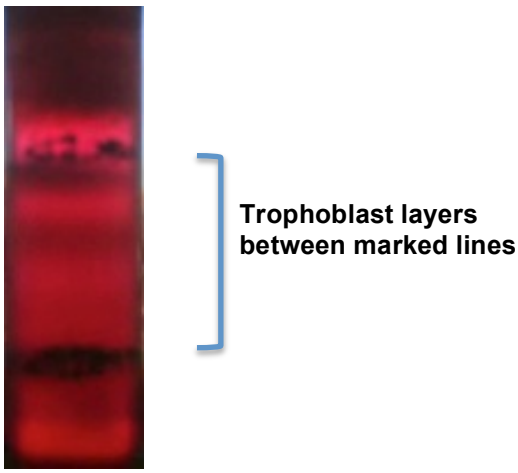

Figure 2.1 Percoll gradient showing the two lines marked at 35% and 55% layers, and the bands of trophoblasts in between these two lines.

2.1.2 Assessment of purity of trophoblasts by flow cytometry

An assessment of the purity of the trophoblasts was performed on day 1 and 2 after the cells were isolated and plated. Cytokeratin 7 and vimentin, for their positive and negative staining respectively, are reliable intracellular markers to assess the purity of trophoblasts (Maldonado-Estrada et al., 2004). Flow cytometry has been to shown to be highly objective and quantitative for this assessment (Pötgens et al., 2001). For the preparation of this experiment, initially the supernatant from the cells in the petri dish was collected into a centrifuge tube. 10ml of Non-enzymatic Cell Dissociation Solution (Sigma-Aldrich, Dorset, UK) was added into the dish and incubated at 37^{o}C for 10 minutes. Then the surface of the dish was gently scraped with a cell scraper to dislodge adherent cells. This suspension of adherent cells was pooled together with the supernatant collected earlier containing floating cells. The combined cell suspension was centrifuged for five minutes at 500RCF. The supernatant was decanted. 1ml of cytomedium was added, the number of cells was counted manually as described in section 2.1.1.4. Single colour flow cytometry was used to analyse the staining of the cells. The cells were aliquoted into three wells at 3 x 10^5 cells/well on a round bottom 96-well plate, for staining with cytokeratin 7, vimentin and isotype primary antibodies separately (Table 2.3). The cells were incubated with human FcR blocking reagent (Miltenyi Biotech Ltd, Bisley,

UK), and permeabilised with Cytofix fixation buffer (BD, Franklin Lakes, NJ, USA). After the washing steps with Cytoperm permeabilisation buffer (BD, Franklin Lakes, NJ, USA), they were incubated in primary antibodies, at 2.5µg/ml in 100µl/well of permeabilisation buffer. Only one primary antibody was used in each well, as this is a mono-colour flow cytometry analysis. The cells were washed again, and incubated further with secondary antibody (Table 2.3), with the volume of 1µl in 50µl of permeabilisation buffer. After more washing steps, the cells were suspended in FACS buffer before analyses in BD FACSCalibur flow cytometer (BD, Franklin Lakes, NJ, USA). Before the experiment samples were being fed through, the machine was set up for optimal data acquisition. The mode of the detectors was set as linear for the forward and side scatters, and log for the other parameters that measure the fluorescent intensities. The voltage and amp gain were adjusted so that the populations of interest were on scale in the dot plots. Then each sample was fed into the machine, left running until the fluid in the FACS tube was at the lowest level of the probe before it was manually stopped; this method allowed the maximal number of cells in each sample to be measured. Data were analysed using Flowjo 8.7.1 (Tree Star, Ashland, OR, USA). A cell was defined as being positive for a particular protein if it was brighter than 95% of the cells that had been treated with the isotype control antibody.

Antibody	Primary/ secondary	Specific/ isotype	Supplier
Monoclonal mouse anti-cytokeratin 7; Clone: OV-TL 12/30; Isotype: IgG1, κ	Primary	Specific	Dako UK Ltd, Ely, UK
Monoclonal mouse anti-vimentin; Clone: V9; Isotype: IgG1, κ	Primary	Specific	Dako UK Ltd, Ely, UK
IgG1, κ isotype control from murine myeloma	Primary	Isotype	Sigma-Aldrich, Dorset, UK
Polyclonal rabbit anti-mouse Ig (FITC)	Secondary	N/A	Dako UK Ltd, Ely, UK

Table 2.3 Antibodies used for assessment of purity of trophoblasts. FITC, fluorescein isothiocyanate.

2.1.3 HEK293 cells maintenance and passage

Wild type HEK293 and HEK293 stably transfected with D6 were maintained for use as control cells in the experiments. They were passaged every two to five days. The cytomedium for wild type HEK293 was made up of DMEM with sodium pyruvate (Gibco, Life Technologies, Paisley, UK), 1% of penicillin-streptomycin 100x solution (Gibco, Life Technologies, Paisley, UK), 10% of non heat-inactivated South American origin fetal bovine serum (Gibco, Life Technologies, Paisley, UK) and 1% of L-Glutamine solution (Sigma-Aldrich, Dorset, UK). For HEK293 transfected with D6, the cytomedium was the same as above but supplemented with G418 at 1mg/ml. The D6-expression plasmid transfected into HEK293 cells included a G418 resistant gene, so inclusion of G418 in the medium ensures that only cells containing the plasmid will grow thereby preventing loss of D6 expression.

2.1.4 Assessment of D6 mRNA expression

On the day of isolation (day 0), trophoblasts were plated out on 24-well plate at 1 x 10^6 trophoblasts per well in 0.5ml cytomedium. Cells in different wells were collected at day 1, 2 and 3 of culture for assessment of mRNA expression. For each RNA sample, four wells of cells from the same placenta were collected. The cytomedium in the four wells was removed. The wells were washed with 0.5ml of cytomedium. After removing this cytomedium, 1ml of TRIzol Reagent (Invitrogen, Life Technologies, Paisley, UK) was added into the first well. The well was gently scraped to dislodge adherent cells. After pipetting up and down several times, the cell suspension was moved to the next well. Similar processes were repeated, until all the 4 wells were treated. The cell suspension was stored in a labelled cryogenic tube for freezing at -80^{o}C. D6 transfected and untransfected HEK293 cells were used as control for comparison of D6 expression. During HEK293 cell passaging, for each RNA sample 4 x 10^6 cells were collected, centrifuged, treated with 1ml of TRIzol Reagent (Invitrogen, Life Technologies, Paisley, UK) and frozen at -80^{o}C.

The samples were passed through 25G needle on a syringe for 10 times. RNA extraction was carried out using TRIzol Reagent (Invitrogen, Life Technologies, Paisley, UK) and chloroform (Sigma-Aldrich, Dorset, UK). The extracted RNA was precipitated using isopropanol (VWR, Lutterworth, UK) and stored in 75% ethanol. Then it was solubilised in nuclease free water. The RNA concentration was determined using NanoDrop ND-1000 spectrophotometer (Thermo Scientific, Wilmington, DE, USA). The samples were stored in -80^{o}C.

The RNA underwent DNAse treatment using a DNAse treatment and removal kit (DNA-free, Ambion, Life Technologies, Paisley, UK). Following that, cDNA syntheses were carried out using High Capacity cDNA Reverse Transcription Kits (Applied Biosystems, Life Technologies, Paisley, UK), plus superasin (Ambion, Life Technologies, Paisley, UK) according to the manufacturer's instructions.

Expression of cytokeratin 7, D6 and CCR2 was measured using the synthesised cDNA. Each biological sample was analysed in duplicate. cDNA, 1x Taqman Universal PCR Mastermix (Applied Biosystems, Life Technologies, Paisley, UK), appropriate probe (Table 2.4), and nuclease free water were added for the

samples for loading into the 7900HT Fast Real-Time PCR System machine (Applied Biosystems, Life Technologies, Paisley, UK). The incubation condition was 95°C for 10 minutes, and then 40 cycles of 95°C for 15 seconds and 60°C for one minute. Data were analysed using 7900HT Sequence Detection Systems v2.3 (Applied Biosystems, Life Technologies, Paisley, UK). The final results were formulated using $2^{-\Delta C}{}_T$. C_T of the endogenous control gene, TOP-1, for each sample was subtracted from C_T of the target gene; this difference was depicted as ΔC_T. ΔC_T was normalised by antilog to base 2, and subsequently multiplied by 100 for displaying the final results in percentages (Goldman and Shalev, 2006).

Target gene (human)	Product ID
D6	Hs00174299_m1
CCR2	Hs00356601_m1
Cytokeratin 7	Hs00818825_m1
GAPDH (*endogenous control)	4310884E
TOP-1 (*endogenous control)	Hs00243257_m1
B-actin (*endogenous control)	4310881E
18s rRNA (*endogenous control)	4310893E

Table 2.4 Target specific and endogenous control human probes used for mRNA expression measurement. All products were from Applied Biosystems, Life Technologies, Paisley, UK.

2.1.5 Assessment of D6 protein expression

In-house monoclonal human D6 antibody is available in our laboratory in Glasgow Biomedical Research Centre at University of Glasgow. The details of the generation and characterisation of this antibody has been described previously (Nibbs et al., 2001). The antibody has been used in many subsequent publications (Weber et al., 2004, Madigan et al., 2010).

2.1.5.1 Western blotting

To prepare the reagents for trophoblast lysis, one tablet of Complete Protease Inhibitor Cocktail (Roche Diagnostics Corporation, Indianapolis, IN, USA) was dissolved in 10ml of CelLytic MT Cell Lysis Reagent (Sigma-Aldrich, Dorset, UK). The lysis reagent was stored in -20^{o}C.

Protein lysates were collected from two placentas, each at different day of trophoblast culture. For the first placenta, lysates were prepared at day 3 of culture. From the petri dish, the culture surface was gently scraped with a cell scraper. The cells were collected, centrifuged and resuspended in cytomedium. Six samples of lysate were prepared from this placenta; they were aliquoted into microcentrifuge tubes at 1 x 10^6 cells each. The samples were centrifuged at 450RCF for 5 minutes, at room temperature. The supernatant was discarded, 1ml of PBS was added to each tube. After this washing step, the tubes were centrifuged as before and the supernatant was discarded. Following this, the cell pellets were resuspended in 250µl of lysis reagent. Then the cell suspensions were vortexed, and left on the shaker on ice for 15 minutes. After the incubation, the cells were passed through a 21G needle on a syringe for ~30 times. The tubes were centrifuged for 15 minutes at 15000RCF, at 4^{o}C. Finally the lysates were collected into new microcentrifuge tubes and stored in -80^{o}C.

The lysates were prepared on day 2 of culture for the second placenta. For this placenta floating and adherent cells where prepared separately for different sets of lysates. The culture media were pooled into a centrifuge tube for the collection of suspension cells. For the adherent cells, each plate was incubated with 10ml of Non-enzymatic Cell Dissociation Solution (Sigma-Aldrich, Dorset, UK) for 10 minutes at 37^{o}C, gently scraped and the resulting cell suspension pooled into a tube. 2.585 x 10^6 of suspending cells and 8.46 x 10^5 of adherent cells were collected. The process of lysate preparation was the same as the first placenta. For each type of cells, 125µl of lysis reagent was used.

In the Western Blotting, each protein sample was prepared, comprising 20µl of the lysate, 5µl of NuPAGE LDS Sample Buffer (Life Technologies, Paisley, UK), and 2.5µl of NuPAGE Sample Reducing Agent (Life Technologies, Paisley, UK). Then the samples were incubated at room temperature for 10 minutes; to

prevent D6 aggregation they were not boiled (Blackburn et al., 2004). The process of electrophoresis of the protein was preformed on NuPAGE 4-12% Bis-Tris Gel 1.0mm, 10 well precast minigels, on the Novex NuPAGE Sodium dodecyl sulphate polyacrylamide gel electrophoresis (SDS-PAGE) Gel System (Life Technologies). First the wells were washed and filled up with NuPAGE MES SDS Running Buffer (Life Technologies, Paisley, UK). The gel was secured in the system, followed by loading of the samples into the wells. The chambers were filled with the running buffer until the wells were fully covered, electrophoresis was run at 200V for 52 minutes. This process was followed by transferring of the protein onto a Whatman nitrocellulose membrane. The gel was sandwiched with the nitrocellulose membrane, carefully rolling out excess air bubbles, and cushioned with filter papers and sponges. The sandwich was placed in the system and covered with the transfer buffer (NuPAGE Transfer Buffer (Life Technologies, Paisley, UK) + 10% methanol). The transferring process was run for 1 hour at 30V. After this, the nitrocellulose membrane was rinsed with distilled water, and incubated in 20ml of non-fat milk (5% Marvel in PBS-0.05% Tween 20 (PBST)) as a blocking agent overnight at 4^{o}C. After the incubation, the nitrocellulose membrane was cut into two parts, for staining separately with in-house D6 antibody (1:10 in 10ml PBST), and cytokeratin 7 antibody (1:1000 in 10ml PBST) (Table 2.3). The staining of cytokeratin 7 was to confirm of the presence of trophoblast cells. This incubation of primary antibodies took 2 hours on the shaker at room temperature. After this, the nitrocellulose membrane was washed with PBST for three times, at room temperature for five minutes in each time, before incubating with the detection antibody (1:10,000 in 10ml PBST) for 60 minutes at room temperature. The detection antibody was anti-mouse IgG HRP linked whole antibody from sheep (GE Healthcare, Little Chalfont Bucks, UK). After this incubation, the membrane was washed for another three times with PBST, covered with 2ml total of Supersignal West Femto Stable Peroxide Buffer and Supersignal West Femto Luminal/ Enhancer Solution at 1:1 ratio, and exposed to the X-ray film. Then the film was developed by Kodak X-Omat processor (Kodak, Rochester, NY, USA).

2.1.5.2 Flow cytometry

2.1.5.2.1 Intracellular staining

The process of mono-colour intracellular staining for D6 is similar to the staining for the assessment of trophoblast purity, as described above. Two different anti human D6 antibodies (mouse and rabbit) were used for the detection of intracellular D6. For the mouse anti-D6 antibody, the primary and secondary antibodies were 2.5µg/ml of in-house mouse anti-human D6 antibody and fluorescein conjugated goat F(ab')2 anti-mouse IgG (R&D Systems Inc., Minneapolis, MN, USA) respectively. Mouse IgG2a (Dako UK Ltd, Ely, UK) was used as isotype control. For the staining using rabbit antibody, the primary and secondary antibodies were 2.5µg/ml of rabbit anti human D6 antibody (Sigma-Aldrich) and fluorescein conjugated goat anti-rabbit IgG (R&D Systems Inc., Minneapolis, MN, USA) respectively. The isotype control was rabbit IgG (Dako UK Ltd, Ely, UK). Untransfected HEK293 cells were used as control cells.

2.1.5.2.2 Surface staining

The process of surface staining was largely similar to the description above, except that the cells were not permeabilised. Following plating on 96-well round bottomed plate, the cells were resuspended in 50µl/well in FACS buffer (PBS + 3% fetal bovine serum + 2mM EDTA + 0.01% NaN_3) containing 2µl human FcR blocking reagent (Miltenyi Biotech Ltd, Bisley, UK). After 10 minutes of incubation, primary in house mouse D6 or isotype antibodies at 2.5µg/ml in 100µl/well FACS buffer were introduced. The cells were incubated for 20 minutes on ice, and washed twice with FACS buffer before further incubation with 1:50 secondary antibody in 50µl/well FACS buffer. The cells had two further FACS buffer washes, and were then resuspended in 350µl of FACS buffer containing 7µl/well of 7-AAD staining solution (BD, Franklin Lakes, NJ, USA) for analysis in BD FACSCalibur. 7-AAD staining was used for dead cell exclusion. Compensation was adjusted for the dual colour staining, where live dot plot was set up with both channels of 7-AAD and fluorescein shown on the axes on the same graph. While running one of the samples prepared for compensation, with only 7-AAD or fluorescein staining, the compensatory controllers were calibrated until the overlapping or underlapping of the spectrum was corrected. The calibration process was repeated using the other untested (7-AAD or fluorescein)

sample, to compensate for the overlapping or underlapping on the opposite channel. Transfected and untransfected HEK293 cells were used as control cells.

2.1.5.3 Immunofluorescence

Trophoblasts, or transfected or untransfected HEK293 cells were seeded on 8-well chamber slides, at 2.4 x 10^4 cells/well with 400µl of corresponding media. Cells were cultured at 37°C, 5% CO_2. During the process of optimisation, different concentration of primary and secondary antibodies were used. The primary in-house mouse D6 and isotype antibodies were the same as those used for flow cytometry; the secondary antibody used was Alexa Fluor 488 F(ab')$_2$ Fragment of Goat Anti-Mouse IgG (Invitrogen, Life Technologies, Paisley, UK) or FITC conjugated Polyclonal rabbit anti-mouse Ig (DAKO UK Ltd, Ely, UK). Immunofluorescent staining was performed on day 2 of cell culture, at room temperature. The media were removed, and the cells washed with PBS. This was followed by ten minutes of fixation with 3.5% paraformaldehyde. The cells were washed twice with PBS, then incubated in 50mM NH_4Cl for 20 minutes to quench autofluorescence of unreacted aldehyde groups. After another step of washing with PBS, the cells were incubated with PGS (PBS, 0.2% gelatine, 0.05% saponin) for 30 minutes. Following that, PGS containing primary anti-D6 or isotype antibodies was introduced. After one hour of incubation, there were two further washes with PGS. Secondary antibody in PGS was introduced, and the cells were protected from light, incubated for 30 minutes. After three washes with PGS, the cells were incubated in 3.5% paraformaldehyde for a further 10 minutes. Finally the supernatant was removed, and the slides mounted with VECTASHIELD mounting medium with DAPI (Vector Laboratories Inc., Burlingame, CA, USA). Nail varnish was applied to secure the coverslips. The slides were viewed under fluorescent microscope Zeiss Imager.M2, the images were processed using Axiovision Rel 4.8 software.

2.1.6 Chemokine uptake assay

2.1.6.1 Immunofluorescence

Trophoblasts and HEK293 cells were incubated with the chemokines before staining with D6 antibodies. Cells were cultured for two days on 8-well chambers slides as described in immunofluorescence protocol above (section 2.1.5.3). The

media were replaced, with fresh medium containing 10nM synthetic human AlexaFluor647 CCL2 (Almac Group Ltd, Craigavon, UK) ($CCL2^{AF647}$) +/- competition of 100nM of CCL2 (Peprotech, Rocky Hill, NJ, USA) into relevant wells. The cells were incubated for one hour in cell culture incubator at 37°C, 5% CO_2. After the incubation period, the cells underwent fixation and staining for D6 protein detection as previously described.

2.1.6.2 Flow cytometry

Day 1 trophoblasts on petri dishes were collected and seeded on 96-well round bottom plate at 3 x 10^5 cells/well as described in previous flow cytometry protocols. The cells were centrifuged, and resuspended in 50µl of cytomedium containing 25nM $CCL2^{AF647}$, with or without 10-fold excess (250nM) of unlabelled competitor chemokines (Peprotech, Rocky Hill, NJ, USA). They were incubated at 37°C, 5% CO_2 for one hour. This was followed by two washes with FACS buffer, and subsequent resuspension of the cells in 350µl FACS buffer containing 7µl 7-AAD staining solution (BD, Franklin Lakes, NJ, USA) for dead cell exclusion, before analysis in BD FACSCalibur. Compensation was adjusted for the two colours. Controls were performed using the HEK293 cells.

2.1.7 Chemokine scavenging assay with quantitation by Western Blot

2.1.7.1 Optimisation process

100ng/µl of synthetic human biotinylated CCL2 (Almac Group Ltd, Craigavon, UK) (bioCCL2) was prepared, by reconstituting 10µg of the lyophilised chemokine with PBS. The chemokine underwent serial dilutions, to allow the determination of the minimum concentration detectable by Western blot. During the optimisation process for the Western blotting, different blocking agents, timings of blocking, enhanced chemiluminescent reagents and chemokine dilution reagents were tried to obtain the best signal to noise ratio on the films. The optimised protocol is outlined in the next section.

2.1.7.2 Chemokine scavenging assay on trophoblasts

1.5 x 10^6 cells/well of primary trophoblasts were seeded on 6-well plates in 1.5ml of cytomedium after cell isolation and purification from placentas and cultured at 37°C, 5% CO_2 overnight. The next morning, at day 1 of culture, 0.75µl of 100ng/µl bioCCL2 was added into all the wells, resulting in a final concentration of 5nM. In relevant wells, 7.5µl of 100ng/µl CCL3L1 (Peprotech, Rocky Hill, NJ, USA) was added as competitor chemokine, to a final concentration (50nM) that was 10x greater than the bioCCL2. Immediately after the chemokines had been introduced into the wells, 60µl of medium was collected from each well; these samples were the 0-hour samples. Following this the trophoblasts were returned to the incubator. At set time points, a series of aliquots of medium were collected from all the wells, up to 72 hours after chemokine addition.

Western blotting was performed on the samples from different time points to determine the level of bioCCL2 in the supernatants. Comparisons were made between samples with and without the competitor CCL3L1 chemokine. Wells without cells were used as negative control. The experiment was also repeated using non-D6 ligand CCL26 as the competitive chemokine. For the preparation of each sample, 20µl of harvested medium was added with 5µl Nupage LDS sample buffer (Invitrogen, Life Technologies, Paisley, UK) and 2.5µl 1x Nupage sample reducing agent (Invitrogen, Life Technologies, Paisley, UK). Samples were boiled at 70°C for 10 minutes, and loaded onto the wells of 10-well precast minigels, for the process of electrophoresis and transferring of the protein on the Novex NuPAGE Sodium dodecyl sulphate polyacrylamide gel electrophoresis (SDS-PAGE) Gel System (Invitrogen, Life Technologies, Paisley, UK). The electrophoresis was run at 200v for 36 minutes, and the transfer was run at 30v for 1 hour. After the transfer, the nitrocellulose membrane was blocked with 5% skimmed milk (Marvel) in PBST for 1 hour at room temperature on the shaker. This was followed by five shake rinses, and 4x five minutes washes with PBST at room temperature on the shaker. Then the membrane was incubated for 60 minutes at room temperature with 1:2500 of streptavidin-HRP (Invitrogen, Life Technologies, Paisley, UK) in 15ml PBST on the shaker. After the washing steps as before, the membrane was dried, placed in a sheet protector and covered with 2ml of Novex ECL Chemiluminescent Substrate Reagent Kit (Invitrogen, Life

Technologies, Paisley, UK). It was placed in the film cassette for exposure to the X-ray film. The films were developed by Kodak X-Omat processor. The films were scanned into TIFF files, for the calculation of Adjusted Volume in Quantity One version 4.6.2 software (Bio-Rad Laboratories Ltd, Hemel Hempstead, UK). The method of drawing the boundaries for calculation of Volume and Background Volume is as shown in Figure 2.2.

a)

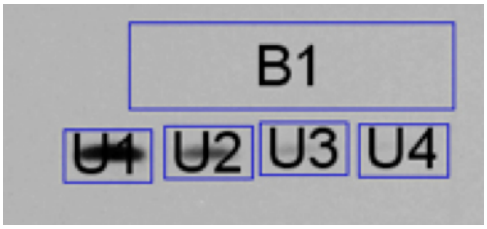

b)

Index	Name	Type	Volume INT*mm2	Adj. Vol. INT*mm2	% Adj. Vol.
1	U1	Unknown	2629.880213	997.6360119	64.40
2	U2	Unknown	2043.085650	410.8414491	26.52
3	U3	Unknown	1741.530678	109.2884775	7.06
4	U4	Unknown	1663.516492	31.27229159	2.02
5	B1	Background	9922.661792	0.000000000	N/A

Figure 2.2 Comparison of the intensities of the pixels of the bands (Adjusted Volume of the boundaries) from four different set time points. Volume is defined as the sum of the intensities of the pixels inside the volume boundary drawn, times the area of a single pixel (in mm^2). a) U1 to U4 were four boundaries of the same size drawn to completely include the four bands of interest from different set time points. The intensities of the pixels (Volume) within the boundaries were calculated by the software. B1 box is the boundary drawn within the unstained area of the nitrocellulose membrane, to determine the average intensity of the pixels in the Background Volume. Adjusted Volume of U1 to U4 were analysed, whereby the average intensity of the pixels in the Background Volume was subtracted from each pixel in these four boundaries. Any pixels inside U1 to U4 that have the same intensity as the average background will be reduced to zero, thereby eliminating them from the quantitation. b) The result of the calculations of Volume and Adjusted Volume.

2.2 In vivo study (mouse model)

2.2.1 Animals

DBA-1 mice, and DBA-1 mice homozygous (D6 KO) and heterozygous (D6 HET) for deletion of the D6 gene, were bred and maintained in the Central Research Facility, University of Glasgow. D6 deficient animals were derived from C57BL/6 D6 deficient mice but had been backcrossed for >10 generations with DBA-1 mice. All procedures were carried out in accordance with the regulations of United Kingdom Home Office. The youngest age for the adult mice used in our experiments was eight weeks and close age-matching was done where possible.

2.2.2 Data on stillbirth, neonatal death and pups weaned/ litter

Data were provided by the staff in Central Research Facility. A cohort of wild type (WT) and D6 KO mice were placed in a breeding programme. Females in late pregnancy were checked for newborns daily. Once all the pups were born and being nursed, the number of live pups and dead carcasses were counted. Carcasses that were noticed when the litter was first discovered were counted as stillbirths; the numbers of live pups were recorded as well. Pups that did not survive to weaning at day 18 to 21 after birth were recorded as neonatal deaths.

2.2.3 Record of perinatal deaths and weight changes during neonatal period

This experiment was carried out over a period of two months. WT or D6 KO females were caged with individual males with the same genetic background. The females that showed sign of pregnancy were removed from their male partners. Females that appeared to be in late stages of pregnancy were checked every 11-13 hours for the appearance of pups. Females that were in labour were subject to minimal disturbance. Once all the pups were born and being nursed, the number of live pups and dead carcasses were counted. The live pups were weighed and returned to the cages with the mothers. This process of counting and weighing live pups was repeated daily until they were six days old, and then alternate days thereafter until either all the pups were successfully weaned at day 18-21 of life, or when there was no live pups left in the litter. Females that were no longer nursing any live pups were caged with individual males with

similar genetic background again until they became pregnant for repeats of the experiment.

2.2.4 Timed mating of the animals

2.2.4.1 WT and D6 KO females

WT and D6 KO females were caged with individual males of the same genetic background overnight. The next morning the females were checked for evidence of a copulation plug demonstrating that copulation had taken place. Those females that exhibited a plug were caged separately, and the day the plug was discovered was recorded as embryonic day, E1, of gestation. At E10, 14 or 18, pregnant females were humanely sacrificed in accordance with Schedule 1 of the Animals (Scientific Procedures) Act for tissue collection. Those females that did not have a plug were placed back into the cage with appropriate males, with repeated timed mating. They continued to be checked daily, and were separated once the copulation plug was observed.

2.2.4.2 D6 HET female

After discovering the difference in the phenotype between the WT and D6 KO pups at E14, a different experiment was designed to ascertain whether the placental defect was due to a maternal or a fetal effect. Females heterozygous for the deleted D6 allele (D6 HET) were bred with D6 KO males, generating D6 HET and D6 KO pups in the same litter. This allowed the phenotype between these two groups of siblings, in a D6 expressing HET mother to be compared. For this study, D6 HET were caged together with individual D6 KO males overnight. They were separated the following morning regardless of the presence of copulation plug. At E14, those females that were pregnant were sacrificed by schedule 1 for tissue collection. Timed mating was repeated for the non-pregnant females until they conceived.

2.2.5 Tissue collection and processing

Pups and placentas were dissected and transported in Dulbecco's phosphate buffered saline (PBS) alongside their respective placentas. The wet weights of the pups and placentas, and also pup/placenta ratios were recorded. The

placentas were sectioned into two equal halves. One-half was stored in RNAlater RNA stabilisation reagent (Qiagen, Manchester, UK) for not more than a week, snap frozen with liquid nitrogen and stored at -80^{o}C, for RNA isolation. The other half was processed for stereology analysis. They were stored in 4% paraformaldehyde/0.1 M 1,4-piperazinediethanesulfonic acid (PIPES) solution overnight at room temperature, and transferred to 0.1 M PIPES buffer the following day. After a night in the PIPES buffer they were ready for tissue processing and embedding in paraffin. If there was any delay in tissue processing, the placentas were transferred to 75% alcohol after two nights in the PIPES buffer. During embedding, the half placentas were orientated such that the hemisectioned side of the placentas was facing downwards, directed towards the surface of the paraffin blocks for cutting. This side of the placentas became the starting point for the microtome sectioning process in stereological analysis.

Pups from D6 HET females were retained for genotyping. The PBS used for transporting was decanted, and the pups were kept in -20^{o}C. Maternal blood was collected and centrifuged; the plasma was collected and frozen at -80^{o}C.

2.2.6 Stereology

2.2.6.1 Microtome sectioning, mounting and staining

Four pregnant mice were used for each of the WT and D6 KO groups for comparison of placental stereology at each time point. For each pregnant mouse, two placentas with the pup/placenta ratio closest to the mean were chosen for stereological analysis.

In the D6 HET model, two D6 HET females were used for the experiment. For each of these females, four placentas with the pup/placenta ratio closest to the mean were chosen for each pup genotype group, resulting in the total of eight placentas for D6 HET and D6 KO siblings in each D6 HET female being used for stereological analysis.

Unfortunately due to the small size of mouse placentas, occasionally they would break during microtoming. If this occurred, the next placenta within the litter with the pup/placenta ratio closest to the mean was chosen.

The technique of stereology for human and mouse placenta has been described in the literature (Mayhew and Burton, 1997, Coan et al., 2004, Coan et al., 2005, Coan et al., 2006, Coan et al., 2008, Coan et al., 2010). To begin this experimental method on the mouse placentas, the selected embedded half placentas were exhaustively sectioned at 8μm until the entire tissue was sectioned. Sections were then collected from the beginning until the end of the sample, aligned according to the sequence of the sections. The total number of sections obtained per placenta was recorded.

15 sections, and backups, from a placenta were chosen systematically for mounting onto microscope slides. At the start of the process, a random number between one and 10 was generated using random integer generator on the internet: www.random.org. That random number generated would represent the first section to be chosen for mounting. The next section was also mounted as backup for the first mounting section. Then the subsequent number of sections left was divided by 15 to obtain a number (n). From the first mounted section, every nth sections were selected for mounting unto the slides until 15 sections and backups (30 in total) were mounted.

The mounted sections underwent haematoxylin and eosin staining. For E14 placentas, all 15 sections for each placenta were analysed by stereology. At E18, due to the higher volume of placenta that was needed to be analysed, eight out of the 15 sections per placenta were chosen for stereology analysis; these 8 sections were randomly selected using the random integer generator, with the number from one to 15 randomly generated. With the introduction of systemic and randomised, unbiased sampling at different levels in stereology, this experimental method validly and efficiently extrapolated three-dimensional (3D) volumes from systemic plotting of areas in two-dimensional (2D) sectional images (Mayhew and Burton, 1997).

2.2.6.2 Image analysis

The sections chosen for inclusion in the stereological analysis were magnified 100x under light microscope. The image was projected onto the computer screen using Image Pro 6.2 Plus (Media Cybernatics, Rockville, MD, USA). With this magnification, a number of fields were captured for a section to be completely

visible. The fields were aligned such that there was no overlapping, and the whole section was included for the analysis (Figure 2.3). Within each field, five grid points were randomly assigned using the grid of LineOrth.grd within the programme, where each grid point was shown as a '+' (Figure 2.4). The functional zones (decidua basalis, junctional zone, labyrinthine zone, chorionic plate) where the centre of each grid point fell upon were recorded. The total numbers of grid points that fell on each zone were added up for each placenta. Then the total number of grid points in each zone were divided by the total number of grid points in the placenta. The result was multiplied by 100 to give the calculation of volume fraction (% of total placental volume for each zone).

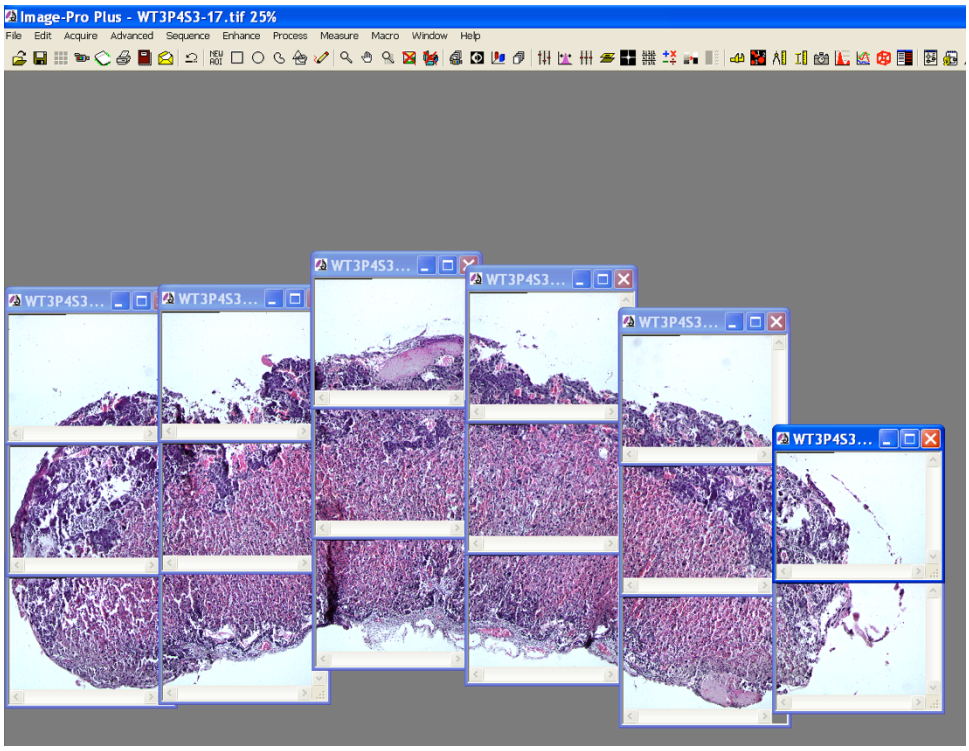

Figure 2.3 An example of the fields for a section of mouse placenta. The fields are non-overlapping, they include the whole section for stereological analysis.

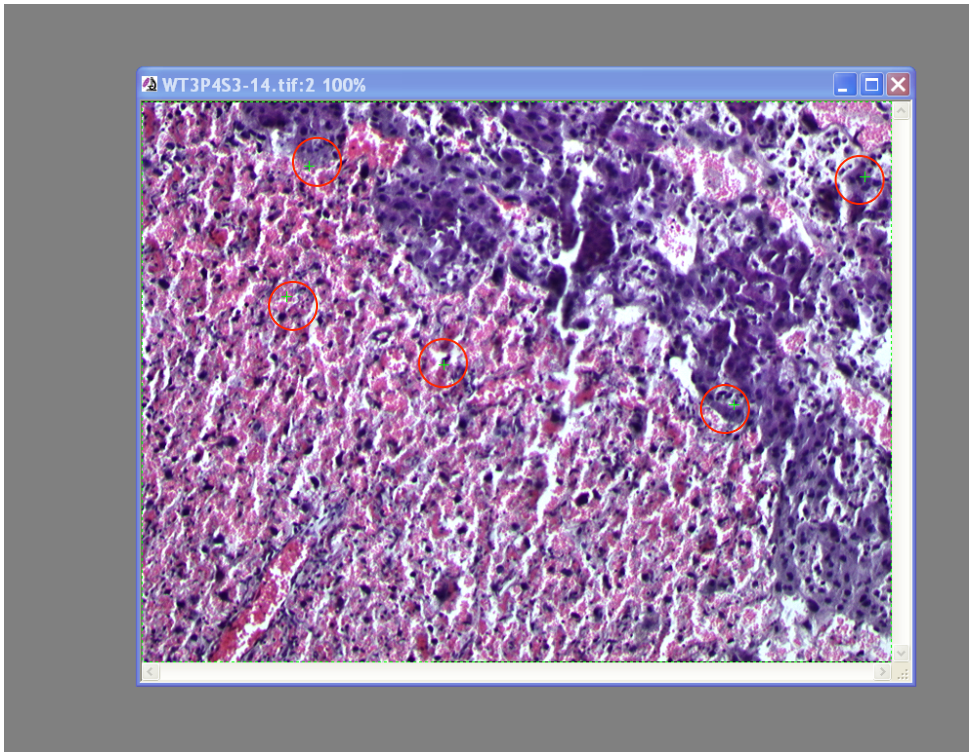

Figure 2.4 An example of five grid points being placed randomly for a field within a section of a mouse placenta.

2.2.7 Relative mRNA expression measurement by quantitative polymerase chain reaction (qPCR)

8 placentas from each of the WT and D6 KO group were chosen for the comparison of mRNA expression. These total of 16 placentas were the same as the ones selected in the experiment of stereology (section 2.2.6.1).

The processes of RNA extraction, DNAse treatment, cDNA synthesis and mRNA expression analysis were the same as the previous description in section 2.1.4, using the primers shown in Table 2.5. Expression of D6, chemokines and leukocyte markers was measured using the synthesised cDNA. $2^{-\Delta C}{}_{T}$ was formulated; the endogenous control gene was GAPDH.

Target gene (mouse)	Product ID
CCL2	Mm00441242_m1
CCL3	Mm99999057_m1
CCL4	Mm00443111_m1
CCL5	Mm01302428_m1
CCL11	Mm00441238_m1
CCL12	Mm01617100_m1
CCL17	Mm00516136_m1
CCL22	Mm00436439_m1
D6	Mm00445551_m1
Foxp3	Mm00475162_m1
F480	Mm00802529_m1
CD3	Mm00438095_m1
GAPDH (*endogenous control)	4352932E
B-actin (*endogenous control)	4352933E

Table 2.5 Target specific and endogenous control mouse probes used for mRNA expression measurement. All products were from Applied Biosystems, Life Technologies, Paisley, UK.

2.2.8 Genotyping of pups from HET females crossbreeding with D6 KO males

5mm of tissues were removed from the head of the pups and incubated with 100µl of lysis buffer (Table 2.6) and 100µl of 100µg/ml proteinase K (Promega, Madison, WI, USA) overnight at 55°C to prepare the samples for the genotyping. The following morning the samples were incubated at 85°C to denature the proteinase K. Then 500µl of sterile water was added to each sample.

Genotyping lysis buffer
100mM Tris-HCL pH 8.5 5mM EDTA 0.2% SDS 200mM NaCl

Table 2.6 Reagents for tail tip lysis buffer.

For each PCR reaction, 2.5µl of primer mix (Table 2.7) and 2µl of each sample were added into a pre-aliquoted ready-mix master mix, flat cap thermo tube (Thermo Fisher Scientific, Waltham, MA, USA). This triplex approach to PCR reveals the 2 bands of 506bp and 357bp, for the wild type and the targeted alleles respectively. The presence of both bands would indicate a D6 HET.

Primer/ solution	DNA sequence	Concentration
D6 wild type	AGC ACG AAG ATC AGG CTG TAG AC	1µM
D6 common	TGG GGA TAC AGT CTT CAT GGT TC	2µM
3 IRES	CCC TAG ATG CAT GCT CGA CG	1µM

Table 2.7 Primer mix for genotyping. The primers were synthesised by Integrated DNA Technologies, Coralville, IA, USA.

PCR was run on a Veriti 96 Well Thermal Cycler (Applied Biosystems, Life Technologies, Paisley, UK). The PCR conditions were 94°C for five minutes,

followed by 35 cycles of 94°C for 15 seconds, 55°C for 30 seconds, 68°C for 45 seconds; and the final step of 68°C for 10 minutes. The gel was made up of 1.5g Seakem LE Agarose (Lonza, Basel, Switzerland) in 100ml TAE buffer (1.5%), with 10µl of SYBR safe DNA gel stain (Invitrogen, Life Technologies, Paisley, UK). Electrophoresis was at 100 volts for 30 minutes. The ladder used was 1Kb Plus DNA Ladder (Invitrogen, Life Technologies, Paisley, UK). After electrophoresis, the gel was transilluminated on the Alphalmager gel imager (Alpha Innotech, Proteinsimple, Santa Clara, CA, USA).

2.2.9 Quantification of chemokine levels in plasma using Luminex multiplex protein assay

Chemokine levels were measured in the plasma from the pregnant females using Luminex protein assay. We used the inventoried singleplex bead kits for the chemokines, plus the buffer reagent kit from Life Technologies, Paisley, UK (Table 2.8).

Mouse singleplex/ buffer reagent kit	Bead region	Product ID
MCP-1(CCL2) bead kit	29	LMC1011
MIP-1α (CCL3) bead kit	26	LMC1021
RANTES (CCL5) bead kit	21	LMC1031
KC (CXCL1) bead kit	41	LMC1061
Extracellular protein buffer reagent kit for mouse or rat	-	LMB0001

Table 2.8 Bead regions for the chemokine singleplex bead kits, and the product ID for the bead kits and buffer reagent kit for the Luminex protein assay. All products were from Life Technologies, Paisley, UK.

The Luminex was run in collaboration with Dr Chris Hansell, postdoctoral researcher in Dr Nibbs's chemokine research group. The assay was carried out following the procedure described in the manual, on the 96 well filter plate

supplied with the buffer reagent kit. All reagents were supplied with the kit. The wash solutions, antibody beads, biotinylated antibodies and streptavidin-RPE were supplied as 10x concentrates: they were diluted to 1x concentration prior to starting the experiment. The antibody beads and biotinylated detector antibodies from the four different chemokines were combined while being diluted into the 1x dilutions. A standard curve was made by preparing serial dilutions of reconstituted lyophilised standards provided with the kits. Aspiration of liquid from the filter plate was performed on a vacuum manifold with gentle vacuum lower than 5mmHg.

For the Luminex assay, the minimum volume required for each reaction was 50µl. The volumes of plasmas obtained were variable. Samples with more than 100µl of volume were run in duplicates. The chemokine levels were determined by using the average of the two wells. Samples with less than 100µl, but more than 50µl available were run as singles. Some samples had less than 50µl of plasma and in these cases we added assay diluent to make the volumes up to 50µl. For this group the concentrations of proteins were adjusted post-hoc according to the dilution factors.

All samples were clarified by 10 minutes centrifugation before the assay. The assay wells were pre-wet with wash solution and incubated for 30 seconds, before the liquid was aspirated. Then 50µl of the vortexed and sonicated diluted bead solution was pipetted into each well. The plate was protected from light from this point as the beads were light sensitive. 200µl of wash solution was added into each well. It was incubated for 30 seconds before liquid aspiration. The wells were washed with 200µl of wash solution. After aspiration, 50µl of incubation buffer was added into each well. For the wells designated for the standard curve, 100µl of relevant standard dilutions were pipetted. For the rest of the wells, 50µl of assay diluent followed by 50µl of samples were added. The plate was incubated for two hours on a shaker. After the incubation, 2 washing steps were performed, before adding 100µl of biotinylated detector antibodies into each well. This was followed by one hour incubation on the shaker. The procedure was followed by two washing steps, before incubated with 100µl of Streptavidin-RPE for 30 minutes on the shaker. After three further washes, 100µl of wash solution was added to each well. The plate was left overnight at 2^{o}C. The next morning, the wash solution on the wells was aspirated before 100µl

fresh washing solution was added. The plate was left on the shaker for 5 minutes to re-suspend the beads before analysed through the Bio-Plex System machine (Bio-Rad Laboratories Ltd, Hemel Hempstead, UK). Data were analysed by Bio-Plex Manager Software 4.0.

2.3 Statistical analysis

Appropriate statistical tests were applied for the analyses of the data using Graphpad Prism Software and are indicated in the legends to the data figures in the results chapters. For the analysis of the result from the mouse serum chemokine levels by Luminex, linear mixed effect modelling was used to take into consideration the different embryonic age of E14 and E18 within the WT and D6 KO groups. Linear mixed effect modelling analysis was performed using SPSS version 19. $P<0.05$ was considered statistically significant for all analyses.

3 Studying the Function of D6 on Cultured Primary Human Trophoblasts

3.1 Selecting primary cell culture over immortalised trophoblast-derived cell lines

D6 protein is abundant in the human placenta (Martinez de la Torre et al., 2007, Madigan et al., 2010). Given the protective effect of D6 observed on mouse reproduction, there is interest in understanding the distribution and function of D6 in human trophoblasts. Studies of the expression, distribution and action of D6 using human choriocarcinoma cell line BeWo have been carried out in the past (Martinez de la Torre et al., 2007, Madigan et al., 2010). Using this cell line for the experiments showed what D6 could potentially do in human trophoblasts, but the results may not be representative of the true property of D6 in the physiological environment in the human placenta. Immortalised cancer-derived cell lines have been modified, maintained, and passaged in a regulated, artificial in vitro environment over a long period of time. Therefore they may have undergone huge transformation, producing very different gene expression profiles and phenotypes in comparison to the original cells (Whitley, 2006). In contrast, primary cells are more closely reflective of the biological process in the human body, and their study brings us closer to the understanding of the role of D6 in the placenta in this instance. Thus for my in vitro study primary human trophoblasts were used.

Using primary trophoblasts from fresh placenta did have some technical disadvantages. Firstly a significant amount of time and effort had to be invested to obtain ethical approval for the research. For each of the experiments, there was the inconvenience of obtaining fresh placenta and culturing trophoblasts. The lifespan for these primary cells is not long; trophoblasts proliferate poorly in culture before undergoing replicative senescence (Whitley, 2006, Orendi et al., 2011). They form multinucleated syncytial complex within 48 to 72 hours (Newby et al., 2005). Due to the above reasons there was limited time to carry out the experiments once the cells were plated. It was appreciated that there was heterogeneity between placentas, and the culture from primary cells will not be as pure as maintained cell lines. Furthermore, at the time when the experiments were conducted, trophoblast isolation and culture had not been performed in the laboratory. The technique had to be established, and the technology for routine primary trophoblast isolation and culture from fresh placentas had to be set up. Despite these difficulties, the efforts of culturing trophoblasts are

worthwhile, because to gain a more realistic insight of D6 function in the human placenta, it is crucial to look at the function of D6 on primary cells.

3.2 Optimising the protocol for trophoblast isolation

The isolation, purification and analysis of trophoblasts was not routinely performed in our laboratory at the beginning of the project. It took much longer than expected to optimise the protocol, due to the fastidious steps and time spent on familiarisation with the batch-to-batch physical and cellular variability of the placentas. The aim of refining the protocol was to achieve high trophoblast purity, and yield optimal number of cells. Flow cytometry was used to assess the purity of trophoblasts, as it is more objective and quantitative than cytospin preparation or staining on the culture plate (Frank et al., 2001). The recommended antibodies for the identification of trophoblasts from other cells are anti-cytokeratin 7 and anti-vimentin. Trophoblasts should express cytokeratin 7 and not vimentin (Pötgens et al., 2001). For the staining for these intracellular cytoskeletal proteins, the cells were permeabilised. Cytokeratin 7 was chosen as it is the most specific protein for all subpopulation of trophoblasts, in comparison to other isoforms of cytokeratin which can be expressed even in the mesenchymal cells of the placenta (Frank et al., 2001). For instance cytokeratin 18 and cytokeratin 8 had been identified in stroma of stem villi and cells from the lineage of a first trimester fibroblast-myofibroblast respectively (Blaschitz et al., 2000).

For trophoblast isolation, it is well recognised that there can be substantial batch-to-batch variability of the purity of the cells. It has been recommended that preparations with 50% or more cytokeratin positive cells should be used in trophoblast research (Frank et al., 2001). In the experiments the number of cells and purity of trophoblasts isolated varied between placentas; however they improved over time as the protocol was being established. After optimisation of the techniques, there was no difficulty in repeatedly obtaining cultures that contained over 50 million cells from a single placenta; more than 70% of the cells were trophoblasts when analysed at day 1 of culture (Fig 3.1). The viability of the cells at day 1 was between 14 to 36%. As the experiments spanned across two to three days, the purity and viability of the cells were also analysed at day 2 of culture. At this time of culture, the purity was maintained at between 67

to 80%, whereas the viability varied between 12 and 34%. The method of physical gating based on forward (FSC) and side-scatter (SSC) characteristics of the trophoblasts was not dissimilar to that previously described (Maldonado-Estrada et al., 2004, Trundley et al., 2006), eliminating events with very small FSC and SSC, which are probably non-viable cell fragments. Figure 3.2 shows views of trophoblasts under light microscope at different days of culture. Typically on day 1, the cultured cells in suspension started to form colonies. By day 2, more cells had adhered to the tissue culture dish but many of the cells had died. On day 3 and 4, most of the cells had adhered together to form larger colonies; at this stage the trophoblasts should have gone through the process of syncytialisation (Newby et al., 2005). The appearance of the cultured cells on the dish was showing the characteristics resembling multinucleated syncytial units. However, more tests would be necessary to confirm that cell fusion has occurred in these cultures.

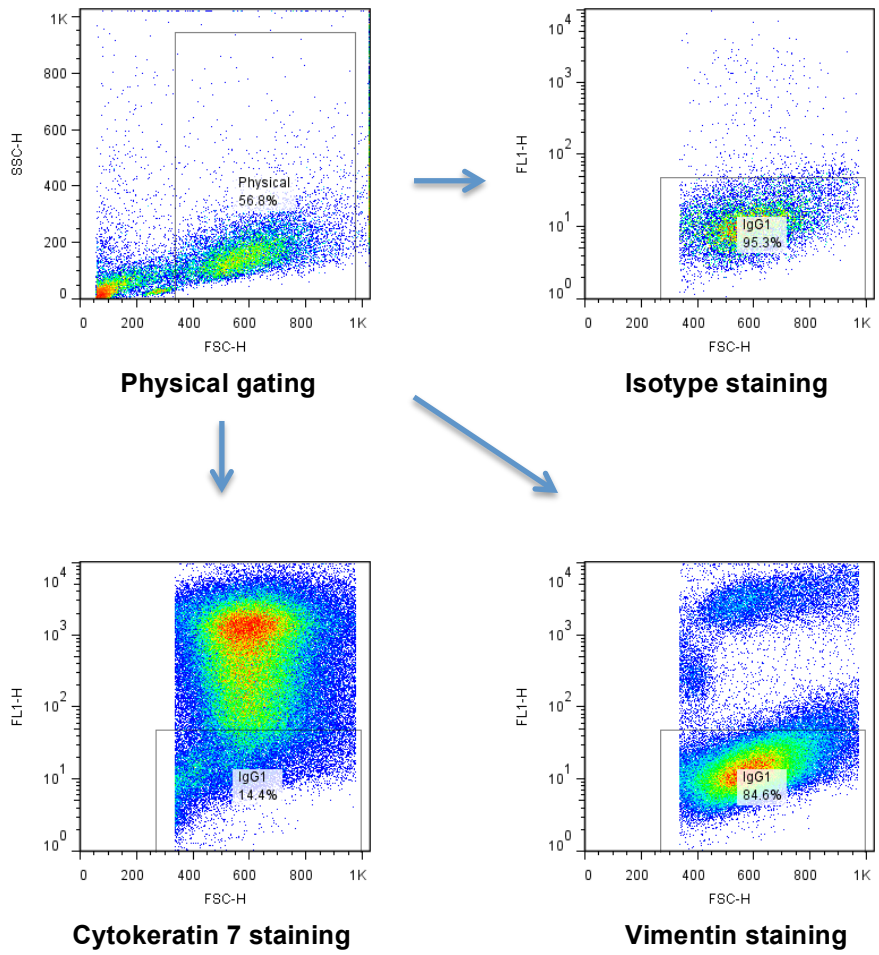

Figure 3.1 Purification process of placental cells using Percoll gradient yields satisfactory purity of trophoblasts. Assessment of trophoblast purity by flow cytometry from the cells isolated and purified from one placenta. Permeabilised cells were stained with either isotype control mIgG1, cytokeratin 7 or vimentin antibodies. First they underwent physical gating (top left); then the negative gating was set to including 95% of cells treated with the isotype control antibody (top right). For this placenta the yield of trophoblasts was 85.6% based on cytokeratin 7 positivity (bottom left), and confirmed by vimentin negativity (84.6%) (bottom right).

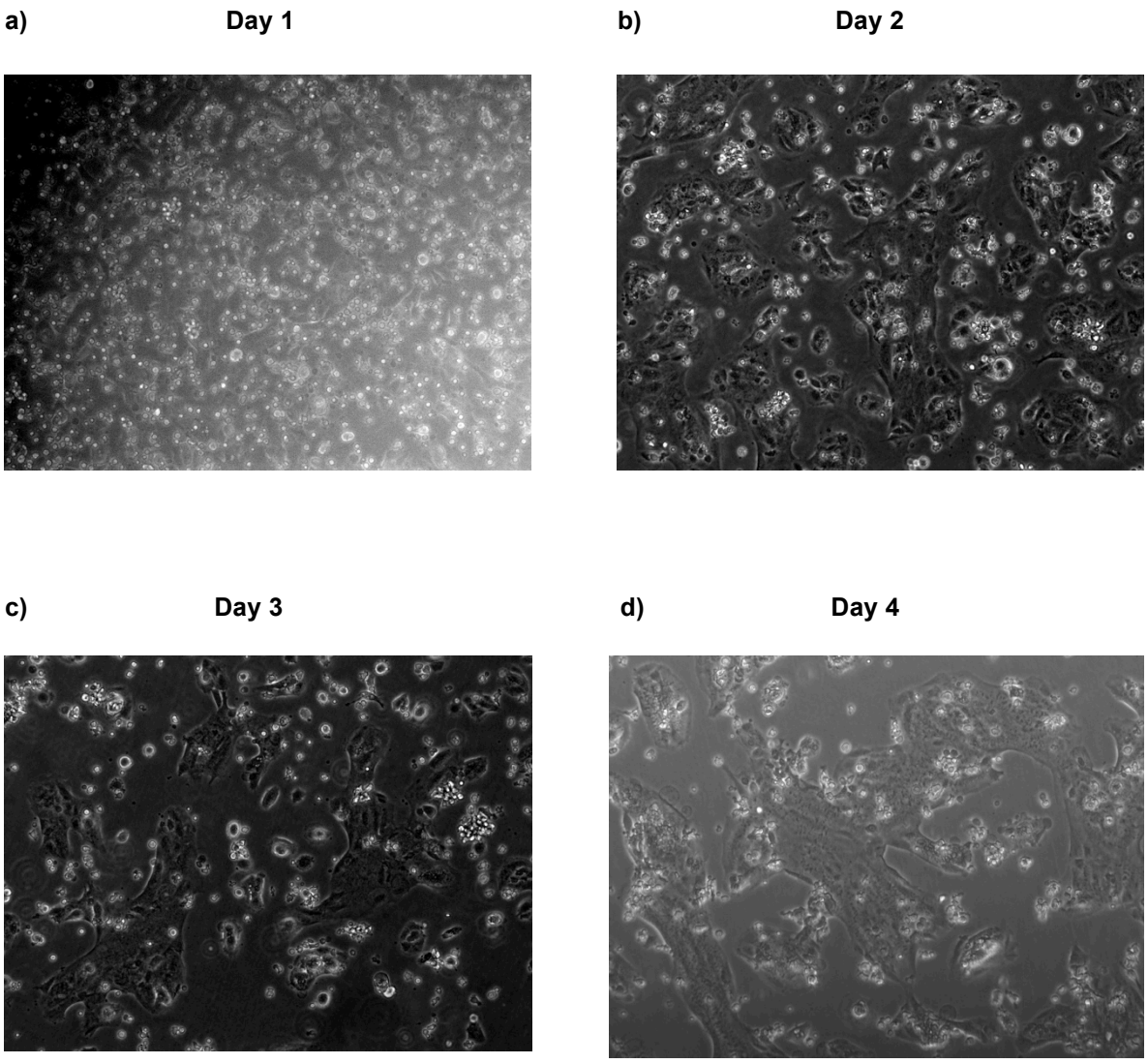

Figure 3.2 **Views of trophoblasts under light microscope at 100x magnification.** Photos of trophoblast culture on 90mm petri dishes on a) day 1; b) day 2; c) day 3 and d) day 4 of culture. Over time the cells adhered and formed colonies, this may be due to the effect of syncytialisation.

3.3 Assessment of D6 mRNA expression in cultured primary trophoblasts

The first step of the experiment in trophoblast culture was to examine if the D6 gene was expressed in the cultured cells. HEK293 cells transfected with D6 expression constructs, and untransfected parental HEK293 cells, were included in the analysis as it was expected that they would act as positive and negative controls, respectively. To study the expression of D6 mRNA, first an appropriate endogenous control gene had to be established. The expression of glyceraldehyde-3-phosphate dehydrogenase (GAPDH), topoisomerase 1 (TOP-1), B-actin and 18s rRNA was assessed in the samples, identifying the ones with low variability of expression between HEK293 cells and trophoblasts at different days

of culture. These housekeeping genes have been used in primary and cell lines for trophoblasts and HEK293 cells (El-Shewy et al., 2006, Goldman and Shalev, 2006, Hannan et al., 2006, Escobar et al., 2011). For my experiment, TOP-1 was chosen as my endogenous control; it was found to have the smallest standard deviation of expressions between trophoblasts and HEK293 cells (data not shown). For assessment of D6 expression, the probe/primer set that spanned an exon junction was chosen to reduce the risk of genomic DNA amplification. CCR2 expression in the primary trophoblasts was also analysed, as it had been reported to be expressed in cells from the fetomaternal interface, and shares some of the ligands with D6 (Hannan et al., 2006). It was planned that later in the experiments, CCL2, a chemokine ligand for D6 and CCR2, was to be used to explore the function of D6 on trophoblasts. Thus, insight into CCR2 expression was considered important at this stage. As a positive control, the expression of cytokeratin 7 was analysed. In these experiments, the genes of interest were analysed by relative quantification, normalising to the expression of the housekeeping gene TOP-1, which had low variability of expression between samples. Thus by qPCR the expression of D6 and other genes could be quantitatively compared between different cells.

In trophoblasts, cytokeratin 7 was expressed at a very high level and D6 was also expressed abundantly. Although there was a drop in cytokeratin 7 expression on day 2 of culture, this was not accompanied by a reduction in D6 expression. The drop in cytokeratin 7 on day 2 may be an artefact due to technical variability, as the high expression of these transcripts was detected using one placenta. There was some expression of CCR2 transcript, albeit detected at a level much lower than D6 (Fig 3.3). Thus, it appears that D6 transcripts are more abundant than those encoding CCR2, although it is possible that differences in the efficiency of the primers used to detect D6 and CCR2 contributed to apparent differences in expression of the two receptors.

Using the same primers, D6 mRNA was not detected in HEK293 cells that had been stably transfected with D6 expression constructs. This was not initially expected. Following this discovery the design of the construct used to make the transfected HEK293 cells was discussed with other team members in the research group, and it was confirmed that the D6 cDNA used did not contain the exon junction of the primers used for the detection. Thus, retrospectively the

result from HEK293 transfected with D6 expression constructs was exactly what would have been expected.

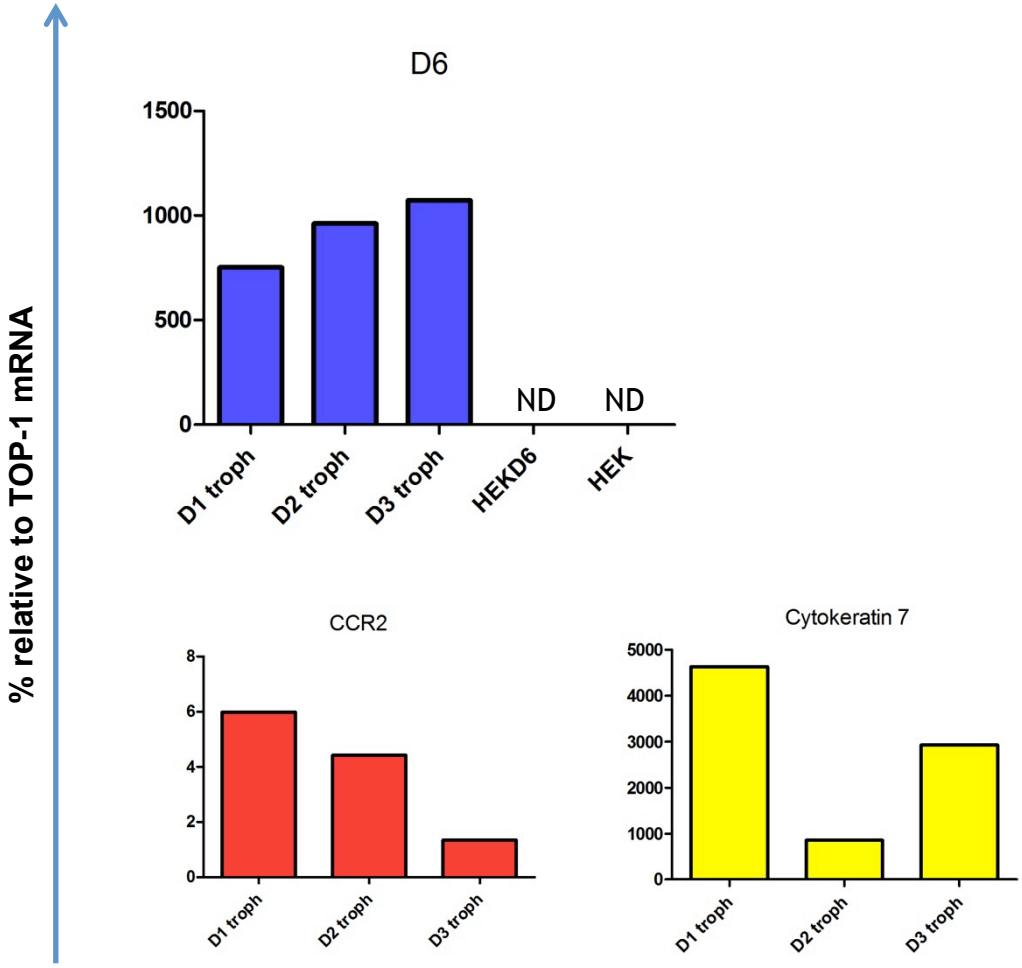

Figure 3.3 D6 is expressed in abundance in trophoblasts at mRNA level. Expression of D6 and CCR2 were detected in trophoblasts. Using our probe, D6 was undetectable on HEKD6 cells, as transfected D6 did not contain the exon junction of the primers used for the detection. Results from one placenta. D1, D2, D3 troph= Day 1, 2 and 3 trophoblast culture. HEKD6= HEK293 transfected with D6 expression constructs. HEK= untransfected HEK293. ND= not detected.

3.4 Assessment of D6 protein expression in cultured primary trophoblasts

3.4.1 Western blotting

The qPCR data suggested strong expression of D6 transcripts by primary cultured trophoblasts from days 1 to 3. Next, the expression of D6 protein in cultured trophoblasts was explored. Two placentas were used in this experiment, and controls were HEK293 +/- transfection with D6 expression constructs. For the first placenta, 8 x 10^4 adherent and floating trophoblasts at day 3 (sample T1)

were pooled together prior to preparing the cell lysate. For the second placenta, lysates were generated separately from 1.35 x 10^5 adherent (sample T2a) and 4.14 x 10^5 floating cells (sample T2b) at day 2. All samples were electrophoresed on polyacrylamide gels and Western blots prepared (Fig 3.4). These blots were probed with antibodies against cytokeratin 7 and D6. All 3 placental samples stained positively for cytokeratin 7, confirming the presence of trophoblasts. Sample T2a clearly contained the most cytokeratin 7 protein followed by T1 and then T2b (Fig 3.4a). This suggested that the quantity of trophoblasts present between the samples was different, either due to them being more abundant in the T2a sample, or that a more concentrated cell lysate had been used. D6 staining showed that the protein was most detectable in sample T2a, but it was also faintly present in sample T1. In sample T2a, there were two weakly stained bands that electrophoresed in a manner similar to those seen in the HEK293 cells transfected with D6 expression constructs (HEK-D6). In HEK-D6 cells there were two major bands on the blot at approximately 46 and 49kDa. The higher molecular weight band is due to N-linked glycosylation which is dispensable for chemokine binding by D6 (Blackburn et al., 2004). Much of the trophoblast D6 protein was slightly larger than the bands in the HEK-D6 cells suggesting that it might have undergone additional post-translational modifications in trophoblasts. Thus, cultures of human trophoblasts prepared fresh from human placentas contain cells expressing D6 protein.

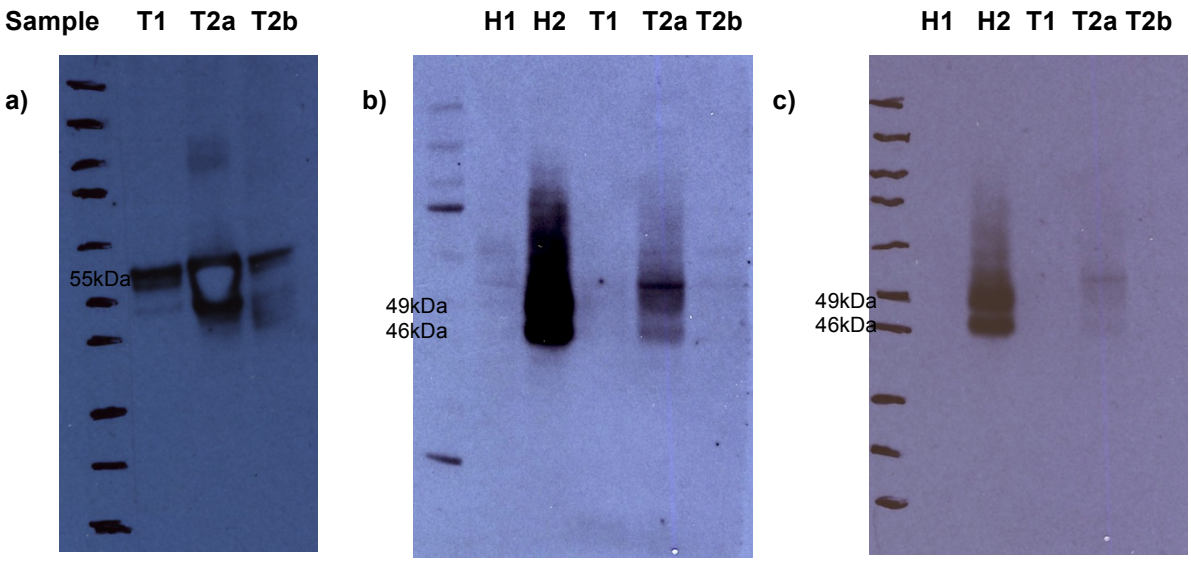

Sample Code	Sample	Number of cells
H1	Untransfected HEK293	80 x 10^3
H2	D6 transfected HEK293	80 x 10^3
T1	Day 3 floating and adherent cells	80 x 10^3
T2a	Day 2 adherent cells	135 x 10^3
T2b	Day 2 floating cells	414 x 10^3

Figure 3.4 D6 protein detected on trophoblasts by Western blot. a) Cytokeratin 7 staining; b) and c) for better appreciation of the bands for both HEK293 and trophoblast cells, two different exposure times were shown for the same blot stained with D6 antibody. In this experiment three lysates were prepared from two placentas. Lysate T1 was prepared from adherent and floating cells from one placenta. Lysates T2a and T2b were adherent and floating cells respectively, from a different placenta. T2a had the strongest staining of D6, corresponding with the highest number of trophoblasts based on its cytokeratin 7 staining.

3.4.2 Immunofluorescence to explore subcellular distribution of D6 in cultured trophoblasts

D6 protein has been successfully detected in and on HEK293 transfected with D6 expression constructs by immunofluorescence. In HEK293, most D6 is inside the cells associated with early and recycling endosomes (Weber et al., 2004, McCulloch et al., 2008), and this also appears to be the case in trophoblasts in placental sections (Madigan et al., 2010). Thus the cells were examined to ascertain whether D6 had a similar subcellular distribution in cultured trophoblasts. The results using HEK-D6 cells shown in previous experiments could be replicated in our laboratory (Fig 3.5). No anti-D6 immunostaining was observed in untransfected HEK293 cells, and isotype-stained HEK-D6 cells were also negative. Using the same staining method, D6 was also detected in trophoblasts on day 2 of culture (Fig 3.6). The experiment was conducted on day 2 because by this time there would be fewer cells being lost during wash steps, as trophoblasts become more adherent in comparison to day 1. The pictures of trophoblasts were not as impressive as the ones on HEK293. The background staining was higher on trophoblasts; the staining of D6 was detectable but not as bright as the control cells. This could be due to the presence of contaminating non-trophoblastic cells from the culture. By day 2, a number of trophoblasts would have syncytialised, causing heterogeneity in cell architecture and D6 expression. The result can also be explained by the lower physiological expression of D6 protein, as opposed to the artificially transfected HEK293 cells. However, in those cells in the trophoblast cultures that were convincingly stained with the anti-D6 antibody, it appeared that the majority of the D6 was inside the cells in a similar manner to that seen in D6 transfected HEK293 cells. Previous work has shown that D6 continuously traffics to and from the cell surface in HEK293, with only <5% on the cell surface at any one time. This is important for its scavenging activity in these cells.

a) x20 magnification

D6 transfected HEK293 cells stained with anti-D6 antibody	D6 transfected HEK293 cells stained with isotype
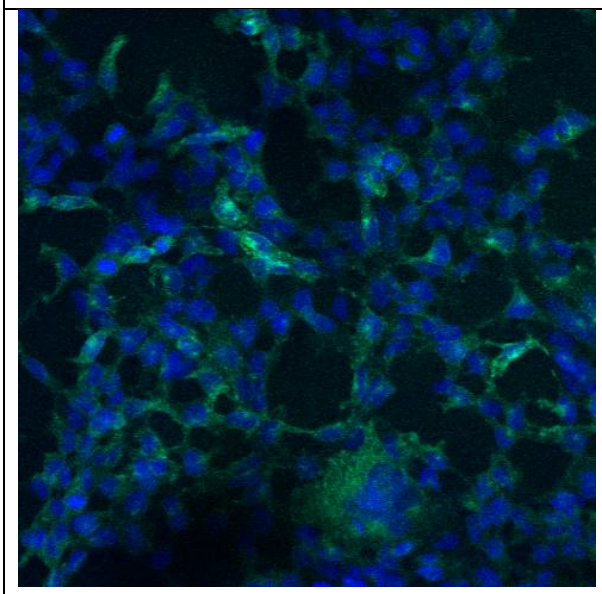	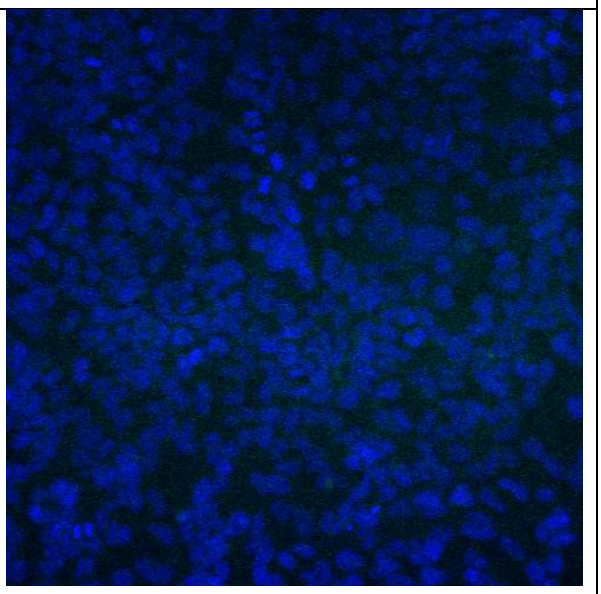
Untransfected HEK293 cells stained with anti-D6 antibody	
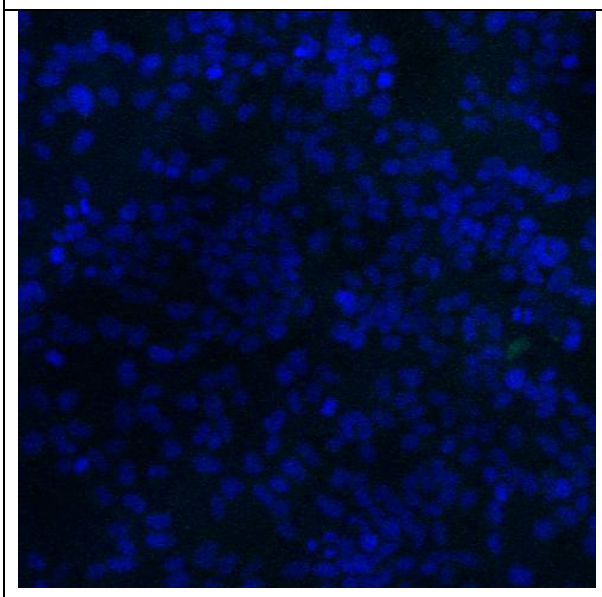	

b) x40 magnification

D6 transfected HEK293 cells stained with anti-D6 antibody	D6 transfected HEK293 cells stained with isotype
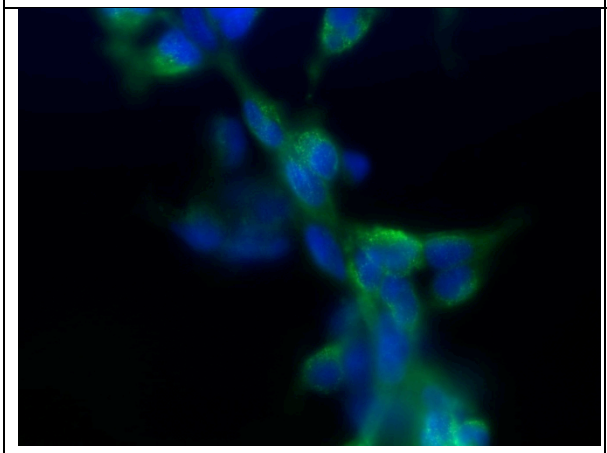	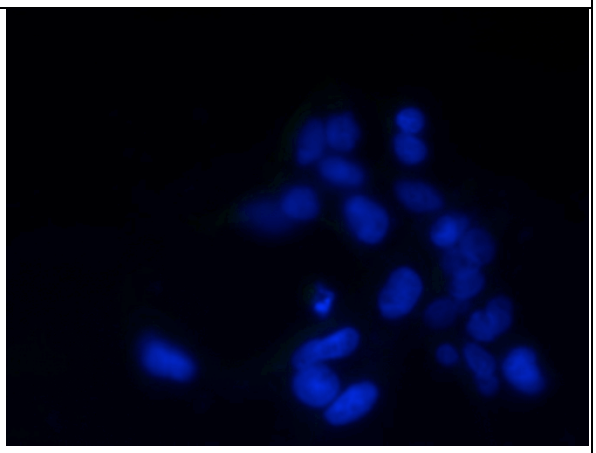
Untransfected HEK293 cells stained with anti-D6 antibody	
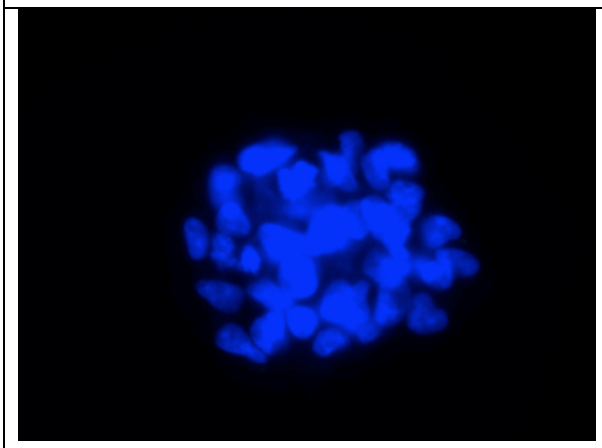	

c)

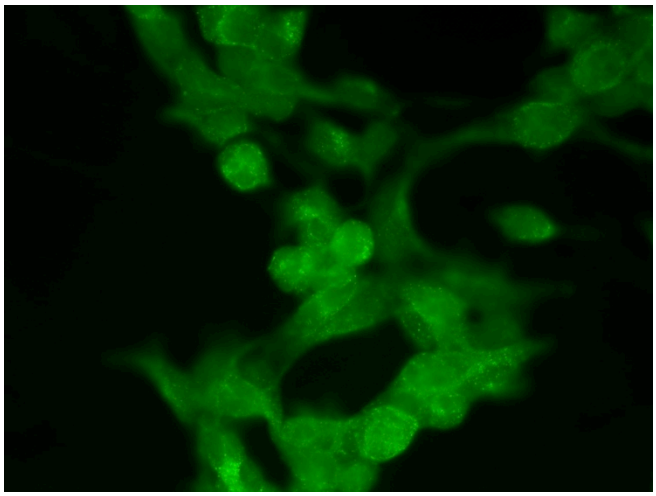

x40 magnification

d)

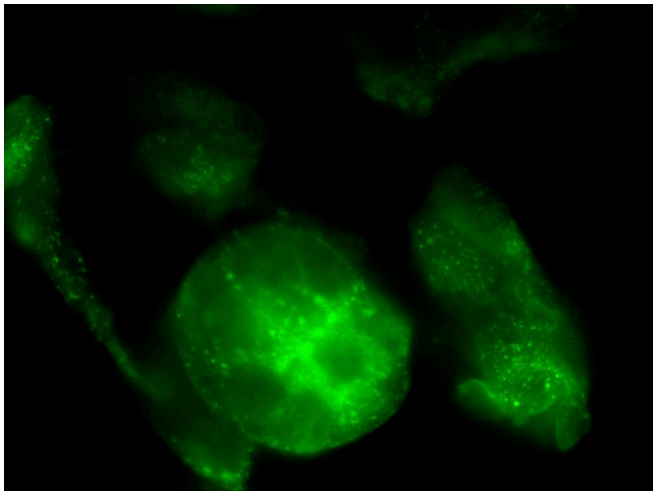

x63 magnification

Figure 3.5 Immunofluorescence protocol optimised for D6 antibody staining on HEK293 cells. Cells were permeabilised, stained with in-house anti-D6 primary antibody or isotype, and AF488 or FITC conjugated secondary antibodies (green). a) and b) Comparison of anti-D6 antibody and isotype staining. Nuclei are stained blue with DAPI. The image settings for the comparative anti-D6 antibody and isotype fields were synchronised for standardisation. c) and d) D6 transfected HEK293 cells stained with anti-D6 antibody at different magnifications; in these two figures the nuclear staining with DAPI is not shown. The staining of anti-D6 antibody can be seen as punctation in the cytoplasm associated with intracellular vesicles.

a) x20 magnification (3 fields)

Anti-D6 antibody	Isotype
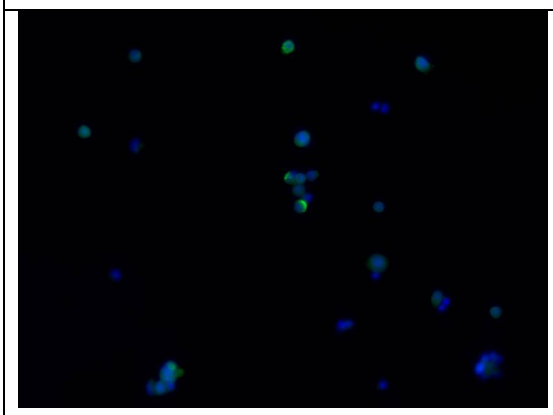	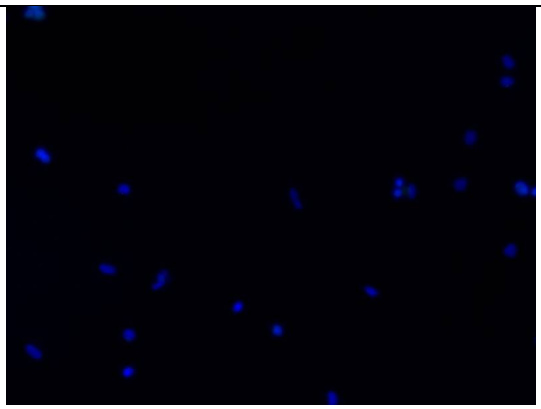
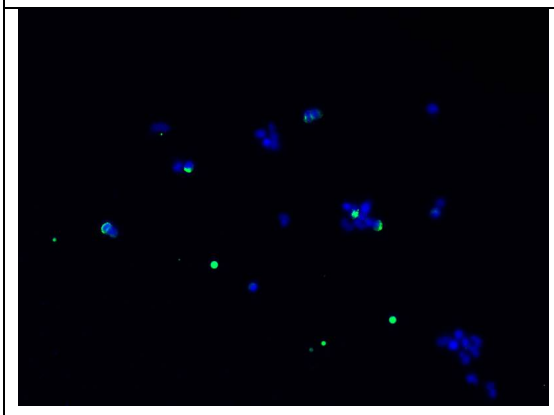	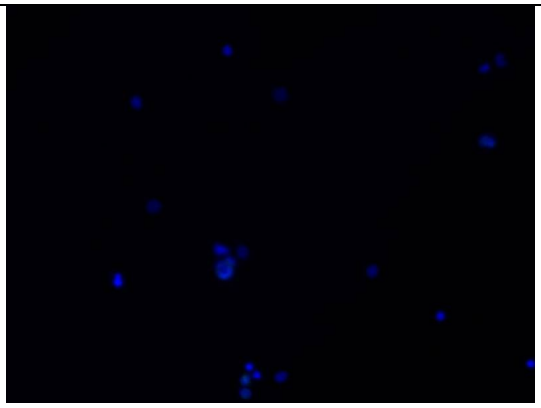
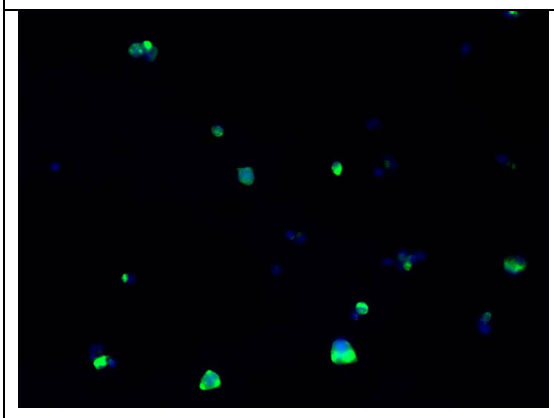	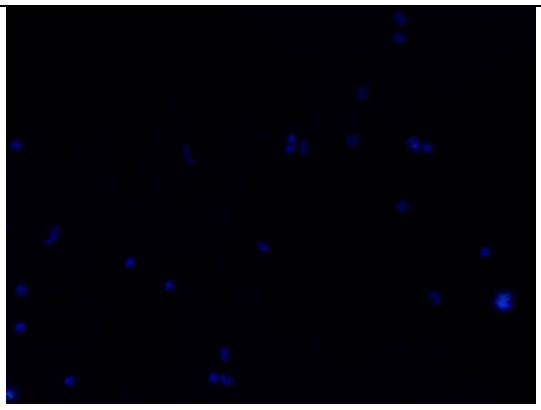

b) x63 magnification (3 fields)

Anti-D6 antibody	Isotype
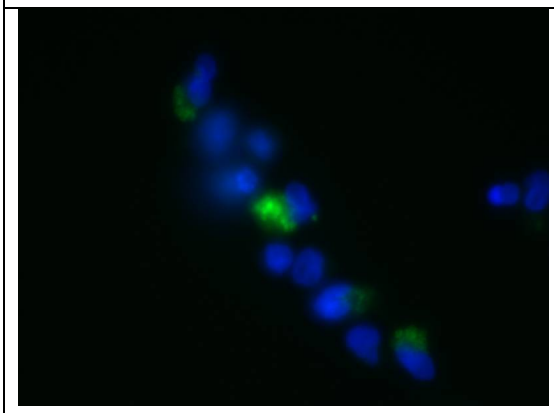	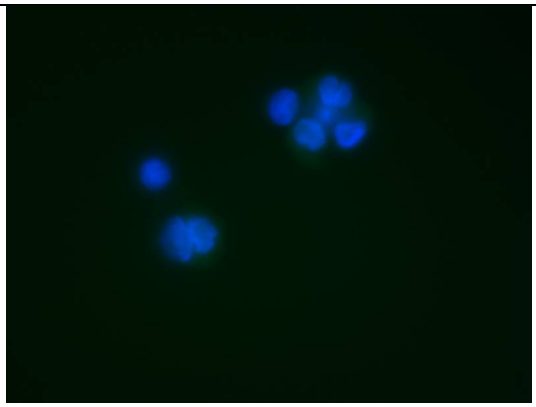
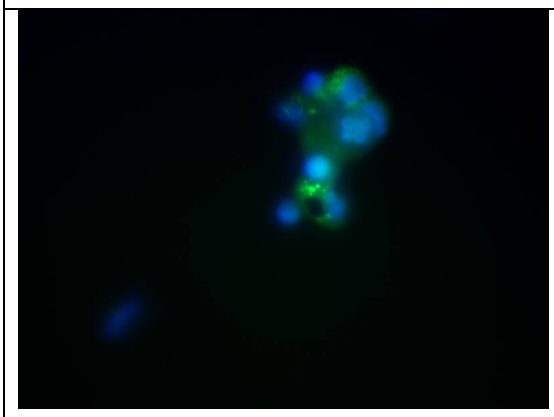	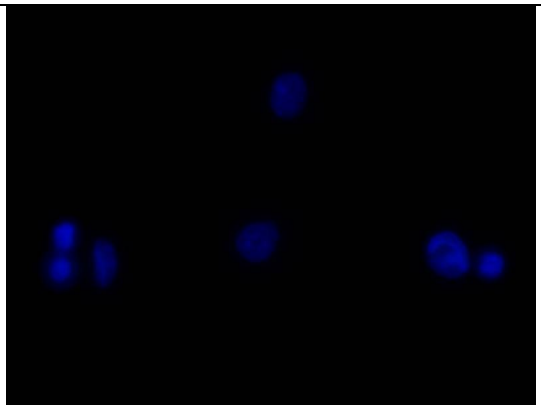
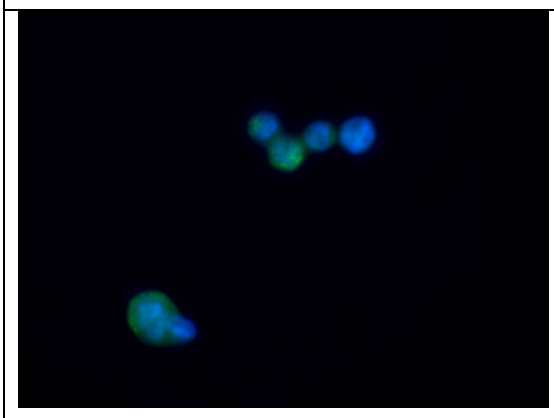	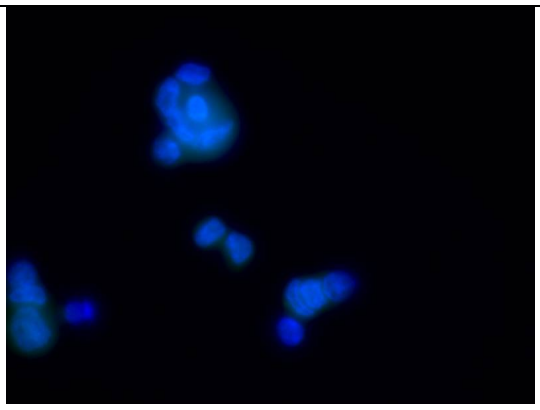

c) x63 magnification (representative photo showing punctate staining with anti-D6 antibody)

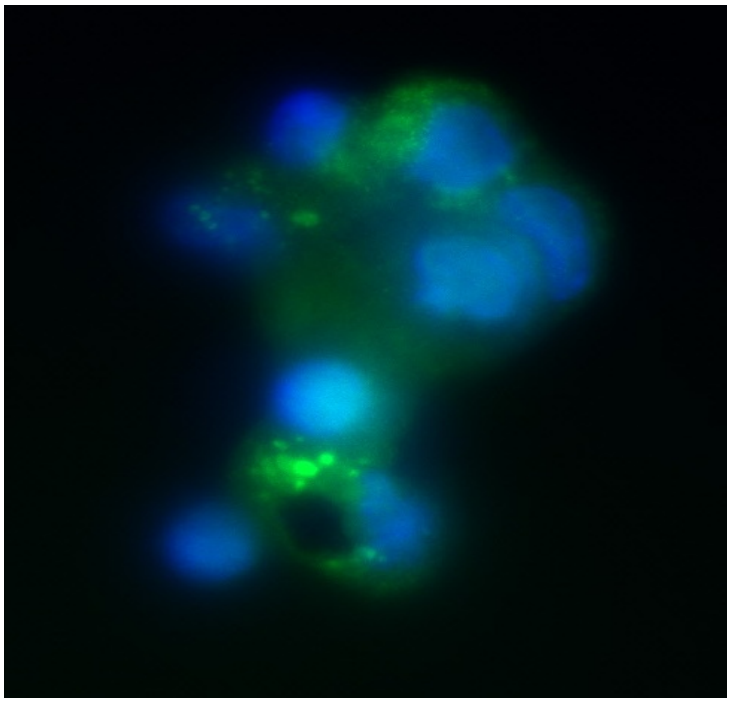

Figure 3.6 D6 protein is stained in trophoblasts and is predominantly in intracellular vesicles. Immunofluorescence of permeabilised primary trophoblast cells. Primary antibody was in-house anti-D6, with AF488 conjugated secondary antibody (green). Nuclei are stained blue with DAPI. The image settings for the comparative D6 antibody and isotype fields were synchronised for standardisation. Z-stack was performed to confirm intracellular staining. The photos of the fields were taken from one representative placenta. 3 biological replicates were performed. In low magnification in a), D6 was seen as bright spots in the cytoplasm. In higher magnification in b) and c), the staining of D6 can be seen in the cytoplasm associated with vesicles.

3.4.3 Flow cytometry

Next surface D6 expression in trophoblast was assessed by flow cytometry (Fig 3.7). HEK-D6 cells were used as controls for this experiment initially and D6 on the surface of these cells was detectable by flow cytometry using anti-D6 antibodies (Fig 3.7a). In contrast surface D6 was virtually undetectable on trophoblasts with only a few cells showing positive staining compared to isotype control stained cells (Fig 3.7b). Intracellular staining on permeabilised trophoblast cells was also performed using two separate anti-D6 antibodies and appropriate isotype controls (Fig 3.8). With mouse anti-human D6 antibodies (Fig 3.8a), there did appear to be some specific intracellular staining and this was also seen in HEK-D6 cells. However, untransfected HEK293 cells gave similar results. This was also the case with the rabbit anti-human D6 antibody (Fig 3.8b). This type of experiment has been performed on other cell types in our department, with similar problems being encountered. Without effective control cells to support the result, it was not possible to conclude that the positive staining inside trophoblasts was truly due to the presence of D6 protein. It is interesting to see that intracellular staining using the same mouse antibody worked on these cells in immunofluorescence; perhaps in flow cytometry the process of detaching the adherent cells into suspension had disrupted the cytoskeletal architecture of the cells, thus resulting in the high background staining from non-specific isotype binding of the antibodies. Nonetheless, it appears that surface D6 is barely detectable on the surface of cultured human trophoblasts even though it was found on HEK-D6 cells. This might be due to the relatively lower level of D6 expression in the physiological environment, as opposed to the artificially transfected HEK293 cells. In addition, perhaps in trophoblasts the predominantly intracellular localisation of D6 is even more pronounced, leaving very low level of D6 detectable on the cell surface.

a)

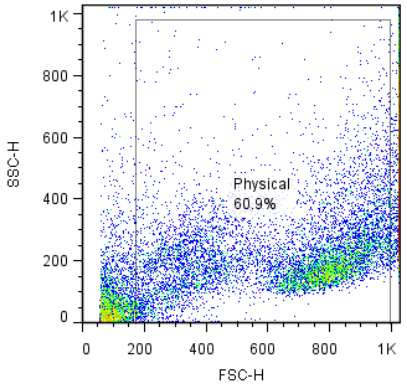

Physical

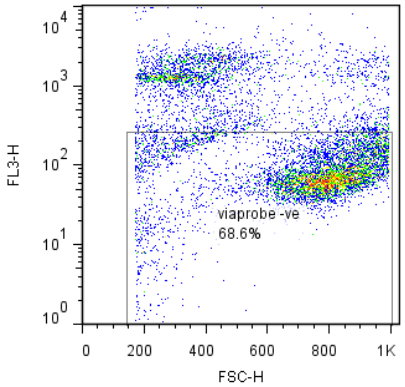

7-AAD viaprobe

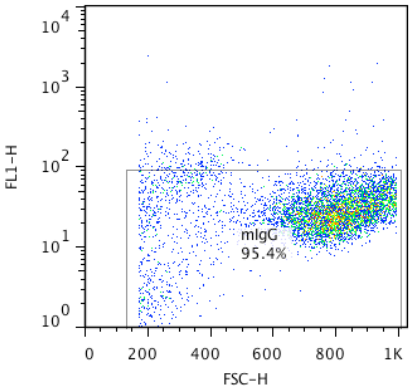

Mouse isotype
4.6% positive

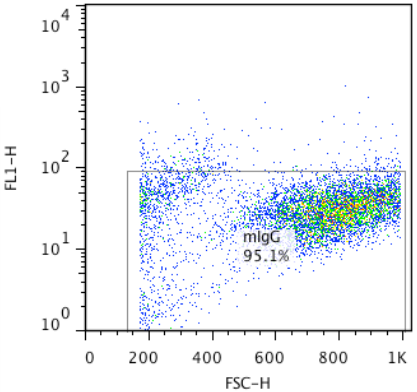

Mouse isotype
4.9% positive

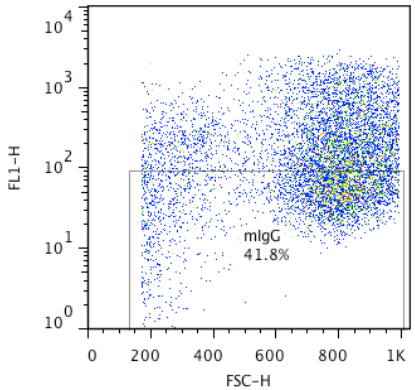

Anti-D6 antibody
58.2% positive

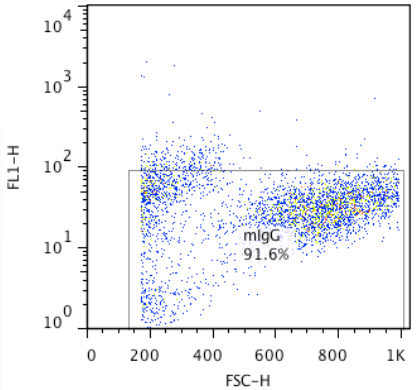

Anti-D6 antibody
8.4% positive

HEK293 cells surface staining

D6 transfected cells

Untransfected cells

b)

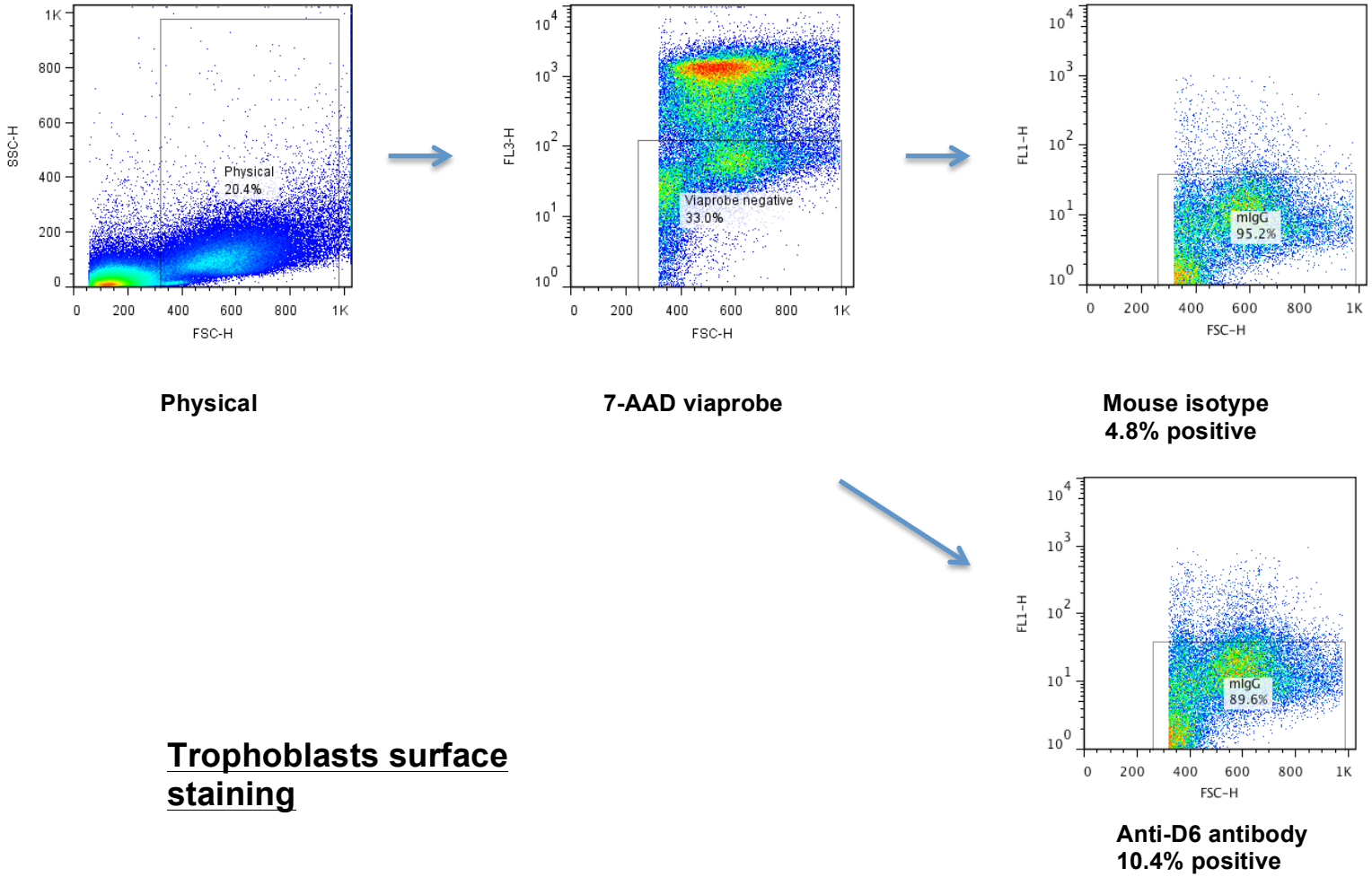

Trophoblasts surface staining

Figure 3.7 D6 protein is virtually undetectable on the surface of trophoblasts. Surface staining of trophoblasts with anti-D6 antibody and isotype; cells were analysed by flow cytometry to detect the presence of D6 protein. HEK293 cells with or without transfected D6 were used as controls for this experiment, as shown in a). The cells underwent physical gating based on FSC and SSC characteristics, then viable cells were selected based on negative staining by 7-AAD viaprobe. 95% inclusion of isotype staining was set as the negative gating for comparison with D6 antibody staining. The result from trophoblasts shown is representative of three biological replicates.

a) Mouse anti-D6 antibody staining

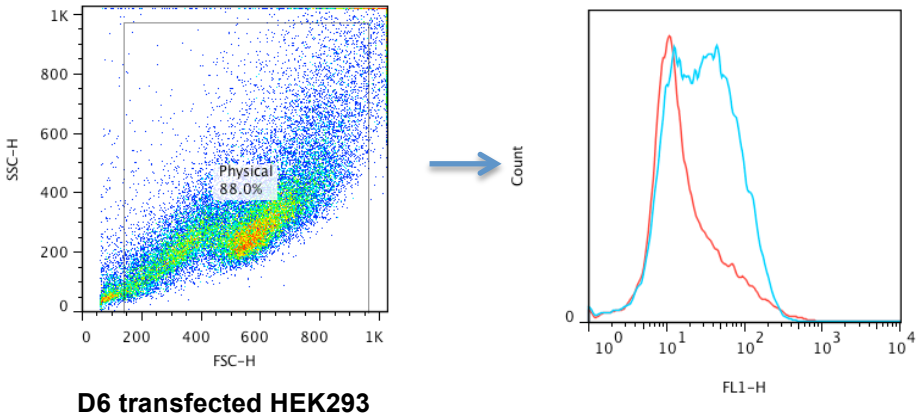

D6 transfected HEK293

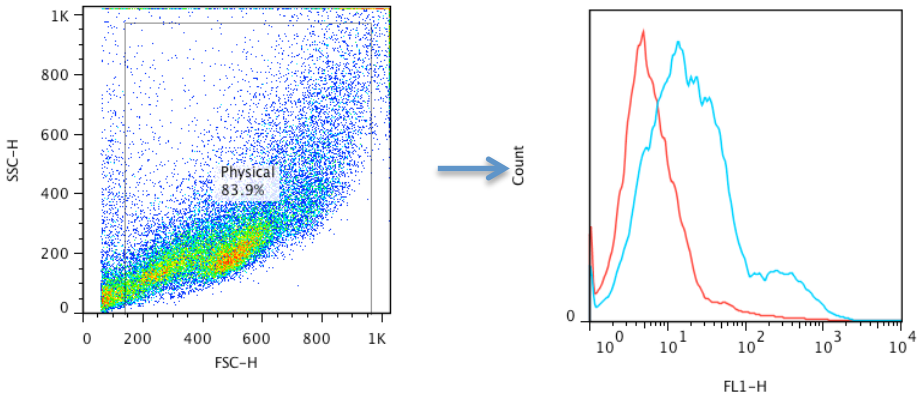

Untransfected HEK293

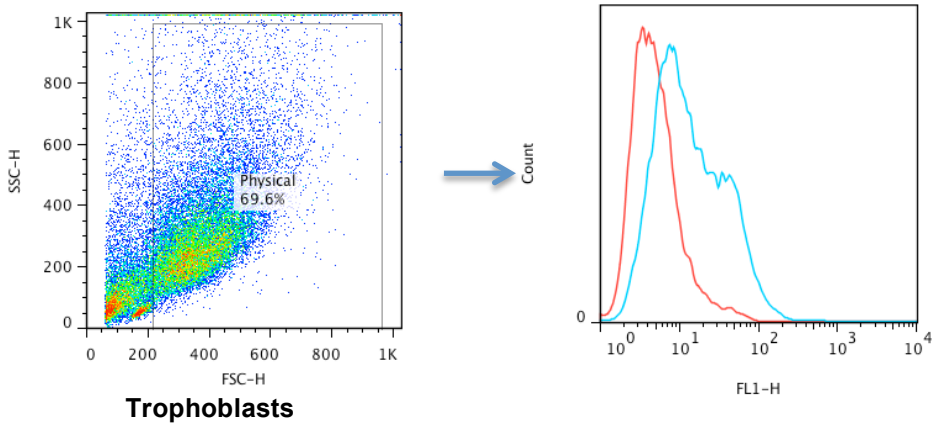

Trophoblasts

Isotype control **Mouse anti-D6**

b) Rabbit anti-D6 antibody staining

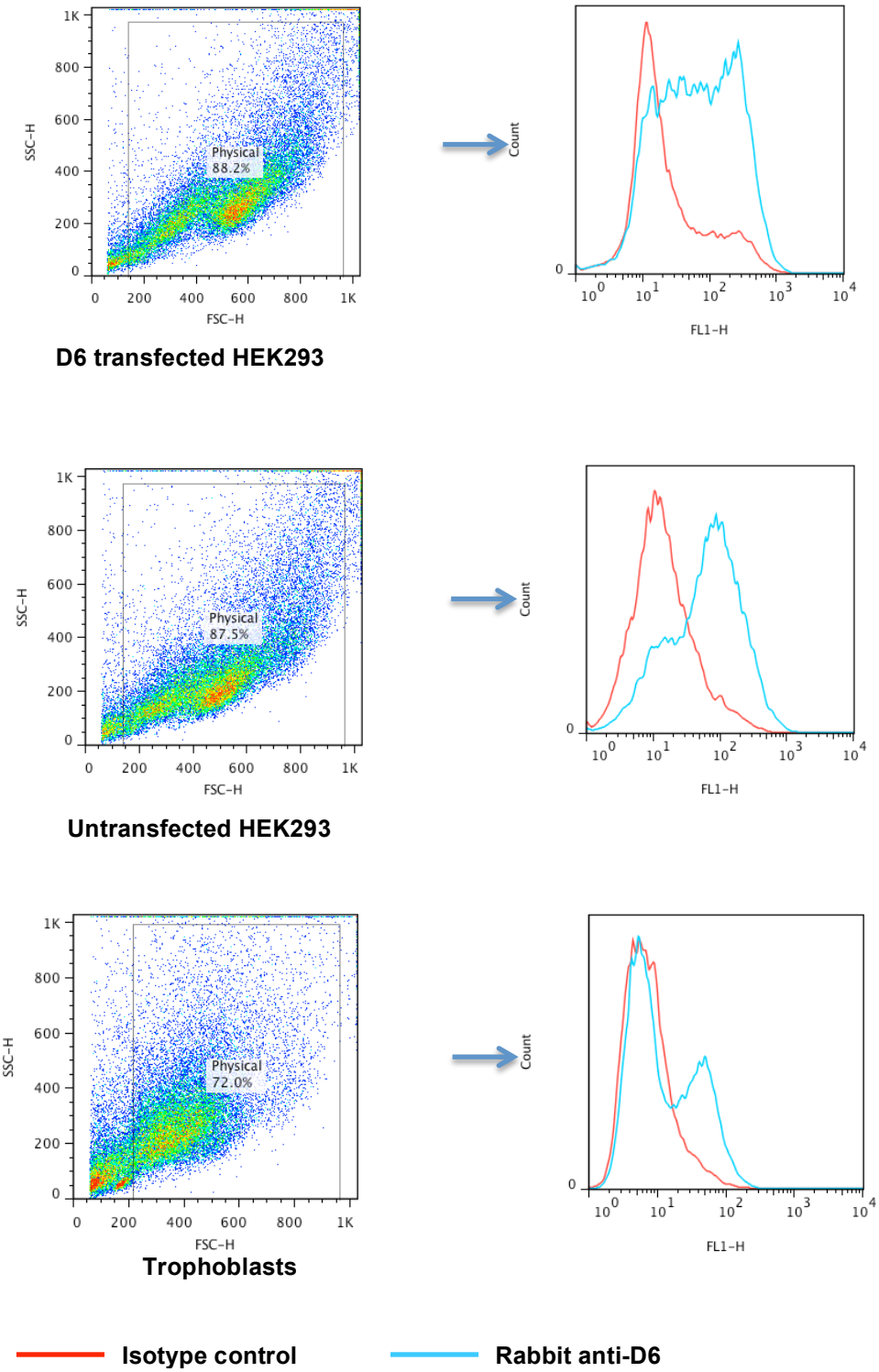

Figure 3.8 Staining permeabilised cells with anti-D6 antibodies. Cells were permeabilised, stained with anti-D6 antibodies or isotype control antibodies and analysed by flow cytometry to detect the presence of D6 protein. The cells underwent physical gating based on FSC and SSC characteristics. Experiments performed using mouse (a) and rabbit (b) antibodies. Trophoblast results were from a single placenta.

3.5 Chemokine uptake assay

3.5.1 Detection using fluorescent microscopy

The observations using qPCR, Western Blotting, immunofluorescence and flow cytometry suggested that D6 is expressed by cultured trophoblasts and shows a subcellular distribution that is not dissimilar to that seen in D6 transfected HEK293 cells. It would be interesting to explore whether this D6 was functional for chemokine uptake and scavenging. To do this, fluorescently labelled CCL2 which has been used successfully to assess D6 activity on mouse leukocytes and D6 transfected HEK293 cells was utilised (Hansell et al., 2011b). Control samples are used in which an excess of unlabelled CCL2 is included. Non-specific pinocytosis of labelled chemokine will not be inhibited by this unlabelled chemokine, but receptor-mediated uptake will be. As expected, $CCL2^{AF647}$ was internalised by HEK-D6 when assessed by fluorescent microscopy although cells were not particularly bright when analysed in this way (Fig 3.9). However, the uptake was successfully competed with a 10-fold molar excess of unlabelled CCL2. Untransfected HEK293 cells were used as negative control and these cells failed to internalise any $CCL2^{AF647}$. This uptake was undetectable when the assay was performed on trophoblasts. There was a concern about the sensitivity of fluorescent microscopy to detect internalised CCL2, so flow cytometry was studied to ascertain whether it was a better approach.

a)

D6 transfected HEK293 cells incubated with $CCL2^{AF647}$	D6 transfected cells with no chemokine during incubation (negative control)
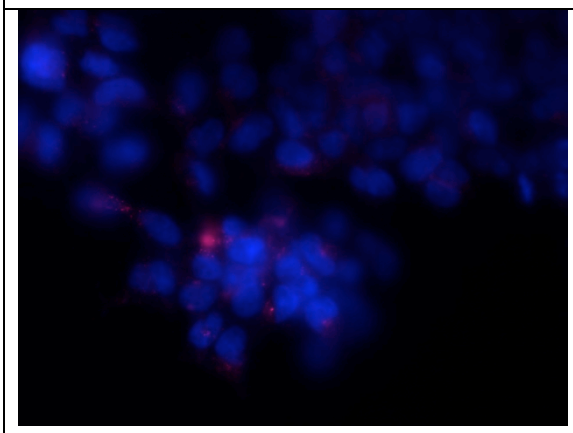	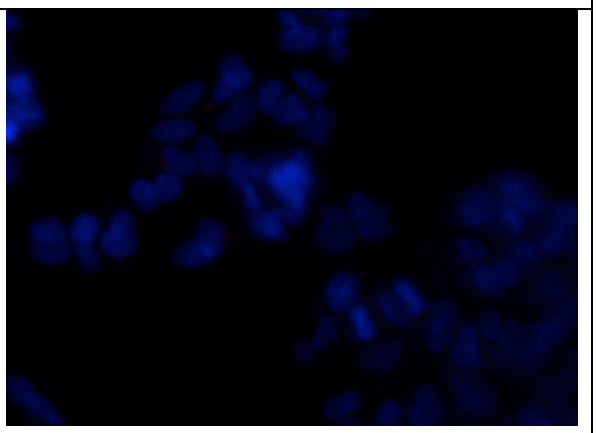
Untransfected cells incubated with $CCL2^{AF647}$ (negative control)	D6 transfected cells incubated with $CCL2^{AF647}$, with a 10-fold molar excess of unlabelled CCL2
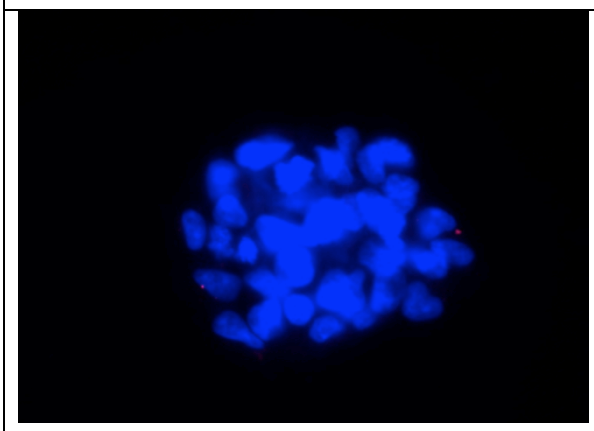	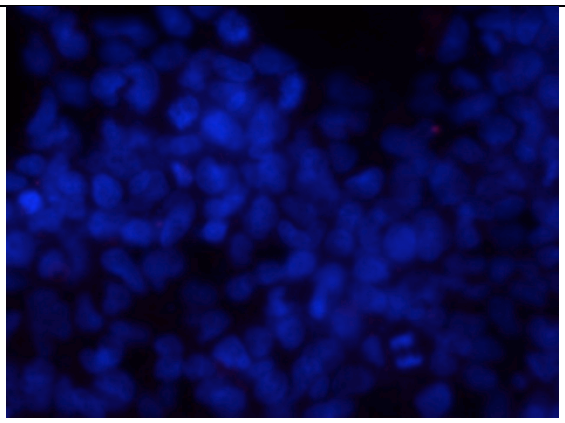

b)

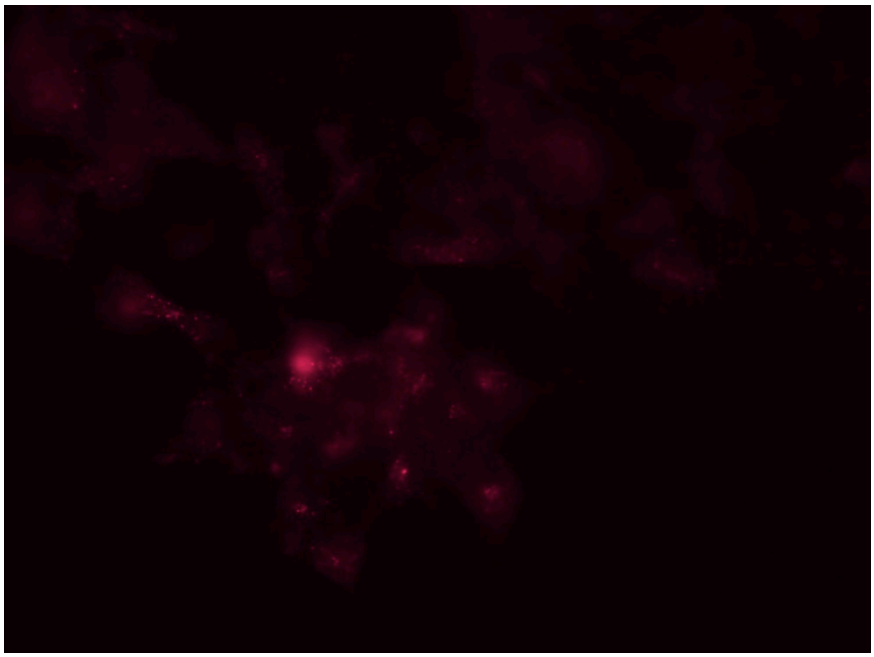

Figure 3.9 Uptake of CCL2 in D6 transfected HEK293 cells. HEK293 cells with or without D6 expression constructs were incubated with $CCL2^{AF647}$ (red) +/- 10-fold molar excess of unlabelled CCL2. Nuclei were stained blue with DAPI. Z-stack was performed to confirm intracellular staining. a) Assessment of CCL2 uptake and competition, comparing with negative controls. Image settings were synchronised for standardisation b) DAPI staining of nuclei turned off, showing positive intracellular $CCL2^{AF647}$ uptake.

3.5.2 Detection of quantitation of $CCL2^{AF647}$ uptake using flow cytometry

In comparison with fluorescent microscopy, flow cytometry proved to be a much more sensitive and quantitative way of detecting uptake of fluorescent chemokine (Fig 3.10-3.13). HEK293 cells expressing human D6 internalised large quantities of $CCL2^{AF647}$, and this uptake could be effectively blocked by inclusion of a large excess of unlabelled human CCL2 (Fig 3.10-3.11). Control untransfected HEK293 cells internalised very little $CCL2^{AF647}$. Moreover, robust $CCL2^{AF647}$ uptake was seen with cultured trophoblasts. Next, competition assays were performed in which a 10-fold molar excess of a range of unlabelled chemokines were individually included along with the $CCL2^{AF647}$ during the uptake incubation period (Fig 3.11-3.12). Known D6 ligands were used as competitors i.e. CCL2, CCL3L1, CCL4, CCL5, CCL7, CCL8, CCL11, CCL13, CCL17 and CCL22. CCL24 and CCL26, which are not thought to be D6 ligands, were also included. As expected, most of the known D6 ligands were able to prevent, to a greater or lesser extent, $CCL2^{AF647}$ uptake by D6-expressing HEK293 cells (Fig 3.11). CCL24 showed some ability to reduce uptake, but CCL26 was ineffective. Surprisingly, CCL4 was also a poor competitor, although it was possible that the batch of CCL4 that was used was defective. No positive control for its bioactivity was undertaken. When cultured trophoblasts were analysed in these assays, a similar profile of competition was observed (Fig 3.12). Cultured trophoblasts from the first placenta analysed showed that unlabelled CCL2 was the most effective competitor, but CCL3L1, CCL5, CCL7, CCL8, CCL11, CCL13, CCL17 and CCL22 all reduced $CCL2^{AF647}$ uptake (Fig 3.12). CCL24 showed some weak activity as a competitor, but CCL26 was ineffective. As with D6-expressing HEK293 cells, CCL4 failed to compete $CCL2^{AF647}$ uptake. Cultured trophoblasts from a further three placentas were then analysed to explore the reproducibility of the findings, and data from all four placentas were combined to produce the graphs show in Figure 3.13a-b. When gating for positive events, there was no statistically significant difference seen by the inclusion of competitor chemokines. When the MFI of the entire population was examined, while clear reductions were apparent these again failed to achieve statistical significance. However, if the MFI of positive events was assessed, then unlabelled CCL2, CCL3L1, CCL5, CCL7, CCL8, CCL13, CCL17 and CCL22 were all able to significantly reduce $CCL2^{AF647}$ uptake by trophoblasts, while CCL4, CCL11, CCL24

and CCL26 were not. These data are consistent with $CCL2^{AF647}$ uptake by cultured trophoblasts being mediated by a receptor that has ligand specificity that is very similar to D6 expressed in HEK293. Bearing in mind the preceding analysis of cultured trophoblasts, this receptor is most likely to be D6.

The uptake assay showed a broad range of $CCL2^{AF647}$ uptake by trophoblasts when they were gated according to the strategy shown in Figure 3.10. Since it was known that trophoblast cultures contained a mixture of cell types, gating was explored to see whether it could be refined to focus more effectively on cells internalising $CCL2^{AF647}$. Thus, histograms of $CCL2^{AF647}$ uptake (in the absence of any competitor chemokine) were back-gated to explore the forward scatter and side scatter characteristics of the $CCL2^{AF647}$-high and $CCL2^{AF647}$-low cells (Fig 3.14). This clearly showed that $CCL2^{AF647}$-high cells were, on average, larger than $CCL2^{AF647}$-low cells, consistent with them being trophoblasts. Bearing this in mind, the $CCL2^{AF647}$ uptake data was reanalysed by drawing a tighter gate with a FSC cut-off greater than 400 (Fig 3.15a). The histogram from this gating method showed a higher proportion of $CCL2^{AF647}$-high cells. Combination of the data from four placentas using this tighter gate (Fig 3.15b) showed broadly similar pattern as the graphs from previous gating (Fig 3.13b), with more significant reductions in $CCL2^{AF647}$ uptake when MFI of the entire population was examined.

Syncytialised BeWo cells were found to have larger size when analysed by flow cytometry in the past (Kudo et al., 2003). Assuming trophoblasts have the same characteristics of syncytialisation as the BeWo cells, it may be possible that the population of $CCL2^{AF647}$-high cells were syncytialised trophoblasts. Further exploration to confirm this theory is worthwhile in future experiments. If there is a low variability in the difference of chemokine uptake between these cell groups, this chemokine uptake assay can potentially be utilised effectively, to become a marker to differentiate subpopulations of trophoblasts in future experiments.

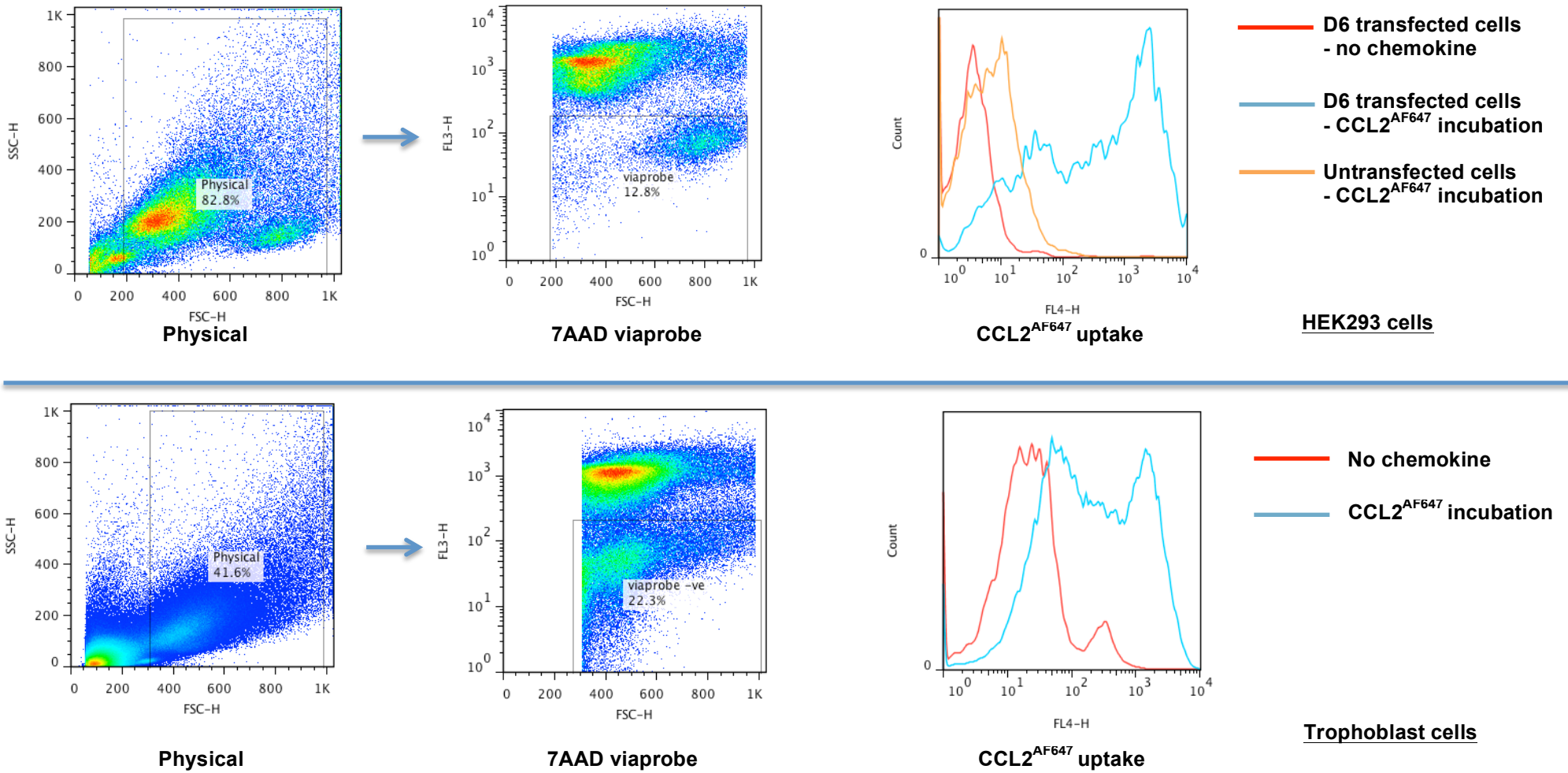

Figure 3.10 Trophoblast cells demonstrated CCL2^{AF647} uptake. Cells were incubated with CCL2^{AF647} and analysed by flow cytometry. The cells underwent physical gating, followed by exclusion of dead cells. HEK293 cells were used as controls. FACS plots and histograms from a representative placenta.

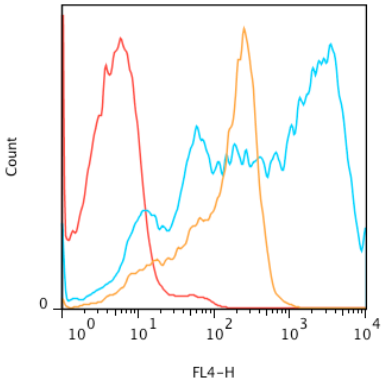

CCL2

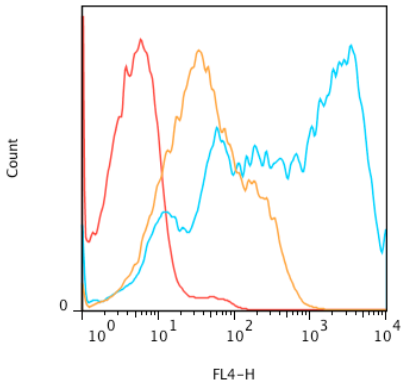

CCL7

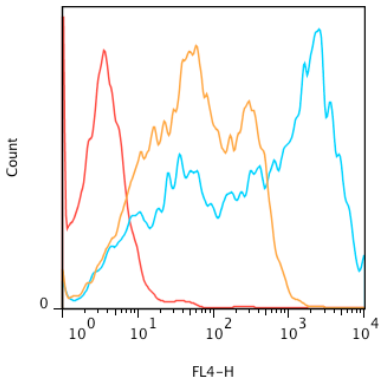

CCL8

No chemokine

$CCL2^{AF647}$ incubation

$CCL2^{AF647}$ + unlabelled competitive chemokine incubation

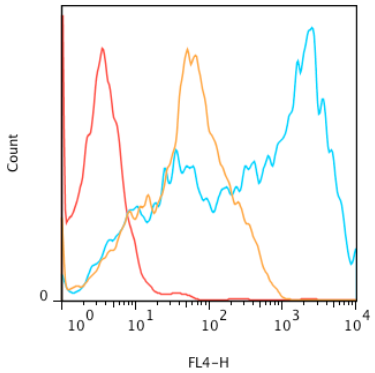

CCL13

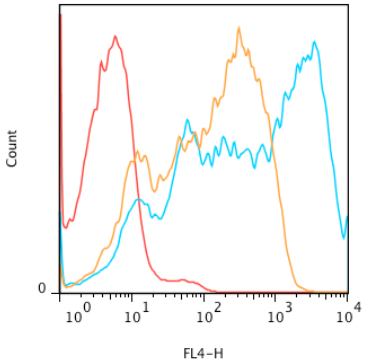

CCL3L1

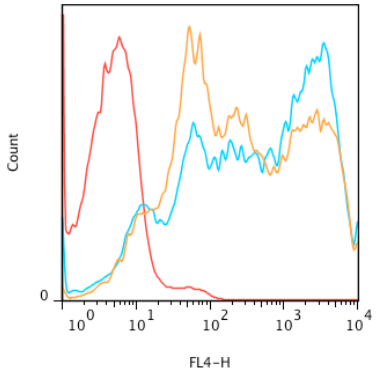

CCL4

D6 transfected HEK293 cells

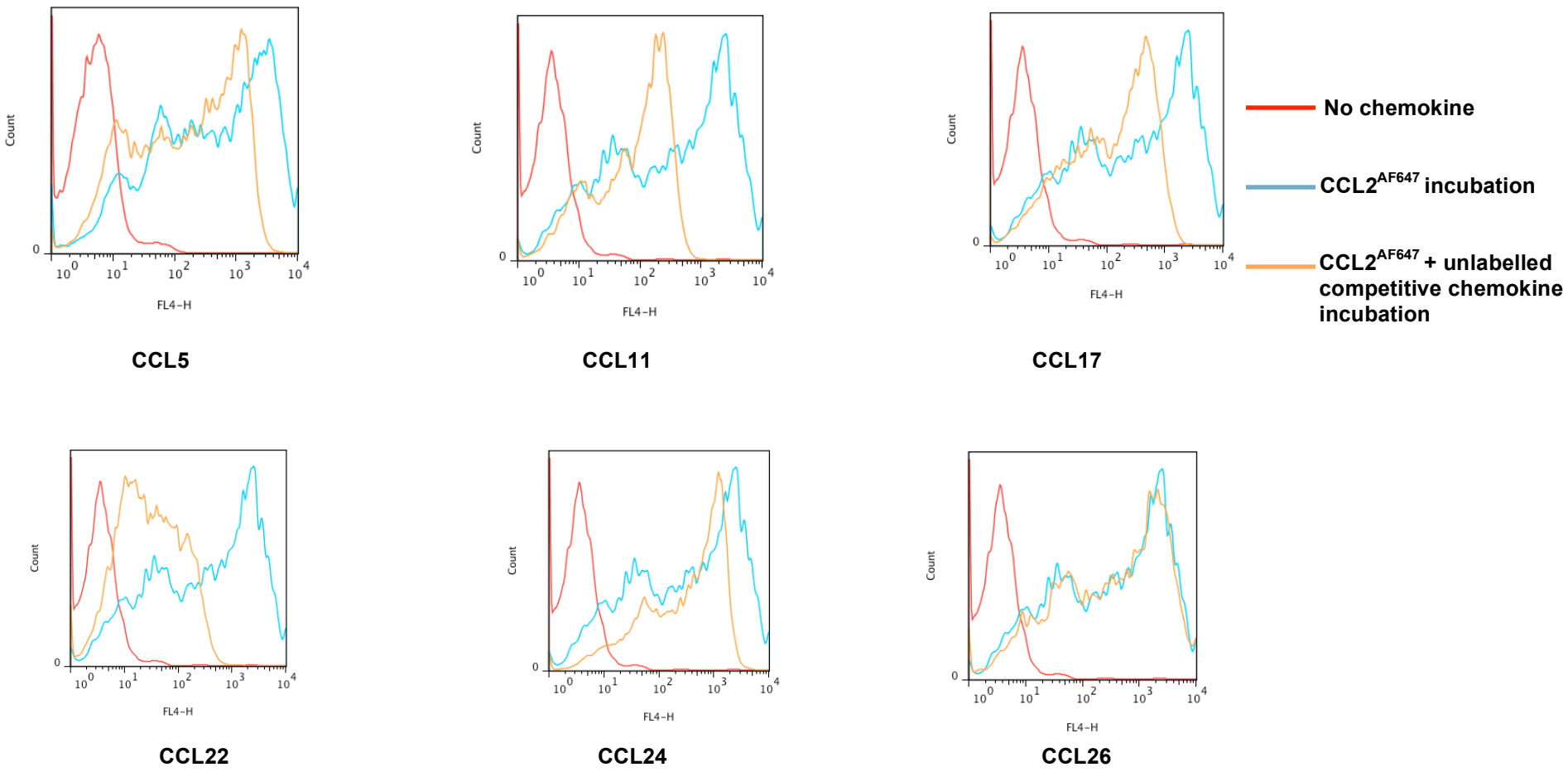

Figure 3.11 D6 ligands effectively compete CCL2^{AF647} uptake by HEK293 cells transfected with D6 expression constructs. Cells were incubated with CCL2^{AF647} +/- a 10-fold excess of unlabelled chemokines and analysed by flow cytometry (page 142 and 143). Gating of the cells was shown in fig 3.10.

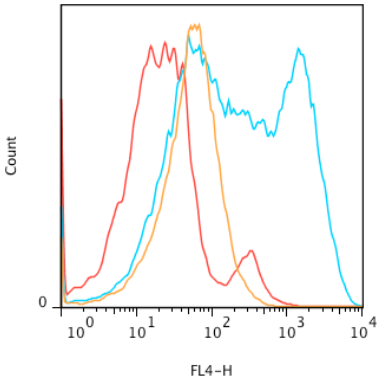

CCL2

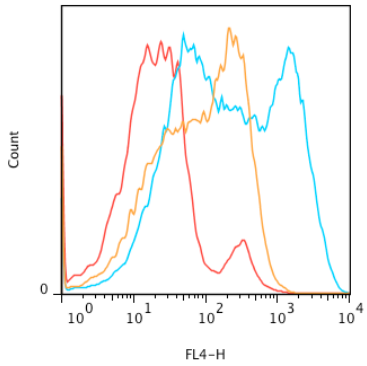

CCL7

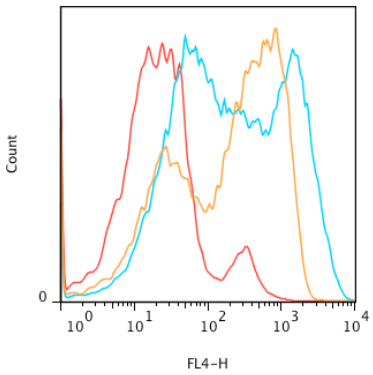

CCL8

No chemokine

$CCL2^{AF647}$ incubation

$CCL2^{AF647}$ + unlabelled competitive chemokine incubation

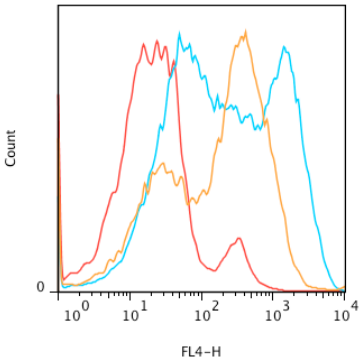

CCL13

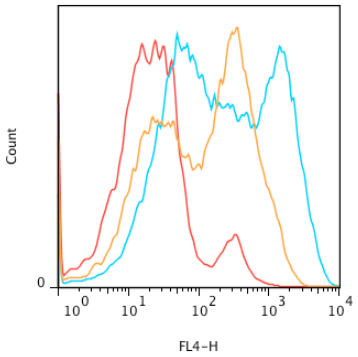

CCL3L1

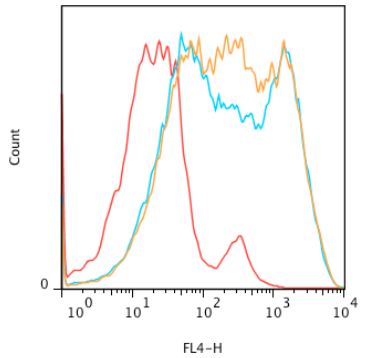

CCL4

Trophoblast cells

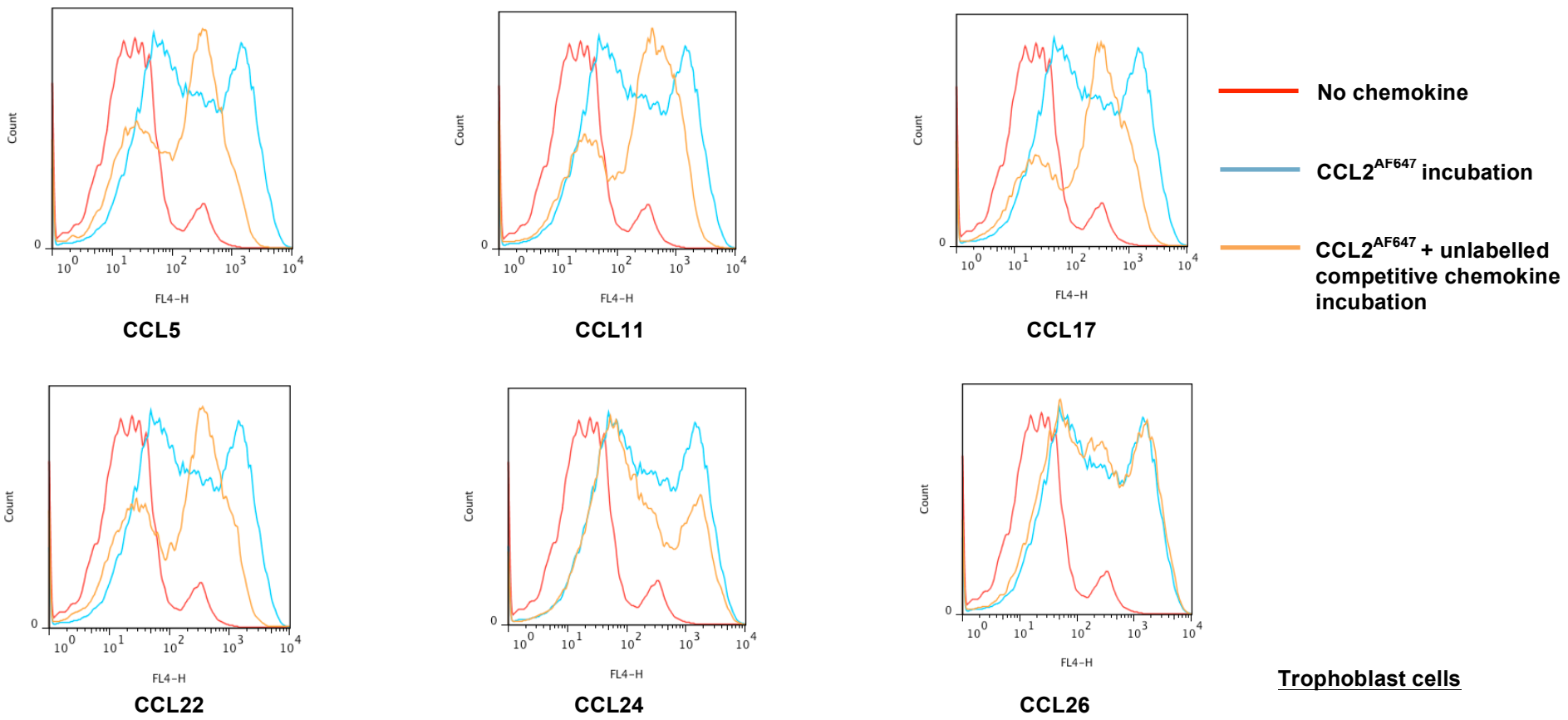

Figure 3.12 D6 mediates CCL2^{AF647} uptake by trophoblasts. Competition chemokine uptake assays revealed the presence of active D6 in trophoblasts. Cells were incubated with CCL2^{AF647} +/- a10-fold excess of unlabelled chemokines. Histograms from a representative placenta (page 144 and 145). Gating of the cells was shown in fig 3.10.

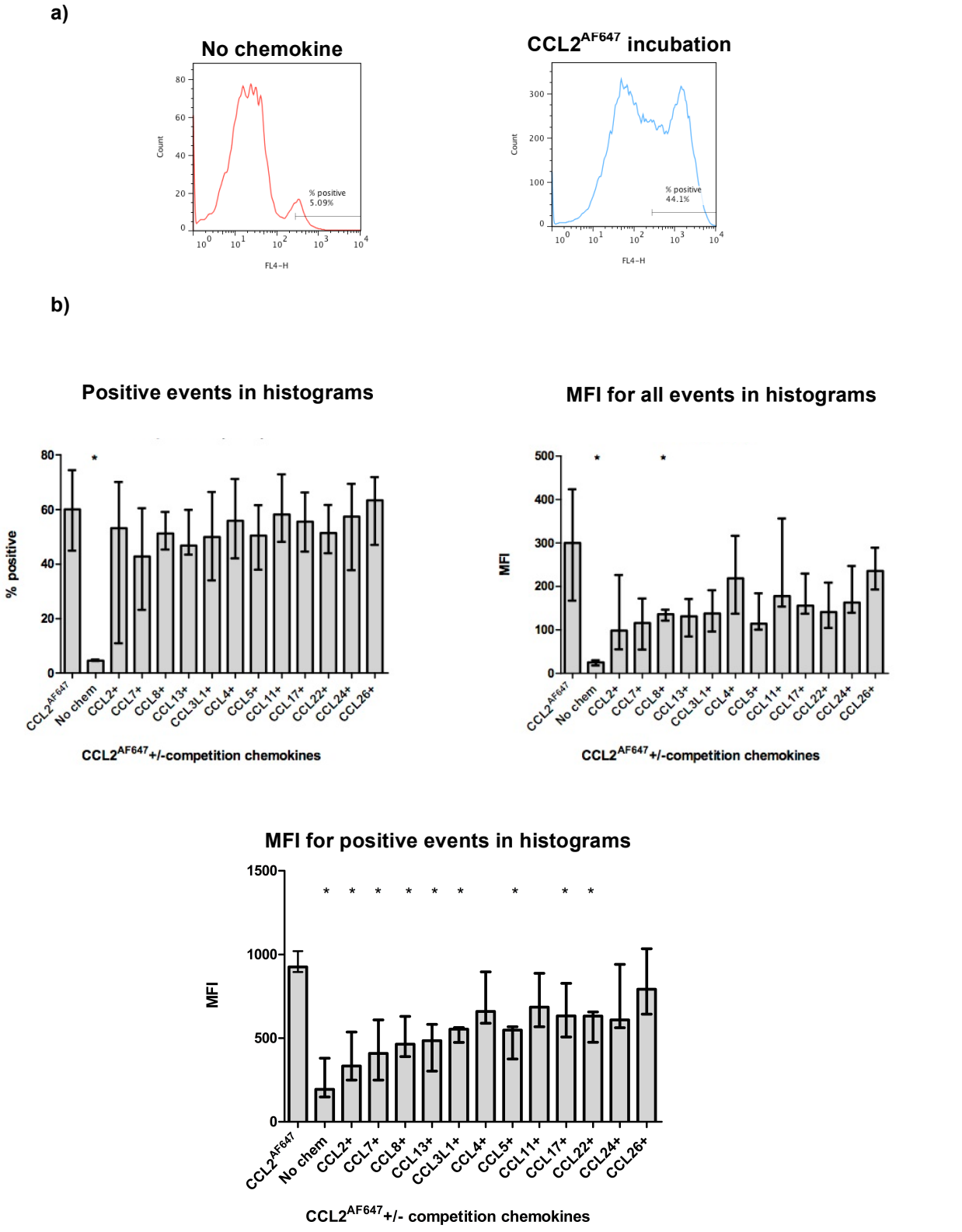

Figure 3.13 Analyses of D6 mediated CCL2^{AF647} uptake by trophoblasts. a) Examples showing calculation of % of positive events. Positive event was defined as any fluorescent events above the 95% threshold from the curve where the cells were not incubated with any chemokine, as shown on the histogram on the left. Thus the percentage of positive events when there was no chemokine was 5%. This threshold was used to compare with other curves where the cells were incubated with CCL2^{AF647} +/- competition chemokines. b) Bar graphs of the positive events, and also mean fluorescence index (MFI) showing median + interquartile range, derived from the histograms of four biological replicates. The first columns show the results with CCL2^{AF647} incubation; the second columns show the results when no chemokine was introduced; from the third columns onwards they show the results with the presence of unlabelled competitive chemokines. * p<0.05 (Mann-Whitney test compared with the first column).

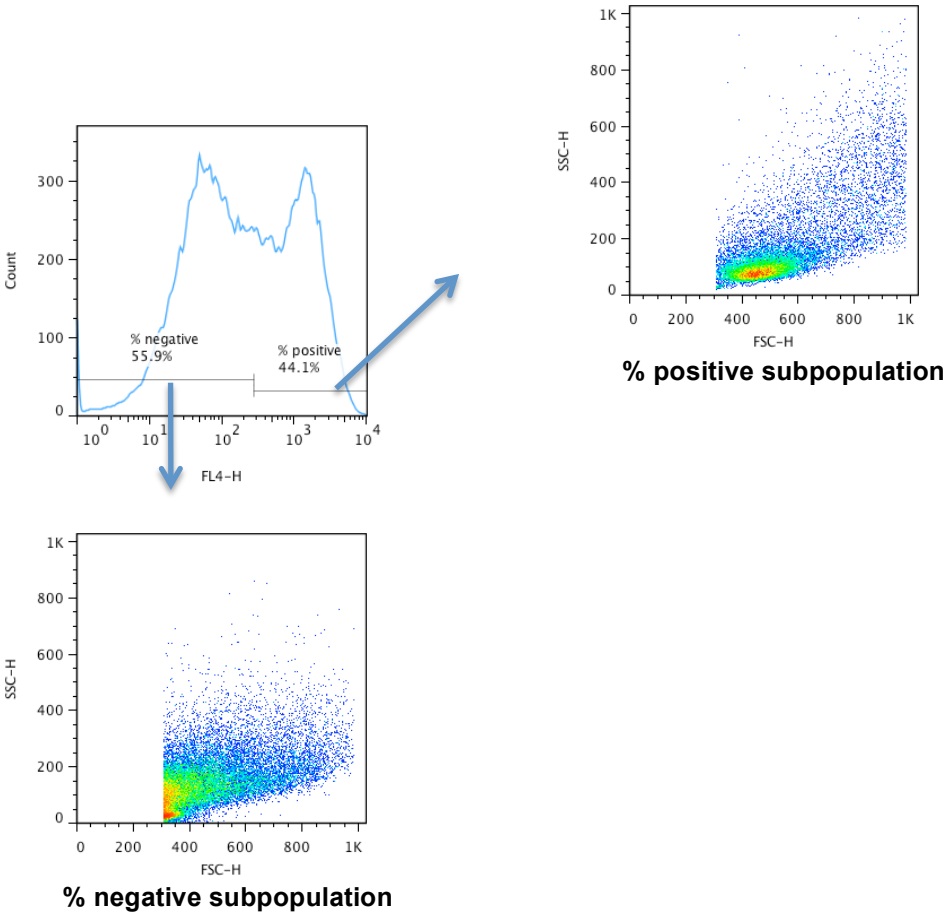

Figure 3.14 Cells in trophoblast cultures positive for chemokine uptake were larger than cells with weak chemokine uptake. Gating method similar to figure 3.13a. Subpopulation of positive and negative cells from the chemokine uptake histogram were backgated to determine forward scatter (size) (FSC) and side scatter (granularity) (SSC). Plots are representative of data from four placentas.

a)

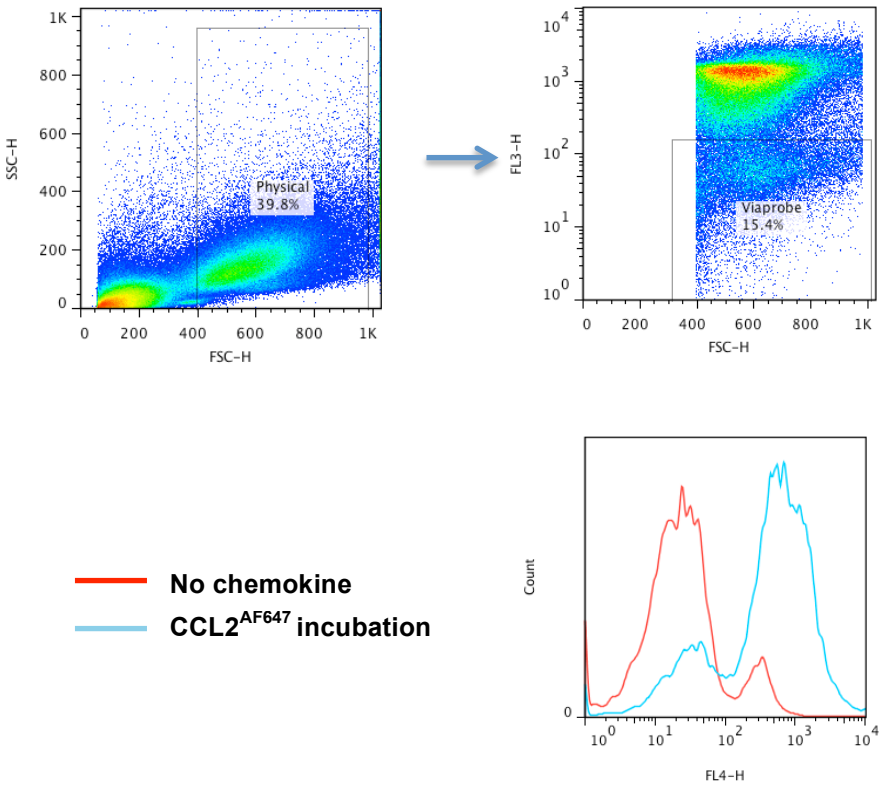
SSC-H
FSC-H
Physical
39.8%
FL3-H
FSC-H
Viaprobe
15.4%
No chemokine
CCL2AF647 incubation
Count
FL4-H

b)

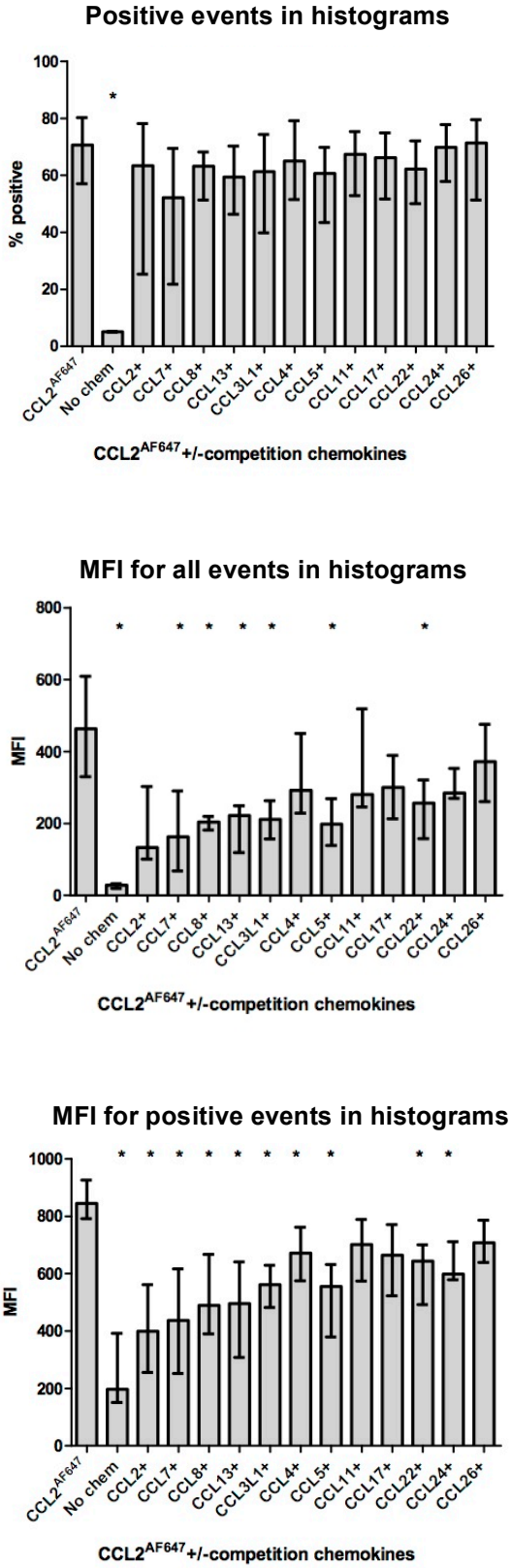

Figure 3.15 Gate with FSC cut-off of greater than 400 contains more CCL2^{AF647}-high cells. a) Gating of cells with FSC cut-off of greater than 400, followed by exclusion of dead cells. FACS plots and histograms from the same samples as Fig 3.12. b) Bar graphs of the positive events, and also mean fluorescence index (MFI) showing median + interquartile range, derived from the histograms of four biological replicates, with FSC cut-off readjusted to greater than 400. The first columns show the results with CCL2^{AF647} incubation; the second columns show the results when no chemokine was introduced; from the third columns onwards they show the results with the presence of unlabelled competitive chemokines. * $p<0.05$ (Mann-Whitney test compared with the first column).

3.6 Chemokine scavenging assay by Western Blot

D6 is believed to act as a chemokine scavenging receptor. To ascertain whether D6 acts as a scavenger in the primary cultured human trophoblasts, chemokine scavenging assays were performed. Biotinylated CCL2 (bioCCL2) was used to study the scavenging of this D6 ligand from the supernatant over time. As this assay had never been performed in our laboratory with trophoblasts, firstly the protocol had to be optimised, and the minimal amount of bioCCL2 detectable by Western blot had to be determined. The result showed 100pg of bioCCL2 was detectable with little background (Fig 3.16). Based on this result, it was concluded that for performing this experiment, at least 1ng of bioCCL2 must be present in an aliquot of medium harvested to effectively study the scavenging effect of the chemokines by quantitative Western blot.

In this experiment, bioCCL2 +/- a 10-fold excess of unlabelled CCL3L1 (D6 ligand) and CCL26 (non-D6 ligand) were added into the wells of trophoblast cultures. An aliquot of medium was harvested from each well immediately after the addition of the chemokines (0 hour samples); this aliquot of medium contained 3ng of bioCCL2, based on the optimisation process described earlier. Subsequently at set time points, a series of aliquots of medium were collected from all the wells to study the scavenging effect mediated by D6. As the bands of bioCCL2 from the medium with trophoblasts faded over time on the Western blots, the result showed bioCCL2 was scavenged by trophoblasts; this effect was attenuated by addition of 10-fold excess of unlabelled CCL3L1 (D6 ligand) (Fig 3.17). Non-D6 ligand CCL26 was used as a negative control for the competition of scavenging, and it failed to prevent bioCCL2 removal by trophoblasts (Fig 3.18).

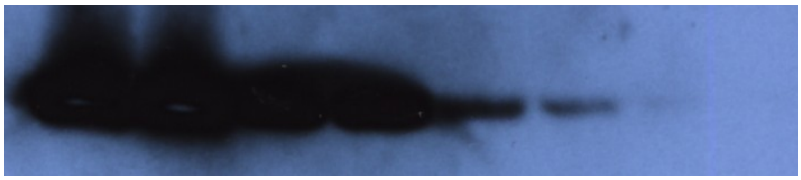

10 10 1 1 0.1 0.1 0.01 0.01

Serial dilutions of biotinylated CCL2 (ng) in duplicates

Figure 3.16 Optimisation process to ascertain the minimal quantity of biotinylated CCL2 (bioCCL2) detectable by Western blot. The indicated quantities of bioCCL2 were run on a polyacrylamide gel and a Western blot prepared. The bioCCL2 was detected with HRP-coupled streptavidin.

a)

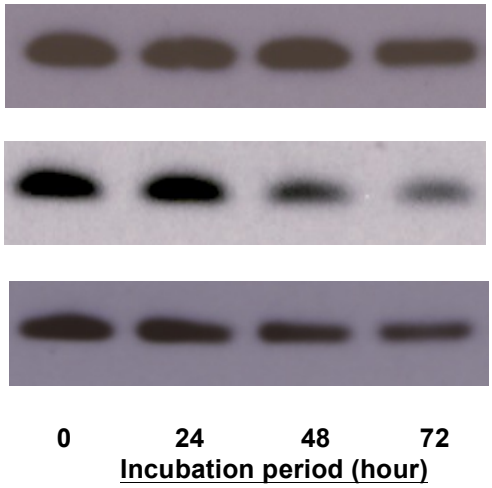

b)

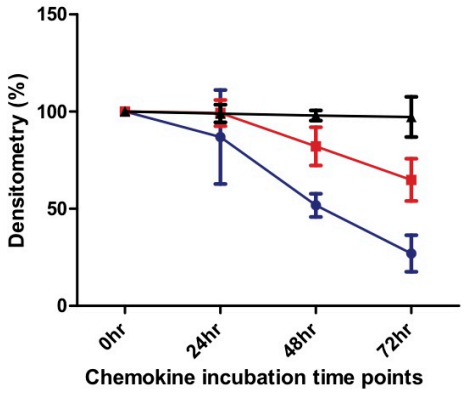

ANOVA statistical analyses

- **Curve C vs. Curve A p = 0.0005**
- **Curve C vs. Curve B p = 0.0057**

Curve	Designation	Description
A		Medium with no cells incubated with biotinylated CCL2 (negative control)
B		1.5 x10^3 cells incubated with biotinylated CCL2 + 10-fold excess unlabelled CCL3L1
C		1.5 x10^3 cells incubated with biotinylated CCL2

Figure 3.17 Trophoblasts contain D6, which scavenges biotinylated CCL2 (bioCCL2) from the medium over time. The scavenging effect can be competed with CCL3L1 (D6 ligand). Scavenging assay of primary trophoblasts was performed; bioCCL2 was added into the wells of trophoblast cultures. At set time points, a series of aliquots of medium were collected from all the wells. Quantification of bioCCL2 was carried out by Western blotting. a) Western blot from the scavenging assay from one representative placenta. The bands of bioCCL2 faded over time due to the scavenging effect of trophoblasts. The effect was noticeably being attenuated with addition of 10-fold excess of unlabelled CCL3L1 (D6 ligand) due to competition. b) Curves showing mean + standard deviation, showing changes of densitometry of the bands of bioCCL2 from four biological replicates of the experiment.

a)

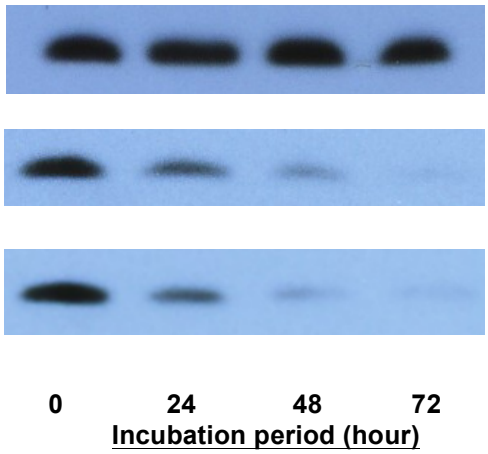

b)

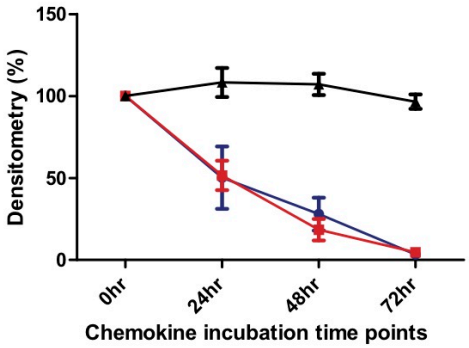

ANOVA statistical analyses

- **Curve C vs. Curve A p = 0.0002**
- **Curve C vs. Curve B p = 0.74**

Curve	Designation	Description
A		Medium with no cells incubated with biotinylated CCL2 (negative control)
B		1.5 x10^3 cells incubated with biotinylated CCL2+10-fold excess unlabelled CCL26
C		1.5 x10^3 cells incubated with biotinylated CCL2

Figure 3.18 Trophoblasts contain D6, which scavenges biotinylated CCL2 (bioCCL2) from the medium over time. The scavenging effect is not competed with CCL26 (non-D6 ligand). To further support the previous finding showing the scavenging effect of D6, we used CCL26, a non-D6 ligand as our negative control for competition. a) Western blot from the scavenging assay from one representative experiment. The bands of bioCCL2 faded over time due to the scavenging effect of trophoblasts. The effect was not being competed with CCL26. b) Curves showing mean + standard deviation, showing changes of densitometry of the bands of bioCCL2 from three technical replicates from a placenta.

3.7 Summary

For greater insight of D6 function in the human placenta, primary human trophoblasts that had been purified and cultured in vitro were used. It was hypothesised that D6 is present in these cells where it serves an important chemokine scavenging role and that this helps to protect the fetus.

The protocol for routine primary trophoblast isolation, purification and culture from fresh placenta was optimised in the laboratory. D6 mRNA was detected in abundance in trophoblasts and Western blotting showed the presence of D6 protein in these primary cells. Despite not producing excellent pictures by immunofluorescence, D6 protein was successfully stained in what appeared to be the intracellular vesicles of trophoblasts and flow cytometry showed D6 protein was barely detectable on the surface of primary trophoblasts. Competition chemokine uptake assays, analysed by flow cytometry, showed that CCL2 was internalised by trophoblasts using D6. Competitive chemokine scavenging assays, analysed by quantitative Western blot, confirmed D6 was functioning as a scavenger for its ligands and that it progressively removed substantial quantities of chemokine from medium bathing the cells.

Collectively these results reaffirmed my initial hypothesis, that D6 is present, and plays a role in scavenging specific chemokines in the human placenta.

3.8 Limitations

Purity and viability of the cells were assessed at day 1 and 2 of culture. All experiments, except the chemokine scavenging assay and Western blotting to assess D6 protein expression, had been completed by day 2; both of these experiments were completed by day 3 (72 hours) of culture. By 72 hours, the cytotrophoblasts would be expected to syncytialise (Kliman et al., 1986, Newby et al., 2005). As shown by the purity assessment, other cells were present in the trophoblast culture due to the nature of the trophoblast isolation.

4 Exploring the Impact of D6 Deletion on Pregnancy in DBA-1 Mice

4.1 Stillbirth, neonatal death and pups weaned/litter in DBA-1 mice

As discussed in the Introduction, D6 deficiency is associated with fetal loss in animal models. Wessels et al demonstrated that arresting porcine attachment sites have reduced expression of D6 in comparison to their viable counterparts (Wessels et al., 2007). Martinez de la Torre et al showed that lack of D6 in mother and pup results in an increased rate of fetal loss when pregnant mice were challenged with LPS and antiphospholipid autoantibodies (Martinez de la Torre et al., 2007). Madigan and colleagues showed that transferred allogeneic D6 deficient fetuses were preferentially lost from wild type recipients (Madigan et al., 2010). In our laboratory, anecdotal evidence suggested that D6 deficient mice on a DBA-1 background generated fewer pups per litter than WT counterparts. Therefore data on the stillbirth rate, neonatal death rate and pups weaned/litter in unchallenged WT and D6 deficient DBA-1 (D6 KO) mice were collected. Interestingly, D6 KO mice had higher stillbirth and neonatal death, resulting in a significant reduction in the number of pups successfully weaned/litter (Fig 4.1). This observed phenotype was not present in C57BL/6 mice (R Nibbs, personal communication, from animal breeding data collected by the Central Research Facility, University of Glasgow). D6 deficient mice on a C57BL/6 background did not show any change in pup survival or pups weaned/litter (data not shown).

WT DBA-1 mice were not particularly good breeders in our facility, and stillborn pups or neonatal death were not uncommon in this strain (Fig 4.1). The combined stillbirth and neonatal death (perinatal death) rate was 27%. The influence of strain on the rate of litter loss has been reported. Mortality rate of up to 32% of the litters in a laboratory mouse strain has been described in the past (Weber et al., 2013). In our laboratory the reason for the high perinatal death rate for DBA-1 mice was not known. A number of antenatal or postnatal factors may be responsible for this phenotype. Postpartum maternal care can vary for different strain of mice, it has been reported that in certain strains the mothers have shorter latencies to nestbuild, and also to retrieve, crouch over and groom their pups (Champagne et al., 2007). However, this variation in maternal behaviour has not been shown to be responsible for the difference in the fetal survival rate during perinatal period. The abnormal behaviour of

maternal cannibalism has also been described in DBA-1 mice (Carter et al., 2002). On the other hand, it is also possible that the low survival rate of DBA-1 pups is due to a suboptimal antenatal development, predisposing them to a compromised phenotype in the neonatal period. The observed phenotype in D6 KO mice may be due a compound effect. The lethal effect of compound mutants has been described before. For example, compound mutants of Tcf1/Lef1 transcription factors resulted in abnormal placentation and death of the pups at mid-gestation, but neither Tcf1 nor Lef1 standalone mutants have any placental phenotypes (Galceran et al., 1999, Rossant and Cross, 2001). Perhaps in DBA-1 there is an inherent defect in placentation and embryogenesis; the compound effect of this defect along with D6 deficiency could be responsible for the higher perinatal loss in the D6 KO group. This model provides a unique opportunity for the exploration of the role of D6 during placentation.

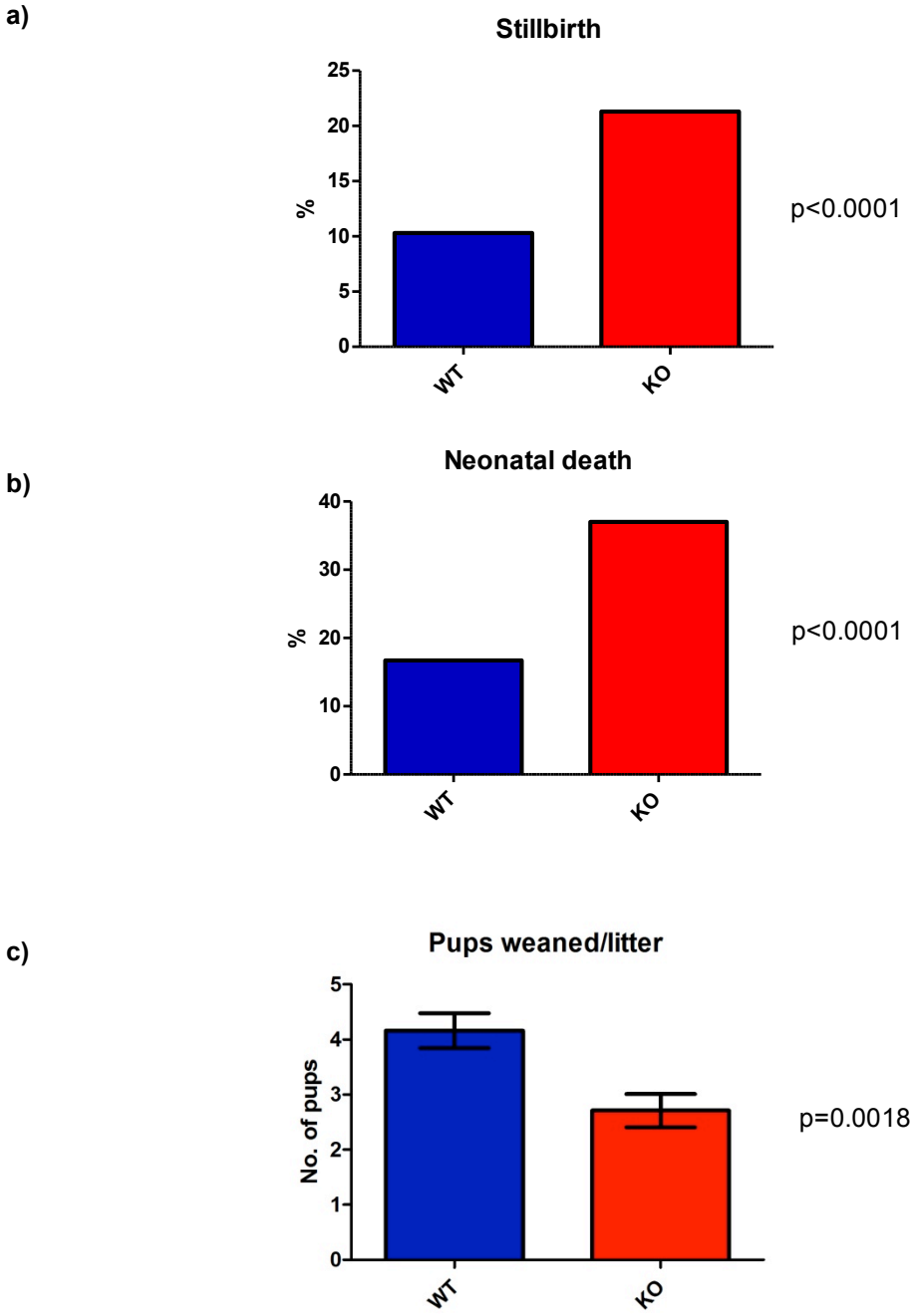

Figure 4.1 D6 KO mice had higher stillbirth and neonatal deaths, resulting in lower pups weaned/litter. Mean numbers of pups born/litter +/- SEM were 5.7 +/- 0.28 (n= 83 litters) for WT, and 5.4 +/- 0.25 (n= 77 litters) for KO; p=0.38 (Mann Whitney). Females in late pregnancy were checked for newborns daily. Once all the pups were born and being nursed, the number of live pups and dead carcasses were counted a) Carcasses that were noticed when the litter was first discovered were counted as stillbirths; n= 474 for WT, n= 418 for D6 KO; p<0.0001 (X^2 test); data from first 3 weeks from birth. b) Pups that did not survive to weaning at day 18 to 21 after birth were recorded as neonatal deaths; n=400 for WT, n=322 for D6 KO; p<0.0001 (X^2 test); data from first 3 weeks from birth. c) Pups weaned per litter; n= 80 litters for WT, n=75 litters for D6 KO; graph shows mean +/- SEM; p= 0.0018 (Mann Whitney).

4.2 Perinatal deaths and weight changes during neonatal period

In view of the evidence of the increase in stillbirth and neonatal death, a more in depth study of the phenotype of the neonates from our DBA-1 mice was performed. Pregnant females were examined twice a day (at 11-13 hours intervals) from the time they appeared to be in late gestation, through delivery and nursing of the pups, for the charting of survival and weight changes of the pups until the neonates reached weaning age. This method allowed me to collect data on the timing of neonatal deaths, and also any evidence of failure to thrive of the pups. D6 KO mice appeared to have a higher perinatal death rate than the WT group, and the majority of deaths occurred either before being born (stillbirth) or within the first week of life. For the surviving pups however, there was no difference in the average weight changes between the two groups (Fig 4.2). The difference of the survival rate between WT and D6 KO was not statistically significant, however the pattern of perinatal death was rather similar to the data generated previously (Fig 4.1). It would be interesting to study the survival curve on a sample size as large as that group. Due to limited resources, a larger sample size could not be generated for this study. Nevertheless, the data reveal that in WT and D6 KO mice, most deaths occurred in the perinatal period within the first week, after which D6 deficiency had no effect on pup weight gain.

a)

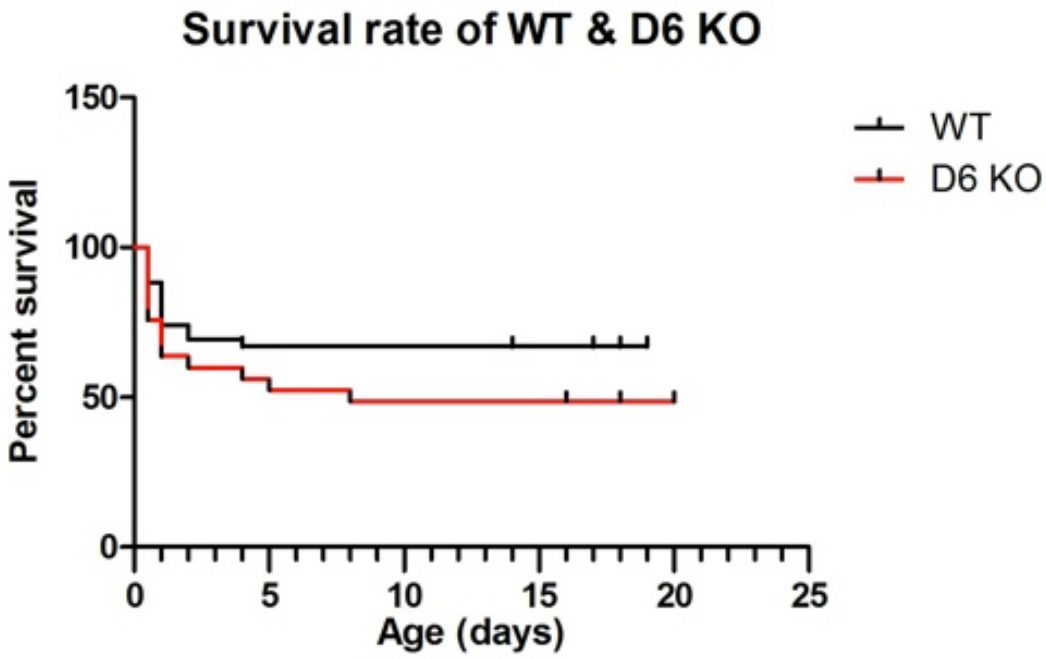

b)

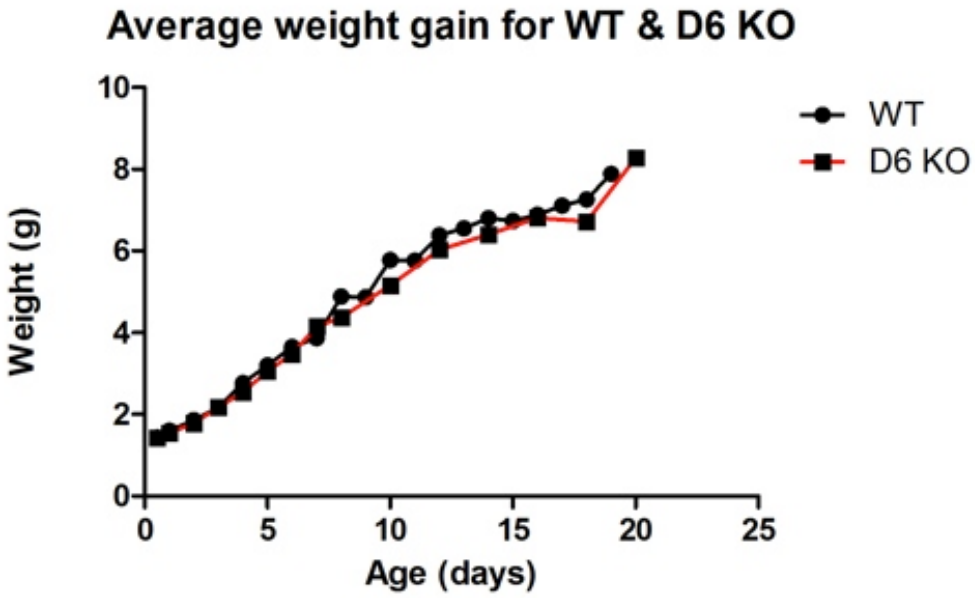

Figure 4.2 D6 KO mice appeared to have a higher perinatal death rate than the WT group. Over a period of 2 months, WT and D6 KO females were mated with males with the same genetic background. The number of live pups and dead carcasses were counted until all the pups were successfully weaned, or when there was no live pups left in the litter. The weight of the live pups was plotted until they were successfully weaned. a) Survival curve covering the period of study. n=43 for WT, n=33 for D6 KO. Majority of deaths occurred either before being born (stillbirth) or within the first week of life. Log rank (Mantel-Cox) test, p= 0.12 b) For the surviving pups, there was no difference in the average weight gain between the two groups. n=10 litters for WT; n= 6 litters for D6 KO.

4.3 Relative mRNA expression of chemokines in mouse placentas

It is well known that in humans and mice, the phenotypes of neonates and fetuses are highly affected by placental function. Placental deficiency is often associated with growth restriction and perinatal death. The postnatal phenotype of D6 deficient mice, and the fact that D6 is expressed by fetal cells in the placenta (Madigan et al., 2010), suggests the reason for perinatal death of D6 deficient pups may lie within the formation and function of the placenta.

To study if there was any evidence of inflammation in D6 deficient placenta the expression of D6 ligands in the placentas of D6 KO mice in comparison to WT was examined. qPCR was carried out to quantify the mRNA expression of CCL2, CCL3, CCL4, CCL5, CCL11, CCL12, CCL17 and CCL22, comparing WT and D6 KO placentas harvested at E18 (Fig 4.3). D6 was also analysed. As an endogenous control that is unlikely to be affected by D6 deficiency, GAPDH and B-actin expression were analysed for each sample. Between the samples, the expression of both of these housekeeping genes was stable; GAPDH was used for normalising all the results for the mouse placentas. Eight placentas from each group were analysed, these placentas are the same ones selected for the stereology study (see section 4.5). As expected, D6 mRNA was readily detected in WT placentas, but not in D6 deficient placentas (Fig 4.3). There was considerable variation in the expression of the chemokines studied, however this can be due to the difference in the efficiency of the primers used for their detection. All the chemokines analysed were not differentially expressed between WT and D6 deficient placentas, with the exception of CCL17 transcripts which were found to be higher in the D6 KO group (discussed further in section 5.2.2.2). This finding was confirmed by qPCR to analyse the expression of CCL17 in all the other available E18 mouse placentas dissected from well-formed pups (Fig 4.4). Thus, D6 deficient E18 placentas show higher expression of the CCL17 gene.

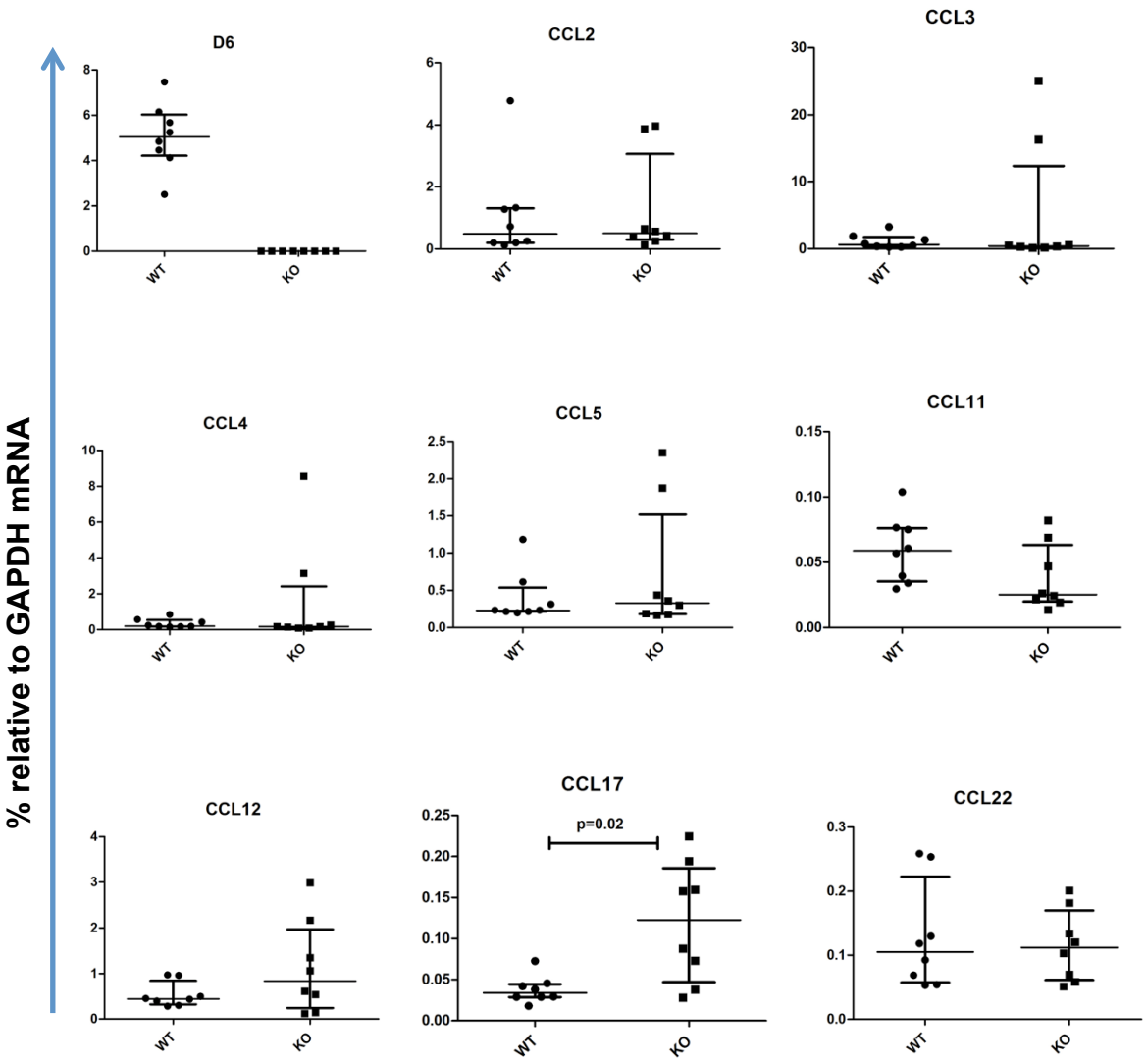

Figure 4.3 mRNA encoding CCL17 was higher in the D6 KO placenta. Analyses of mRNA expression of D6 and its ligands by qPCR. n= 8 in each group. Placentas were harvested at E18. RNA was extracted, cDNA was generated and the samples were then subjected to qPCR analyses. Graphs show median + interquartile range and individual data points. Mann-Whitney test.

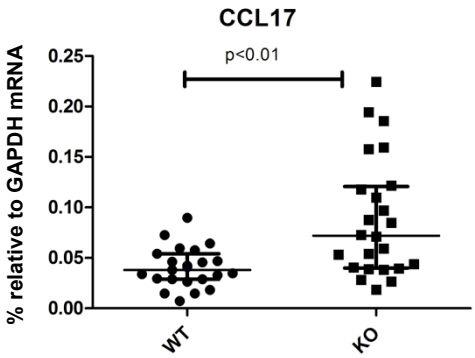

Figure 4.4 Confirmation of higher mRNA expression of CCL17. More placentas from well formed pups were analysed to confirm earlier finding from eight placentas in each group. WT n= 23, D6 KO n= 24. Graphs show median + interquartile range and individual data points. Mann-Whitney test.

4.4 Relative mRNA expressions of white cell markers in the mouse placentas

D6 may regulate chemokine abundance, and D6 deficient placentas contain higher levels of CCL17 mRNA. Thus, more leukocytes may be recruited to D6 deficient placentas. To examine this the expression of white cell markers in the placentas was studied. Besides D6, CCL17 is also a ligand for CCR4, which is expressed in regulatory T cells (Treg) (Leber et al., 2010). Perhaps without D6, a higher expression of CCL17 in the D6 KO group acts as a compensatory mechanism to regulate inflammation by attracting more Treg to localise in the area. Apart from Treg, monocyte/macrophages and T cells also migrate in response to D6 ligands. Therefore D6 deficiency may also affect the level of the markers for these white cells. However, analysis of the same 8 placentas used earlier for chemokine expression showed there were no differences in the expression of Foxp3 (Treg), F480 (macrophages) or CD3 (T cells) between the groups (Fig 4.5). Thus, there appears to be no detectable increase in the recruitment of these cells to the D6 deficient placenta.

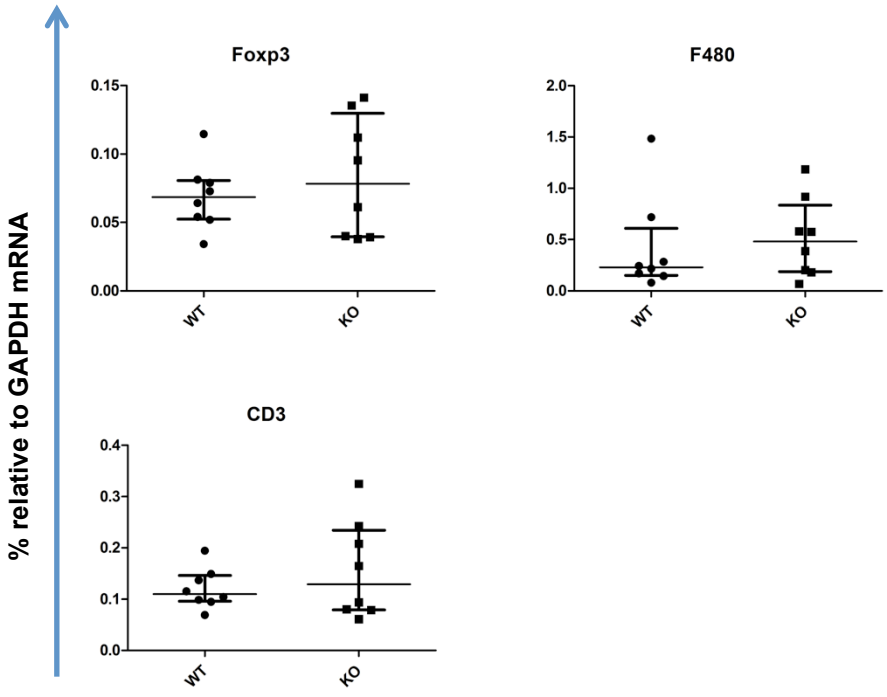

Figure 4.5 No difference in the expression of white cell markers between WT and D6 KO placentas. Analyses of mRNA expression of white cell markers by qPCR. n= 8 in each group, the same samples used in Figure 4.3. Graphs showing median + interquartile range and individual data points. Mann-Whitney test.

4.5 Stereology of mouse placentas

To gain further insight into the D6 deficient placenta, pup weights, placental weights and pup/placenta ratios were examined; stereology on the placentas at early (E10), mid (E14) and late (E18) gestations of the mice was also performed.

Stereology is a well established technique using systemic uniform random sections (Coan et al., 2004), allowing minimally-biased and economical quantitation of the 3D structure and function of the placenta from cellular to whole tissue levels (Mayhew, 2009). In the experiments the volume fractions (percentages of total volumes) of different functional zones of the murine placentas were studied. These 4 different functional zones were: decidua basalis (DB), junctional zone (JZ), labyrinthine zone (LZ) and chorionic plate (CP). There was a particularly interest in the LZ. This is the zone where the irregularly shaped maternal blood spaces are closely juxtaposed to fetal capillaries. This fetal-maternal interface represents the principal site of haemotrophic exchange (Coan et al., 2004). Previous studies have shown that genetic or environmental factors that result in low pup weights are associated with reduced LZ volume in mice (Coan et al., 2008, Coan et al., 2010).

Experiments at E10 were abandoned because the placentas at that stage were too small, friable and technically challenging to section. Professor Burton's group at the Centre of Trophoblast Research, University of Cambridge was consulted for advice regarding this difficulty. They confirmed that mouse placentas in very early gestations are unsuitable to be used for stereology study due to this technical issue.

Comparison of WT and D6 KO pups at E18 showed there was no difference in pup weight, placental weight and pup/placenta weight ratio (Fig 4.6). Stereology of the placentas did not show any differences in all the functional zones at E18 (Fig 4.7). However, at E14 the pup weight was lower for D6 KO than WT (Fig 4.8). The functional volumes were lower for LZ, and higher for JZ in the D6 KO group compared with WT counterparts (Fig 4.9).

This phenotype in the D6 deficient placenta at E14 could potentially be due to a maternal or a fetal effect of D6 deficiency. To examine this, females

heterozygous for the deleted D6 allele (D6 HET) were bred with D6 KO males, generating D6 HET and D6 KO siblings in the same D6 HET mother. Pups were genotyped to ascertain their genetic background. Out of the total of 20 pups from two D6 HET females, there were 11 D6 HET and nine D6 KO pups, close to the expected ratio of 1:1 (Fig 4.10).

Stereology of the placentas showed reduced LZ and increased CP volume fractions in the D6 KO siblings at this gestation (Fig 4.11). However, pup weight, placental weight and pup/placenta weight ratio were the same between the 2 groups of D6 HET and D6 KO siblings (Fig 4.12). The result of placental stereology from the two HET mothers was similar to the finding in the experiment comparing WT and KO mice, therefore we did not have to sacrifice more HET females for this study. Collectively, the stereology report indicates that formation of placenta early to mid gestation is dependent on the D6 genotype of fetus. However, the weight of the D6 KO pups was not affected by fetal D6 deficiency in the presence of D6 expression by the mother and siblings; although the group size is smaller this result is different from the data comparing the offspring from WT and D6 KO females.

To ascertain the importance of labyrinthine zone in supporting fetal growth, the correlations between the volume fraction of different functional zones and pup/placenta weight ratio were analysed. It is more reasonable to compare the placental function with pup/placenta weight ratio rather than pup weight, to normalise the size of the placenta in the analysis. For this analysis, all the placentas with data from stereology as described above were included. At E18, the placentas from WT and D6 KO females bred with males of the same genetic background were included. At E14, the placentas included were from WT and D6 KO females bred with males of the same genetic background, and also from D6 HET females bred with D6 KO males. There were significant positive correlations between pup/placenta weight ratio and labyrinthine zone volume fraction at both E18 and E14 (Fig 4.13 and 4.14). The volume fractions of junctional zone (E14 and E18), and to a certain extent chorionic plate (E14), were negatively correlated to pup/placenta weight ratio, presumably as a result of replacement of the loss in the volume of labyrinthine zone.

Collectively, stereology of mouse placentas showed D6 deficiency of the fetus leads to a decrease in the functional volume of labyrinthine zone in the placenta in early to mid gestation. The functional volume of labyrinthine zone is essential in supporting fetal growth, as there are significant positive correlations between pup/placenta ratio and labyrinthine zone volume fraction.

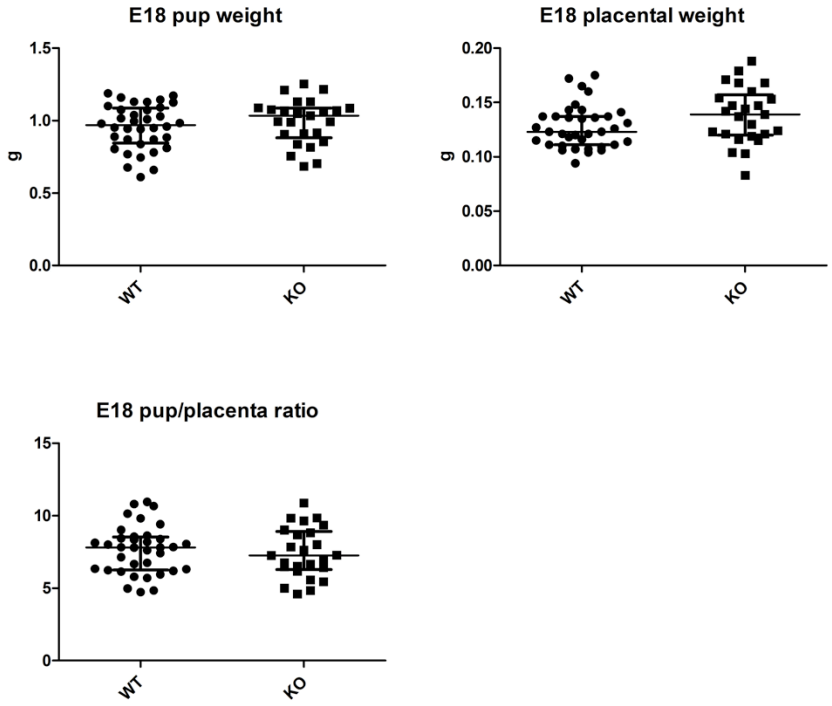

Figure 4.6 No differences in pup weight, placental weight and pup/placenta weight ratio between WT and D6 KO at E18. Comparisons of wet weight of pups and placentas, and also pup/placenta ratio at E18 between the two groups. WT n=36; D6 KO n=25. Graphs showing median + interquartile range and individual data points. Mann-Whitney test.

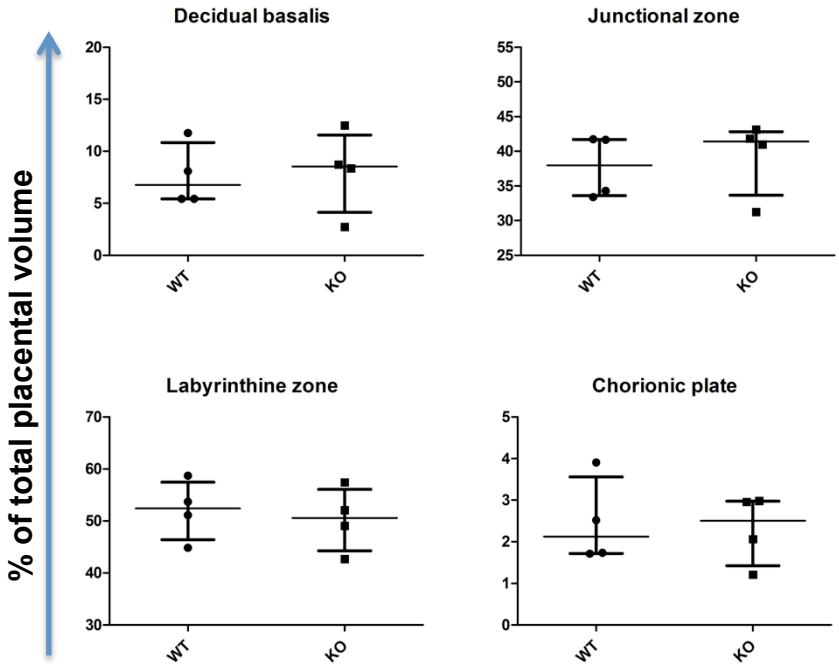

Figure 4.7 No difference in the volume of the functional zones in the placentas between WT and D6 KO at E18. One half of each placenta was serially sectioned at 8μm, and aligned in the correct order from the beginning until the end. At fixed interval, representative sections from each placenta were mounted on slides, and stained with haematoxylin and eosin. Stereology was carried out where the sections were gridded and randomly plotted to compare the volume of different functional zones. n=2 placentas from each litter, four litters for each group. Graphs showing the mean of each litter and median + interquartile range for each group. Mann-Whitney test.

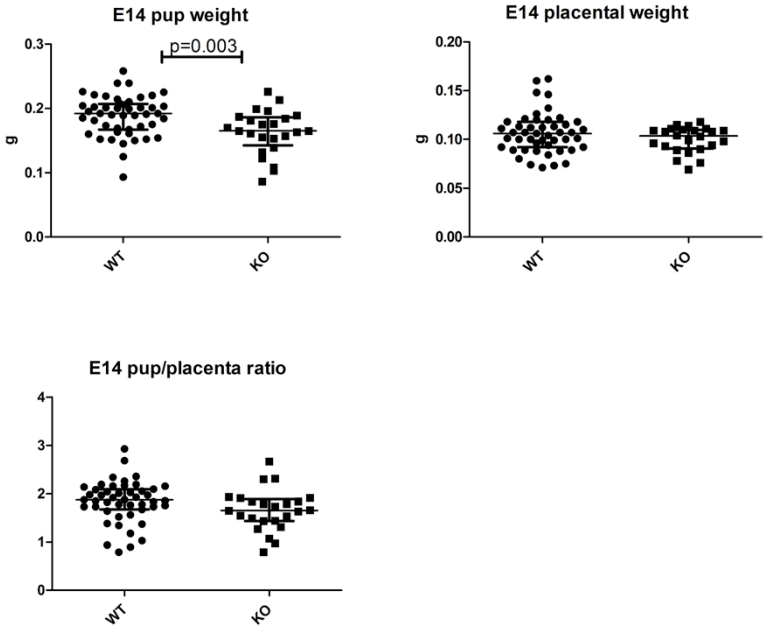

Figure 4.8 Pup weight was significantly less in D6 KO in comparison to WT at E14. Comparisons of wet weight of pups and placentas, and also pup/placenta ratio at E14 between the two groups. Placental weight and pup/placenta ratio were similar between the two groups. WT n=47; D6 KO n=24. Graphs showing median + interquartile range and individual data points. Mann-Whitney test.

a)

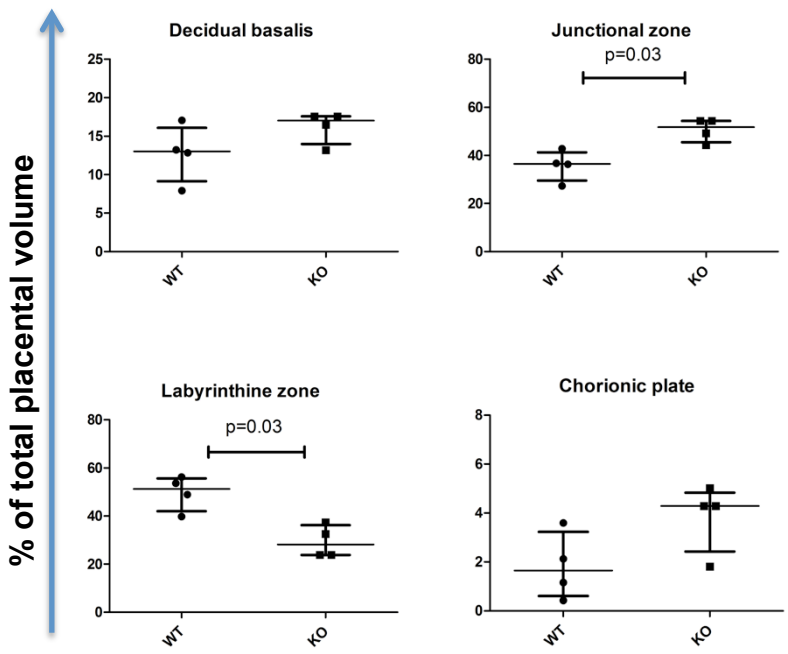

b)

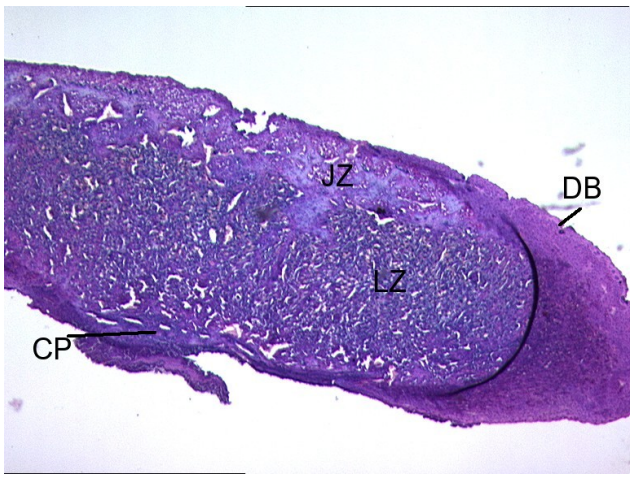

E14 WT mouse placenta

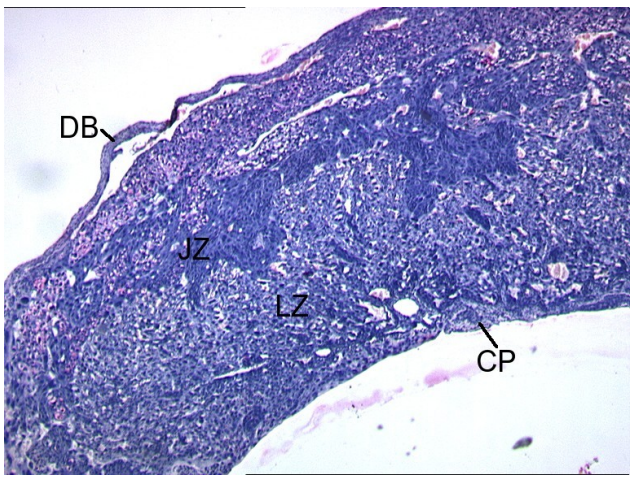

E14 D6 KO mouse placenta

Figure 4.9 Decreased labyrinthine zone and increased junctional zone in D6 KO at E14. Stereology analyses of the placentas comparing WT and D6 KO groups at E14. a) n=2 placentas from each litter, four litters for each group. Graphs showing the mean of each litter and median + interquartile range for each group. Mann-Whitney test. b) Histological sections showing thickened junctional zone and smaller labyrinthine zone in D6 KO at E14. DB= decidua basalis; JZ= junctional zone; LZ= labyrinthine zone; CP= chorionic plate.

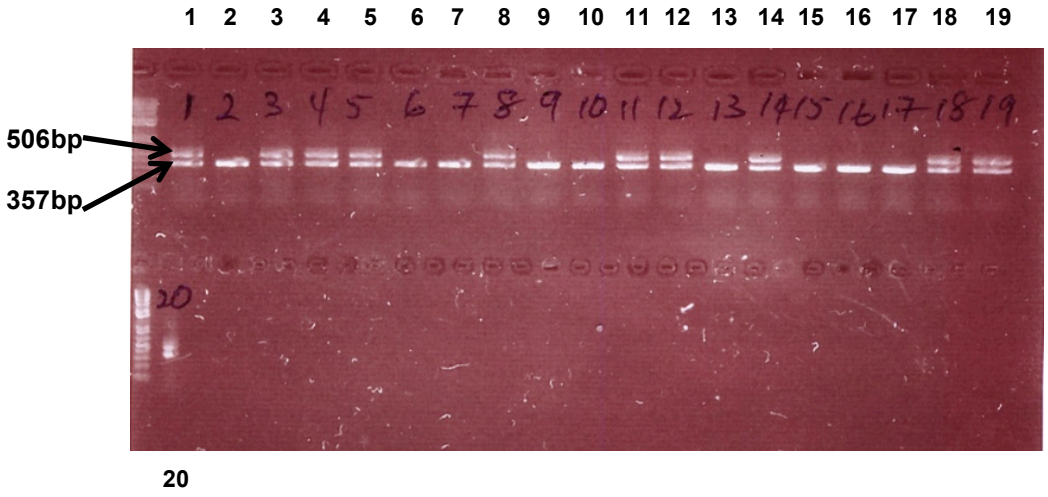

Figure 4.10 1:1 ratio of D6 HET and D6 KO pups. Genotype of pups from two D6 HET females bred with D6 KO males. Columns with two bands depicted genotype of D6 HET pups; one band depicted genotype of D6 KO pups. One HET female had 12 pups (columns 1 to 12); the other had 8 pups (columns 13 to 20). Samples taken from pups, and genomic DNA isolated. PCR was performed using three primers, one common to both WT and D6 KO alleles, and one specific to each allele.

a)

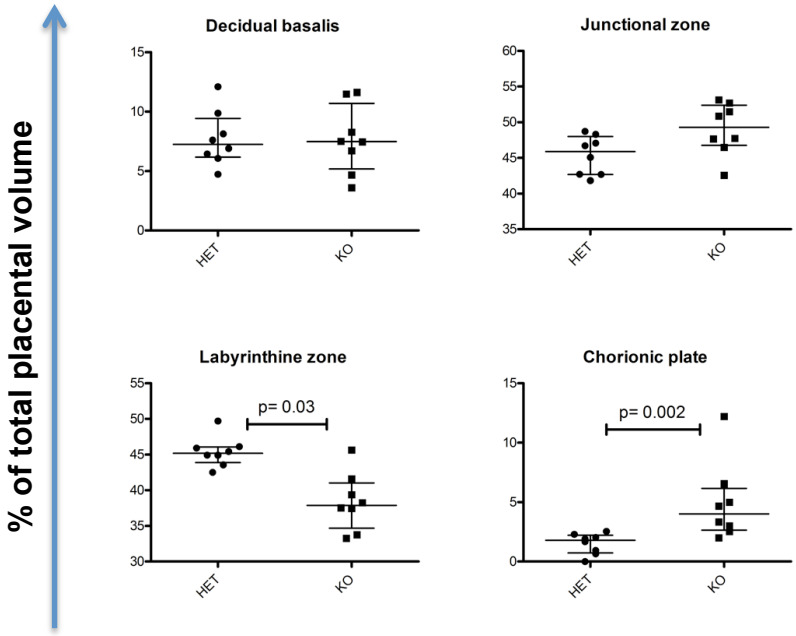

b)

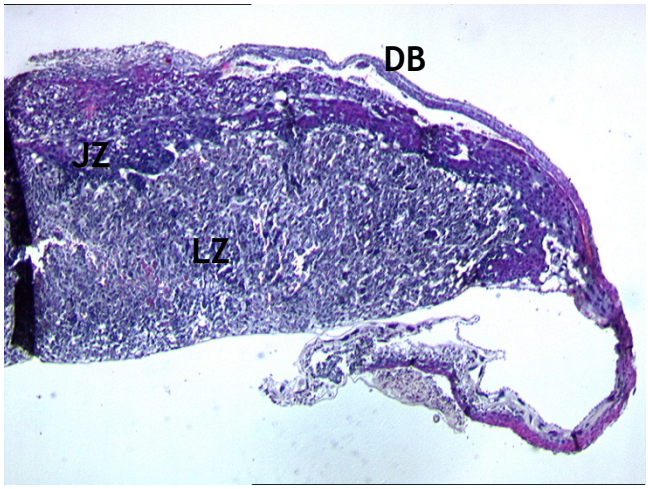

E14 D6 HET mouse placenta

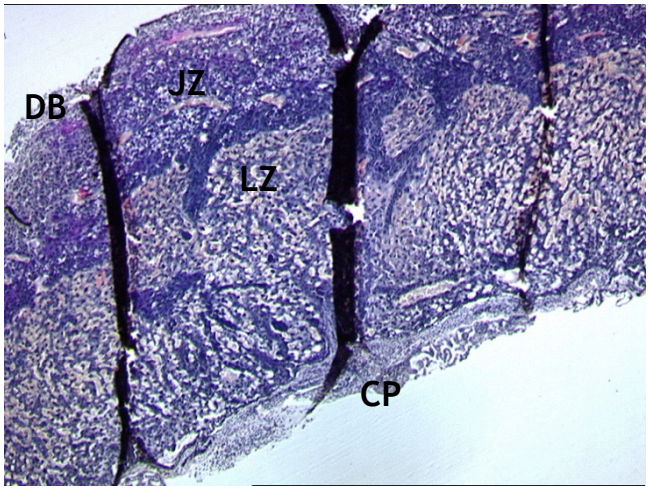

E14 D6 KO mouse placenta

Figure 4.11 Decreased labyrinthine zone and increased chorionic plate in D6 KO comparing with their D6 HET siblings at E14. Stereology analyses of the placentas comparing D6 KO and their D6 HET siblings at E14. The pups were genotyped. a) n= 4 placentas for each litter for each group, two litters in total. Graphs showing the result for each placenta and median + interquartile range for each group. Mann-Whitney test. b) Histological sections showing thickened chorionic plate in D6 KO at E14. DB=decidua basalis; JZ=junctional zone; LZ=labyrinthine zone; CP=chorionic plate.

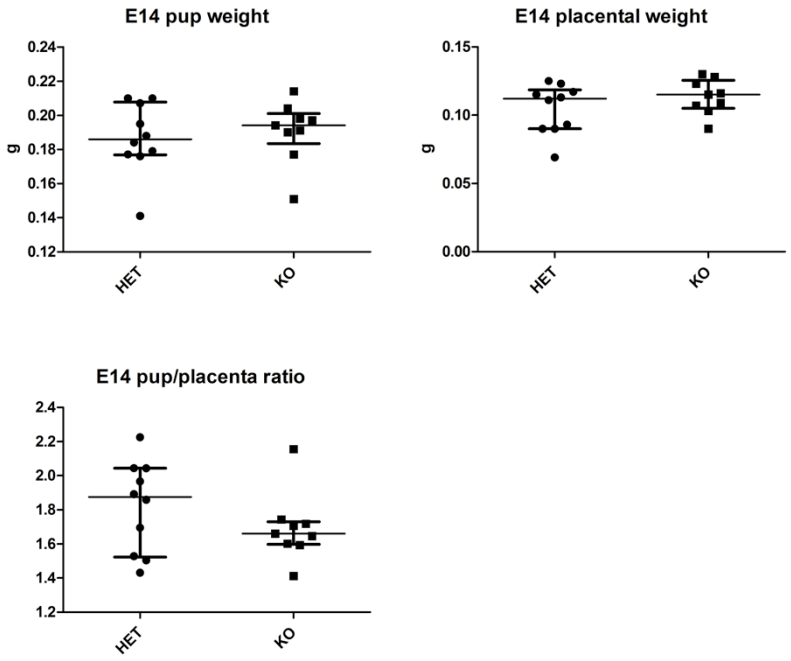

Figure 4.12 No differences in pup weight, placental weight and pup/placenta ratio between D6 HET and their D6 KO siblings at E14. Comparisons of wet weight of pups and placentas, and also pup/placenta ratio at E14 between the two groups. The pups were genotyped. D6 HET n=10; D6 KO n=9. Graphs showing median + interquartile range and individual data points. Mann-Whitney test.

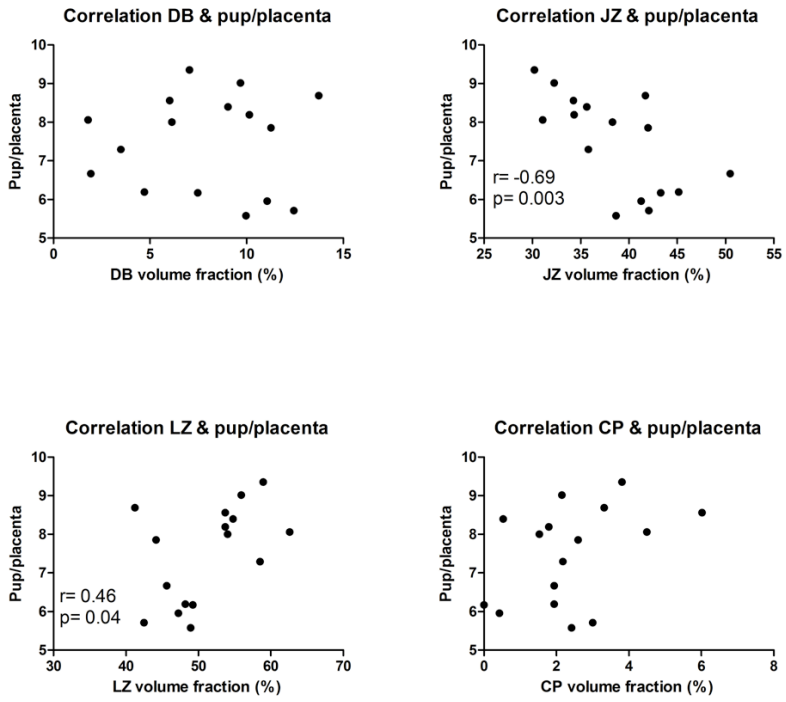

Figure 4.13 Pup/placenta ratio significantly correlates to labyrinthine zone volume fraction at E18. Significant positive correlations to labyrinthine zone and negative correlations to junctional zone. Spearman rank correlation coefficient. n=16; placentas from WT and D6 KO females bred with males of the same genetic background.. DB= decidua basalis; JZ= junctional zone; LZ= labyrinthine zone; CP= chorionic plate.

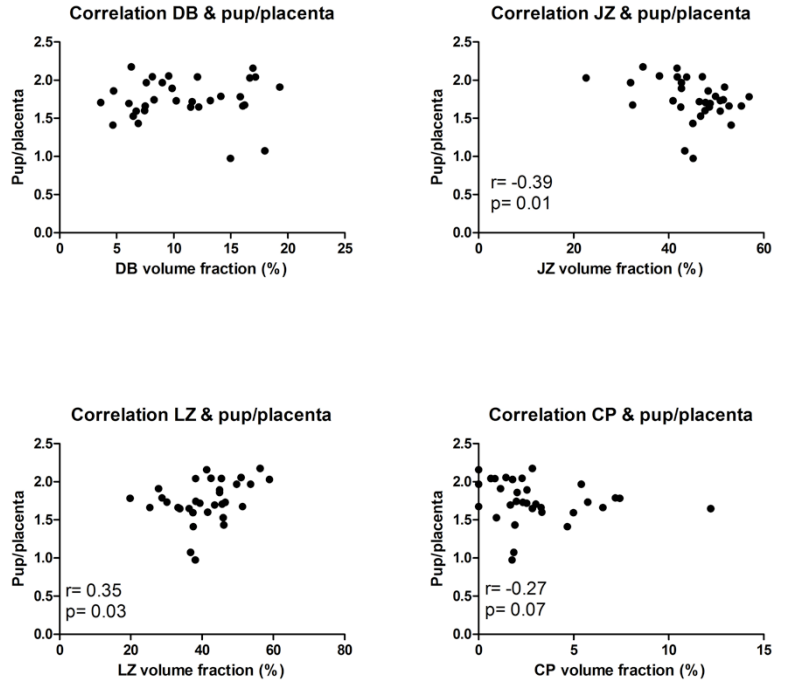

Figure 4.14 Pup/placenta ratio significantly correlates to labyrinthine zone volume fraction at E14. Significant positive correlations to labyrinthine zone and negative correlations to junctional zone. There is also a trend showing negative correlations to chorionic plate. Spearman rank correlation coefficient. n=32; placentas from WT and D6 KO females bred with males of the same genetic background, and also from D6 HET females bred with D6 KO males. DB=decidua basalis; JZ=junctional zone; LZ=labyrinthine zone; CP=chorionic plate.

4.6 Quantification of chemokine levels in plasma using Luminex multiplex protein assay

In humans, D6 is much more highly expressed in the placenta in comparison to other solid tissues (Nibbs et al., 1997b) . Furthermore, in term human placenta, the chorionic villi are thought to have a surface area of about $10m^2$ (Biswas et al., 2008). One would expect the level of D6 ligands to be reduced in pregnancy, as the maternal blood flows through the large surface area of D6 abundance in the placenta. The results from Madigan et al suggest that this postulation is true in humans (Madigan et al., 2010).

In mouse, D6 is also expressed in the placenta, albeit at a lower level than in humans (Nibbs et al., 1997a). Stereological analysis shows the surface area of maternal blood space in a mouse placenta at E18.5 to be $23.87cm^2$ (Coan et al., 2004). Given that a litter can consist of more than 10 pups, the combined surface area of maternal blood space in the placentas of a pregnant mouse is substantial. Thus the placentas in a pregnant mouse may have a major contribution in regulating the level of D6 ligands in the blood. Perhaps if there are differences in the systemic levels of D6 binding pro-inflammatory chemokines between WT and D6 KO, they also play a major role in determining the phenotype of the offspring.

Luminex multiplex protein assay showed that in mouse plasma, the level of CCL2 (D6 ligand) is higher in pregnant D6 KO mice than pregnant WT animals. The difference is more marked at E14 in comparison to E18. However, due to insufficient power, the difference of CCL2 between WT and D6 KO did not reach statistical significance when E14 and E18 were analysed separately. There is no difference in the level of D6 ligands CCL3 and CCL5, or the non-D6 ligand CXCL1 between the two groups of mice (Fig 4.15).

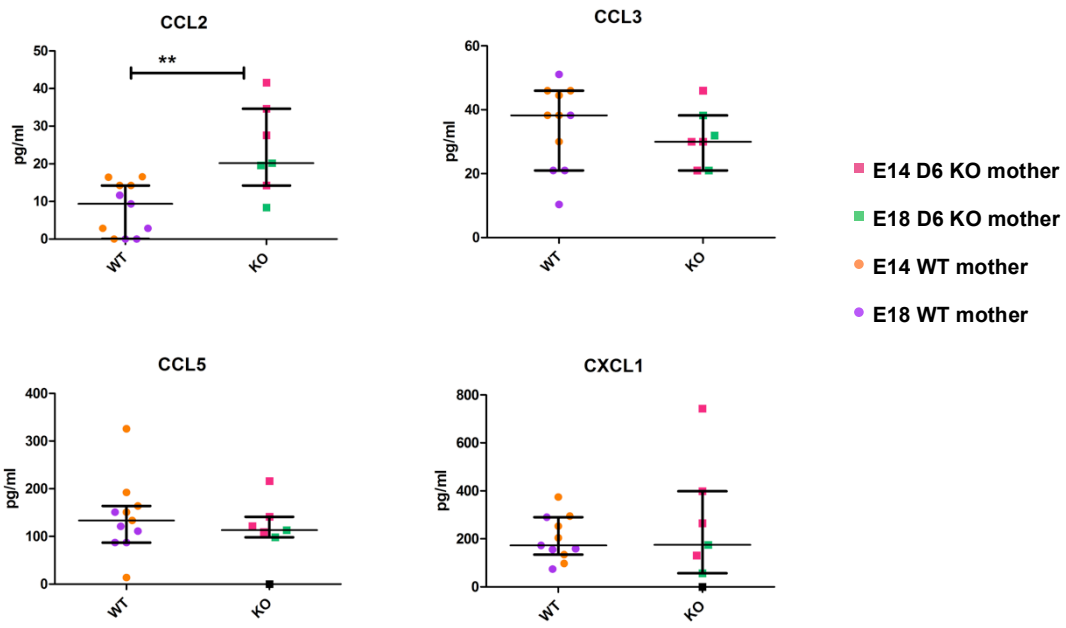

Figure 4.15 D6 KO pregnant mice had significantly higher CCL2 in the plasma. Quantification of chemokine levels in the plasma for pregnant mice at E14 and E18 by Luminex multiplex protein assay. CCL2, CCL3 and CCL5 are known D6 ligands. CXCL1 is a non-D6 ligand, used as a negative control. **Linear mixed effect statistical modelling; difference between WT and D6 KO p= 0.001; difference between E14 and E18 p= 0.03. n=11 for WT and n=7 for D6 KO; one sample was excluded each for WT and D6 KO due to the level of chemokines clearly not representative of the rest of the group, shown as significant outliers from the rest by Grubbs' test (http://graphpad.com/quickcalcs/Grubbs1.cfm). Individual analysis of CCL2 level at E14 and E18 showed the difference between WT and D6 KO was more marked at E14, however this did not reach statistical significance due to inadequate sample size, resulting in an underpowered study.

4.7 Summary

Animal models showed that D6 deficiency is associated with fetal loss. In this chapter, the phenotypes of D6 deficiency in the placentas and pups of DBA-1 mouse was studied in order to understand the pathophysiology underlying these compromised features. The initial hypothesis was that, the suboptimal reproductive outcome in D6 KO pups was due to a fundamental defect in the formation of functional anatomy of the placenta.

D6 KO DBA-1 mice cohort had higher stillbirth and neonatal deaths, resulting in lower pups weaned/litter in comparison to their WT counterpart. A more detailed analysis showed the majority of deaths in both groups occurred either

before birth (stillbirth) or within the first week of life. For the surviving pups, there was no difference in the average weight gain between the two groups.

At E18, there was no difference in mRNA expression of D6 ligands in the placentas apart from CCL17. mRNA expression of CCL17 was higher in D6 KO placentas. Despite the higher level of expression of this chemokine in the D6 KO group, there were no differences in the expression of the markers for Treg, macrophages or T cells.

At E18, no differences were detected in the pup weight, placental weight and pup/placenta weight ratio between WT and D6 KO. At this gestation, stereology showed no difference in the volume fractions of the functional zones in the placentas between WT and D6 KO. However at the earlier gestational age of E14, the pup weight was significantly smaller in the D6 KO mice. Stereology analysis at this gestation showed a decrease in labyrinthine zone volume fraction. The experiment at E14 was extended, breeding D6 HET DBA-1 females with D6 KO males, to compare the phenotypes of D6 KO pups and placentas with their D6 HET siblings that developed in a mother expressing some D6 (i.e. D6 HET). Although there were no differences in pup weight, placental weight and pup/placenta ratio between these two groups, stereology revealed a decrease in labyrinthine zone volume fraction in the D6 KO placentas in comparison to their D6 HET siblings.

Analysis of the correlation between pup/placenta ratio and different functional zones of the placentas showed that at all gestations there were significant positive correlations of the pup/placenta ratio to the labyrinthine zone volume fraction, and significant negative correlations to the junctional zone volume fraction.

Quantification of chemokine levels in plasma using Luminex multiplex protein assay showed D6 KO pregnant mice had significantly higher CCL2 in the serum in comparison to the WT counterpart. No differences were detected in the level of CCL3 and CCL5 (both D6 ligands), and also CXCL1 (non D6 ligand).

Thus, D6 deficiency in DBA-1 mice is associated with increased neonatal death, reduced labyrinthine zone size, and dysregulation of circulating chemokine levels. These findings are discussed in greater depth in the Discussion section.

4.8 Limitations

WT and KO mice have been bred as separate colonies for many generations, thus genetic drift could have occurred as a result and affected the phenotypes of the mice. For the WT and KO comparison, we relied on the detection of copulation plug for the determination of the gestational age. This technique is known to be an efficient way for conducting mouse experiments within a set time limit, albeit not the most accurate method of dating mouse pregnancies. The results from HET mice from subsequent experiments were helpful in confirming the findings on WT and KO mice; in this experiment the method of timing of gestational period was improved.

The frequent intervention of weighing the pups in the neonatal period could have caused distress to the mothers and pups, this may have also affected the behaviour of the mothers. However, despite the intervention in the neonatal period, the rate of neonatal death is similar to the data provided by the staff in the Central Research Facility.

The study of mRNA expression of the chemokines in the mouse placentas indicated the pattern of protein synthesis, however the level of protein in the tissues may not be truly reflected by this experiment. On a related note, the study of mRNA expression of white blood cell markers would not have shown any difference in the pattern of distribution of the cells. These experiments can be complemented by studies of protein levels.

The sample size of the animals needed was difficult to be determined before starting the stereology experiment. Prior to the experiment, it was not known whether the expression of D6 would have caused any difference in stereological analysis. Taking the welfare of the animals into consideration, the aim was to sacrifice as few mice as possible. We started the stereology experiment with four litters in each arm. As shown in the results, no difference was detected in our first experiment at E18. In this instance it is difficult to gauge whether any

difference will be detected if a larger sample size is used. However by studying the patterns of pup/placenta ratio at E18 and also the correlations between labyrinthine zone volume fraction and pup/placenta ratio, it is postulated that no difference will be detected even if a larger sample size is used.

5 Discussion

During implantation, the decidua has to be receptive to the implantation of the semi-allogeneic embryo. This delicate process, along with the formation of the placenta, requires intimate cross-talk between fetal trophoblasts cells, maternal stromal cells in the uterine wall, and specialised maternal decidual leukocytes, which are recruited to the decidua during pregnancy.

The placenta serves to support the nutrition, survival and wellbeing of mammalian fetuses until they are mature and ready to be delivered from the uterus. A good pregnancy outcome is greatly dependent on successful placentation, with adequate depth of invasion into the myometrium. Abnormal placentation is one of the common findings in pregnancies that lead to intrauterine growth restriction and stillbirth (Khong et al., 1986, Bukowski et al., 2011); it has also been shown to be related to late sporadic miscarriage and preterm labour (Kim et al., 2003, Ball et al., 2006, Brosens et al., 2011, Kovo et al., 2013). There is also a report that a risk of stillbirth can be predicted by placental function in the first ten weeks after conception (Smith et al., 2004). Placentas that invade too deeply into the myometrium result in placenta accreta, which poses a great risk of haemorrhage to pregnant women during delivery. On the contrary, inadequate placentation in human is associated with the above complications in pregnancy and also pre-eclampsia and eclampsia, with significant risk of fetal and maternal morbidity and mortality in pregnancy.

Chemokines play a major role in regulating the process of placentation. By binding to G-protein coupled receptors, chemokines become important communication tools between leukocytes and trophoblasts. They are believed to be one of the central mechanisms that control the infiltration and localisation of specific cells in the placenta and decidua. In the decidua, the distribution of expression of different chemokines and their receptors are distinctive, defining the specific role they play in the process of placentation (Red-Horse et al., 2004, Hannan and Salamonsen, 2007)

D6, an atypical chemokine receptor, is highly expressed in the placenta, and is postulated to exert its role as a scavenger of CC chemokines in the organ. It is expressed by fetal trophoblasts at the feto-maternal interface that separates fetal cells from the maternal tissues, and it has been proposed to play a role in protecting the embryo from immunological detection and attack from maternal

leukocytes (Madigan et al., 2010). Previous in vivo experiments showed that D6 has an indispensible protective role in pregnancy in challenged and fully allogeneic models (Martinez de la Torre et al., 2007, Madigan et al., 2010, Kliman et al., 1986). In vivo experiments using BeWo cells reported D6 is present in this trophoblast-derived choriocarcinoma cell line, and acts as a chemokine scavenger (Madigan et al., 2010).

At present, the pathophysiology of abnormal placentation, a process that starts at early gestation, is poorly understood. Based on previous findings, it is plausible that dysfunction in chemokine regulation could greatly affect this delicate process, resulting in the pregnancy disorders described. The abundance and precise localisation of D6 in the placenta indicate that it plays an important role in regulating the bioavailability of chemokines at specific microanatomical locations. The findings in this thesis lend further support to the idea that D6 on trophoblasts scavenges chemokines. Moreover, they demonstrate that loss of D6 can lead to fundamental defects in placental structure that appear to compromise the health of neonates.

5.1 Molecular function of D6

5.1.1 Approaches to exploring D6 function in vitro

Much of what we know about the function of D6 has come from the analysis of its behaviour when it is over-expressed in an immortalised cell line. In this context, D6 binds with high affinity to many pro-inflammatory CC chemokines but appears unable to couple to signal transduction pathways that are typically activated by chemokine receptors. However, because of its trafficking properties in these cells lines, D6 can continuously remove chemokines from the extracellular environment and it is this behaviour that has led to the concept that the function of D6 in vivo is to act as a non-signalling chemokine scavenger in vivo. This idea has been supported by the analysis of D6 function in immortalised choriocarcinoma cells (BeWo) and is consistent with many of the phenotypes observed in D6 deficient mice. However, the function of D6 had not been explored on primary human cells, yet this is important to get a more reliable insight into D6 function in vivo.

Primary cultured human trophoblasts are arguably the most representative cells in which to explore the function of D6 in the human placenta. This approach is far more technically challenging than using immortalised cell lines, which are easy to culture, store and analyse, and there is no limitation on the number of cells that can be generated. In contrast, when working with primary trophoblasts careful planning was required to obtain a regular supply of fresh placentas and isolate the cells, and these cells only have a limited lifespan and undergo syncytialisation within 48 to 72 hours of isolation (Whitley, 2006, Orendi et al., 2011). Moreover, only a limited number of cells could be purified from each placenta, and the time period available for performing experiments was restricted by the time that these cells survive in culture. A considerable amount of time was spent establishing and developing this technique to effectively and reproducibly isolate and culture trophoblasts from fresh samples. Nonetheless, despite the difficulties and inconveniences, using primary human trophoblasts is the optimal method of studying D6, because it is in these cells that it will show its characteristics closest to its biological form in the body. Importantly, this work is the first experimental report of D6 on primary human cells.

In my experiments, human placentas underwent enzymatic digestion and cells were purified in layered Percoll gradients. This technique was first described by Kliman et al., and is known as a high-yielding protocol of isolating primary trophoblasts with sufficient purity (Kliman et al., 1986). This approach of trophoblast isolation and purification was adopted even in experiments in recent years (Aye et al., 2010, Desforges and Westwood, 2011). Immunoselection methods may produce a higher purity of trophoblasts (Pötgens et al., 2003), but this was not practical in our laboratory, due to the scale and time required for the experiments. For each placenta collected, limited time was available for performing different experiments before the cells lost viability or syncytialised.

Concentration of oxygen may affect the behaviour of the cells in trophoblast culture. In vivo, the level of oxygen in the placenta fluctuates from the start of placentation until the end of the first trimester. As described earlier, after implantation endovascular extravillous trophoblast cells migrate to the lumens of the spiral arteries and occlude them. This limits the maternal blood flow into the placenta. At this stage the partial pressure of oxygen in the placenta is less than 20mmHg; thus the embryo is protected from free radicals (Rodesch et al.,

1992, Burton and Jauniaux, 2004). Incomplete plugging of the arteries leads to premature intervillous circulation, which can result in abnormal placental development and pathological conditions in pregnancy (Jauniaux et al., 2003, Burton and Jauniaux, 2004). Normally the low oxygen environment is maintained until about 10-12 weeks of gestation, and begins to rise when maternal blood starts entering the intervillous space. After the twelfth week of gestation, the oxygen partial pressure rises to 40-60mmHg (5-8% oxygen); the oxygen concentration continues at this level until the third trimester (Rodesch et al., 1992, Burton and Jauniaux, 2004). In vitro studies showed that when trophoblasts were exposed to hypoxic conditions with oxygen concentration of 2% or below, the epigenetic profile, and also gene and protein expression of the cells altered (Newby et al., 2005, Oh et al., 2011, Yuen et al., 2013). In this environment the cells also differentiated poorly, and did not cease to proliferate; this regulatory mechanism that influence the behaviour of trophoblasts is thought to be crucial in determining the success of placental development (Genbacev et al., 1997). Interesting, in the same experiments the authors did not detect any change in the phenotype of the trophoblasts when they were cultured in 8% oxygen concentration in comparison to the standard incubating oxygen concentration of 20% (Oh et al., 2011, Yuen et al., 2013). In my experiment, the trophoblasts from term pregnancies were cultured in the standard oxygen concentration of 20% to avoid the conditioning effect of hypoxia.

The purity of trophoblasts was assessed using flow cytometry, the most objective and quantitative technique described (Frank et al., 2001). Recommended reliable markers cytokeratin 7 and vimentin were used for staining (Frank et al., 2001, Pötgens et al., 2001). Despite initial poor yields and low viability, routine cultures of placental cells that contained 50-100 x 10^6 cells, with 70-85% of which were trophoblasts based on expression of cytokeratin 7 and lack of vimentin were established. With these cultures, experiments were carried out to explore D6 expression and function.

5.1.2 Expression and function of D6 in primary human trophoblasts

By examining RNA and protein, the results clearly demonstrated high expression of D6 in primary cultured trophoblasts. Moreover, immunofluorescence stained D6 protein predominantly intracellular, with no detectable receptor on the surface. This is interesting because this subcellular distribution of D6 is similar to that observed for endogenous D6 in BeWo cells, D6 in trophoblasts in situ in gestational membranes (Madigan et al., 2010), and exogenous D6 overexpressed in HEK293 cells (Weber et al., 2004, Madigan et al., 2010). In HEK293 cells, this distribution is caused by the ability of D6 to rapidly internalise into endosomes after reaching the cell surface, a process that is critical for the ability of D6 to scavenge chemokines in these cells. Thus, this observation implied that D6 might show similar trafficking properties in primary cultured trophoblasts. More importantly, the chemokine uptake and scavenging assays directly demonstrated that D6 in primary trophoblasts can act as a chemokine scavenger and lead to the progressive removal of extracellular pro-inflammatory CC chemokines. Therefore, in many respects, D6 in trophoblasts is behaving as reported in previous studies using immortalised cell lines.

In the experiments assessing the chemokine uptake activity of D6, a slight variation in its specificity in primary trophoblasts in comparison to the D6 transfected HEK293 cells was discovered. D6 in trophoblasts was shown to have a broadly similar ligand binding profile as D6 in HEK293 cells, but CCL11 appeared not to be a ligand for D6 in trophoblasts, despite binding D6 in HEK293. In addition, D6 in HEK293 appeared to have a much stronger affinity for CCL22 than CCL2, but this was not apparent in primary trophoblasts. The molecular basis for these discrepancies is not clear. However, it is worth noting that Western blotting revealed differences in the molecular weights of D6 protein between HEK293 cells and primary trophoblasts. Much of the D6 protein in trophoblasts was of a higher molecular weight than that seen in HEK293 overexpressing exogenous D6. Higher molecular weight of D6 has been reported in the past, and found to be due to N-linked glycosylation of the molecule. It was shown to be dispensable for CCL3 binding by the molecule, but a full analysis of ligand specificity of glycosylation-free D6 was not performed (Blackburn et al., 2004).

Thus, it is possible that differences in the post-translational modification of D6 in HEK293 cells and trophoblasts are responsible for subtle alterations in ligand binding specificity. This would not be surprising as negative charge on chemokine receptors (in the form of negatively-charged amino acids, sulphated tyrosine residues, and/or glycosylation) is important for forming initial interactions with chemokines during the binding process. An alternative explanation is that D6 in trophoblasts contains additional protein-coding exons and that this alters ligand specificity and affinity. It is possible that the splice sites within the intron of D6 gene are different, resulting in the variations in the mRNA generated. This phenomenon has been observed with other human chemokine receptors, most notably CXCR3. It exists in two forms, CXCR3A and CXCR3B, which differ at their extreme C-terminus. This alters ligand specificity and signalling activity (Lasagni et al., 2003). Further work will be required to more fully analyse the specificity and affinity of chemokines for D6 in trophoblasts, and define the molecular basis for any differences between its properties in trophoblasts and HEK293 cells.

Due to time constraints, the analysis of D6 expression and chemokine uptake by subgroups of trophoblasts in the cultures was not carried out. However, gating of the histograms from the flow cytometry for $CCL2^{AF647}$ uptake showed that the $CCL2^{AF647}$-high group consisted of larger cells than the $CCL2^{AF647}$-low group. Perhaps this difference in $CCL2^{AF647}$ uptake was due to the presence of different groups of trophoblasts (villous cytotrophoblasts, extravillous cytotrophoblasts and syncytiotrophoblasts) (Pötgens et al., 2003). Syncytiotrophoblasts are known to be larger than cytotrophoblasts in flow cytometry analysis (Kudo et al., 2003). Further experiments may be able to differentiate the subgroups with $CCL2^{AF647}$-high and $CCL2^{AF647}$-low cells. D6 may have a different scavenging activity depending on the type of trophoblast that expresses it. Alternatively, the difference in $CCL2^{AF647}$ uptake can also be due to distinctive pattern of D6 expression in different group of trophoblasts. With further studies, it may be possible to use $CCL2^{AF647}$ uptake to purify certain types of trophoblasts directly from the culture.

Following the findings from the above studies, the experiments of D6 in trophoblasts could be expanded to further understand the regulation of expression, function and distribution of this protein in these cells. For instance,

trophoblasts could be exposed to different pH's to assess the ability of D6 to bind its ligands. One would expect the affinity of the receptor to its ligand to be reduced in low pH environment. This character of D6 is believed to ensure chemokines bound to D6 are retained inside cells, as when D6 encounter low pH in the endosomes, it releases them for endosomal passage instead of bringing them back to the surface of the cells (Weber et al., 2004).

Trophoblasts could also be pretreated with unlabelled D6 ligands before chemokine uptake and scavenging assays are performed. This would assess whether the receptor is desensitised over time, after repeated exposure to the ligands. In HEK293 cell line, there was no apparent desensitisation of this receptor to subsequent chemokine uptake (Weber et al., 2004).

The scavenging property of D6 can be complemented by experiments using radioligand degradation assays. After introducing radiolabelled chemokine e.g. ^{125}I-mCCL3 to trophoblasts, the degree of degradation of the ligand over time can be measured, correlating to the emergence of non-trichloroacetic acid (TCA) precipitable radioactivity of the supernatant. SDS-PAGE analysis of the supernatants may be able to detect these degraded radioiodinated amino acids or short peptides, represented by diffuse bands with slower electrophoretic mobility than intact ^{125}I-mCCL3 (Weber et al., 2004). Over time, the bands of intact and degraded ^{125}I-mCCL3 from cell lysate and supernatant can be compared quantitatively to picture the pattern of chemokine scavenging activity of D6. The degradation of D6 ligands by lysosomes has been shown to be inhibited by neutralisation of vesicle acidification by NH_4Cl in HEK293 cell line, this study can be carried out in trophoblasts to explore whether similar results are shown (Weber et al., 2004).

By regulating the availability of chemokines, D6 probably has a role to play in orchestrating the chemotactic migration of white cells, and perhaps trophoblasts in the decidua. To investigate this further, migration assays could be performed to explore whether trophoblasts have the ability to migrate towards D6 ligands. In addition, white cells e.g. THP1, a human monocytic cell line, and also Treg or NK cells can be used to study their migratory potential towards trophoblast medium supplemented with chemokine ligands.

The expression of D6 in BeWo cell line has been successfully subdued by the siRNA approach (Madigan et al., 2010). If by using this method the protein expression is significantly reduced, my experiments on chemokine uptake and scavenging, and also migration assays could be repeated to assess the impact of D6 downregulation. D6 activity could also be potentially interfered by using transient transfection methodology to introduce mutant versions of proteins known to interfere with endocytotic pathways, as shown in HEK293 cells in the study by Weber et al (Weber et al., 2004).

In summary, this work demonstrates that cultured primary trophoblasts express D6 protein, and that, in this context, D6 is capable of efficiently scavenging extracellular chemokines. These data lend important support to the idea, developed using immortalised cell lines, that D6 protein regulates chemokine abundance in vivo particularly at the fetomaternal interface, which is by far the richest source of D6 in the human body.

5.2 Role of D6 during reproduction in DBA-1 mice

Two previous studies have investigated the impact of D6 deficiency on pregnancy. In one study, it was shown that D6 deficient mothers carrying D6 deficient pups were more susceptible to LPS- or aPL-induced fetal loss (Martinez de la Torre et al., 2007). In the second study, D6 was demonstrated to enhance the survival of embryos transferred into allogeneic pseudopregnant recipients (Madigan et al., 2010). The data in this thesis clearly show that the survival of fully syngeneic pups is compromised in D6 deficient DBA-1 mice in comparison to WT DBA-1 counterparts. This is the first time that exaggerated perinatal death has been observed in D6 KO mice, and it is not seen when D6 is deleted from C57BL/6 mice. The majority of deaths observed in DBA-1 were stillbirths, or neonatal deaths that occurred within the first week of life. The surviving pups for both WT and D6 KO continued to thrive postnatally. It appears that WT DBA-1 pups, even in an unchallenged environment, are prone to neonatal death and many WT DBA-1 pups were stillborn or died shortly after birth. This was enhanced by loss of D6. Perhaps in this strain of mouse the trophoblasts and leukocytes are highly sensitive to the precise localisation of chemokines required for successful placentation and that lack of D6, by causing deregulation of this

process, results in dire consequences for some of the pups. Clinically this is an exciting finding because it shows that D6, influenced by other genetic factors, can play an indispensible role in protecting fetuses, even in an unchallenged environment. Due to the known expression of D6 by fetal cells in the placenta (Madigan et al., 2010), it seemed likely that the enhanced neonatal death of D6 deficient pups could be due to a defect in the placenta. Indeed, stereology revealed a marked difference in the structure of the placenta feeding D6 deficient pups at E14 in mothers homozygous or heterozygous for the deleted D6 allele.

5.2.1 Stereology reveals labyrinthine zone defects in the E14 D6 deficient placenta

Stereology is an effective, albeit time consuming, way to study the structure and function of an organ. In contrary to two dimensional (2D) histological sections, this systematic, and randomised method allows nonbiased, accurate assessment of the sample, making it possible to obtain a three dimensional (3D) picture of the functional architecture.

On discovering the enhanced neonatal death of D6 deficient pups, one of the key subsequent aims of the project was to examine whether there were fundamental defects in the structure of the D6 deficient placenta. By stereology, it was possible to compare the volumes of different functional zones in the placentas of the mice. The labyrinthine zone (LZ) is the main area where the placenta performs its function in supporting the fetus. This is the zone where maternal blood spaces are interfacing with the fetal blood vessels, supplying nutrients and gases, and removing waste. The fact that the size of the LZ significantly correlated with pup/placenta ratio at all gestations studied shows its importance for feto-maternal exchanges, and for supporting the wellbeing of the fetus. Thus, the smaller the LZ volume, the smaller the fetus.

Comparison between WT and D6 KO mice at E14 showed significant reduction in the LZ functional volume in the D6 KO group, supporting the initial hypothesis that D6 deficiency is responsible for a defect in the structural formation of the placenta. This defect in the functional volume of feto-maternal interface

resulted in a significant reduction in the pup weight, and a trend towards reduced pup/placenta ratio. In the model where we crossbred D6 HET females with D6 KO males, there was also a difference between the placentas supporting D6 HET and their D6 KO siblings. D6 deficiency caused a significant reduction in LZ functional volume, and a trend towards reduced pup/placenta ratio. This confirmed that the placental phenotype associated with D6 deficiency was caused by a fetal effect rather than lack of D6 in the mother.

It was notable that the placental phenotype and reduced pup weight observed at E14 were not apparent at E18. Perhaps at the later stages of pregnancy, D6 is dispensable for the subsequent development of the placenta, and the LZ continues to grow up to E18 of mouse gestation (Coan et al., 2004). Thus, it appears that the functional volume of the LZ in the placenta of D6 KO pups catches up with their WT counterparts and normalises as pregnancy advances. The placental defect and fetal compromise at the early ages of pregnancy may have a long lasting effect on the wellbeing of the offspring, leading to the increase in perinatal deaths in the D6 deficient group in DBA-1 mice. In human, illnesses in adulthood are linked to relatively brief periods of fetal compromise during a sensitive stage of in utero development (Lapillonne and Griffin, 2013). The detrimental effect may not be reversed even if the child's growth is normalised during early infancy. For this study while the link between the phenotypes in early pregnancy and perinatal period is biologically plausible, more experiments are needed to confirm the hypothesis.

The reduction of LZ volume fraction in the mouse placenta reflects a reduction of the area available for fetal-maternal exchanges. The evidence of poor pup growth associated with the reduction in LZ volume in mouse pregnancies has already been shown by stereology in the past. Environmental and genetic factors can cause the reduction in LZ volume, and subsequently affecting the growth of the pups (Coan et al., 2008, Coan et al., 2010). This finding of placental insufficiency can be translated to human pregnancies. Reduced efficiency of maternal-fetal exchanges in the human placenta is known clinically to be a cause of fetal growth restriction, resulting in fetal compromise. Recently there is interest in confirming this placental pathology by stereology, first described by Mayhew et al in 1997 (Mayhew, 1997). Reductions in the volume of syncytiotrophoblast and placental villi have been associated with exposure to

polychlorinated biphenyls (PCBs), and also in pregnancies associated with pre-eclampsia and fetal growth restriction (Odibo et al., 2011, Tsuji et al., 2013). Syncytiotrophoblast and placental villi are important areas for maternal-fetal exchanges in human placenta, playing similar role to LZ in mouse placenta. PCBs are an environmental pollutant, whereas pre-eclampsia is an illness in human pregnancy, but both are known to be associated with fetal growth restriction. In clinical practice there have been many instances where placental insufficiencies are detected by histology in pregnancies with fetal growth restriction and fetal death; often no aetiology has been found to be the cause of this defect. Perhaps in a number of these patients there is a lack of, or reduced expression of D6. D6 expression in the human placenta may be regulated by more complex mechanisms, for example single nucleotide polymorphisms (SNPs). Further exploration of D6 expression in the human placentas associated with growth restriction, pre-eclampsia or other conditions that affect fetal growth could prove informative and interesting.

5.2.2 Role of D6 in the regulation of chemokine abundance

Based on the studies of D6 in immortalised cell lines, and this work here using primary human trophoblasts, it seems likely that D6 in the placenta functions primarily to control chemokine abundance and distribution. As outlined in the introduction, chemokines likely serve several roles during placentation; therefore elevated level of chemokines arising from loss of D6 could deregulate leukocyte recruitment into the placenta and/or alter the behaviour of trophoblasts.

5.2.2.1 D6 regulates the plasma level of chemokines in pregnancy

There is evidence of chemokine dysregulation in pregnant D6 deficient mice. The protein levels of D6 binding chemokines in the blood have been studied on pregnant mice injected with LPS. D6 binding CCL2, CCL11 and CCL22 were found to be higher in the D6 KO mice than WT controls, whereas there was no difference in the level of non-D6 ligand CXCL2 (Martinez de la Torre et al., 2007). The surface area of placenta where the maternal blood flows through is significant in size. Together with other mouse organs, the placenta probably makes a major contribution in scavenging the ligands, affecting their levels

systematically. In human, plasma level of chemokine ligands CCL2, CCL3, CCL4 and CCL11 is reduced from the first to the third trimester of pregnancy, as the placenta grew when pregnancy advanced. In contrast, the level of CXCL10, a non-D6 ligand, did not change between those different periods of pregnancy. Interestingly, in women with pre-eclampsia CXCL10 was significantly elevated, while no significant difference was detected in the earlier D6 ligands between these women and the control group (Madigan et al., 2010). This suggests that the levels of D6-binding ligands are well regulated in pregnancy, even in an environment when there is robust expression of these pro-inflammatory chemokines.

In the Luminex multiplex protein assay of DBA-1 mouse plasma in my work, among all the D6 binding chemokines studied (CCL2, CCL3 and CCL5), only CCL2 showed a significant difference in DBA-1 mice. The reason for this selective difference is yet to be explored. In the study of Martinez de la Torre, the level of plasma CCL3 in challenged pregnant mice was similar between WT and D6 KO mice, while the levels of other D6 binding chemokines (CCL2, CCL11, CCL22) were elevated in the D6 KO group (Martinez de la Torre et al., 2007). In comparison to the other D6 ligands, CCL3 disappeared very quickly from the circulation after LPS administration, even in the WT mice. The explanation of the quick disappearance of CCL3 is yet to be discovered. However from the result D6 seems to be dispensable in removing CCL3 from the circulation. In this experiment, no difference was detected in the plasma protein level of CCL3 and CCL5 between WT and D6 KO mice in an unchallenged environment. Perhaps the level of CCL5, like CCL3, fluctuates quickly in the mouse circulation. D6 may be more important in the regulation of the systemic level of ligands with higher protein stability in the circulation. The significantly higher plasma level of CCL2 in the D6 KO mice was not due to the differences in placental expression of this chemokine. Like almost all the other chemokines examined this experiment, the expression of CCL2 transcript was not different between WT and D6 KO placentas at E18.

Following the interesting findings above, further investigations of chemokine abundance in the plasma of D6 deficient mice are worthwhile in future experiments. First, as the difference in chemokine abundance discovered was more marked at E14, the experiments should be repeated with an increased

sample size for E14 to enable the study of more D6 binding ligands with sufficient power. In addition, it will also be interesting to see if non-pregnant D6 deficient DBA-1 mice have elevated levels of CCL2 (and other D6-binding chemokines) in their plasma.

The relationship between fetal survival and the plasma level of D6 binding chemokines is still unclear. It is possible that the elevated systemic level of D6 ligands in the D6 KO mice affects the structure and function of the placenta, or alternatively it may directly influence the survival of the pups in this group. The answer may be found by examining circulating chemokine levels in pregnant D6 heterozygous mothers carrying a mixture of D6 heterozygous and D6 deficient pups. In this experiment D6 deficient placentas in the pregnancies of D6 heterozygous mothers were abnormal. The presence of D6 expression by the mother and by the D6 heterozygous placentas might be expected to prevent elevated CCL2 in the plasma, if this is true perhaps the local regulation of chemokines in the placenta itself might be more important than systemic chemokine control.

5.2.2.2 Role of D6 in the local regulation of chemokines in the placenta

In the study the abundance of transcripts encoding chemokines in WT and D6 deficient placentas was compared. Apart from CCL17, there were no significant differences between the placentas of WT and D6 KO mice. These results show that D6 does not affect the production of most chemokines locally, and it will now be interesting to examine protein levels of D6 binding chemokines. It would not be surprising to find that the levels for these chemokines are lower in the WT group, due to the scavenging effect from D6. These subdued protein levels of D6 binding chemokines have been demonstrated in a study. In comparison to the D6 KO mice, the pregnant WT animals injected with LPS were found to have lower protein levels of CCL2, CCL3, CCL11 and CCL22; the non-D6 binding CXCL2 level was similar between the 2 groups (Martinez de la Torre et al., 2007). The higher level of CCL17 transcript in D6 KO than WT DBA-1 placentas in this experiment was unexpected. The placentas might elevate CCL17 production to counteract the effect of D6 deficiency. If this is a compensatory mechanism, the exact pathway is still unknown. By expressing CCR4, regulatory T cells are known

to respond to CCL17 and could be recruited more effectively to the D6 KO placenta. However, there was no difference in expression of FoxP3, a marker of regulatory T cells, between WT and D6 deficient placentas. In addition, there were no differences in the expression of markers for macrophages (F480) or T cells (CD3). Thus, my study provided no evidence of altered leukocyte recruitment to the placenta in response to D6 loss. However, in future, the experiment could be expanded to include other populations of white cells, such as mast cells, NK cells and neutrophils. Moreover, these various cell types should be enumerated and localised in WT and D6 deficient placentas by immunocytochemistry.

5.3 Conclusions and future directions

This project brings our understanding of the importance of D6 in reproductive tissues to a higher level. Together the results from animal in vivo and human in vitro cellular studies provide valuable information on function of D6 in the placenta.

By studying D6, for the first time, in primary human cells it showed that it is capable of performing the scavenging function ascribed to it in transfected HEK293 and BeWo cells (Weber et al., 2004, Madigan et al., 2010). In DBA-1 mice, D6 deficiency affects the growth of fetus in the early gestational age (E14), and has a detrimental effect of fetal survival in the neonatal period. A fundamental defect in the formation of labyrinthine zone at E14 was detected in D6 KO placenta, which, by using D6 HET females, was shown to be due to D6 deficiency in fetal cells, most likely the trophoblasts of the placenta.

Further experiments are required to determine the exact mechanism by which D6 protects offspring. Chemokines may exert chemotactic effect to trophoblasts, controlling its migration into desired location. By scavenging chemokines, D6 may directly influence the character of trophoblasts and their responsiveness to chemokines when invading the decidua, modifying existing and forming new blood vessels, and shaping the formation of functional units of the placenta. In addition, D6 may also alter the signalling behaviour of trophoblasts with other cells. The ability of D6 in affecting the migratory potential of the cells

expressing the receptor has been demonstrated before (Hansell et al., 2011b). Innate-like B cells in mouse uniquely and universally express D6. D6 was shown to suppress the chemotactic responsiveness of these cells to CXCL13, a non-D6 ligand. It was thought that D6 regulates this response by controlling ß-arrestin redistribution, therefore alters signalling and subsequent migratory responses of the B cells to CXCL13 mediated by CXCR5.

The abundance of CC chemokine is also likely to influence leukocyte recruitment. Perhaps the efficiency of embryo implantation, and the process of placentation, is indirectly influenced by the interaction between trophoblasts and leukocytes locally and systemically. Locally in the gestation tissues, precise control of the level of chemokines could steer and localise leukocytes to assist, or play a direct role, in ensuring a successful implantation and placentation. Delicate orchestration of the level of chemokines may also prevent inappropriate leukocyte adhesion on the vessels of gestational tissue, which could possibly reduce the efficiency of gaseous and nutrient exchange in the feto-maternal interface. Systematically, uncontrolled, overabundance of chemokines could lead to the desensitisation, and subsequently inadequate response of the leukocytes to chemokine stimulation. The phenomenon of desensitisation of chemotactic response of leukocytes towards ligand chemokines has been demonstrated. Leukocytes overexposed to chemokines have been shown to have reduced migratory responsiveness (Noso et al., 1994, Uguccioni et al., 1995). Many G-protein coupled chemokine receptors on these cells, unlike D6, are internalised and desensitised to further ligand uptake following prolonged exposure to agonist activation (Uguccioni et al., 1995, Vila-Coro et al., 1999, Weber et al., 2004, Escola et al., 2010). Thus by regulating the level of chemokine systematically, D6 might ensure the robust response of leukocytes to chemokines is maintained, and thus increasing leukocyte migratory potential.

To complement the findings from the in vitro study, further cellular and molecular experiments of D6 can be performed on first trimester placentas, and also placentas from abnormal pregnancies, for examples miscarriages, and pregnancies with pre-eclampsia, or being diagnosed with placental insufficiency. Early pre-eclampsia occurring before 34 weeks is often more severe and associated with a worse perinatal outcome in comparison to the later onset disease (Gong et al., 2012). It would be interesting to compare the status of D6

expression from the placentas between these two groups. Besides the techniques that have been described in this project, other techniques like stereology could be utilised in human placentas to further understand the three-dimensional pattern of distribution of D6 and leukocytes. Considering that variation in D6 expression might be due to the presence of single nucleotide polymorphisms (SNPs), studies could be carried out to detect any such variants and whether they are associated with any particular placental defects.

In conclusion, the phenotype and cellular discoveries from this project provide novel physiologically significant insight into D6 function in the placenta. It also opens the door to aid the design of future experiments to reveal the code of chemokine regulations of D6, and its precise role in determining the outcome of pregnancies.

References

ABI-YOUNES, S., SAUTY, A., MACH, F., SUKHOVA, G. K., LIBBY, P. & LUSTER, A. D. 2000. The stromal cell-derived factor-1 chemokine is a potent platelet agonist highly expressed in atherosclerotic plaques. *Circ Res,* 86**,** 131-8.

ADAMSON, S. L., LU, Y., WHITELEY, K. J., HOLMYARD, D., HEMBERGER, M., PFARRER, C. & CROSS, J. C. 2002. Interactions between trophoblast cells and the maternal and fetal circulation in the mouse placenta. *Dev Biol,* 250**,** 358-73.

ADDISON, C. L., ARENBERG, D. A., MORRIS, S. B., XUE, Y. Y., BURDICK, M. D., MULLIGAN, M. S., IANNETTONI, M. D. & STRIETER, R. M. 2000. The CXC chemokine, monokine induced by interferon-gamma, inhibits non-small cell lung carcinoma tumor growth and metastasis. *Hum Gene Ther,* 11**,** 247-61.

AHMED, M. S., ALEKSUNES, L. M., BOEUF, P., CHUNG, M. K., DAOUD, G., DESOYE, G., DIAZ, P., GOLOS, T. G., ILLSLEY, N. P., KIKUCHI, K., KOMATSU, R., LAO, T., MORALES-PRIETO, D. M., NANOVSKAYA, T., NOBUZANE, T., ROBERTS, C. T., SAFFERY, R., TAMURA, I., TAMURA, K., THAN, N. G., TOMI, M., UMBERS, A., WANG, B., WEEDON-FEKJAER, S., YAMADA, S., YAMAZAKI, K., YOSHIE, M. & LASH, G. E. 2012. IFPA Meeting 2012 Workshop Report II: Epigenetics and imprinting in the placenta. *Placenta*.

ALDERS, M., HODGES, M., HADJANTONAKIS, A. K., POSTMUS, J., VAN WIJK, I., BLIEK, J., DE MEULEMEESTER, M., WESTERVELD, A., GUILLEMOT, F., OUDEJANS, C., LITTLE, P. & MANNENS, M. 1997. The human Achaete-Scute homologue 2 (ASCL2,HASH2) maps to chromosome 11p15.5, close to IGF2 and is expressed in extravillus trophoblasts. *Hum Mol Genet,* 6**,** 859-67.

ALUVIHARE, V. R., KALLIKOURDIS, M. & BETZ, A. G. 2004. Regulatory T cells mediate maternal tolerance to the fetus. *Nat Immunol,* 5**,** 266-71.

ANDERS, H. J., VIELHAUER, V. & SCHLONDORFF, D. 2003. Chemokines and chemokine receptors are involved in the resolution or progression of renal disease. *Kidney Int,* 63**,** 401-15.

ARCURI, F., RICCI, C., IETTA, F., CINTORINO, M., TRIPODI, S. A., CETIN, I., GARZIA, E., SCHATZ, F., KLEMI, P., SANTOPIETRO, R. & PAULESU, L. 2001. Macrophage migration inhibitory factor in the human endometrium: expression and localization during the menstrual cycle and early pregnancy. *Biol Reprod,* 64**,** 1200-5.

ARENBERG, D. A., KEANE, M. P., DIGIOVINE, B., KUNKEL, S. L., MORRIS, S. B., XUE, Y. Y., BURDICK, M. D., GLASS, M. C., IANNETTONI, M. D. & STRIETER, R. M. 1998. Epithelial-neutrophil activating peptide (ENA-78) is an important angiogenic factor in non-small cell lung cancer. *J Clin Invest,* 102**,** 465-72.

ARENBERG, D. A., KUNKEL, S. L., POLVERINI, P. J., MORRIS, S. B., BURDICK, M. D., GLASS, M. C., TAUB, D. T., IANNETTONI, M. D., WHYTE, R. I. & STRIETER, R. M. 1996. Interferon-gamma-inducible protein 10 (IP-10) is an angiostatic factor that inhibits human non-small cell lung cancer (NSCLC) tumorigenesis and spontaneous metastases. *J Exp Med,* 184**,** 981-92.

AYE, I. L., WADDELL, B. J., MARK, P. J. & KEELAN, J. A. 2010. Placental ABCA1 and ABCG1 transporters efflux cholesterol and protect trophoblasts from oxysterol induced toxicity. *Biochim Biophys Acta,* 1801**,** 1013-24.

BAAL, N., WIDMER-TESKE, R., MCKINNON, T., PREISSNER, K. T. & ZYGMUNT, M. T. 2009. In vitro spheroid model of placental vasculogenesis: does it work? *Lab Invest,* 89**,** 152-63.

BACHELERIE, F., BEN-BARUCH, A., BURKHARDT, A. M., COMBADIERE, C., FARBER, J. M., GRAHAM, G. J., HORUK, R., SPARRE-ULRICH, A. H., LOCATI, M., LUSTER, A. D., MANTOVANI, A., MATSUSHIMA, K., MURPHY, P. M., NIBBS, R., NOMIYAMA, H., POWER, C. A., PROUDFOOT, A. E., ROSENKILDE, M. M., ROT, A., SOZZANI, S., THELEN, M., YOSHIE, O. & ZLOTNIK, A. 2014. International Union of Pharmacology. LXXXIX. Update on the Extended Family of Chemokine Receptors and Introducing a New Nomenclature for Atypical Chemokine Receptors. *Pharmacol Rev,* 66**,** 1-79.

BACON, K., BAGGIOLINI, M., BROXMEYER, H., HORUK, R., LINDLEY, I., MANTOVANI, A., MAYSUSHIMA, K., MURPHY, P., NOMIYAMA, H., OPPENHEIM, J., ROT, A., SCHALL, T., TSANG, M., THORPE, R., VAN DAMME, J., WADHWA, M., YOSHIE, O., ZLOTNIK, A. & ZOON, K. 2002. Chemokine/chemokine receptor nomenclature. *J Interferon Cytokine Res,* 22**,** 1067-8.

BALASHOV, K. E., ROTTMAN, J. B., WEINER, H. L. & HANCOCK, W. W. 1999. CCR5(+) and CXCR3(+) T cells are increased in multiple sclerosis and their ligands MIP-1alpha and IP-10 are expressed in demyelinating brain lesions. *Proc Natl Acad Sci U S A,* 96**,** 6873-8.

BALL, E., BULMER, J. N., AYIS, S., LYALL, F. & ROBSON, S. C. 2006. Late sporadic miscarriage is associated with abnormalities in spiral artery transformation and trophoblast invasion. *J Pathol,* 208**,** 535-42.

BARRIENTOS, G., TIRADO-GONZALEZ, I., FREITAG, N., KOBELT, P., MOSCHANSKY, P., KLAPP, B. F., THIJSSEN, V. L. & BLOIS, S. M. 2013. CXCR4(+) dendritic cells promote angiogenesis during embryo implantation in mice. *Angiogenesis,* 16**,** 417-27.

BENIRSCHKE, K., BURTON, G. J. & BAERGEN, R. N. 2012. *Pathology of the human placenta***,** 13-15.

BERRES, M. L., TRAUTWEIN, C., ZALDIVAR, M. M., SCHMITZ, P., PAUELS, K., LIRA, S. A., TACKE, F. & WASMUTH, H. E. 2009. The chemokine scavenging receptor D6 limits acute toxic liver injury in vivo. *Biol Chem,* 390**,** 1039-45.

BISWAS, S., GHOSH, S. K. & CHHABRA, S. 2008. Surface area of chorionic villi of placentas: an index of intrauterine growth restriction of fetuses. *J Obstet Gynaecol Res.* Japan.

BLACKBURN, P. E., SIMPSON, C. V., NIBBS, R. J., O'HARA, M., BOOTH, R., POULOS, J., ISAACS, N. W. & GRAHAM, G. J. 2004. Purification and biochemical characterization of the D6 chemokine receptor. *Biochem J,* 379**,** 263-72.

BLASCHITZ, A., WEISS, U., DOHR, G. & DESOYE, G. 2000. Antibody reaction patterns in first trimester placenta: implications for trophoblast isolation and purity screening. *Placenta,* 21**,** 733-41.

BOISVERT, W. A., SANTIAGO, R., CURTISS, L. K. & TERKELTAUB, R. A. 1998. A leukocyte homologue of the IL-8 receptor CXCR-2 mediates the accumulation of macrophages in atherosclerotic lesions of LDL receptor-deficient mice. *J Clin Invest,* 101**,** 353-63.

BORDON, Y., HANSELL, C. A., SESTER, D. P., CLARKE, M., MOWAT, A. M. & NIBBS, R. J. 2009. The atypical chemokine receptor D6 contributes to the development of experimental colitis. *J Immunol,* 182**,** 5032-40.

BORING, L., GOSLING, J., CLEARY, M. & CHARO, I. F. 1998. Decreased lesion formation in CCR2-/- mice reveals a role for chemokines in the initiation of atherosclerosis. *Nature,* 394**,** 894-7.

BORLAND, R. 1975. Placenta as an allograft. *In:* STEVEN, D. H. (ed.) *Comparative placentation.* London: Academic Press.

BORRONI, E., BONECCHI, R., BURACCHI, C., SAVINO, B., MANTOVANI, A. & LOCATI, M. 2008. Chemokine decoy receptors: new players in reproductive immunology. *Immunol Invest,* 37**,** 483-97.

BREW, R., ERIKSON, J. S., WEST, D. C., KINSELLA, A. R., SLAVIN, J. & CHRISTMAS, S. E. 2000. Interleukin-8 as an autocrine growth factor for human colon carcinoma cells in vitro. *Cytokine,* 12**,** 78-85.

BREW, R., SOUTHERN, S. A., FLANAGAN, B. F., MCDICKEN, I. W. & CHRISTMAS, S. E. 1996. Detection of interleukin-8 mRNA and protein in human colorectal carcinoma cells. *Eur J Cancer,* 32a**,** 2142-7.

BROSENS, I., PIJNENBORG, R., VERCRUYSSE, L. & ROMERO, R. 2011. The "Great Obstetrical Syndromes" are associated with disorders of deep placentation. *Am J Obstet Gynecol,* 204**,** 193-201.

BUKOWSKI, R., CARPENTER, M., CONWAY, D., COUSTAN, D., DUDLEY, D. J., GOLDENBERG, R. L., HOGUE, C. J., KOCH, M. A., PARKER, C. B., PINAR, H., REDDY, U. M., SAADE, G. R., SILVER, R. M., STOLL, B. J., VARNER, M. W. & WILLINGER, M. 2011. Causes of death among stillbirths. *JAMA,* 306**,** 2459-68.

BULMER, J. N., MORRISON, L., LONGFELLOW, M., RITSON, A. & PACE, D. 1991. Granulated lymphocytes in human endometrium: histochemical and immunohistochemical studies. *Hum Reprod,* 6**,** 791-8.

BULMER, J. N., WILLIAMS, P. J. & LASH, G. E. 2010. Immune cells in the placental bed. *Int J Dev Biol,* 54**,** 281-94.

BUNTING, M. D., COMERFORD, I., SEACH, N., HAMMETT, M. V., ASQUITH, D. L., KORNER, H., BOYD, R. L., NIBBS, R. J. & MCCOLL, S. R. 2013. CCX-CKR deficiency alters thymic stroma impairing thymocyte development and promoting autoimmunity. *Blood,* 121**,** 118-28.

BURGER, M., BURGER, J. A., HOCH, R. C., OADES, Z., TAKAMORI, H. & SCHRAUFSTATTER, I. U. 1999. Point mutation causing constitutive signaling of CXCR2 leads to transforming activity similar to Kaposi's sarcoma herpesvirus-G protein-coupled receptor. *J Immunol,* 163**,** 2017-22.

BURNS, J. M., SUMMERS, B. C., WANG, Y., MELIKIAN, A., BERAHOVICH, R., MIAO, Z., PENFOLD, M. E., SUNSHINE, M. J., LITTMAN, D. R., KUO, C. J., WEI, K., MCMASTER, B. E., WRIGHT, K., HOWARD, M. C. & SCHALL, T. J. 2006. A novel chemokine receptor for SDF-1 and I-TAC involved in cell survival, cell adhesion, and tumor development. *J Exp Med,* 203**,** 2201-13.

BURTON, G. J. & JAUNIAUX, E. 2004. Placental oxidative stress: from miscarriage to preeclampsia. *J Soc Gynecol Investig,* 11**,** 342-52.

BURTON, G. J., JAUNIAUX, E. & CHARNOCK-JONES, D. S. 2010. The influence of the intrauterine environment on human placental development. *Int J Dev Biol,* 54**,** 303-12.

CALDERON, T. M., BERMAN, J. W. & LISA, M. S. 2005. Overview and History of Chemokines and Their Receptors. *Current Topics in Membranes.* Academic Press.

CALUWAERTS, S., VERCRUYSSE, L., LUYTEN, C. & PIJNENBORG, R. 2005. Endovascular trophoblast invasion and associated structural changes in uterine spiral arteries of the pregnant rat. *Placenta,* 26**,** 574-84.

CAO, Q., CHEN, H., DENG, Z., YUE, J., CHEN, Q., CAO, Y., NING, L., LEI, X. & DUAN, E. 2013. Genetic deletion of Cxcl14 in mice alters uterine NK cells. *Biochem Biophys Res Commun,* 435**,** 664-70.

CARLINO, C., STABILE, H., MORRONE, S., BULLA, R., SORIANI, A., AGOSTINIS, C., BOSSI, F., MOCCI, C., SARAZANI, F., TEDESCO, F., SANTONI, A. & GISMONDI, A. 2008. Recruitment of circulating NK cells through decidual tissues: a possible mechanism controlling NK cell accumulation in the uterus during early pregnancy. *Blood,* 111**,** 3108-15.

CARTER, A. M., ENDERS, A. C., JONES, C. J., MESS, A., PFARRER, C., PIJNENBORG, R. & SOMA, H. 2006. Comparative placentation and animal models: patterns of trophoblast invasion -- a workshop report. *Placenta.* England.

CARTER, A. M. & PIJNENBORG, R. 2011. Evolution of invasive placentation with special reference to non-human primates. *Best Pract Res Clin Obstet Gynaecol,* 25**,** 249-57.

CARTER, D. B., KENNETT, M. J. & FRANKLIN, C. L. 2002. Use of perphenazine to control cannibalism in DBA/1 mice. *Comp Med,* 52**,** 452-5.

CAVANAGH, P. C., DUNK, C., PAMPILLO, M., SZERESZEWSKI, J. M., TAYLOR, J. E., KAHIRI, C., HAN, V., LYE, S., BHATTACHARYA, M. & BABWAH, A. V. 2009. Gonadotropin-releasing hormone-regulated chemokine expression in human placentation. *Am J Physiol Cell Physiol,* 297**,** C17-27.

CHAMPAGNE, F. A., CURLEY, J. P., KEVERNE, E. B. & BATESON, P. P. 2007. Natural variations in postpartum maternal care in inbred and outbred mice. *Physiol Behav,* 91**,** 325-34.

CHANTAKRU, S., MILLER, C., ROACH, L. E., KUZIEL, W. A., MAEDA, N., WANG, W. C., EVANS, S. S. & CROY, B. A. 2002. Contributions from self-renewal and trafficking to the uterine NK cell population of early pregnancy. *J Immunol,* 168**,** 22-8.

CHAOUAT, G. 2007. The Th1/Th2 paradigm: still important in pregnancy? *Semin Immunopathol,* 29**,** 95-113.

CHARO, I. F. & RANSOHOFF, R. M. 2006. The many roles of chemokines and chemokine receptors in inflammation. *N Engl J Med,* 354**,** 610-21.

CHAUDHURI, A., POLYAKOVA, J., ZBRZEZNA, V., WILLIAMS, K., GULATI, S. & POGO, A. O. 1993. Cloning of glycoprotein D cDNA, which encodes the major subunit of the Duffy blood group system and the receptor for the Plasmodium vivax malaria parasite. *Proc Natl Acad Sci U S A,* 90**,** 10793-7.

CHAZARA, O., XIONG, S. & MOFFETT, A. 2011. Maternal KIR and fetal HLA-C: a fine balance. *J Leukoc Biol,* 90**,** 703-16.

CHEN, S. U., CHOU, C. H., CHAO, K. H., LEE, H., LIN, C. W., LU, H. F. & YANG, Y. S. 2010. Lysophosphatidic acid up-regulates expression of growth-regulated oncogene-alpha, interleukin-8, and monocyte chemoattractant protein-1 in human first-trimester trophoblasts: possible roles in angiogenesis and immune regulation. *Endocrinology,* 151**,** 369-79.

CHEN, T., BAI, H., SHAO, Y., ARZIGIAN, M., JANZEN, V., ATTAR, E., XIE, Y., SCADDEN, D. T. & WANG, Z. Z. 2007. Stromal cell-derived factor-1/CXCR4 signaling modifies the capillary-like organization of human embryonic stem cell-derived endothelium in vitro. *Stem Cells,* 25**,** 392-401.

CHENG, C. W., BIELBY, H., LICENCE, D., SMITH, S. K., PRINT, C. G. & CHARNOCK-JONES, D. S. 2007. Quantitative cellular and molecular analysis of the effect of progesterone withdrawal in a murine model of decidualization. *Biol Reprod,* 76**,** 871-83.

CHRISTIANSEN, O. B., NIELSEN, H. S. & KOLTE, A. M. 2006. Future directions of failed implantation and recurrent miscarriage research. *Reprod Biomed Online,* 13**,** 71-83.

COAN, P., FERGUSON-SMITH, A. & BURTON, G. 2004. Developmental dynamics of the definitive mouse placenta assessed by stereology. *Biol Reprod,* 70**,** 1806-13.

COAN, P., FOWDEN, A., CONSTANCIA, M., FERGUSON-SMITH, A., BURTON, G. & SIBLEY, C. 2008. Disproportional effects of Igf2 knockout on placental morphology and diffusional exchange characteristics in the mouse. *J Physiol,* 586**,** 5023-32.

COAN, P. M., CONROY, N., BURTON, G. J. & FERGUSON-SMITH, A. C. 2006. Origin and characteristics of glycogen cells in the developing murine placenta. *Dev Dyn,* 235**,** 3280-94.
COAN, P. M., FERGUSON-SMITH, A. C. & BURTON, G. J. 2005. Ultrastructural changes in the interhaemal membrane and junctional zone of the murine chorioallantoic placenta across gestation. *J Anat,* 207**,** 783-96.
COAN, P. M., VAUGHAN, O. R., SEKITA, Y., FINN, S. L., BURTON, G. J., CONSTANCIA, M. & FOWDEN, A. L. 2010. Adaptations in placental phenotype support fetal growth during undernutrition of pregnant mice. *J Physiol,* 588**,** 527-38.
COCHAIN, C., AUVYNET, C., POUPEL, L., VILAR, J., DUMEAU, E., RICHART, A., RECALDE, A., ZOUGGARI, Y., YIN, K. Y., BRUNEVAL, P., RENAULT, G., MARCHIOL, C., BONNIN, P., LEVY, B., BONECCHI, R., LOCATI, M., COMBADIERE, C. & SILVESTRE, J. S. 2012. The chemokine decoy receptor D6 prevents excessive inflammation and adverse ventricular remodeling after myocardial infarction. *Arterioscler Thromb Vasc Biol,* 32**,** 2206-13.
COLE, L. A. 2009. hCG and hyperglycosylated hCG in the establishment and evolution of hemochorial placentation. *J Reprod Immunol,* 82**,** 112-8.
COLLINS, M. K., TAY, C. S. & ERLEBACHER, A. 2009. Dendritic cell entrapment within the pregnant uterus inhibits immune surveillance of the maternal/fetal interface in mice. *J Clin Invest,* 119**,** 2062-73.
COMBADIERE, C., POTTEAUX, S., GAO, J. L., ESPOSITO, B., CASANOVA, S., LEE, E. J., DEBRE, P., TEDGUI, A., MURPHY, P. M. & MALLAT, Z. 2003. Decreased atherosclerotic lesion formation in CX3CR1/apolipoprotein E double knockout mice. *Circulation,* 107**,** 1009-16.
COMERFORD, I., LITCHFIELD, W., HARATA-LEE, Y., NIBBS, R. J. & MCCOLL, S. R. 2007. Regulation of chemotactic networks by 'atypical' receptors. *Bioessays,* 29**,** 237-47.
COMERFORD, I., MILASTA, S., MORROW, V., MILLIGAN, G. & NIBBS, R. 2006. The chemokine receptor CCX-CKR mediates effective scavenging of CCL19 in vitro. *Eur J Immunol,* 36**,** 1904-16.
CONTINI, P., GHIO, M., POGGI, A., FILACI, G., INDIVERI, F., FERRONE, S. & PUPPO, F. 2003. Soluble HLA-A,-B,-C and -G molecules induce apoptosis in T and NK CD8+ cells and inhibit cytotoxic T cell activity through CD8 ligation. *Eur J Immunol,* 33**,** 125-34.
COOPER, M. A., FEHNIGER, T. A. & CALIGIURI, M. A. 2001. The biology of human natural killer-cell subsets. *Trends Immunol,* 22**,** 633-40.
CROSS, J. C. 2000. Genetic insights into trophoblast differentiation and placental morphogenesis. *Semin Cell Dev Biol,* 11**,** 105-13.
CROSS, J. C., SIMMONS, D. G. & WATSON, E. D. 2003. Chorioallantoic morphogenesis and formation of the placental villous tree. *Ann N Y Acad Sci,* 995**,** 84-93.
CRUZ-ORENGO, L., CHEN, Y. J., KIM, J. H., DORSEY, D., SONG, S. K. & KLEIN, R. S. 2011a. CXCR7 antagonism prevents axonal injury during experimental autoimmune encephalomyelitis as revealed by in vivo axial diffusivity. *J Neuroinflammation,* 8**,** 170.
CRUZ-ORENGO, L., HOLMAN, D. W., DORSEY, D., ZHOU, L., ZHANG, P., WRIGHT, M., MCCANDLESS, E. E., PATEL, J. R., LUKER, G. D., LITTMAN, D. R., RUSSELL, J. H. & KLEIN, R. S. 2011b. CXCR7 influences leukocyte entry into the CNS parenchyma by controlling abluminal CXCL12 abundance during autoimmunity. *J Exp Med,* 208**,** 327-39.
CURIEL, T. J., COUKOS, G., ZOU, L., ALVAREZ, X., CHENG, P., MOTTRAM, P., EVDEMON-HOGAN, M., CONEJO-GARCIA, J. R., ZHANG, L., BUROW, M., ZHU, Y., WEI, S., KRYCZEK, I., DANIEL, B., GORDON, A., MYERS, L., LACKNER, A., DISIS, M. L., KNUTSON, K. L., CHEN, L. & ZOU, W. 2004. Specific recruitment of regulatory T cells in ovarian carcinoma fosters immune privilege and predicts reduced survival. *Nat Med,* 10**,** 942-9.
DAMSKY, C. H., FITZGERALD, M. L. & FISHER, S. J. 1992. Distribution patterns of extracellular matrix components and adhesion receptors are intricately modulated during first trimester cytotrophoblast differentiation along the invasive pathway, in vivo. *J Clin Invest,* 89**,** 210-22.
DARBONNE, W. C., RICE, G. C., MOHLER, M. A., APPLE, T., HEBERT, C. A., VALENTE, A. J. & BAKER, J. B. 1991. Red blood cells are a sink for interleukin 8, a leukocyte chemotaxin. *J Clin Invest,* 88**,** 1362-9.
DAWSON, T. C., LENTSCH, A. B., WANG, Z., COWHIG, J. E., ROT, A., MAEDA, N. & PEIPER, S. C. 2000. Exaggerated response to endotoxin in mice lacking the Duffy antigen/receptor for chemokines (DARC). *Blood,* 96**,** 1681-4.
DE OLIVEIRA, L. G., LASH, G. E., MURRAY-DUNNING, C., BULMER, J. N., INNES, B. A., SEARLE, R. F., SASS, N. & ROBSON, S. C. 2010. Role of interleukin 8 in uterine natural killer cell regulation of extravillous trophoblast cell invasion. *Placenta,* 31**,** 595-601.
DESFORGES, M. & WESTWOOD, M. 2011. A limitation of the method for siRNA delivery into primary human cytotrophoblast cells. *Placenta,* 32**,** 192-4.
DI LIBERTO, D., LOCATI, M., CACCAMO, N., VECCHI, A., MERAVIGLIA, S., SALERNO, A., SIRECI, G., NEBULONI, M., CACERES, N., CARDONA, P. J., DIELI, F. & MANTOVANI, A. 2008. Role of the chemokine decoy receptor D6 in balancing inflammation, immune activation, and antimicrobial resistance in Mycobacterium tuberculosis infection. *J Exp Med,* 205**,** 2075-84.
DIMITRIADIS, E., NIE, G., HANNAN, N., PAIVA, P. & SALAMONSEN, L. 2010. Local regulation of implantation at the human fetal-maternal interface. *Int J Dev Biol,* 54**,** 313-22.
DRAKE, P. M., GUNN, M. D., CHARO, I. F., TSOU, C. L., ZHOU, Y., HUANG, L. & FISHER, S. J. 2001. Human placental cytotrophoblasts attract monocytes and CD56(bright) natural killer cells via the actions of monocyte inflammatory protein 1alpha. *J Exp Med,* 193**,** 1199-212.
DU, J., LUAN, J., LIU, H., DANIEL, T. O., PEIPER, S., CHEN, T. S., YU, Y., HORTON, L. W., NANNEY, L. B., STRIETER, R. M. & RICHMOND, A. 2002. Potential role for Duffy antigen chemokine-binding protein in angiogenesis and maintenance of homeostasis in response to stress. *J Leukoc Biol,* 71**,** 141-53.
EIDE, I. P., ROLFSENG, T., ISAKSEN, C. V., MECSEI, R., ROALD, B., LYDERSEN, S., SALVESEN, K. A., HARSEM, N. K. & AUSTGULEN, R. 2006. Serious foetal growth restriction is associated with reduced proportions of natural killer cells in decidua basalis. *Virchows Arch,* 448**,** 269-76.
EL-SHEWY, H. M., JOHNSON, K. R., LEE, M. H., JAFFA, A. A., OBEID, L. M. & LUTTRELL, L. M. 2006. Insulin-like growth factors mediate heterotrimeric G protein-dependent ERK1/2 activation by transactivating sphingosine 1-phosphate receptors. *J Biol Chem,* 281**,** 31399-407.
ELLERY, P. M., CINDROVA-DAVIES, T., JAUNIAUX, E., FERGUSON-SMITH, A. C. & BURTON, G. J. 2009. Evidence for transcriptional activity in the syncytiotrophoblast of the human placenta. *Placenta,* 30**,** 329-34.
ERLEBACHER, A. 2013. Immunology of the maternal-fetal interface. *Annu Rev Immunol,* 31**,** 387-411.
ERLEBACHER, A., VENCATO, D., PRICE, K. A., ZHANG, D. & GLIMCHER, L. H. 2007. Constraints in antigen presentation severely restrict T cell recognition of the allogeneic fetus. *J Clin Invest,* 117**,** 1399-411.

ESCOBAR, J. C., PATEL, S. S., BESHAY, V. E., SUZUKI, T. & CARR, B. R. 2011. The human placenta expresses CYP17 and generates androgens de novo. *J Clin Endocrinol Metab,* 96**,** 1385-92.

ESCOLA, J. M., KUENZI, G., GAERTNER, H., FOTI, M. & HARTLEY, O. 2010. CC chemokine receptor 5 (CCR5) desensitization: cycling receptors accumulate in the trans-Golgi network. *J Biol Chem,* 285**,** 41772-80.

EVANS, J. & SALAMONSEN, L. A. 2012. Inflammation, leukocytes and menstruation. *Rev Endocr Metab Disord,* 13**,** 277-88.

FARZAN, M., MIRZABEKOV, T., KOLCHINSKY, P., WYATT, R., CAYABYAB, M., GERARD, N. P., GERARD, C., SODROSKI, J. & CHOE, H. 1999. Tyrosine sulfation of the amino terminus of CCR5 facilitates HIV-1 entry. *Cell,* 96**,** 667-76.

FENG, L., CHEN, S., GARCIA, G. E., XIA, Y., SIANI, M. A., BOTTI, P., WILSON, C. B., HARRISON, J. K. & BACON, K. B. 1999. Prevention of crescentic glomerulonephritis by immunoneutralization of the fractalkine receptor CX3CR1 rapid communication. *Kidney Int,* 56**,** 612-20.

FERNANDEZ, E. J. & LOLIS, E. 2002. Structure, function, and inhibition of chemokines. *Annu Rev Pharmacol Toxicol,* 42**,** 469-99.

FLIER, J., BOORSMA, D. M., VAN BEEK, P. J., NIEBOER, C., STOOF, T. J., WILLEMZE, R. & TENSEN, C. P. 2001. Differential expression of CXCR3 targeting chemokines CXCL10, CXCL9, and CXCL11 in different types of skin inflammation. *J Pathol,* 194**,** 398-405.

FONTENOT, J. D., GAVIN, M. A. & RUDENSKY, A. Y. 2003. Foxp3 programs the development and function of CD4+CD25+ regulatory T cells. *Nat Immunol,* 4**,** 330-6.

FOX, J. M. & PEASE, J. E. 2005. The Molecular and Cellular Biology of CC Chemokines and Their Receptors. *In:* LISA, M. S. (ed.) *Current Topics in Membranes.* Academic Press.

FRANK, H. G., MORRISH, D. W., PÖTGENS, A., GENBACEV, O., KUMPEL, B. & CANIGGIA, I. 2001. Cell culture models of human trophoblast: primary culture of trophoblast--a workshop report. *Placenta,* 22 Suppl A**,** S107-9.

FREDERICK, M. J. & CLAYMAN, G. L. 2001. Chemokines in cancer. *Expert Rev Mol Med,* 3**,** 1-18.

FREUD, A. G., BECKNELL, B., ROYCHOWDHURY, S., MAO, H. C., FERKETICH, A. K., NUOVO, G. J., HUGHES, T. L., MARBURGER, T. B., SUNG, J., BAIOCCHI, R. A., GUIMOND, M. & CALIGIURI, M. A. 2005. A human CD34(+) subset resides in lymph nodes and differentiates into CD56bright natural killer cells. *Immunity,* 22**,** 295-304.

FUJISAWA, N., SAKAO, Y., HAYASHI, S., HADDEN, W. A., 3RD, HARMON, C. L. & MILLER, E. J. 2000. alpha-Chemokine growth factors for adenocarcinomas; a synthetic peptide inhibitor for alpha-chemokines inhibits the growth of adenocarcinoma cell lines. *J Cancer Res Clin Oncol,* 126**,** 19-26.

FUKUMA, N., AKIMITSU, N., HAMAMOTO, H., KUSUHARA, H., SUGIYAMA, Y. & SEKIMIZU, K. 2003. A role of the Duffy antigen for the maintenance of plasma chemokine concentrations. *Biochem Biophys Res Commun,* 303**,** 137-9.

GALCERAN, J., FARINAS, I., DEPEW, M. J., CLEVERS, H. & GROSSCHEDL, R. 1999. Wnt3a-/--like phenotype and limb deficiency in Lef1(-/-)Tcf1(-/-) mice. *Genes Dev,* 13**,** 709-17.

GARDNER, L., PATTERSON, A. M., ASHTON, B. A., STONE, M. A. & MIDDLETON, J. 2004. The human Duffy antigen binds selected inflammatory but not homeostatic chemokines. *Biochem Biophys Res Commun,* 321**,** 306-12.

GARLANDA, C., MAINA, V., MARTINEZ DE LA TORRE, Y., NEBULONI, M. & LOCATI, M. 2008. Inflammatory reaction and implantation: the new entries PTX3 and D6. *Placenta,* 29 Suppl B**,** 129-34.

GEELHOED, J. J., FRASER, A., TILLING, K., BENFIELD, L., DAVEY SMITH, G., SATTAR, N., NELSON, S. M. & LAWLOR, D. A. 2010. Preeclampsia and gestational hypertension are associated with childhood blood pressure independently of family adiposity measures: the Avon Longitudinal Study of Parents and Children. *Circulation.* United States.

GENBACEV, O., ZHOU, Y., LUDLOW, J. W. & FISHER, S. J. 1997. Regulation of human placental development by oxygen tension. *Science,* 277**,** 1669-72.

GENBACEV, O. D., PRAKOBPHOL, A., FOULK, R. A., KRTOLICA, A. R., ILIC, D., SINGER, M. S., YANG, Z. Q., KIESSLING, L. L., ROSEN, S. D. & FISHER, S. J. 2003. Trophoblast L-selectin-mediated adhesion at the maternal-fetal interface. *Science,* 299**,** 405-8.

GEORGIADES, P., FERGUSON-SMITH, A. C. & BURTON, G. J. 2002. Comparative developmental anatomy of the murine and human definitive placentae. *Placenta,* 23**,** 3-19.

GEUSENS, N., HERING, L., VERLOHREN, S., LUYTEN, C., DRIJKONINGEN, K., TAUBE, M., VERCRUYSSE, L., HANSSENS, M., DECHEND, R. & PIJNENBORG, R. 2010. Changes in endovascular trophoblast invasion and spiral artery remodelling at term in a transgenic preeclamptic rat model. *Placenta,* 31**,** 320-6.

GIBBONS, A. 1998. Solving the brain's energy crisis. *Science,* 280**,** 1345-7.

GODISKA, R., CHANTRY, D., DIETSCH, G. N. & GRAY, P. W. 1995. Chemokine expression in murine experimental allergic encephalomyelitis. *J Neuroimmunol,* 58**,** 167-76.

GOLDMAN, S. & SHALEV, E. 2006. Difference in progesterone-receptor isoforms ratio between early and late first-trimester human trophoblast is associated with differential cell invasion and matrix metalloproteinase 2 expression. *Biol Reprod,* 74**,** 13-22.

GONG, Y. H., JIA, J., LU, D. H., DAI, L., BAI, Y. & ZHOU, R. 2012. Outcome and risk factors of early onset severe preeclampsia. *Chin Med J (Engl),* 125**,** 2623-7.

GOSLING, J., DAIRAGHI, D. J., WANG, Y., HANLEY, M., TALBOT, D., MIAO, Z. & SCHALL, T. J. 2000. Cutting edge: identification of a novel chemokine receptor that binds dendritic cell- and T cell-active chemokines including ELC, SLC, and TECK. *J Immunol,* 164**,** 2851-6.

GOSLING, J., SLAYMAKER, S., GU, L., TSENG, S., ZLOT, C. H., YOUNG, S. G., ROLLINS, B. J. & CHARO, I. F. 1999. MCP-1 deficiency reduces susceptibility to atherosclerosis in mice that overexpress human apolipoprotein B. *J Clin Invest,* 103**,** 773-8.

GRAHAM, G. J. 2009. D6 and the atypical chemokine receptor family: novel regulators of immune and inflammatory processes. *Eur J Immunol,* 39**,** 342-51.

GRAHAM, G. J., LOCATI, M., MANTOVANI, A., ROT, A. & THELEN, M. 2012. The biochemistry and biology of the atypical chemokine receptors. *Immunol Lett,* 145**,** 30-8.

GREAVES, D. R., HAKKINEN, T., LUCAS, A. D., LIDDIARD, K., JONES, E., QUINN, C. M., SENARATNE, J., GREEN, F. R., TYSON, K., BOYLE, J., SHANAHAN, C., WEISSBERG, P. L., GORDON, S. & YLA-HERTUALLA, S. 2001. Linked chromosome 16q13 chemokines, macrophage-derived chemokine, fractalkine, and thymus- and activation-regulated chemokine, are expressed in human atherosclerotic lesions. *Arterioscler Thromb Vasc Biol,* 21**,** 923-9.

GULERIA, I., KHOSROSHAHI, A., ANSARI, M. J., HABICHT, A., AZUMA, M., YAGITA, H., NOELLE, R. J., COYLE, A., MELLOR, A. L., KHOURY, S. J. & SAYEGH, M. H. 2005. A critical role for the programmed death ligand 1 in fetomaternal tolerance. *J Exp Med,* 202**,** 231-7.

GUSTAFSSON, C., MJOSBERG, J., MATUSSEK, A., GEFFERS, R., MATTHIESEN, L., BERG, G., SHARMA, S., BUER, J. & ERNERUDH, J. 2008. Gene expression profiling of human decidual macrophages: evidence for immunosuppressive phenotype. *PLoS One,* 3**,** e2078.

HADLEY, T. J. & PEIPER, S. C. 1997. From malaria to chemokine receptor: the emerging physiologic role of the Duffy blood group antigen. *Blood,* 89**,** 3077-91.

HAMILTON, W. J. & BOYD, J. D. 1966. Trophoblast in human utero-placental arteries. *Nature,* 212**,** 906-8.

HANNA, J., GOLDMAN-WOHL, D., HAMANI, Y., AVRAHAM, I., GREENFIELD, C., NATANSON-YARON, S., PRUS, D., COHEN-DANIEL, L., ARNON, T. I., MANASTER, I., GAZIT, R., YUTKIN, V., BENHARROCH, D., PORGADOR, A., KESHET, E., YAGEL, S. & MANDELBOIM, O. 2006. Decidual NK cells regulate key developmental processes at the human fetal-maternal interface. *Nat Med,* 12**,** 1065-74.

HANNA, J., WALD, O., GOLDMAN-WOHL, D., PRUS, D., MARKEL, G., GAZIT, R., KATZ, G., HAIMOV-KOCHMAN, R., FUJII, N., YAGEL, S., PELED, A. & MANDELBOIM, O. 2003. CXCL12 expression by invasive trophoblasts induces the specific migration of CD16- human natural killer cells. *Blood,* 102**,** 1569-77.

HANNAN, N., JONES, R., WHITE, C. & SALAMONSEN, L. 2006. The chemokines, CX3CL1, CCL14, and CCL4, promote human trophoblast migration at the feto-maternal interface. *Biol Reprod,* 74**,** 896-904.

HANNAN, N. J., JONES, R. L., CRITCHLEY, H. O., KOVACS, G. J., ROGERS, P. A., AFFANDI, B. & SALAMONSEN, L. A. 2004. Coexpression of fractalkine and its receptor in normal human endometrium and in endometrium from users of progestin-only contraception supports a role for fractalkine in leukocyte recruitment and endometrial remodeling. *J Clin Endocrinol Metab,* 89**,** 6119-29.

HANNAN, N. J. & SALAMONSEN, L. A. 2007. Role of chemokines in the endometrium and in embryo implantation. *Curr Opin Obstet Gynecol,* 19**,** 266-72.

HANNON, T., INNES, B. A., LASH, G. E., BULMER, J. N. & ROBSON, S. C. 2012. Effects of local decidua on trophoblast invasion and spiral artery remodeling in focal placenta creta - an immunohistochemical study. *Placenta,* 33**,** 998-1004.

HANSELL, C. A., HURSON, C. E. & NIBBS, R. J. 2011a. DARC and D6: silent partners in chemokine regulation? *Immunol Cell Biol,* 89**,** 197-206.

HANSELL, C. A., SCHIERING, C., KINSTRIE, R., FORD, L., BORDON, Y., MCINNES, I. B., GOODYEAR, C. S. & NIBBS, R. J. 2011b. Universal expression and dual function of the atypical chemokine receptor D6 on innate-like B cells in mice. *Blood,* 117**,** 5413-24.

HEINZEL, K., BENZ, C. & BLEUL, C. C. 2007. A silent chemokine receptor regulates steady-state leukocyte homing in vivo. *Proc Natl Acad Sci U S A,* 104**,** 8421-6.

HELIGE, C., AHAMMER, H., MOSER, G., HAMMER, A., DOHR, G., HUPPERTZ, B. & SEDLMAYR, P. 2013. Distribution of decidual natural killer cells and macrophages in the neighbourhood of the trophoblast invasion front: a quantitative evaluation. *Hum Reprod*.

HESS, A. P., HAMILTON, A. E., TALBI, S., DOSIOU, C., NYEGAARD, M., NAYAK, N., GENBECEV-KRTOLICA, O., MAVROGIANIS, P., FERRER, K., KRUESSEL, J., FAZLEABAS, A. T., FISHER, S. J. & GIUDICE, L. C. 2007. Decidual stromal cell response to paracrine signals from the trophoblast: amplification of immune and angiogenic modulators. *Biol Reprod,* 76**,** 102-17.

HIBY, S. E., APPS, R., SHARKEY, A. M., FARRELL, L. E., GARDNER, L., MULDER, A., CLAAS, F. H., WALKER, J. J., REDMAN, C. W., MORGAN, L., TOWER, C., REGAN, L., MOORE, G. E., CARRINGTON, M. & MOFFETT, A. 2010. Maternal activating KIRs protect against human reproductive failure mediated by fetal HLA-C2. *J Clin Invest,* 120**,** 4102-10.

HIBY, S. E., REGAN, L., LO, W., FARRELL, L., CARRINGTON, M. & MOFFETT, A. 2008. Association of maternal killer-cell immunoglobulin-like receptors and parental HLA-C genotypes with recurrent miscarriage. *Hum Reprod,* 23**,** 972-6.

HIBY, S. E., WALKER, J. J., O'SHAUGHNESSY K, M., REDMAN, C. W., CARRINGTON, M., TROWSDALE, J. & MOFFETT, A. 2004. Combinations of maternal KIR and fetal HLA-C genes influence the risk of preeclampsia and reproductive success. *J Exp Med,* 200**,** 957-65.

HIROTA, Y., OSUGA, Y., KOGA, K., YOSHINO, O., HIRATA, T., MORIMOTO, C., HARADA, M., TAKEMURA, Y., NOSE, E., YANO, T., TSUTSUMI, O. & TAKETANI, Y. 2006. The expression and possible roles of chemokine CXCL11 and its receptor CXCR3 in the human endometrium. *J Immunol,* 177**,** 8813-21.

HOLMES, C. H., SIMPSON, K. L., OKADA, H., OKADA, N., WAINWRIGHT, S. D., PURCELL, D. F. & HOULIHAN, J. M. 1992. Complement regulatory proteins at the feto-maternal interface during human placental development: distribution of CD59 by comparison with membrane cofactor protein (CD46) and decay accelerating factor (CD55). *Eur J Immunol,* 22**,** 1579-85.

HOUSER, B. L. 2012. Decidual macrophages and their roles at the maternal-fetal interface. *Yale J Biol Med,* 85**,** 105-18.

HOUSER, B. L., TILBURGS, T., HILL, J., NICOTRA, M. L. & STROMINGER, J. L. 2011. Two unique human decidual macrophage populations. *J Immunol,* 186**,** 2633-42.

HU, Y., DUTZ, J. P., MACCALMAN, C. D., YONG, P., TAN, R. & VON DADELSZEN, P. 2006. Decidual NK cells alter in vitro first trimester extravillous cytotrophoblast migration: a role for IFN-gamma. *J Immunol,* 177**,** 8522-30.

HUANG, S. J., SCHATZ, F., MASCH, R., RAHMAN, M., BUCHWALDER, L., NIVEN-FAIRCHILD, T., TANG, C., ABRAHAMS, V. M., KRIKUN, G. & LOCKWOOD, C. J. 2006. Regulation of chemokine production in response to pro-inflammatory cytokines in first trimester decidual cells. *J Reprod Immunol,* 72**,** 60-73.

HUB, E. & ROT, A. 1998. Binding of RANTES, MCP-1, MCP-3, and MIP-1alpha to cells in human skin. *Am J Pathol,* 152**,** 749-57.

HUNT, J. S., ANDREWS, G. K. & WOOD, G. W. 1987. Normal trophoblasts resist induction of class I HLA. *J Immunol,* 138**,** 2481-7.

HUNT, J. S., PETROFF, M. G., MCINTIRE, R. H. & OBER, C. 2005. HLA-G and immune tolerance in pregnancy. *Faseb j,* 19**,** 681-93.

HUPPERTZ, B. 2007. The feto-maternal interface: setting the stage for potential immune interactions. *Semin Immunopathol,* 29**,** 83-94.

HUSTIN, J. & SCHAAPS, J. P. 1987. Echographic [corrected] and anatomic studies of the maternotrophoblastic border during the first trimester of pregnancy. *Am J Obstet Gynecol,* 157**,** 162-8.

ISHITANI, A., SAGESHIMA, N., LEE, N., DOROFEEVA, N., HATAKE, K., MARQUARDT, H. & GERAGHTY, D. E. 2003. Protein expression and peptide binding suggest unique and interacting functional roles for HLA-E, F, and G in maternal-placental immune recognition. *J Immunol,* 171**,** 1376-84.

IVARSSON, K., EKERYDH, A., FYHR, I. M., JANSON, P. O. & BRANNSTROM, M. 2000. Upregulation of interleukin-8 and polarized epithelial expression of interleukin-8 receptor A in ovarian carcinomas. *Acta Obstet Gynecol Scand,* 79**,** 777-84.

JACOBS, D. J., VREEBURG, S. A., DEKKER, G. A., HEARD, A. R., PRIEST, K. R. & CHAN, A. 2003. Risk factors for hypertension during pregnancy in South Australia. *Aust N Z J Obstet Gynaecol,* 43**,** 421-8.

JAMIESON, T., COOK, D. N., NIBBS, R. J., ROT, A., NIXON, C., MCLEAN, P., ALCAMI, A., LIRA, S. A., WIEKOWSKI, M. & GRAHAM, G. J. 2005. The chemokine receptor D6 limits the inflammatory response in vivo. *Nat Immunol,* 6**,** 403-11.

JANATPOUR, M. J., UTSET, M. F., CROSS, J. C., ROSSANT, J., DONG, J., ISRAEL, M. A. & FISHER, S. J. 1999. A repertoire of differentially expressed transcription factors that offers insight into mechanisms of human cytotrophoblast differentiation. *Dev Genet,* 25**,** 146-57.

JAUNIAUX, E., HEMPSTOCK, J., GREENWOLD, N. & BURTON, G. J. 2003. Trophoblastic oxidative stress in relation to temporal and regional differences in maternal placental blood flow in normal and abnormal early pregnancies. *Am J Pathol,* 162**,** 115-25.

JILMA-STOHLAWETZ, P., HOMONCIK, M., DRUCKER, C., MARSIK, C., ROT, A., MAYR, W. R., SEIBOLD, B. & JILMA, B. 2001. Fy phenotype and gender determine plasma levels of monocyte chemotactic protein. *Transfusion,* 41**,** 378-81.

JIN, L. P., ZHOU, Y. H., WANG, M. Y., ZHU, X. Y. & LI, D. J. 2005. Blockade of CD80 and CD86 at the time of implantation inhibits maternal rejection to the allogeneic fetus in abortion-prone matings. *J Reprod Immunol,* 65**,** 133-46.

JONES, R. L., HANNAN, N. J., KAITU'U, T. J., ZHANG, J. & SALAMONSEN, L. A. 2004. Identification of chemokines important for leukocyte recruitment to the human endometrium at the times of embryo implantation and menstruation. *J Clin Endocrinol Metab,* 89**,** 6155-67.

JURISICOVA, A., CASPER, R. F., MACLUSKY, N. J. & LIBRACH, C. L. 1996a. Embryonic human leukocyte antigen-G expression: possible implications for human preimplantation development. *Fertil Steril,* 65**,** 997-1002.

JURISICOVA, A., CASPER, R. F., MACLUSKY, N. J., MILLS, G. B. & LIBRACH, C. L. 1996b. HLA-G expression during preimplantation human embryo development. *Proc Natl Acad Sci U S A,* 93**,** 161-5.

KALLIKOURDIS, M., ANDERSEN, K. G., WELCH, K. A. & BETZ, A. G. 2007. Alloantigen-enhanced accumulation of CCR5+ 'effector' regulatory T cells in the gravid uterus. *Proc Natl Acad Sci U S A,* 104**,** 594-9.

KAMMERER, U., EGGERT, A. O., KAPP, M., MCLELLAN, A. D., GEIJTENBEEK, T. B., DIETL, J., VAN KOOYK, Y. & KAMPGEN, E. 2003. Unique appearance of proliferating antigen-presenting cells expressing DC-SIGN (CD209) in the decidua of early human pregnancy. *Am J Pathol,* 162**,** 887-96.

KARPUS, W. J. & KENNEDY, K. J. 1997. MIP-1alpha and MCP-1 differentially regulate acute and relapsing autoimmune encephalomyelitis as well as Th1/Th2 lymphocyte differentiation. *J Leukoc Biol,* 62**,** 681-7.

KAUFMAN, K. A., BOWEN, J. A., TSAI, A. F., BLUESTONE, J. A., HUNT, J. S. & OBER, C. 1999. The CTLA-4 gene is expressed in placental fibroblasts. *Mol Hum Reprod,* 5**,** 84-7.

KAUFMANN, P., SEN, D. K. & SCHWEIKHART, G. 1979. Classification of human placental villi. I. Histology. *Cell Tissue Res,* 200**,** 409-23.

KHONG, T. Y., DE WOLF, F., ROBERTSON, W. B. & BROSENS, I. 1986. Inadequate maternal vascular response to placentation in pregnancies complicated by pre-eclampsia and by small-for-gestational age infants. *Br J Obstet Gynaecol,* 93**,** 1049-59.

KHOURY, S. J. & SAYEGH, M. H. 2004. The roles of the new negative T cell costimulatory pathways in regulating autoimmunity. *Immunity,* 20**,** 529-38.

KIM, Y. M., BUJOLD, E., CHAIWORAPONGSA, T., GOMEZ, R., YOON, B. H., THALER, H. T., ROTMENSCH, S. & ROMERO, R. 2003. Failure of physiologic transformation of the spiral arteries in patients with preterm labor and intact membranes. *Am J Obstet Gynecol,* 189**,** 1063-9.

KING, A., BURROWS, T. D., HIBY, S. E., BOWEN, J. M., JOSEPH, S., VERMA, S., LIM, P. B., GARDNER, L., LE BOUTEILLER, P., ZIEGLER, A., UCHANSKA-ZIEGLER, B. & LOKE, Y. W. 2000. Surface expression of HLA-C antigen by human extravillous trophoblast. *Placenta,* 21**,** 376-87.

KITAYA, K. 2008. Accumulation of uterine CD16(-) natural killer (NK) cells: friends, foes, or Jekyll-and-Hyde relationship for the conceptus? *Immunol Invest,* 37**,** 467-81.

KIVISAKK, P., MAHAD, D. J., CALLAHAN, M. K., SIKORA, K., TREBST, C., TUCKY, B., WUJEK, J., RAVID, R., STAUGAITIS, S. M., LASSMANN, H. & RANSOHOFF, R. M. 2004. Expression of CCR7 in multiple sclerosis: implications for CNS immunity. *Ann Neurol,* 55**,** 627-38.

KLIMAN, H. J., NESTLER, J. E., SERMASI, E., SANGER, J. M. & STRAUSS, J. F. 1986. Purification, characterization, and in vitro differentiation of cytotrophoblasts from human term placentae. *Endocrinology,* 118**,** 1567-82.

KNOFLER, M. & POLLHEIMER, J. 2013. Human placental trophoblast invasion and differentiation: a particular focus on Wnt signaling. *Front Genet,* 4**,** 190.

KOOPMAN, L. A., KOPCOW, H. D., RYBALOV, B., BOYSON, J. E., ORANGE, J. S., SCHATZ, F., MASCH, R., LOCKWOOD, C. J., SCHACHTER, A. D., PARK, P. J. & STROMINGER, J. L. 2003. Human decidual natural killer cells are a unique NK cell subset with immunomodulatory potential. *J Exp Med,* 198**,** 1201-12.

KOPCOW, H. D., ERIKSSON, M., MSELLE, T. F., DAMRAUER, S. M., WIRA, C. R., SENTMAN, C. L. & STROMINGER, J. L. 2010. Human decidual NK cells from gravid uteri and NK cells from cycling endometrium are distinct NK cell subsets. *Placenta,* 31**,** 334-8.

KOVO, M., SCHREIBER, L. & BAR, J. 2013. Placental vascular pathology as a mechanism of disease in pregnancy complications. *Thromb Res,* 131 Suppl 1**,** S18-21.

KUDO, Y., BOYD, C. A., KIMURA, H., COOK, P. R., REDMAN, C. W. & SARGENT, I. L. 2003. Quantifying the syncytialisation of human placental trophoblast BeWo cells grown in vitro. *Biochim Biophys Acta,* 1640**,** 25-31.

KUNZ, M., HARTMANN, A., FLORY, E., TOKSOY, A., KOCZAN, D., THIESEN, H. J., MUKAIDA, N., NEUMANN, M., RAPP, U. R., BROCKER, E. B. & GILLITZER, R. 1999. Anoxia-induced up-regulation of interleukin-8 in human malignant melanoma. A potential mechanism for high tumor aggressiveness. *Am J Pathol,* 155**,** 753-63.

KUZIEL, W. A., DAWSON, T. C., QUINONES, M., GARAVITO, E., CHENAUX, G., AHUJA, S. S., REDDICK, R. L. & MAEDA, N. 2003. CCR5 deficiency is not protective in the early stages of atherogenesis in apoE knockout mice. *Atherosclerosis,* 167**,** 25-32.

LAMBERT, D., NAISH, D. & WYSE, E. 2001. *Encyclopedia of dinosaurs and prehistoric life,* Great Britain, Dorling Kindersley Limited.

LAMKHIOUED, B., GARCIA-ZEPEDA, E. A., ABI-YOUNES, S., NAKAMURA, H., JEDRZKIEWICZ, S., WAGNER, L., RENZI, P. M., ALLAKHVERDI, Z., LILLY, C., HAMID, Q. & LUSTER, A. D. 2000. Monocyte chemoattractant protein (MCP)-4

expression in the airways of patients with asthma. Induction in epithelial cells and mononuclear cells by proinflammatory cytokines. *Am J Respir Crit Care Med,* 162**,** 723-32.
LAPILLONNE, A. & GRIFFIN, I. J. 2013. Feeding preterm infants today for later metabolic and cardiovascular outcomes. *J Pediatr,* 162**,** S7-16.
LASAGNI, L., FRANCALANCI, M., ANNUNZIATO, F., LAZZERI, E., GIANNINI, S., COSMI, L., SAGRINATI, C., MAZZINGHI, B., ORLANDO, C., MAGGI, E., MARRA, F., ROMAGNANI, S., SERIO, M. & ROMAGNANI, P. 2003. An alternatively spliced variant of CXCR3 mediates the inhibition of endothelial cell growth induced by IP-10, Mig, and I-TAC, and acts as functional receptor for platelet factor 4. *J Exp Med,* 197**,** 1537-49.
LASH, G. E., SCHIESSL, B., KIRKLEY, M., INNES, B. A., COOPER, A., SEARLE, R. F., ROBSON, S. C. & BULMER, J. N. 2006. Expression of angiogenic growth factors by uterine natural killer cells during early pregnancy. *J Leukoc Biol,* 80**,** 572-80.
LE BELLEGO, F., VAILLANCOURT, C. & LAFOND, J. 2009. Isolation and culture of term human cytotrophoblast cells and in vitro methods for studying human cytotrophoblast cells' calcium uptake. *Methods Mol Biol,* 550**,** 73-87.
LE ROND, S., AZEMA, C., KRAWICE-RADANNE, I., DURRBACH, A., GUETTIER, C., CAROSELLA, E. D. & ROUAS-FREISS, N. 2006. Evidence to support the role of HLA-G5 in allograft acceptance through induction of immunosuppressive/ regulatory T cells. *J Immunol,* 176**,** 3266-76.
LE, Y., ZHOU, Y., IRIBARREN, P. & WANG, J. 2004. Chemokines and chemokine receptors: their manifold roles in homeostasis and disease. *Cell Mol Immunol,* 1**,** 95-104.
LEBER, A., TELES, A. & ZENCLUSSEN, A. 2010. Regulatory T cells and their role in pregnancy. *Am J Reprod Immunol,* 63**,** 445-59.
LEE, J. S., FREVERT, C. W., THORNING, D. R., SEGERER, S., ALPERS, C. E., CARTRON, J. P., COLIN, Y., WONG, V. A., MARTIN, T. R. & GOODMAN, R. B. 2003a. Enhanced expression of Duffy antigen in the lungs during suppurative pneumonia. *J Histochem Cytochem,* 51**,** 159-66.
LEE, J. S., FREVERT, C. W., WURFEL, M. M., PEIPER, S. C., WONG, V. A., BALLMAN, K. K., RUZINSKI, J. T., RHIM, J. S., MARTIN, T. R. & GOODMAN, R. B. 2003b. Duffy antigen facilitates movement of chemokine across the endothelium in vitro and promotes neutrophil transmigration in vitro and in vivo. *J Immunol,* 170**,** 5244-51.
LEE, K. M., MCKIMMIE, C. S., GILCHRIST, D. S., PALLAS, K. J., NIBBS, R. J., GARSIDE, P., MCDONALD, V., JENKINS, C., RANSOHOFF, R., LIU, L., MILLING, S., CEROVIC, V. & GRAHAM, G. J. 2011. D6 facilitates cellular migration and fluid flow to lymph nodes by suppressing lymphatic congestion. *Blood,* 118**,** 6220-9.
LEE, W., O'CONNELL, C. M. & BASKETT, T. F. 2004. Maternal and perinatal outcomes of eclampsia: Nova Scotia, 1981-2000. *J Obstet Gynaecol Can,* 26**,** 119-23.
LEMAOULT, J., KRAWICE-RADANNE, I., DAUSSET, J. & CAROSELLA, E. D. 2004. HLA-G1-expressing antigen-presenting cells induce immunosuppressive CD4+ T cells. *Proc Natl Acad Sci U S A,* 101**,** 7064-9.
LENTSCH, A. B. 2002. The Duffy antigen/receptor for chemokines (DARC) and prostate cancer. A role as clear as black and white? *Faseb j,* 16**,** 1093-5.
LESSIN, D. L., HUNT, J. S., KING, C. R. & WOOD, G. W. 1988. Antigen expression by cells near the maternal-fetal interface. *Am J Reprod Immunol Microbiol,* 16**,** 1-7.
LI, C., HOUSER, B. L., NICOTRA, M. L. & STROMINGER, J. L. 2009. HLA-G homodimer-induced cytokine secretion through HLA-G receptors on human decidual macrophages and natural killer cells. *Proc Natl Acad Sci U S A,* 106**,** 5767-72.
LIDSTROM, C., MATTHIESEN, L., BERG, G., SHARMA, S., ERNERUDH, J. & EKERFELT, C. 2003. Cytokine secretion patterns of NK cells and macrophages in early human pregnancy decidua and blood: implications for suppressor macrophages in decidua. *Am J Reprod Immunol,* 50**,** 444-52.
LIN, G. J., HUANG, S. H., CHEN, Y. W., HUENG, D. Y., CHIA, W. T., CHIEN, M. W., YEN, B. L. & SYTWU, H. K. 2011. Transgenic expression of murine chemokine decoy receptor D6 by islets reveals the role of inflammatory CC chemokines in the development of autoimmune diabetes in NOD mice. *Diabetologia,* 54**,** 1777-87.
LIU, L., GRAHAM, G. J., DAMODARAN, A., HU, T., LIRA, S. A., SASSE, M., CANASTO-CHIBUQUE, C., COOK, D. N. & RANSOHOFF, R. M. 2006. Cutting edge: the silent chemokine receptor D6 is required for generating T cell responses that mediate experimental autoimmune encephalomyelitis. *J Immunol,* 177**,** 17-21.
LIU, M. T., KEIRSTEAD, H. S. & LANE, T. E. 2001. Neutralization of the chemokine CXCL10 reduces inflammatory cell invasion and demyelination and improves neurological function in a viral model of multiple sclerosis. *J Immunol,* 167**,** 4091-7.
LLOYD, C. M., MINTO, A. W., DORF, M. E., PROUDFOOT, A., WELLS, T. N., SALANT, D. J. & GUTIERREZ-RAMOS, J. C. 1997. RANTES and monocyte chemoattractant protein-1 (MCP-1) play an important role in the inflammatory phase of crescentic nephritis, but only MCP-1 is involved in crescent formation and interstitial fibrosis. *J Exp Med,* 185**,** 1371-80.
LOCKWOOD, C. J., MATTA, P., KRIKUN, G., KOOPMAN, L. A., MASCH, R., TOTI, P., ARCURI, F., HUANG, S. T., FUNAI, E. F. & SCHATZ, F. 2006. Regulation of monocyte chemoattractant protein-1 expression by tumor necrosis factor-alpha and interleukin-1beta in first trimester human decidual cells: implications for preeclampsia. *Am J Pathol,* 168**,** 445-52.
LUAN, J., SHATTUCK-BRANDT, R., HAGHNEGAHDAR, H., OWEN, J. D., STRIETER, R., BURDICK, M., NIRODI, C., BEAUCHAMP, D., JOHNSON, K. N. & RICHMOND, A. 1997. Mechanism and biological significance of constitutive expression of MGSA/GRO chemokines in malignant melanoma tumor progression. *J Leukoc Biol,* 62**,** 588-97.
LUKACS, N. W. 2001. Role of chemokines in the pathogenesis of asthma. *Nat Rev Immunol,* 1**,** 108-16.
LYALL, F., ROBSON, S. C. & BULMER, J. N. 2013. Spiral Artery Remodeling and Trophoblast Invasion in Preeclampsia and Fetal Growth Restriction: Relationship to Clinical Outcome. *Hypertension*.
LYNCH, L., GOLDEN-MASON, L., EOGAN, M., O'HERLIHY, C. & O'FARRELLY, C. 2007. Cells with haematopoietic stem cell phenotype in adult human endometrium: relevance to infertility? *Hum Reprod,* 22**,** 919-26.
MACKAY, C. R. 2001. Chemokines: immunology's high impact factors. *Nat Immunol,* 2**,** 95-101.
MACKLON, N. S., GERAEDTS, J. P. & FAUSER, B. C. 2002. Conception to ongoing pregnancy: the 'black box' of early pregnancy loss. *Hum Reprod Update,* 8**,** 333-43.
MADIGAN, J., FREEMAN, D., MENZIES, F., FORROW, S., NELSON, S., YOUNG, A., SHARKEY, A., MOFFETT, A., GRAHAM, G., GREER, I., ROT, A. & NIBBS, R. 2010. Chemokine Scavenger D6 Is Expressed by Trophoblasts and Aids the Survival of Mouse Embryos Transferred into Allogeneic Recipients. *J Immunol*.
MALDONADO-ESTRADA, J., MENU, E., ROQUES, P., BARRÉ-SINOUSSI, F. & CHAOUAT, G. 2004. Evaluation of Cytokeratin 7 as an accurate intracellular marker with which to assess the purity of human placental villous trophoblast cells by flow cytometry. *J Immunol Methods,* 286**,** 21-34.

MALE, V., SHARKEY, A., MASTERS, L., KENNEDY, P. R., FARRELL, L. E. & MOFFETT, A. 2011. The effect of pregnancy on the uterine NK cell KIR repertoire. *Eur J Immunol,* 41**,** 3017-27.
MANGALE, S. S. & REDDY, K. V. 2007. Expression pattern of integrins and their ligands in mouse feto-maternal tissues during pregnancy. *Reprod Fertil Dev,* 19**,** 452-60.
MANTOVANI, A., BONECCHI, R. & LOCATI, M. 2006. Tuning inflammation and immunity by chemokine sequestration: decoys and more. *Nat Rev Immunol,* 6**,** 907-18.
MANTOVANI, A., SICA, A., SOZZANI, S., ALLAVENA, P., VECCHI, A. & LOCATI, M. 2004. The chemokine system in diverse forms of macrophage activation and polarization. *Trends Immunol,* 25**,** 677-86.
MARTINEZ DE LA TORRE, Y., BURACCHI, C., BORRONI, E., DUPOR, J., BONECCHI, R., NEBULONI, M., PASQUALINI, F., DONI, A., LAURI, E., AGOSTINIS, C., BULLA, R., COOK, D., HARIBABU, B., MERONI, P., RUKAVINA, D., VAGO, L., TEDESCO, F., VECCHI, A., LIRA, S., LOCATI, M. & MANTOVANI, A. 2007. Protection against inflammation- and autoantibody-caused fetal loss by the chemokine decoy receptor D6. *Proc Natl Acad Sci U S A,* 104**,** 2319-24.
MARTINEZ DE LA TORRE, Y., LOCATI, M., BURACCHI, C., DUPOR, J., COOK, D. N., BONECCHI, R., NEBULONI, M., RUKAVINA, D., VAGO, L., VECCHI, A., LIRA, S. A. & MANTOVANI, A. 2005. Increased inflammation in mice deficient for the chemokine decoy receptor D6. *Eur J Immunol,* 35**,** 1342-6.
MATSUKAWA, A., HOGABOAM, C. M., LUKACS, N. W., LINCOLN, P. M., EVANOFF, H. L. & KUNKEL, S. L. 2000. Pivotal role of the CC chemokine, macrophage-derived chemokine, in the innate immune response. *J Immunol,* 164**,** 5362-8.
MATSUKAWA, A., HOGABOAM, C. M., LUKACS, N. W., LINCOLN, P. M., STRIETER, R. M. & KUNKEL, S. L. 1999. Endogenous monocyte chemoattractant protein-1 (MCP-1) protects mice in a model of acute septic peritonitis: cross-talk between MCP-1 and leukotriene B4. *J Immunol,* 163**,** 6148-54.
MATSUURA-SAWADA, R., MURAKAMI, T., OZAWA, Y., NABESHIMA, H., AKAHIRA, J., SATO, Y., KOYANAGI, Y., ITO, M., TERADA, Y. & OKAMURA, K. 2005. Reproduction of menstrual changes in transplanted human endometrial tissue in immunodeficient mice. *Hum Reprod,* 20**,** 1477-84.
MATTSSON, R. 1998. The non-expression of MHC class II in trophoblast cells. *Am J Reprod Immunol,* 40**,** 383-4.
MAYHEW, T. M. 1997. Recent applications of the new stereology have thrown fresh light on how the human placenta grows and develops its form. *J Microsc,* 186**,** 153-63.
MAYHEW, T. M. 2009. A stereological perspective on placental morphology in normal and complicated pregnancies. *J Anat,* 215**,** 77-90.
MAYHEW, T. M. & BURTON, G. J. 1997. Stereology and its impact on our understanding of human placental functional morphology. *Microsc Res Tech,* 38**,** 195-205.
MCCULLOCH, C., MORROW, V., MILASTA, S., COMERFORD, I., MILLIGAN, G., GRAHAM, G., ISAACS, N. & NIBBS, R. 2008. Multiple roles for the C-terminal tail of the chemokine scavenger D6. *J Biol Chem,* 283**,** 7972-82.
MCDERMOTT, D. H., FONG, A. M., YANG, Q., SECHLER, J. M., CUPPLES, L. A., MERRELL, M. N., WILSON, P. W., D'AGOSTINO, R. B., O'DONNELL, C. J., PATEL, D. D. & MURPHY, P. M. 2003. Chemokine receptor mutant CX3CR1-M280 has impaired adhesive function and correlates with protection from cardiovascular disease in humans. *J Clin Invest,* 111**,** 1241-50.
MCKIMMIE, C., FRASER, A., HANSELL, C., GUTIÉRREZ, L., PHILIPSEN, S., CONNELL, L., ROT, A., KUROWSKA-STOLARSKA, M., CARRENO, P., PRUENSTER, M., CHU, C., LOMBARDI, G., HALSEY, C., MCINNES, I., LIEW, F., NIBBS, R. & GRAHAM, G. 2008. Hemopoietic cell expression of the chemokine decoy receptor D6 is dynamic and regulated by GATA1. *J Immunol,* 181**,** 3353-63.
MEDOFF, B. D., SAUTY, A., TAGER, A. M., MACLEAN, J. A., SMITH, R. N., MATHEW, A., DUFOUR, J. H. & LUSTER, A. D. 2002. IFN-gamma-inducible protein 10 (CXCL10) contributes to airway hyperreactivity and airway inflammation in a mouse model of asthma. *J Immunol,* 168**,** 5278-86.
METZNER, B., HOFMANN, C., HEINEMANN, C., ZIMPFER, U., SCHRAUFSTATTER, I., SCHOPF, E. & NORGAUER, J. 1999. Overexpression of CXC-chemokines and CXC-chemokine receptor type II constitute an autocrine growth mechanism in the epidermoid carcinoma cells KB and A431. *Oncol Rep,* 6**,** 1405-10.
MIDDLETON, J., NEIL, S., WINTLE, J., CLARK-LEWIS, I., MOORE, H., LAM, C., AUER, M., HUB, E. & ROT, A. 1997. Transcytosis and surface presentation of IL-8 by venular endothelial cells. *Cell,* 91**,** 385-95.
MILLER, L. H., MASON, S. J., CLYDE, D. F. & MCGINNISS, M. H. 1976. The resistance factor to Plasmodium vivax in blacks. The Duffy-blood-group genotype, FyFy. *N Engl J Med,* 295**,** 302-4.
MIYAMOTO, M., SHIMIZU, Y., OKADA, K., KASHII, Y., HIGUCHI, K. & WATANABE, A. 1998. Effect of interleukin-8 on production of tumor-associated substances and autocrine growth of human liver and pancreatic cancer cells. *Cancer Immunol Immunother,* 47**,** 47-57.
MOFFETT-KING, A. 2002. Natural killer cells and pregnancy. *Nat Rev Immunol,* 2**,** 656-63.
MOKHTAR, N. M., CHENG, C. W., COOK, E., BIELBY, H., SMITH, S. K. & CHARNOCK-JONES, D. S. 2010. Progestin regulates chemokine (C-X-C motif) ligand 14 transcript level in human endometrium. *Mol Hum Reprod,* 16**,** 170-7.
MOORE, K. L., PERSAUD, T. V. N. & TORCHIA, M. G. 2013. *The developing human: Clinically orientated embryology,* Philadelphia, PA, Saunders.
MULLER, A., HOMEY, B., SOTO, H., GE, N., CATRON, D., BUCHANAN, M. E., MCCLANAHAN, T., MURPHY, E., YUAN, W., WAGNER, S. N., BARRERA, J. L., MOHAR, A., VERASTEGUI, E. & ZLOTNIK, A. 2001. Involvement of chemokine receptors in breast cancer metastasis. *Nature,* 410**,** 50-6.
MURPHY, P. M. 2002. International Union of Pharmacology. XXX. Update on chemokine receptor nomenclature. *Pharmacol Rev,* 54**,** 227-9.
NAIT-OUMESMAR, B., COPPERMAN, A. B. & LAZZARINI, R. A. 2000. Placental expression and chromosomal localization of the human Gcm 1 gene. *J Histochem Cytochem,* 48**,** 915-22.
NANCY, P., TAGLIANI, E., TAY, C. S., ASP, P., LEVY, D. E. & ERLEBACHER, A. 2012. Chemokine gene silencing in decidual stromal cells limits T cell access to the maternal-fetal interface. *Science,* 336**,** 1317-21.
NANKI, T., HAYASHIDA, K., EL-GABALAWY, H. S., SUSON, S., SHI, K., GIRSCHICK, H. J., YAVUZ, S. & LIPSKY, P. E. 2000. Stromal cell-derived factor-1-CXC chemokine receptor 4 interactions play a central role in CD4+ T cell accumulation in rheumatoid arthritis synovium. *J Immunol,* 165**,** 6590-8.
NASU, K., FUJISAWA, K., ARIMA, K., KAI, K., SUGANO, T. & MIYAKAWA, I. 2001. Expression and regulation of growth-regulated oncogene alpha in human endometrial stromal cells. *Mol Hum Reprod,* 7**,** 741-6.
NELKEN, N. A., COUGHLIN, S. R., GORDON, D. & WILCOX, J. N. 1991. Monocyte chemoattractant protein-1 in human atheromatous plaques. *J Clin Invest,* 88**,** 1121-7.
NELSON, J. L., HUGHES, K. A., SMITH, A. G., NISPEROS, B. B., BRANCHAUD, A. M. & HANSEN, J. A. 1993. Maternal-fetal disparity in HLA class II alloantigens and the pregnancy-induced. *N Engl J Med,* 329**,** 466-71.

NEWBY, D., COUSINS, F., MYATT, L. & LYALL, F. 2005. Heme oxygenase expression in cultured human trophoblast cells during in vitro differentiation: effects of hypoxia. *Placenta,* 26**,** 201-9.
NIBBS, R., GRAHAM, G. & ROT, A. 2003. Chemokines on the move: control by the chemokine "interceptors" Duffy blood group antigen and D6. *Semin Immunol,* 15**,** 287-94.
NIBBS, R., KRIEHUBER, E., PONATH, P., PARENT, D., QIN, S., CAMPBELL, J., HENDERSON, A., KERJASCHKI, D., MAURER, D., GRAHAM, G. & ROT, A. 2001. The beta-chemokine receptor D6 is expressed by lymphatic endothelium and a subset of vascular tumors. *Am J Pathol,* 158**,** 867-77.
NIBBS, R., MCLEAN, P., MCCULLOCH, C., RIBOLDI-TUNNICLIFFE, A., BLAIR, E., ZHU, Y., ISAACS, N. & GRAHAM, G. 2009. Structure-function dissection of D6, an atypical scavenger receptor. *Methods Enzymol,* 460**,** 245-61.
NIBBS, R. J., GILCHRIST, D. S., KING, V., FERRA, A., FORROW, S., HUNTER, K. D. & GRAHAM, G. J. 2007. The atypical chemokine receptor D6 suppresses the development of chemically induced skin tumors. *J Clin Invest,* 117**,** 1884-92.
NIBBS, R. J., WYLIE, S. M., PRAGNELL, I. B. & GRAHAM, G. J. 1997a. Cloning and characterization of a novel murine beta chemokine receptor, D6. Comparison to three other related macrophage inflammatory protein-1alpha receptors, CCR-1, CCR-3, and CCR-5. *J Biol Chem,* 272**,** 12495-504.
NIBBS, R. J., WYLIE, S. M., YANG, J., LANDAU, N. R. & GRAHAM, G. J. 1997b. Cloning and characterization of a novel promiscuous human beta-chemokine receptor D6. *J Biol Chem,* 272**,** 32078-83.
NIBBS, R. J. B. & GRAHAM, G. J. 2013. Immune regulation by atypical chemokine receptors. *Nature Reviews Immunology,* 13**,** 815-829.
NORWITZ, E., DJ, S. & SJ, F. 2001. Implantation and the survival of early pregnancy. *N Engl J Med,* 345**,** 1400-1408.
NOSO, N., PROOST, P., VAN DAMME, J. & SCHRODER, J. M. 1994. Human monocyte chemotactic proteins-2 and 3 (MCP-2 and MCP-3) attract human eosinophils and desensitize the chemotactic responses towards RANTES. *Biochem Biophys Res Commun,* 200**,** 1470-6.
NOWAK, I., MALINOWSKI, A., TCHORZEWSKI, H., BARCZ, E., WILCZYNSKI, J. R., BANASIK, M., GRYBOS, M., KURPISZ, M., LUSZCZEK, W., MAJORCZYK, E., WISNIEWSKI, A., SENITZER, D., SUN, J. Y. & KUSNIERCZYK, P. 2011. HLA-C C1C2 heterozygosity may protect women bearing the killer immunoglobulin-like receptor AA genotype from spontaneous abortion. *J Reprod Immunol,* 88**,** 32-7.
OBER, C. 1998. HLA and pregnancy: the paradox of the fetal allograft. *Am J Hum Genet,* 62**,** 1-5.
ODIBO, A. O., ZHONG, Y., LONGTINE, M., TUULI, M., ODIBO, L., CAHILL, A. G., MACONES, G. A. & NELSON, D. M. 2011. First-trimester serum analytes, biophysical tests and the association with pathological morphometry in the placenta of pregnancies with preeclampsia and fetal growth restriction. *Placenta,* 32**,** 333-8.
OH, S. Y., CHU, T. & SADOVSKY, Y. 2011. The timing and duration of hypoxia determine gene expression patterns in cultured human trophoblasts. *Placenta,* 32**,** 1004-9.
OLIVARES, E. G., MONTES, M. J., OLIVER, C., GALINDO, J. A. & RUIZ, C. 1997. Cultured human decidual stromal cells express B7-1 (CD80) and B7-2 (CD86) and stimulate allogeneic T cells. *Biol Reprod,* 57**,** 609-15.
ORENDI, K., KIVITY, V., SAMMAR, M., GRIMPEL, Y., GONEN, R., MEIRI, H., LUBZENS, E. & HUPPERTZ, B. 2011. Placental and trophoblastic in vitro models to study preventive and therapeutic agents for preeclampsia. *Placenta,* 32 Suppl**,** S49-54.
PARK, B., LEE, S., KIM, E., CHANG, S., JIN, M. & AHN, K. 2001. The truncated cytoplasmic tail of HLA-G serves a quality-control function in post-ER compartments. *Immunity,* 15**,** 213-24.
PASHOVER-SCHALLINGER, E., ASWAD, M., SCHIF-ZUCK, S., SHAPIRO, H., SINGER, P. & ARIEL, A. 2012. The atypical chemokine receptor D6 controls macrophage efferocytosis and cytokine secretion during the resolution of inflammation. *Faseb j,* 26**,** 3891-900.
PATHAK, S., HOOK, E., HACKETT, G., MURDOCH, E., SEBIRE, N. J., JESSOP, F. & LEES, C. 2010. Cord coiling, umbilical cord insertion and placental shape in an unselected cohort delivering at term: relationship with common obstetric outcomes. *Placenta,* 31**,** 963-8.
PETROFF, M. G., CHEN, L., PHILLIPS, T. A., AZZOLA, D., SEDLMAYR, P. & HUNT, J. S. 2003. B7 family molecules are favorably positioned at the human maternal-fetal interface. *Biol Reprod,* 68**,** 1496-504.
PHILLIPS, R. J., BURDICK, M. D., LUTZ, M., BELPERIO, J. A., KEANE, M. P. & STRIETER, R. M. 2003. The stromal derived factor-1/CXCL12-CXC chemokine receptor 4 biological axis in non-small cell lung cancer metastases. *Am J Respir Crit Care Med,* 167**,** 1676-86.
PIJNENBORG, R., DIXON, G., ROBERTSON, W. B. & BROSENS, I. 1980. Trophoblastic invasion of human decidua from 8 to 18 weeks of pregnancy. *Placenta,* 1**,** 3-19.
PIJNENBORG, R., VERCRUYSSE, L. & HANSSENS, M. 2006. The uterine spiral arteries in human pregnancy: facts and controversies. *Placenta,* 27**,** 939-58.
PITMAN, H., INNES, B. A., ROBSON, S. C., BULMER, J. N. & LASH, G. E. 2013. Altered expression of interleukin-6, interleukin-8 and their receptors in decidua of women with sporadic miscarriage. *Hum Reprod,* 28**,** 2075-86.
POLANCZYK, M. J., CARSON, B. D., SUBRAMANIAN, S., AFENTOULIS, M., VANDENBARK, A. A., ZIEGLER, S. F. & OFFNER, H. 2004. Cutting edge: estrogen drives expansion of the CD4+CD25+ regulatory T cell compartment. *J Immunol,* 173**,** 2227-30.
PÖTGENS, A. J., GAUS, G., FRANK, H. G. & KAUFMANN, P. 2001. Characterization of trophoblast cell isolations by a modified flow cytometry assay. *Placenta,* 22**,** 251-5.
PÖTGENS, A. J., KATAOKA, H., FERSTL, S., FRANK, H. G. & KAUFMANN, P. 2003. A positive immunoselection method to isolate villous cytotrophoblast cells from first trimester and term placenta to high purity. *Placenta,* 24**,** 412-23.
QUENBY, S., BATES, M., DOIG, T., BREWSTER, J., LEWIS-JONES, D. I., JOHNSON, P. M. & VINCE, G. 1999. Pre-implantation endometrial leukocytes in women with recurrent miscarriage. *Hum Reprod,* 14**,** 2386-91.
RAJAGOPALAN, S., FU, J. & LONG, E. O. 2001. Cutting edge: induction of IFN-gamma production but not cytotoxicity by the killer cell Ig-like receptor KIR2DL4 (CD158d) in resting NK cells. *J Immunol,* 167**,** 1877-81.
REAPE, T. J. & GROOT, P. H. 1999. Chemokines and atherosclerosis. *Atherosclerosis,* 147**,** 213-25.
RED-HORSE, K., DRAKE, P. & FISHER, S. 2004. Human pregnancy: the role of chemokine networks at the fetal-maternal interface. *Expert Rev Mol Med,* 6**,** 1-14.
RED-HORSE, K., DRAKE, P. M., GUNN, M. D. & FISHER, S. J. 2001. Chemokine ligand and receptor expression in the pregnant uterus: reciprocal patterns in complementary cell subsets suggest functional roles. *Am J Pathol,* 159**,** 2199-213.

REISTER, F., FRANK, H. G., HEYL, W., KOSANKE, G., HUPPERTZ, B., SCHRODER, W., KAUFMANN, P. & RATH, W. 1999. The distribution of macrophages in spiral arteries of the placental bed in pre-eclampsia differs from that in healthy patients. *Placenta,* 20**,** 229-33.
RENFREE, M. B. 1972. Influence of the embryo on the marsupial uterus. *Nature,* 240**,** 475-7.
RENFREE, M. B. 2000. Maternal recognition of pregnancy in marsupials. *Rev Reprod,* 5**,** 6-11.
RICHMOND, A., BALENTIEN, E., THOMAS, H. G., FLAGGS, G., BARTON, D. E., SPIESS, J., BORDONI, R., FRANCKE, U. & DERYNCK, R. 1988. Molecular characterization and chromosomal mapping of melanoma growth stimulatory activity, a growth factor structurally related to beta-thromboglobulin. *Embo j,* 7**,** 2025-33.
RILEY, J. K. & YOKOYAMA, W. M. 2008. NK cell tolerance and the maternal-fetal interface. *Am J Reprod Immunol,* 59**,** 371-87.
RIZZO, R., VERCAMMEN, M., VAN DE VELDE, H., HORN, P. A. & REBMANN, V. 2011. The importance of HLA-G expression in embryos, trophoblast cells, and embryonic stem cells. *Cell Mol Life Sci,* 68**,** 341-52.
ROBERTS, C. L., ALGERT, C. S., MORRIS, J. M., FORD, J. B. & HENDERSON-SMART, D. J. 2005. Hypertensive disorders in pregnancy: a population-based study. *Med J Aust.* Australia.
RODESCH, F., SIMON, P., DONNER, C. & JAUNIAUX, E. 1992. Oxygen measurements in endometrial and trophoblastic tissues during early pregnancy. *Obstet Gynecol,* 80**,** 283-5.
RODRIGUEZ-SANABRIA, F., RULL, A., BELTRAN-DEBON, R., ARAGONES, G., CAMPS, J., MACKNESS, B., MACKNESS, M. & JOVEN, J. 2010. Tissue distribution and expression of paraoxonases and chemokines in mouse: the ubiquitous and joint localisation suggest a systemic and coordinated role. *J Mol Histol,* 41**,** 379-86.
ROSENBERG, K. R. & TREVATHAN, W. R. 2007. An anthropological perspective on the evolutionary context of preeclampsia in humans. *J Reprod Immunol,* 76**,** 91-7.
ROSENKILDE, M. M. & SCHWARTZ, T. W. 2004. The chemokine system -- a major regulator of angiogenesis in health and disease. *Apmis,* 112**,** 481-95.
ROSS, R. 1993. The pathogenesis of atherosclerosis: a perspective for the 1990s. *Nature,* 362**,** 801-9.
ROSSANT, J. & CROSS, J. C. 2001. Placental development: lessons from mouse mutants. *Nat Rev Genet,* 2**,** 538-48.
ROSSI, D. & ZLOTNIK, A. 2003. The Biology of Chemokines and their Receptors. *Annual Review of Immunology,* 18**,** 217-242.
ROT, A. 2005. Contribution of Duffy antigen to chemokine function. *Cytokine Growth Factor Rev,* 16**,** 687-94.
ROVIN, B. H., LU, L. & SAXENA, R. 1999. A novel polymorphism in the MCP-1 gene regulatory region that influences MCP-1 expression. *Biochem Biophys Res Commun,* 259**,** 344-8.
ROZNER, A. E., DAMBAEVA, S. V., DRENZEK, J. G., DURNING, M. & GOLOS, T. G. 2011. Modulation of cytokine and chemokine secretions in rhesus monkey trophoblast co-culture with decidual but not peripheral blood monocyte-derived macrophages. *Am J Reprod Immunol,* 66**,** 115-27.
RUBANYL, G. M., FRYE, R. L., HOLMES, D. R., JR. & VANHOUTTE, P. M. 1987. Vasoconstrictor activity of coronary sinus plasma from patients with coronary artery disease. *J Am Coll Cardiol,* 9**,** 1243-9.
SAETTA, M., MARIANI, M., PANINA-BORDIGNON, P., TURATO, G., BUONSANTI, C., BARALDO, S., BELLETTATO, C. M., PAPI, A., CORBETTA, L., ZUIN, R., SINIGAGLIA, F. & FABBRI, L. M. 2002. Increased expression of the chemokine receptor CXCR3 and its ligand CXCL10 in peripheral airways of smokers with chronic obstructive pulmonary disease. *Am J Respir Crit Care Med,* 165**,** 1404-9.
SAITO, S., SASAKI, Y. & SAKAI, M. 2005. CD4(+)CD25high regulatory T cells in human pregnancy. *J Reprod Immunol,* 65**,** 111-20.
SAITO, S., SHIOZAKI, A., SASAKI, Y., NAKASHIMA, A., SHIMA, T. & ITO, M. 2007. Regulatory T cells and regulatory natural killer (NK) cells play important roles in feto-maternal tolerance. *Semin Immunopathol,* 29**,** 115-22.
SALAFIA, C. M., YAMPOLSKY, M., MISRA, D. P., SHLAKHTER, O., HAAS, D., EUCKER, B. & THORP, J. 2010. Placental surface shape, function, and effects of maternal and fetal vascular pathology. *Placenta,* 31**,** 958-62.
SALCEDO, R., WASSERMAN, K., YOUNG, H. A., GRIMM, M. C., HOWARD, O. M., ANVER, M. R., KLEINMAN, H. K., MURPHY, W. J. & OPPENHEIM, J. J. 1999. Vascular endothelial growth factor and basic fibroblast growth factor induce expression of CXCR4 on human endothelial cells: In vivo neovascularization induced by stromal-derived factor-1alpha. *Am J Pathol,* 154**,** 1125-35.
SATO, Y., HIGUCHI, T., YOSHIOKA, S., TATSUMI, K., FUJIWARA, H. & FUJII, S. 2003. Trophoblasts acquire a chemokine receptor, CCR1, as they differentiate towards invasive phenotype. *Development,* 130**,** 5519-32.
SAVINO, B., CASTOR, M. G., CARONNI, N., SARUKHAN, A., ANSELMO, A., BURACCHI, C., BENVENUTI, F., PINHO, V., TEIXEIRA, M. M., MANTOVANI, A., LOCATI, M. & BONECCHI, R. 2012. Control of murine Ly6C(high) monocyte traffic and immunosuppressive activities by atypical chemokine receptor D6. *Blood,* 119**,** 5250-60.
SCHACTER, B., MUIR, A., GYVES, M. & TASIN, M. 1979. HLA-A,B compatibility in parents of offspring with neural-tube defects or couples experiencing involuntary fetal wastage. *Lancet,* 1**,** 796-9.
SCHECTER, A. D., ROLLINS, B. J., ZHANG, Y. J., CHARO, I. F., FALLON, J. T., ROSSIKHINA, M., GIESEN, P. L., NEMERSON, Y. & TAUBMAN, M. B. 1997. Tissue factor is induced by monocyte chemoattractant protein-1 in human aortic smooth muscle and THP-1 cells. *J Biol Chem,* 272**,** 28568-73.
SCHOENWOLF, G. C., BLEYL, S. B., BRAUER, P. R. & FRANCIS-WEST, P. H. 2009. *Larsen's human embryology,* Philadelphia, PA, Churchill Livingstone.
SEPULVEDA, W. 2006. Velamentous insertion of the umbilical cord: a first-trimester sonographic screening study. *J Ultrasound Med,* 25**,** 963-8; quiz 970.
SHARKEY, A. M., GARDNER, L., HIBY, S., FARRELL, L., APPS, R., MASTERS, L., GOODRIDGE, J., LATHBURY, L., STEWART, C. A., VERMA, S. & MOFFETT, A. 2008. Killer Ig-like receptor expression in uterine NK cells is biased toward recognition of HLA-C and alters with gestational age. *J Immunol,* 181**,** 39-46.
SHEN, H., SCHUSTER, R., STRINGER, K. F., WALTZ, S. E. & LENTSCH, A. B. 2006. The Duffy antigen/receptor for chemokines (DARC) regulates prostate tumor growth. *Faseb j,* 20**,** 59-64.
SHIH, J. C., CHIEN, C. L., HO, H. N., LEE, W. C. & HSIEH, F. J. 2006. Stellate transformation of invasive trophoblast: a distinct phenotype of trophoblast that is involved in decidual vascular remodelling and controlled invasion during pregnancy. *Hum Reprod,* 21**,** 1299-304.
SIERRO, F., BIBEN, C., MARTINEZ-MUNOZ, L., MELLADO, M., RANSOHOFF, R. M., LI, M., WOEHL, B., LEUNG, H., GROOM, J., BATTEN, M., HARVEY, R. P., MARTINEZ, A. C., MACKAY, C. R. & MACKAY, F. 2007. Disrupted cardiac development but normal hematopoiesis in mice deficient in the second CXCL12/SDF-1 receptor, CXCR7. *Proc Natl Acad Sci U S A,* 104**,** 14759-64.

SIMPSON, J., REZAIE, P., NEWCOMBE, J., CUZNER, M. L., MALE, D. & WOODROOFE, M. N. 2000. Expression of the beta-chemokine receptors CCR2, CCR3 and CCR5 in multiple sclerosis central nervous system tissue. *J Neuroimmunol,* 108**,** 192-200.

SINGH, M. D., KING, V., BALDWIN, H., BURDEN, D., THORRAT, A., HOLMES, S., MCINNES, I. B., NICOLL, R., SHAMS, K., PALLAS, K., JAMIESON, T., LEE, K. M., CARBALLIDO, J. M., ROT, A. & GRAHAM, G. J. 2012. Elevated expression of the chemokine-scavenging receptor D6 is associated with impaired lesion development in psoriasis. *Am J Pathol,* 181**,** 1158-64.

SMITH, D. R., POLVERINI, P. J., KUNKEL, S. L., ORRINGER, M. B., WHYTE, R. I., BURDICK, M. D., WILKE, C. A. & STRIETER, R. M. 1994. Inhibition of interleukin 8 attenuates angiogenesis in bronchogenic carcinoma. *J Exp Med,* 179**,** 1409-15.

SMITH, G. C., CROSSLEY, J. A., AITKEN, D. A., PELL, J. P., CAMERON, A. D., CONNOR, J. M. & DOBBIE, R. 2004. First-trimester placentation and the risk of antepartum stillbirth. *JAMA.* United States.

SOMERSET, D. A., ZHENG, Y., KILBY, M. D., SANSOM, D. M. & DRAYSON, M. T. 2004. Normal human pregnancy is associated with an elevation in the immune suppressive CD25+ CD4+ regulatory T-cell subset. *Immunology,* 112**,** 38-43.

STALLMACH, A., GIESE, T., SCHMIDT, C., LUDWIG, B., MUELLER-MOLAIAN, I. & MEUER, S. C. 2004. Cytokine/chemokine transcript profiles reflect mucosal inflammation in Crohn's disease. *Int J Colorectal Dis,* 19**,** 308-15.

STANDIFORD, T. J., KUNKEL, S. L., LUKACS, N. W., GREENBERGER, M. J., DANFORTH, J. M., KUNKEL, R. G. & STRIETER, R. M. 1995. Macrophage inflammatory protein-1 alpha mediates lung leukocyte recruitment, lung capillary leak, and early mortality in murine endotoxemia. *J Immunol,* 155**,** 1515-24.

STELLATO, C., COLLINS, P., PONATH, P. D., SOLER, D., NEWMAN, W., LA ROSA, G., LI, H., WHITE, J., SCHWIEBERT, L. M., BICKEL, C., LIU, M., BOCHNER, B. S., WILLIAMS, T. & SCHLEIMER, R. P. 1997. Production of the novel C-C chemokine MCP-4 by airway cells and comparison of its biological activity to other C-C chemokines. *J Clin Invest,* 99**,** 926-36.

STOKNES, M., ANDERSEN, G. L., DAHLSENG, M. O., SKRANES, J., SALVESEN, K. A., IRGENS, L. M., KURINCZUK, J. J. & VIK, T. 2012. Cerebral palsy and neonatal death in term singletons born small for gestational age. *Pediatrics.* United States.

STRIETER, R. M., POLVERINI, P. J., KUNKEL, S. L., ARENBERG, D. A., BURDICK, M. D., KASPER, J., DZUIBA, J., VAN DAMME, J., WALZ, A., MARRIOTT, D. & ET AL. 1995. The functional role of the ELR motif in CXC chemokine-mediated angiogenesis. *J Biol Chem,* 270**,** 27348-57.

SZALAI, C., DUBA, J., PROHASZKA, Z., KALINA, A., SZABO, T., NAGY, B., HORVATH, L. & CSASZAR, A. 2001. Involvement of polymorphisms in the chemokine system in the susceptibility for coronary artery disease (CAD). Coincidence of elevated Lp(a) and MCP-1 -2518 G/G genotype in CAD patients. *Atherosclerosis,* 158**,** 233-9.

SZEKANECZ, Z., PAKOZDI, A., SZENTPETERY, A., BESENYEI, T. & KOCH, A. E. 2009. Chemokines and angiogenesis in rheumatoid arthritis. *Front Biosci (Elite Ed),* 1**,** 44-51.

TANTBIROJN, P., CRUM, C. P. & PARAST, M. M. 2008. Pathophysiology of placenta creta: the role of decidua and extravillous trophoblast. *Placenta,* 29**,** 639-45.

TENG, F., ZHOU, Y., JIN, R., CHEN, Y., PEI, X., LIU, Y., DONG, J., WANG, W., PANG, X., QIAN, X., CHEN, W. F., ZHANG, Y. & GE, Q. 2011. The molecular signature underlying the thymic migration and maturation of TCRalphabeta+ CD4+ CD8 thymocytes. *PLoS One,* 6**,** e25567.

THORNTON, J. G. & ONWUDE, J. L. 1992. Convulsions in pregnancy in related gorillas. *Am J Obstet Gynecol,* 167**,** 240-1.

TILLIE-LEBLOND, I., HAMMAD, H., DESURMONT, S., PUGIN, J., WALLAERT, B., TONNEL, A. B. & GOSSET, P. 2000. CC chemokines and interleukin-5 in bronchial lavage fluid from patients with status asthmaticus. Potential implication in eosinophil recruitment. *Am J Respir Crit Care Med,* 162**,** 586-92.

TODROS, T., BONTEMPO, S., PICCOLI, E., IETTA, F., ROMAGNOLI, R., BIOLCATI, M., CASTELLUCCI, M. & PAULESU, L. 2005. Increased levels of macrophage migration inhibitory factor (MIF) in preeclampsia. *Eur J Obstet Gynecol Reprod Biol,* 123**,** 162-6.

TRAUGOTT, U., REINHERZ, E. L. & RAINE, C. S. 1983. Multiple sclerosis: distribution of T cell subsets within active chronic lesions. *Science,* 219**,** 308-10.

TREBST, C., SORENSEN, T. L., KIVISAKK, P., CATHCART, M. K., HESSELGESSER, J., HORUK, R., SELLEBJERG, F., LASSMANN, H. & RANSOHOFF, R. M. 2001. CCR1+/CCR5+ mononuclear phagocytes accumulate in the central nervous system of patients with multiple sclerosis. *Am J Pathol,* 159**,** 1701-10.

TROTT, J. F., SIMPSON, K. J., MOYLE, R. L., HEARN, C. M., SHAW, G., NICHOLAS, K. R. & RENFREE, M. B. 2003. Maternal regulation of milk composition, milk production, and pouch young development during lactation in the tammar wallaby (Macropus eugenii). *Biol Reprod,* 68**,** 929-36.

TRUNDLEY, A., GARDNER, L., NORTHFIELD, J., CHANG, C. & MOFFETT, A. 2006. Methods for isolation of cells from the human fetal-maternal interface. *Methods Mol Med,* 122**,** 109-22.

TSAI, W. C., STRIETER, R. M., WILKOWSKI, J. M., BUCKNELL, K. A., BURDICK, M. D., LIRA, S. A. & STANDIFORD, T. J. 1998. Lung-specific transgenic expression of KC enhances resistance to Klebsiella pneumoniae in mice. *J Immunol,* 161**,** 2435-40.

TSUJI, M., AIKO, Y., KAWAMOTO, T., HACHISUGA, T., KOORIYAMA, C., MYOGA, M., TOMONAGA, C., MATSUMURA, F., ANAN, A., TANAKA, M., YU, H. S., FUJISAWA, Y., SUGA, R. & SHIBATA, E. 2013. Polychlorinated biphenyls (PCBs) decrease the placental syncytiotrophoblast volume and increase Placental Growth Factor (PlGF) in the placenta of normal pregnancy. *Placenta*.

UGUCCIONI, M., D'APUZZO, M., LOETSCHER, M., DEWALD, B. & BAGGIOLINI, M. 1995. Actions of the chemotactic cytokines MCP-1, MCP-2, MCP-3, RANTES, MIP-1 alpha and MIP-1 beta on human monocytes. *Eur J Immunol,* 25**,** 64-8.

VALENTIN, G., HAAS, P. & GILMOUR, D. 2007. The chemokine SDF1a coordinates tissue migration through the spatially restricted activation of Cxcr7 and Cxcr4b. *Curr Biol,* 17**,** 1026-31.

VALLES, C. S. & DOMÍNGUEZ, F. 2006. Embryo-endometrial interaction. *Chang Gung Med J,* 29**,** 9-14.

VAN DEN HEUVEL, M., PERALTA, C., BASHAR, S., TAYLOR, S., HORROCKS, J. & CROY, B. A. 2005. Trafficking of peripheral blood CD56(bright) cells to the decidualizing uterus--new tricks for old dogmas? *J Reprod Immunol,* 67**,** 21-34.

VANOTTEREN, G. M., STRIETER, R. M., KUNKEL, S. L., PAINE, R., 3RD, GREENBERGER, M. J., DANFORTH, J. M., BURDICK, M. D. & STANDIFORD, T. J. 1995. Compartmentalized expression of RANTES in a murine model of endotoxemia. *J Immunol,* 154**,** 1900-8.

VASSILIADOU, N. & BULMER, J. N. 1996. Immunohistochemical evidence for increased numbers of 'classic' CD57+ natural killer cells in the endometrium of women suffering spontaneous early pregnancy loss. *Hum Reprod,* 11**,** 1569-74.
VERCRUYSSE, L., CALUWAERTS, S., LUYTEN, C. & PIJNENBORG, R. 2006. Interstitial trophoblast invasion in the decidua and mesometrial triangle during the last third of pregnancy in the rat. *Placenta,* 27**,** 22-33.
VERMA, S., KING, A. & LOKE, Y. W. 1997. Expression of killer cell inhibitory receptors on human uterine natural killer cells. *Eur J Immunol,* 27**,** 979-83.
VETRANO, S., BORRONI, E. M., SARUKHAN, A., SAVINO, B., BONECCHI, R., CORREALE, C., ARENA, V., FANTINI, M., RONCALLI, M., MALESCI, A., MANTOVANI, A., LOCATI, M. & DANESE, S. 2010. The lymphatic system controls intestinal inflammation and inflammation-associated Colon Cancer through the chemokine decoy receptor D6. *Gut,* 59**,** 197-206.
VIGANO, P., CINTORINO, M., SCHATZ, F., LOCKWOOD, C. J. & ARCURI, F. 2007. The role of macrophage migration inhibitory factor in maintaining the immune privilege at the fetal-maternal interface. *Semin Immunopathol,* 29**,** 135-50.
VILA-CORO, A. J., MELLADO, M., MARTIN DE ANA, A., MARTINEZ, A. C. & RODRIGUEZ-FRADE, J. M. 1999. Characterization of RANTES- and aminooxypentane-RANTES-triggered desensitization signals reveals differences in recruitment of the G protein-coupled receptor complex. *J Immunol,* 163**,** 3037-44.
VOSSHENRICH, C. A., GARCIA-OJEDA, M. E., SAMSON-VILLEGER, S. I., PASQUALETTO, V., ENAULT, L., RICHARD-LE GOFF, O., CORCUFF, E., GUY-GRAND, D., ROCHA, B., CUMANO, A., ROGGE, L., EZINE, S. & DI SANTO, J. P. 2006. A thymic pathway of mouse natural killer cell development characterized by expression of GATA-3 and CD127. *Nat Immunol,* 7**,** 1217-24.
WANG, J., OU, Z. L., HOU, Y. F., LUO, J. M., SHEN, Z. Z., DING, J. & SHAO, Z. M. 2006a. Enhanced expression of Duffy antigen receptor for chemokines by breast cancer cells attenuates growth and metastasis potential. *Oncogene,* 25**,** 7201-11.
WANG, J. H., DEVALIA, J. L., XIA, C., SAPSFORD, R. J. & DAVIES, R. J. 1996. Expression of RANTES by human bronchial epithelial cells in vitro and in vivo and the effect of corticosteroids. *Am J Respir Cell Mol Biol,* 14**,** 27-35.
WANG, X., MA, Z., HONG, Y., LU, P. & LIN, Q. 2006b. Expression of CD28 and cytotoxic T lymphocyte antigen 4 at the maternal-fetal interface in women with unexplained pregnancy loss. *Int J Gynaecol Obstet,* 93**,** 123-9.
WANG, Y. & ZHAO, S. 2010. Placental blood circulation. *Vascular biology of the placenta.* Morgan & Claypool Life Sciences.
WATANABE, K., PENFOLD, M. E., MATSUDA, A., OHYANAGI, N., KANEKO, K., MIYABE, Y., MATSUMOTO, K., SCHALL, T. J., MIYASAKA, N. & NANKI, T. 2010. Pathogenic role of CXCR7 in rheumatoid arthritis. *Arthritis Rheum,* 62**,** 3211-20.
WATANABE, T., PAKALA, R., KATAGIRI, T. & BENEDICT, C. R. 2001. Monocyte chemotactic protein 1 amplifies serotonin-induced vascular smooth muscle cell proliferation. *J Vasc Res,* 38**,** 341-9.
WATSON, E. D. & CROSS, J. C. 2005. Development of structures and transport functions in the mouse placenta. *Physiology (Bethesda),* 20**,** 180-93.
WEBER, E. M., ALGERS, B., WURBEL, H., HULTGREN, J. & OLSSON, I. A. 2013. Influence of strain and parity on the risk of litter loss in laboratory mice. *Reprod Domest Anim,* 48**,** 292-6.
WEBER, M., BLAIR, E., SIMPSON, C., O'HARA, M., BLACKBURN, P., ROT, A., GRAHAM, G. & NIBBS, R. 2004. The chemokine receptor D6 constitutively traffics to and from the cell surface to internalize and degrade chemokines. *Mol Biol Cell,* 15**,** 2492-508.
WENZEL, U., SCHNEIDER, A., VALENTE, A. J., ABBOUD, H. E., THAISS, F., HELMCHEN, U. M. & STAHL, R. A. 1997. Monocyte chemoattractant protein-1 mediates monocyte/macrophage influx in anti-thymocyte antibody-induced glomerulonephritis. *Kidney Int,* 51**,** 770-6.
WESSELS, J., LINTON, N., CROY, B. & TAYADE, C. 2007. A review of molecular contrasts between arresting and viable porcine attachment sites. *Am J Reprod Immunol,* 58**,** 470-80.
WHITEHEAD, G. S., WANG, T., DEGRAFF, L. M., CARD, J. W., LIRA, S. A., GRAHAM, G. J. & COOK, D. N. 2007. The chemokine receptor D6 has opposing effects on allergic inflammation and airway reactivity. *Am J Respir Crit Care Med,* 175**,** 243-9.
WHITLEY, G. S. 2006. Production of human trophoblast cell lines. *Methods Mol Med,* 121**,** 219-28.
WILMUT, I., SALES, D. I. & ASHWORTH, C. J. 1986. Maternal and embryonic factors associated with prenatal loss in mammals. *J Reprod Fertil,* 76**,** 851-64.
WU, F. Y., OU, Z. L., FENG, L. Y., LUO, J. M., WANG, L. P., SHEN, Z. Z. & SHAO, Z. M. 2008. Chemokine decoy receptor d6 plays a negative role in human breast cancer. *Mol Cancer Res,* 6**,** 1276-88.
XIE, X., KANG, Z., ANDERSON, L. N., HE, H., LU, B. & CROY, B. A. 2005. Analysis of the contributions of L-selectin and CXCR3 in mediating leukocyte homing to pregnant mouse uterus. *Am J Reprod Immunol,* 53**,** 1-12.
XU, C., MAO, D., HOLERS, V. M., PALANCA, B., CHENG, A. M. & MOLINA, H. 2000. A critical role for murine complement regulator crry in fetomaternal tolerance. *Science,* 287**,** 498-501.
YAMADA, H., KATO, E. H., MORIKAWA, M., SHIMADA, S., SAITO, H., WATARI, M., MINAKAMI, H. & NISHIHIRA, J. 2003. Decreased serum levels of macrophage migration inhibition factor in miscarriages with normal chromosome karyotype. *Hum Reprod,* 18**,** 616-20.
YAMPOLSKY, M., SALAFIA, C. M., SHLAKHTER, O., HAAS, D., EUCKER, B. & THORP, J. 2009. Centrality of the umbilical cord insertion in a human placenta influences the placental efficiency. *Placenta,* 30**,** 1058-64.
YANG, T. Y., CHEN, S. C., LEACH, M. W., MANFRA, D., HOMEY, B., WIEKOWSKI, M., SULLIVAN, L., JENH, C. H., NARULA, S. K., CHENSUE, S. W. & LIRA, S. A. 2000. Transgenic expression of the chemokine receptor encoded by human herpesvirus 8 induces an angioproliferative disease resembling Kaposi's sarcoma. *J Exp Med,* 191**,** 445-54.
YONEYAMA, H., HARADA, A., IMAI, T., BABA, M., YOSHIE, O., ZHANG, Y., HIGASHI, H., MURAI, M., ASAKURA, H. & MATSUSHIMA, K. 1998. Pivotal role of TARC, a CC chemokine, in bacteria-induced fulminant hepatic failure in mice. *J Clin Invest,* 102**,** 1933-41.
YUE, T. L., WANG, X., SUNG, C. P., OLSON, B., MCKENNA, P. J., GU, J. L. & FEUERSTEIN, G. Z. 1994. Interleukin-8. A mitogen and chemoattractant for vascular smooth muscle cells. *Circ Res,* 75**,** 1-7.
YUEN, R. K., CHEN, B., BLAIR, J. D., ROBINSON, W. P. & NELSON, D. M. 2013. Hypoxia alters the epigenetic profile in cultured human placental trophoblasts. *Epigenetics,* 8**,** 192-202.
ZENCLUSSEN, A. C., FEST, S., SEHMSDORF, U. S., HAGEN, E., KLAPP, B. F. & ARCK, P. C. 2001. Upregulation of decidual P-selectin expression is associated with an increased number of Th1 cell populations in patients suffering from spontaneous abortions. *Cell Immunol.* United States.
ZENCLUSSEN, A. C., GERLOF, K., ZENCLUSSEN, M. L., SOLLWEDEL, A., BERTOJA, A. Z., RITTER, T., KOTSCH, K., LEBER, J. & VOLK, H. D. 2005. Abnormal T-cell reactivity against paternal antigens in spontaneous abortion: adoptive

transfer of pregnancy-induced CD4+CD25+ T regulatory cells prevents fetal rejection in a murine abortion model. *Am J Pathol,* 166**,** 811-22.

ZHANG, J., CHEN, Z., SMITH, G. N. & CROY, B. A. 2011. Natural killer cell-triggered vascular transformation: maternal care before birth? *Cell Mol Immunol,* 8**,** 1-11.

ZLOTNIK, A. & YOSHIE, O. 2000. Chemokines: a new classification system and their role in immunity. *Immunity,* 12**,** 121-7.